UDK 66:54(05) CODEN HMIDA 8 ISSN 0367–598 X

6

Hemijska industrija

Vol. 67

Časopis Saveza hemijskih inženjera

Chemical Industry

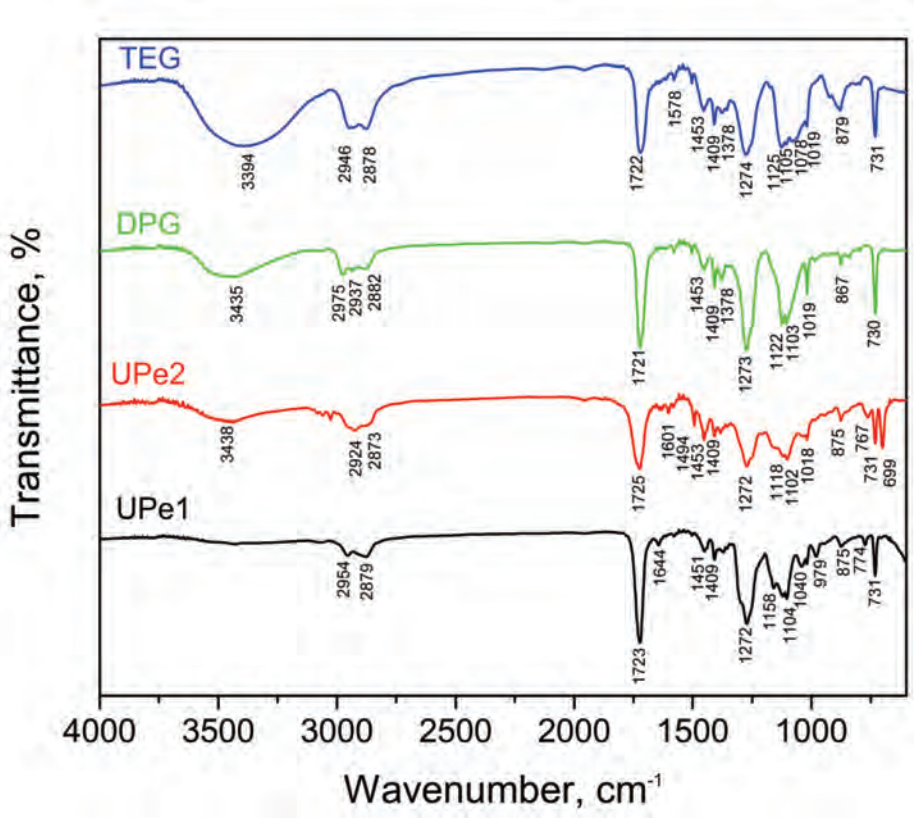

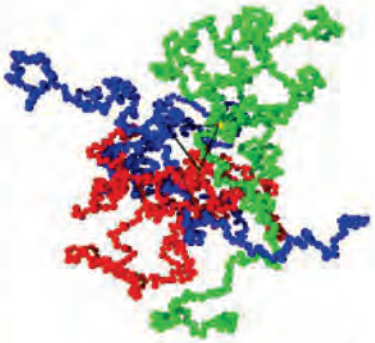

Posebna sekcija:
Polimeri

BEOGRAD, NOVEMBAR-DECEMBAR 2013. HMIDA 8, 67 (6) 861-1025 (2013)

GENERALNI POKROVITELJ

Hemofarm

HEMOFARM KONCERN

VRŠAC, Beogradski put bb, tel. 013/821-345, 821-027, 821-129
BEOGRAD, Prote Mateje 70, tel. 011/344-26-63, faks: 344-17-87
E-pošta: info@hemofarm.com

IZDAVANJE ČASOPISA POMOGLA JE:

INŽENJERSKA KOMORA SRBIJE
Bulevar vojvode Mišića 37
11000 Beograd

SUIZDAVAČI

Tehnološko-metalurški fakultet
Univerziteta u Beogradu, Beograd

Prirodno-matematički fakultet Univerziteta
u Novom Sadu, Novi Sad

Hemijski fakutet
Univerziteta u Beogradu
Beograd

ITNMS
Institut za tehnologiju nuklearnih i drugih
mineralnih sirovina, Beograd

HIP PETROHEMIJA
HIP Petrohemija a.d. Pančevo

Tehnološki fakultet Univerziteta
u Novom Sadu, Novi Sad

NU Institut za hemiju,
tehnologiju i metalurgiju
Univerziteta u Beogradu,
Beograd

nevena
„Nevena Color“ d.o.o.
Leskovac

Tehnološki fakultet Univerziteta
u Nišu, Leskovac

dcp-hemigal®
DCP Hemigal, Leskovac

Beograd Srbija SHI

Chemical Industry
Химическая промышленность

Hemijska industrija

Časopis Saveza hemijskih inženjera Srbije
Journal of the Association of Chemical Engineers of Serbia
Журнал Союза химических инженеров Сербии

VOL. 67 **Beograd, novembar–decembar 2013** **Broj 6**

Izdavač
Savez hemijskih inženjera Srbije
Beograd, Kneza Miloša 9/I

Glavni urednik
Branko Bugarski

Urednici
Katarina Jeremić, Ivana Banković-Ilić, Maja Obradović, Dušan Mijin

Članovi uredništva
Milorad Cakić, Željko Čupić, Željko Grbavčić, Katarina Jeremić, Miodrag Lazić, Slobodan Petrović, Milovan Purenović, Aleksandar Spasić, Dragoslav Stoiljković, Radmila Šećerov-Sokolović, Slobodan Šerbanović, Nikola Nikačević, Svetomir Milojević

Članovi uredništva iz inostranstva
Dragomir Bukur (SAD), Jiri Hanika (Češka Republika), Valerij Meshalkin (Rusija), Ljubiša Radović (SAD), Constantinos Vayenas (Grčka)

Likovno-grafičko rešenje naslovne strane
Milan Jovanović

Redakcija
11000 Beograd, Kneza Miloša 9/I
Tel/fax: 011/3240-018
E-pošta: shi@yubc.net
www.ache.org.rs

Izlazi dvomesečno, rukopisi se ne vraćaju

Za izdavača
Tatijana Dudukoviċ

Sekretar redakcije
Slavica Desnica

Izdavanje časopisa pomaže
Republika Srbija, Ministarstvo prosvete, nauke i tehnološkog razvoja

Uplata pretplate i oglasnog prostora vrši se na tekući račun Saveza hemijskih inženjera Srbije, Beograd, broj 205-2172-71, Komercijalna banka a.d., Beograd

Kompjuterska priprema
Vladimir Panić

Štampa
Razvojno-istraživački centar grafičkog inženjerstva, Tehnološko-metalurški fakultet, Univerzitet u Beogradu, Karnegijeva 4, 11000 Beograd

Indeksiranje
Radovi koji se publikuju u časopisu *Hemijska Industrija* ideksiraju se preko *Thompson Reuters Scietific®* servisa *Science Citation Index - Expanded™* i *Journal Citation Report (JCR)*, kao i domaćeg *SCIndeks* servisa Centra za evaluaciju u obrazovanju i nauci

SADRŽAJ

SADRŽAJ nastavak

CONTENTS

Polymers

CONTENTS Continued

Karakterizacija nanofotoničnih mekih kontaktnih sočiva na bazi poli(2-hidroksietil-metakrilata) i fulerena

Aleksandra D. Debeljković, Lidija R. Matija, Đuro Lj. Koruga

Univerzitet u Beogradu, NanoLab, Mašinski fakultet, Beograd, Srbija

Izvod

U ovom radu predstavljeno je uporedno ispitivanje karakteristika baznog i novog nanofotoničnog materijala koji je dobijen inkorporiranjem nanomaterijala u bazni materijal za meka kontaktna sočiva. Bazni (SL38) i nanofotonični materijal (SL38-A) za meka kontaktna sočiva dobijeni su radikalnom polimerizacijom 2-hidroksietil-metakrilata, odnosno 2-hidroksietil-metakrilata i fulerena koja je izvedena po tehnologiji i u proizvodnim laboratorijama kompanije Soleko (Milano, Italija). Fulereni su dodati zbog apsorpcionih transmisionih karakteristika u ultraljubičastom, vidljivom i bliskom infracrvenom spektru. Od dobijenih materijala napravljena su meka kontaktna sočiva u kompaniji Optix (Beograd, Srbija). Izračunati su parametri mreže, urađena je SEM analiza i merene su optičke karakteristike ispitivanih mekih kontaktnih sočiva. Utvrđeno je da transport tečnosti kroz hidrogel prati Fikov zakon i da bazni i nanofotonični materijal spadaju u grupu neporoznih hidrogelova. Dobijeni rezultati pokazuju bolja optička svojstva sintetisanih nanofotoničnih mekih kontaktnih sočiva u poređenju sa baznim sočivom.

Ključne reči: *nanofotonična meka kontaktna sočiva, PHEMA, fulereni, optička snaga.*

Dostupno na Internetu sa adrese časopisa: http://www.ache.org.rs/HI/

Polimeri

NAUČNI RAD

UDK 617.7–089.243:678:54

Hem. Ind. **67** (6) 861–870 (2013)

doi: 10.2298/HEMIND120830019D

Hidrogelovi su slabo umreženi hidrofilni polimeri sposobni da apsorbuju velike količine vode ili bioloških fluida, pri čemu bubre, ali se ne rastvaraju [1,2]. Kao takvi, hidrogelovi imaju primenu u biomedicini odnosno kod kontaktnih sočiva i za kontrolisano otpuštanje aktivnih supstanci. Jedan od najčešće korišćenih hidrogelova za izradu kontaktnih sočiva je poli(2-hidroksietil-metakrilat), PHEMA, koji služi kao osnovna komponenta u mekim kontaktnim sočivima. Utvrđeno je da je biokompatibilnost ovog materijala odraz sadržaja vode, kiseonika, permeabilnosti i kvašenja površine [3–5].

Sočiva se mogu sintetisati tako da sadrže optimalnu količinu vode odnosno bioloških fluida u vodenoj sredini, da imaju odgovarajuća mehanička svojstva, propustljivost za kiseonik, biokompatibilnost, stabilnost oblika i mekoću sličnu onoj koju poseduju meka tkiva [6–8]. Brojna su istraživanja [9–14] koja za cilj imaju razvoj i unapređenje karakteristika materijala za meka kontaktna sočiva, a sve sa svrhom postizanja što kvalitetnije korekcije vida, veće udobnosti nošenja, obezbeđivanja dovoljne količine kiseonika za rožnjaču i sve manje medicinskih komplikacija pri nošenju mekih kontaktnih sočiva.

Takođe, u oblasti optike i materijala za meka kontaktna sočiva, potrebno je da se razvije novi materijal koji bi posle obrade trebalo da poboljša optička svojstva transmisije vidljive i blisko vidljive svetlosti.

Prepiska: A.D. Debeljković, NanoLab, Mašinski fakultet, Kraljice Marije 16, 11000 Beograd, Srbija.
E-pošta: adebeljkovic@mas.bg.ac.rs
Rad primljen: 31. avgust, 2012
Rad prihvaćen: 5. februar, 2013

Jedan od načina koji može da se iskoristi za poboljšanje karakteristika materijala za meka kontaktna sočiva jeste primena nanotehnologija. Nanotehnologije se već dve decenije najčešće koriste u naučnim oblastima kao što su elektronika, primenjena fizika i inženjerstvo. U ovim oblastima pokazale su ogroman napredak, međutim, u biomedicini i farmaciji njihove mogućnosti tek treba istraživati. Tokom poslednjih nekoliko decenija polimeri modifikovani nanočesticama su od posebnog interesa za istraživanje i razvoj materijala za izradu kontaktnih sočiva [4].

Kada se nekom optičkom materijalu doda nanomaterijal u procentu koji značajno menja optička svojstva baznog materijala, dobija se nanofotonični materijal. Nanofotonični materijali sa ugrađenim C_{60} daju različita optička svojstva jer ikosaedarska grupa ima više simetrijskih elemenata koji određuju sopstvene energetske vrednosti (T1u, T2u,...) nanofotoničnog materijala.

Veliki broj radova predstavlja rezultate istraživanja i eksperimenata u domenu inkorporiranja fulerena u strukturu polimera [15–18]. Fuleren je molekul koji sadrži 60 atoma ugljenika koji su raspoređeni po površini sfere u pentagone (12) i heksagone (20). Kao individualni molekul, C_{60} je čvršći od dijamanta, međutim, kada kristališe, kristalna rešetka mu je meka skoro kao kod grafita. Iako vrlo stabilan, molekul C_{60} lako reaguje, tako da je danas poznato više od 6500 potpuno novih jedinjenja na bazi ovog molekula. Molekul C_{60} ima značajne mogućnosti primene koje se očekuju u narednim decenijama [19,20].

Međutim, nije poznato da su rađena istraživanja i objavljivani rezultati koji se bave sintezom i karakteri-

zacijom mekih kontaktnih sočiva sa fulerenima u strukturi materijala. Inkorporiranjem fulerena može se uticati na optička svojstva materijala što ih čini veoma interesantnim za ispitivanja. Fulereni manje propuštaju svetlost u domenu ultraljubičastog, plavog i infracrvenog spektra, koji oštećuju očno tkivo, dok je u oblasti zelenog i žutog spektra propuštanje svetlosti veće, što odgovara ljudskom oku.

Do sada su samo ispitivana gas-propusna kontaktna sočiva na bazi poli (metil metakrilata), PMMA, sa inkorporiranim fulerenom. Stamenković i saradnici [21,22] su pokazali da su optičke i mehaničke karakteristike nanofotoničnih materijala na bazi PMMA i fulerena (transmitivnost talasnih dužina vidljivog spektra u skladu sa spektralnom efikasnošću oka, zaštita od ultraljubičastog i infracrvenog zračenja, zaštita od ljubičasto-plavog dela vidljivog spektra, kvašenja površine i kvalitet obrađenih površina-hrapavost) značajno poboljšane ugradnjom fulerena u sočivo na bazi PMMA.

Cilj ovog rada je da se uporedno ispitaju svojstva baznog i nanofotoničnog materijala, koji su sintetisani u kompaniji Soleko (Milano, Italija). Bazni (SL38) i nanofotonični materijal (SL38-A) za meka kontaktna sočiva dobijeni su radikalnom polimerizacijom 2-hidroksietil-metakrilata odnosno 2-hidroksietil-metakrilata i fulerena. Od dobijenih materijala napravljena su meka kontaktna sočiva u kompaniji Optix (Beograd, Srbija). Ispitano je bubrenje baznog i nanofotoničnog materijala u puferskom rastvoru pH vrednosti 7,3. Na osnovu dobijenih rezultata izračunati su parametri mreže, molarna masa između dve tačke umreženja i veličina pora. Urađene su mikrografije skenirajuće elektronske mikroskopije (SEM), određene su i optička snaga i mape defekata ispitivanih uzoraka mekih kontaktnih sočiva.

EKSPERIMENTALNI DEO

Materijal

Materijali su dobijeni na osnovu ugovora o naučno-tehničko-poslovnoj saradnji između kompanija Optix (Beograd, Srbija) i Soleko (Milano, Italija) sa Mašinskim fakultetom Univerziteta u Beogradu. Polimerizacija novih nanofotoničnih materijala za meka kontaktna sočiva izvedena je po tehnologiji i u proizvodnim laboratorijama kompanije Soleko (Milano, Italija). U njihov bazni materijal za meka kontaktna sočiva, SL38, koji se dobija radikalnom polimerizacijom 2-hidroksietil-metakrilata, dodat je fuleren kako bi se dobio nanofotonični materijal, SL38-A. U reakciji polimerizacije korišćen je 2-hidroksietil-metakrilat, HEMA, (Sigma Aldrich, ≥99%) kao monomer, etilen-glikol-dimetakrilat (Sigma Aldrich, 98 %) je upotrebljen kao umreživač, fuleren C_{60} (MER Corporation, SAD, ≥99%), a kao inicijator je korišćen benzoil-peroksid (Sigma Aldrich, 75%). Od dobijenih materijala napravljena su meka kontaktna sočiva.

Za ispitivanje bubrenja, parametara mreže i SEM analize korišćeni su bazni i nanofotonični materijal za meka kontaktna sočiva, dok su za određivanje optičke snage i mape defekata korišćena na strugu obrađena bazna i nanofotonična meka kontaktna sočiva. Gustina baznog i nanofotoničnog materijala je određena piknometrom.

Sintetisani materijali su u obliku diska dimenzija: SL38 (R = 12,16 mm, h = 3,83 mm) i SL38-A (R = 12,50 mm, h = 3,73 mm). Za bubrenje korišćen je puferski rastvor (pH 7,3) sastava: natrijum-hlorid (Sigma Aldrich, BioXtra, ≥99.5%), borna kiselina (Sigma Aldrich, 4%) i borax – dinatrijum-tetraborat (Sigma Aldrich, 50 g/l).

Karakterizacija

Bubrenje hidrogelova

Suvi, izmereni uzorci su potopljeni u 50 ml puferskog rastvora pH vrednosti 7,3 (pH vrednost suznog filma). Prosečna masa SL38 iznosila je 0,1055 g, dok je za SL38-A iznosila 0,1155 g. Proces bubrenja je praćen gravimetrijski na 25 °C. U određenim vremenskim intervalima, gelovi su vađeni iz rastvora i nakon odstranjivanja viška pufera sa površine gela, merena je masa nabubrelog gela, a stepen bubrenja, q_t, je računat prema jednačini [23–25] :

$$q_t = (m_t/m_o) \quad (1)$$

gde je m_o - masa suvog uzorka, m_t - masa nabubrelog gela u trenutku t.

Ravnotežni stepen bubrenja, q_e, je određen kao odnos mase nabubrelog gela nakon dostizanja ravnoteže i mase suvog uzorka:

$$q_e = m_e/m_o \quad (2)$$

gde je: m_e - masa nabubrelog gela po dostizanju ravnoteže.

Dobijeni eksperimentalni rezultati predstavljaju srednju vrednost tri nezavisna merenja.

Skenirajuća elektronska mikroskopija

Ispitivanja su izvedena na elektronskom mikroskopu Tescan Mira 3XMU (Tescan, Republika Češka). Pre snimanja uzorci sintetisanih materijala u obliku diska su potopljeni u tečni azot da bi se izbegle deformacije prilikom loma. Nakon toga su uzorci stavljeni u evaporator Polaron SC502 (Fisons Instruments, England) kako bi se metalizirali pomoću platine.

Optička snaga

Ispitivanja optičke snage izvršena su na topografu optičke snage, uređaju Rotlex® CONTEST Plus (Intra-Ocular Lens analizer, Izrael). Specifikacija Rotlex uređaja: opseg, -30 do +30 D, rezolucija, 0,01 D, tačnost, 0,5%, cilindar, do 6 D i vreme merenja, 4 s.

Merenja optičke snage su izvedena u strogo kontrolisanim uslovima, pod konstantnom kontrolom tem-

perature (25 °C), kontrolom vlažnosti vazduha (do 38%) i kvaliteta samog vazduha.

Za oba kontaktna sočiva, SL38 i SL38-A, nominalna tražena snaga je +3,00 D. Indeks prelamanja za oba kontaktna sočiva je n = 1,4950. Ova vrednost predstavlja teorijsku vrednost indeksa prelamanja izračunatu u kompaniji Soleko (Milano, Italija). Indeks prelamanja za puferski rastvor pH 7,3 u kiveti je n = 1,3350. Sočivo je rađeno sa baznom krivinom kao r = 8,6 mm. Debljina sočiva u centru je 0,21 mm. Ispitivana kontaktna sočiva su sferna i sabirna. Merena snaga je računata za prečnik od 7,40 mm. Meka kontaktna sočiva u suvom stanju podležu hidrataciji u puferskom rastvoru pH 7,3, a posle hidratacije idu u autoklav na sterilizaciju. Minimalno vreme za hidrataciju je 2 h na 50 °C.

Proces u autoklavu traje 1 h na 50 °C, dok sterilizacija traje 15 min na 120 °C. Optička snaga mekih kontaktnih sočiva je merena nakon sterilizacije.

REZULTATI I DISKUSIJA

Određivanje ravnotežnog stepena bubrenja

Jedno od najvažnijih svojstava sočiva pri kontaktu sa vodom je bubrenje usled apsorpcije vode, pri čemu im se povećava zapremina. Kada se suv uzorak potopi u vodu, molekuli vode prvo hidratišu najpolarnije hidrofilne grupe, jonske grupe (ako su prisutne) i grupe koje mogu da obrazuju vodonične veze. Sadržaj vode u mekim kontaktnim sočivima može da dostigne vrednost između 38 i 79%. Apsorbovana voda čini da sočivo bude meko i fleksibilno. Na slici 1 prikazana je vremenska zavisnost stepena bubrenja sintetisanih sočiva na pH 7,3.

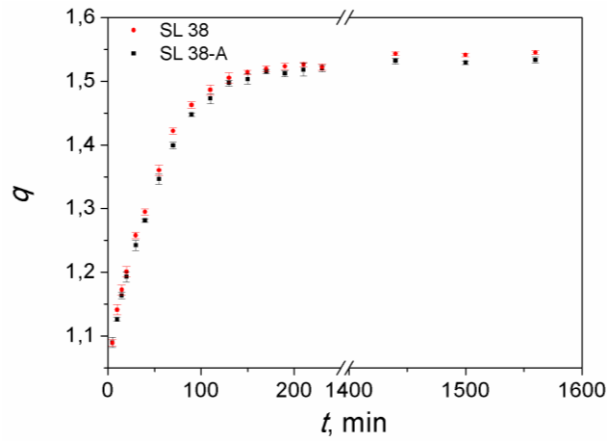

Slika 1. Vremenska zavisnost stepena bubrenja materijala za meka kontaktna sočiva SL38 i SL38-A.
Figure 1. Time dependence of swelling of the material for soft contact lenses SL38 and SL38-A.

Sadržaj vode u baznom materijalu, SL38 određen je u kompaniji Soleko (Milano, Italija) i iznosi 38%. Poređenjem krivih bubrenja za uzorak SL38 i SL38-A može se zaključiti da ugradnjom fulerena u bazni materijal ne dolazi do značajnije promene stepena bubrenja, odnosno sadržaja vode. Na osnovu dobijenog rezultata pretpostavlja se da sintetisani nanofotonični materijal može da obezbedi potrebnu i dovoljnu elastičnost i mekoću sočiva kao i bazni materijal.

Ispitivanje difuzije u baznom i nanofotoničnom materijalu

Poznato je da je difuzija u hidrogelovima povezana sa fizičkim svojstvima mreže i interakcijama između polimera i penetrirajućeg medijuma [24,26]. Kada suv uzorak dođe u kontakt sa vodom molekuli vode difunduju u polimernu mrežu, smeštaju se u prostore između polimernih lanaca i pri tome prouzrokuju njihovo razdvajanje i bubrenje mreže. Praćenje mehanizma transporta vode sa vremenom, do postizanja ravnoteže, se može izvesti primenom sledeće poluempirijske jednačine [27–31]:

$$\frac{w_t}{w_e} = kt^n \tag{3}$$

gde su: w_t – masa apsorbovane vode u trenutku t, w_e – masa apsorbovane vode u stanju ravnoteže, k – konstanta karakteristična za određenu vrstu gela, t – vreme i n – difuzioni eksponent.

Jednačina (3) važi uz uslov $w_t/w_e < 0{,}6$.

Na osnovu vrednosti difuzionog eksponenta dobija se informacija o mehanizmu apsorpcije vode. Ukoliko je vrednost difuzionog eksponenta $n \leq 0{,}5$, transport tečnosti u hidrogel prati Fikov (Fick) zakon, odnosno difuzija vode kontroliše bubrenje, jer je to sporiji proces od relaksacije polimernih lanaca. Kada je n = 1 relaksacija polimernih lanaca kontroliše proces bubrenja (tzv. tip II, engl. *case II*). Za vrednosti n u intervalu $0{,}5 < n < 1$ mehanizam bubrenja ne prati Fikov zakon, a difuzija tečnosti i relaksacija polimernih lanaca kontrolišu proces bubrenja. Za vrednosti $n > 1$ mehanizam odgovara tipu III (engl. *super case II*).

Na slici 2 prikazan je grafik pravolinijske zavisnosti između $\ln(w_t/w_e)$ i $\ln t$.

Vrednosti konstante k i vrednosti eksponenta n za početnu fazu procesa bubrenja materijala za meka kontaktna sočiva izračunate su iz odsečka i nagiba prave, kada je zavisnost stepena bubrenja od proteklog vremena pravolinijska. To je vreme za koje gel apsorbuje 60% od ukupno apsorbovane vode odnosno rastvora. Dobijeni rezultati su prikazani u tabeli 1.

Na osnovu ovih podataka može se zaključiti da vrednost difizionog eksponenta nije u značajnoj meri veća od 0,5 tako da se transport fluida kroz uzorak može smatrati bliskim Fikovoj difuziji. tj. difuzija vode kontroliše proces bubrenja. Takođe se može uočiti da se dodatkom fulerena ne menja vrednost difuzionog eksponenta.

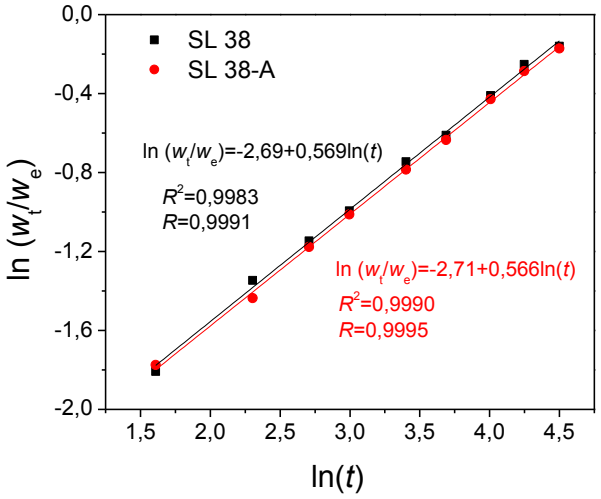

Slika 2. Logaritamska zavisnost ln(w_t/w_e) od ln t za ispitivane materijale za meka kontaktna sočiva.
Figure 2. Logarithmic dependence of ln(wt/we) vs ln(t) for investigated materials for soft contact lenses.

Tabela 1. Kinetički parametri bubrenja
Table 1. Kinetic parameters of swelling

Uzorak	$k\times10^2$ / min$^{-1/2}$	n	R^2
SL 38	6,77	0,57	0,9989
SL 38-A	6,66	0,57	0,9998

Parametri mreže

Da bi se okarakterisala jedna polimerna mreža potrebno je odrediti molarnu masu polimernih lanaca između dve susedne tačke umreženja (M_c), veličinu pora (ξ), zapreminski udeo polimera u nabubrelom stanju ($\upsilon_{2,s}$), parametar interakcije polimer-rastvarač (χ) i efektivnu gustinu umreženja (V_e).

Molarna masa između dve tačke umreženja se izračunava pomoću Flori-Renerove (Flory–Rehner-ove) jednačine [32]:

$$M_c = -d_p V_s^{1/3}[\ln(1-\upsilon_{2,s}) + \upsilon_{2,s} + \chi\,\upsilon_{2,s}^2]^{-1} \quad (4)$$

gde je d_p – gustina hidrogela [33,34], V_s – molarna zapremina rastvarača, χ – Flory–Haginsov (Flori–Huggins) parametar interakcije polimer–rastvarač [32]:

$$\chi = \frac{\ln(1-v_{2m}) + v_{2m}}{v_{2m}^2} \quad (5)$$

Zapreminski udeo polimera u nabubrelom stanju se računa pomoću sledeće jednačine:

$$\upsilon_{2,s} = [1+[\frac{d_p}{d_s}(\frac{m_a}{m_b}) - \frac{d_p}{d_s}]]^{-1} \quad (6)$$

gde je d_s – gustina rastvarača, m_a – masa materijala posle bubrenja, m_b – masa materijala pre bubrenja.

Efektivna gustina umreženja se računa prema sledećoj formuli:

$$V_e = \frac{d_p N_A}{M_c} \quad (7)$$

gde je N_A – Avogadrov broj.

Veličina pora se može izračunati pomoću sledeće jednačine [35]:

$$\xi = \left(\frac{2C_n\bar{M}_c}{M_o}\right)^{1/2} l\upsilon_{2,s}^{-1/3} \quad (8)$$

gde je: M_o - molarna masa osnovne jedinice od koje je polimerni lanac sastavljen, M_c – molarna masa polimernih lanaca između dve susedne tačke umreženja, C_n – karakterističan odnos koji definiše konformaciju polimera i konstantan je za dati sistem polimer-rastvarač i l dužina C–C veze (1,54 Å=1,54×10^{-10} m).

Vrednosti parametara mreže hidrogela (udeo zapremine polimera u nabubrelom gelu, molarna masa polimernih lanaca između dve susedne tačke umreženja, efektivna gustina umreženja i veličina pora) prikazane su u tabeli 2.

Na osnovu prikazanih vrednosti parametara mreže, uočeno je da nanofotonični materijal SL38-A ima manju molarnu masu između dve tačke umreženja i veličinu pora u poređenju sa SL38, dok je efektivna gustina umreženja i parametar interakcije polimer-rastvarač za SL38-A veći u odnosu na bazni materijal SL38 (tabela 2). Dobijeni rezultati su u skladu sa rezultatima bubrenja. Male vrednosti za M_c su očekivane s obzirom na mali ravnotežni stepen bubrenja posmatranih sintetisanih materijala. Što je manja molarna masa između dve tačke umreženja, efektivna gustina umreženja je veća, a bubrenje je manje. Vrednosti parametra interakcije su u skladu sa rezultatima bubrenja.

Prema izračunatim vrednostima za veličinu pora, ispitivani hidrogelovi se mogu klasifikovati kao neporozni jer je veličina pora manja od 10 nm [36].

Tabela 2. Parametri mreže materijala za meka kontaktna sočiva dobijeni primenom teorije ravnotežnog bubrenja
Table 2. Network parameters of the material for soft contact lenses obtained by equilibrium swelling theory

Uzorak	q_e	d_p g/cm^3	v_{2m}	χ	$M_c\times10^3$ g/mol	$V_e\times10^{22}$ mol/cm^3	$\xi\times10^{10}$ m
SL 38	1,54	1,36	0,72	0,85	0,0367	0,23	0,365
SL 38-A	1,53	1,24	0,73	0,88	0,0297	0,69	0,324

SEM analiza

Morfologija sintetisanog baznog i nanofotoničnog materijala za meka kontaktna sočiva je ispitana skenirajućom elektronskom mikroskopijom (Slika 3). SEM mikrografije pokazuju da ovi materijali imaju slabo poroznu strukturu.

Optička snaga i mape defekata

Optička snaga (optička jačina) jednog dioptera (površine koja razdvaja dve optičke sredine različitih indeksa prelamanja), optičkog elementa (sočiva) ili optičkog sistema (npr. optičkog sistema oka) je mera prelamanja optičkih zraka. Sočivo je optički "snažnije" ili "jače" ako više skreće – prelama zrake od drugog sočiva. Optička snaga se izražava u dioptrijama (D) i može da bude pozitivna (+) ili negativna (–). Za precizna merenja i analizu optičke snage po celoj površini sočiva koriste se topografi optičke snage koji kao rezultat daju vrednosti optičke snage u svakoj tački površine sočiva. Materijal kontaktnog sočiva mora da bude optički homogen tj. njegov indeks prelamanja treba da je konstantan. S obzirom da je optička snaga sočiva direktno proporcionalna indeksu prelamanja materijala, bilo kakva optička nehomogenost može da prouzrokuje razlike u indeksu prelamanja u pojedinim zonama sočiva, što će izazvati neravnomernu refrakciju, odnosno optičku snagu, koja utiče na kvalitet vida [37].

Princip merenja optičke snage je baziran na tehnologiji poznatoj još kao Moare deflektometrija (*Moiré Deflectometry*). Nekoliko rešetki je fiksirano na određenoj distanci. Kada zrak svetlosti prođe kroz ovakav par rešetki, formira se mreža. Kada sočivo nije postavljeno u kivetu za merenje, mreža ima pravilan izgled (slika 4a). Nakon postavljanja sočiva u sistem, mreža se za-

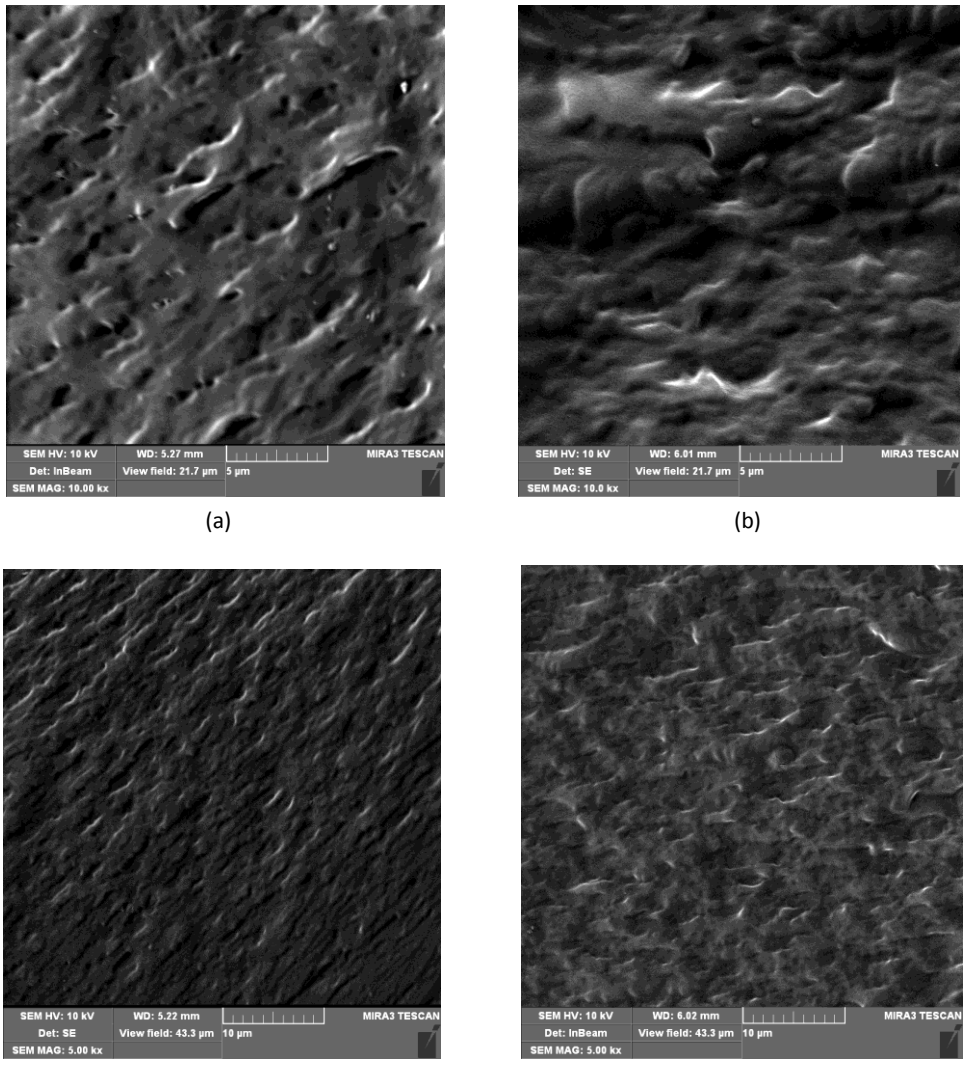

(a) (b)

(c) (d)

Slika 3. SEM mikrografije: a) SL38 (uvećanje 10000×); b) SL38-A (uvećanje 10000x); c) SL38 (uvećanje 5000×); d) SL38 (uvećanje 5000×).
Figure 3. SEM Micrographs: a) SL38 (magnification 10000×); b) SL38-A (magnification 10000×); c) SL38 (magnification 5000×); d) SL38-A (magnification 5000×).

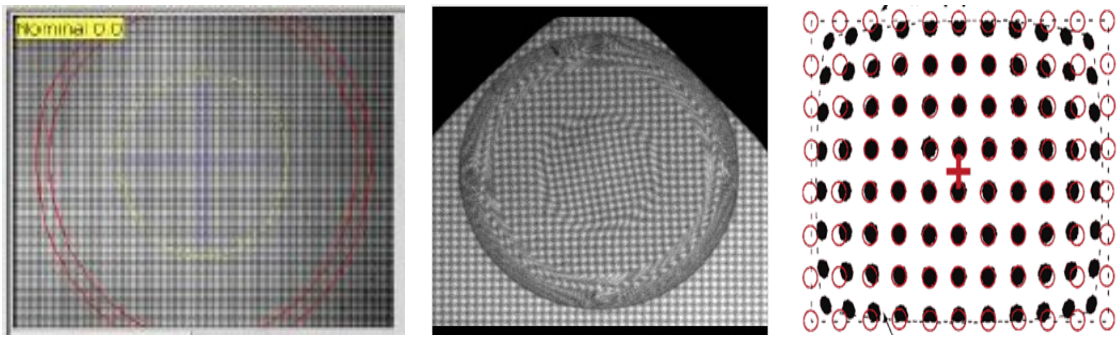

(a) (b) (c)

Slika 4. Izgled mreže: a) kada kontaktno sočivo nije postavljeno u kiveti, b) nakon postavljanja kontaktnog sočiva u kivetu i c) distorzije slike kontaktnog sočiva postavljenog u kivetu.
Figure 4. Grid layout: a) when the contact lens is not set in the cuvette, b) after placing the contact lens in the cuvette and c) image distortion of contact lens placed in the cuvette.

kreće u zavisnosti od lokalne sferne i cilindrične snage sočiva (slika 4b i c). Zakrivljenost svake od rešetki se javlja usled različitih uvećanja sočiva tj. distorzije [22,37].

Na slici 5 prikazana je raspodela snage na baznom sočivu. Na osnovu vertikalnih i horizontalnih resica može se uočiti da nema deformacija između kvadratića tj. da nema većih distorzija slike.

Sa slike 5, se uočavaju promene boje od žute do svetlo plave, što odgovara promeni optičke snage od +2,75 pa do +2,15 D. Dominacija svetlo zelene boje odgovara optičkoj snazi +2,65 D i ukazuje da sočivo ima skoro uniformnu raspodelu optičke snage. Granica tolerancije oka je ±0,25 D u odnosu na nominalnu optičku snagu, što ukazuje da ovakvo sočivo ne bi moglo da izađe iz proizvodnje.

Kvalitet kontaktnog sočiva predstavlja merenje optičke homogenosti u području merenja [37]. Ukoliko je optička homogenost veća, rezultat će biti bliži vrednosti 10. Broj koji odredjuje kvalitet se računa kao broj svih tačaka koje nose vrednosti o optičkoj snazi koje se nalaze u određenom okruženju srednje snage podeljen sa ukupnim brojem piksela u zoni merenja i pomnožen sa 10.

Na osnovu izmerenih parametara dobijeno je da je kvalitet kontaktnog sočiva 9,9/10. Na krajevima sočiva postoji slaba distorzija, koja može biti uzrok prelaska sa optičke zone na perifernu zonu. Žuti prsten na mapi snage daje malo veću optičku snagu, koja može biti prouzrokovana različitim radijusom ili indeksom prelamanja.

Na osnovu dijagrama defekata mogu se uočiti nepravilnosti na sočivu, tj. koji fragmenti sočiva više, a koji manje prelamaju svetlost. Na mapi defekata sočiva SL 38, slika 6, nema značajnijih nepravilnosti.

Raspodela snage na nanofotoničnom sočivu prikazana je na slici 7. Izmerena snaga sočiva je +3,00 D, što je ista vrednost nominalne optičke snage. Za razliku od sočiva SL38, ovakvo sočivo bi moglo da izađe iz proizvodnje. Dobijeni kvalitet sočiva iznosi 10/10.

Sa slike 7 uočava se da su u većoj meri zastupljene zelena i svetlo plava boja, što ukazuje da sočivo ima uniformnu raspodelu snage, i da optička snaga varira od +3,00 pa do +2,60 D.

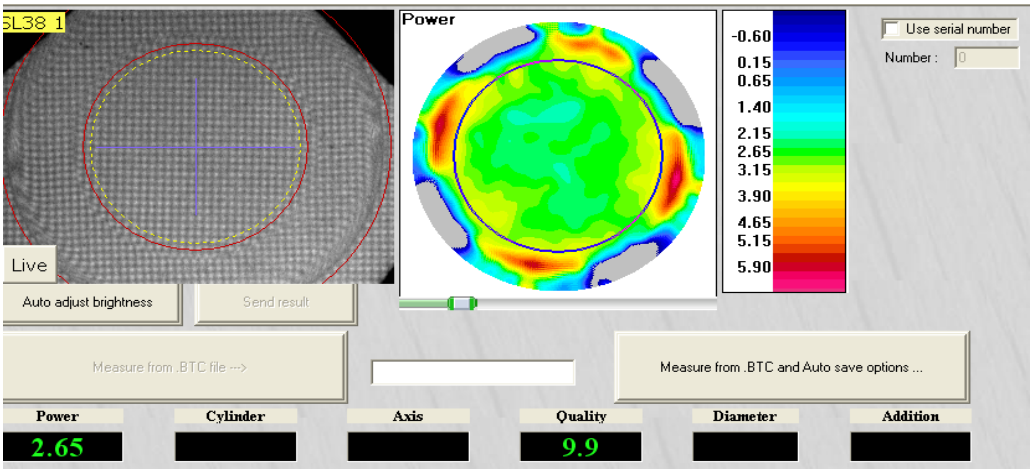

Slika 5. Prikaz raspodele optičke snage mekog kontaktnog sočiva SL38.
Figure 5. Distribution of optical power of the soft contact lens SL38.

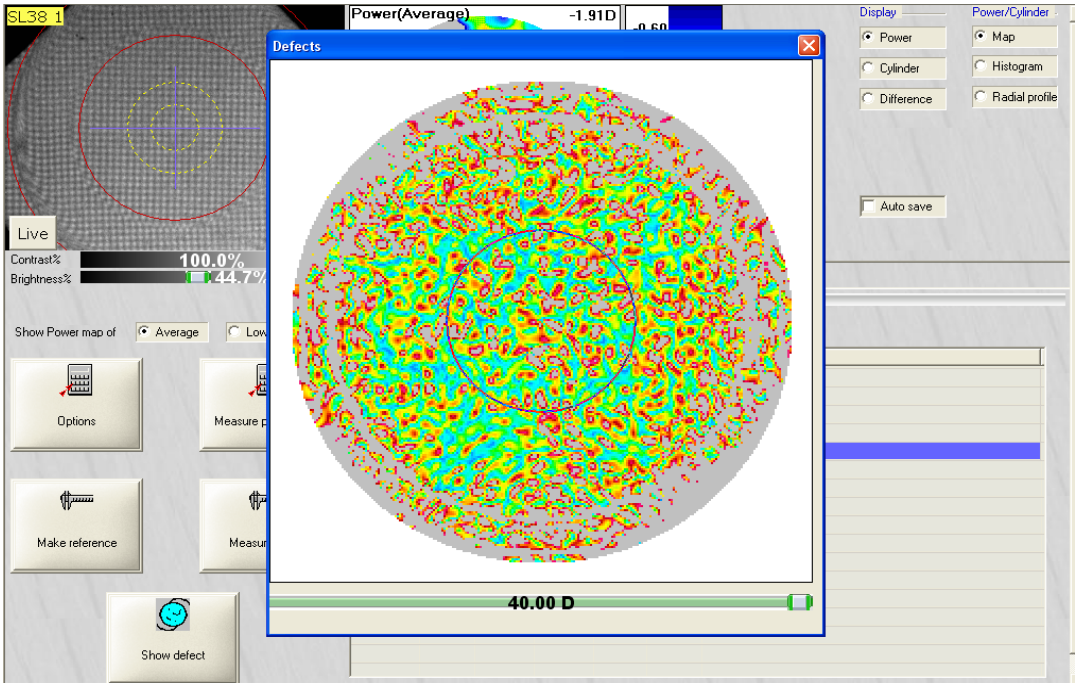

Slika 6. Prikaz mape defekata za meko kontaktno sočivo SL38.
Figure 6. Map of defects for soft contact lens SL38.

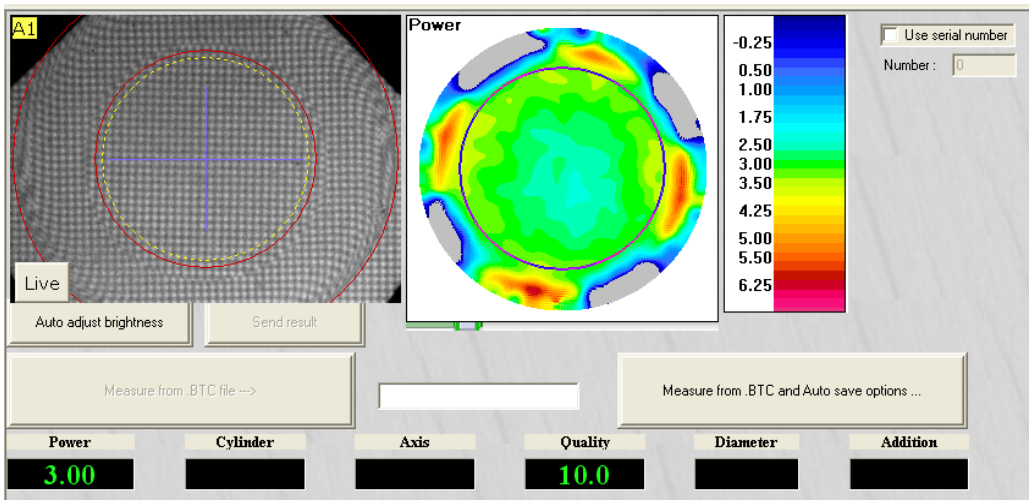

Slika 7. Prikaz raspodele snage mekog kontaktnog sočiva SL38-A.
Figure 7. Distribution of optical power of soft the contact lens SL38-A.

Posmatrajući mapu defekata, slika 8, može se zaključiti da ne postoje veće promene u homogenosti materijala za nanofotonično kontaktno sočivo.

Na osnovu poređenja dobijenih rezultata može se zaključiti da nanofotonično sočivo pokazuje bolja optička svojstva u pogledu optičke snage i kvaliteta u odnosu na bazno sočivo.

ZAKLJUČAK

U ovom radu su ispitana i upoređena svojstva baznog i novog nanofotoničnog materijala. Zaključeno je da ugradnjom fulerena u bazni materijal ne dolazi do značajnije promene stepena bubrenja, odnosno sadržaja vode, zatim da transport tečnosti kroz sintetisane materijale prati Fikov zakon difuzije, kao i da se ovi sintetisani materijali mogu svrstati u grupu neporoznih hidrogelova.

Iz prikazanih rezultata analize optičkih karakteristika baznog i nanofotoničnog sočiva, može da se zaključi da novo nanofotonično sočivo pokazuje optičku snagu koja je bliža nominalnoj u poređenju sa baznim sočivom. Ne postoje značajne promene optičke snage kod nanofotoničnih sočiva jer izmerena snaga ima istu vrednost kao i nominalna optička snaga. Mapa defekata pokazuje da ne postoje veće promene u homogenosti materijala za

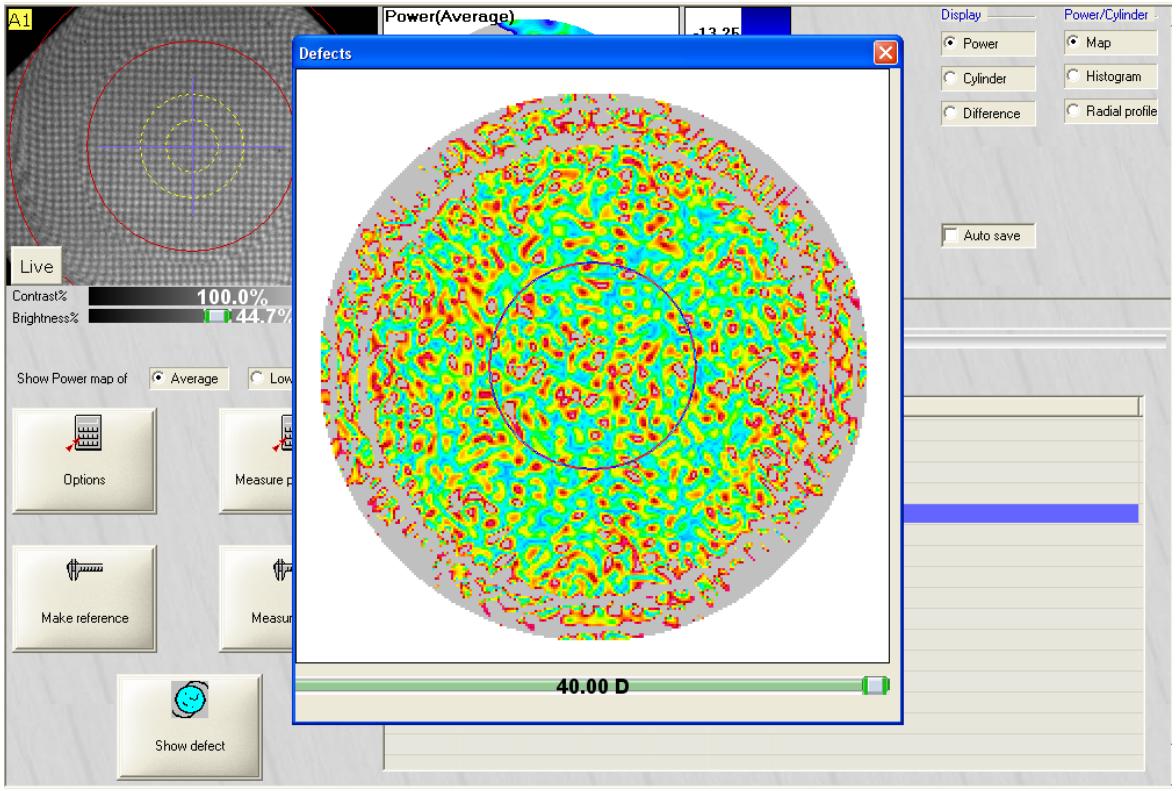

Slika 8. Prikaz mape defekata za meko kontaktno sočivo SL38-A.
Figure 8. Map of defects for soft contact lens SL38-A.

nanofotonično sočivo. Na osnovu dobijenih rezultata, nanofotonični materijal za kontaktno sočivo bi mogao da ima potencijalnu primenu za izradu mekih kontaktnih sočiva.

Zahvalnica

Autori se zahvaljuju Ministarstvu prosvete, nauke i tehnološkog razvoja Republike Srbije za finansijsku podršku ovom radu u okviru projekta br. III 45009, „Funkcionalizacija nanomaterijala za dobijanje nove vrste kontaktinh sočiva i ranu dijagnostiku dijabetesa“. Takođe, autori se zahvaljuju i firmi Optix (Beograd, Srbija) za korišćenje merne instrumentacije pri određivanju optičke snage mekih kontaktnih sočiva.

LITERATURA

[1] N.A. Peppas, P. Bures, W. Leobandung, H. Ichikawa, Hydrogels in pharmaceutical formulations, Eur. J. Pharm. Biopharm. **50** (2000) 27–46.

[2] L. Brannon-Peppas, R.S. Harland, Preparation and characterization of crosslinked hydrophilic networks, u Absorbent Polymer Technology, Elsevier, Amsterdam, 1990, pp. 45–66.

[3] H.A. Ketelson, D.L. Meadows, R.P. Stone, Dynamic wettability properties of a soft contact lens hydrogel, Colloids Surfaces, B **40** (2005) 1–9.

[4] A.P. Kumar, D. Depan, N.S. Tomer, R.P. Singh, Nanoscale particles for polymer degradation and stabilization – Trendsand future perspectives, Prog. Polym. Sci. **34** (2009) 479–515.

[5] N. Efron, Contact lenses Practice, Vision Science (111303), Australia, 2001.

[6] A. Safrany, Radiation processing: Synthesis and modification of biomaterials for medical use, Nucl. Instr. Meth., B **131** (1997) 376–381.

[7] J.M. Rosiak, F. Yoshii, Hydrogels and their medical applications, Nucl. Instr. Meth., B **151** (1999) 56–64.

[8] T. Yu, C.K. Ober, Methods for the Topographical Patterning and Patterned Surface Modification of Hydrogels Based on Hydroxyethyl Methacrylate, Biomacromolecules **4** (2003) 1126–1131.

[9] C. Monis, Hydrogel Contact Lenses, San Jose State University, 2002.

[10] R.M. Ahmed, S.M. El-Bashir, Structure and Physical Properties of Polymer Composite Films Doped with Fullerene Nanoparticles, Int. J. Photoenergy, doi: 10.1155/ /2011/801409 (2011).

[11] A. Opdahl,S.H. Kim,T.S. Koffas, C. Marmo, G.A. Somorjai, Surface mechanical properties of PHEMA contact lenses: Viscoelastic and adhesive property changes on exposure to controlled humidity, J. Biomed. Mater. Res., A **67** (2003) 350–356.

[12] S.H. Kim, A. Opdahl, C. Marmo, G.A. Somorjai, AFM and SFG studies of PHEMA-based hydrogel contact lens surfaces in saline solution: adhesion, friction, and the presence of non-crosslinked polymer chains at the surface, Biomaterials **23** (2002) 1657–1666.

[13] I. Tranoudis, N. Efron, Water properties of soft contact lens materials, Cont. Lens Anterior Eye **27** (2004) 193––208.

[14] J. Kopeček, Hydrogels: From Soft Contact Lenses and Implants to Self-Assembled films, J. Appl. Phys. **743** (1993) 669–672.

[15] F. Giacalone, N. Martýn, Fullerene Polymers: Synthesis and Properties, Chem. Rev. **106** (2006) 5136–5190.

[16] R.M. Ahmed, S.M. El-Bashir, Structure and Physical Properties of Polymer Composite Films Doped with Fullerene Nanoparticles, Int. J. Photoenergy, 2011.

[17] J.E. Riggs, Y.P. Sun, Optical Limiting Properties of (60) Fullerene and Methano(60)fullerene Derivative in Solution versus in Polymer Matrix, J. Phys. Chem., A **103** (1999) 485–495.

[18] N. Peng, F.S.M. Leung, Novel Fullerene Materials with Unique Optical Transmission Characteristics, Chem. Mater. **16** (2004) 4790-4798.

[19] L. Matija, D. Kojić, A. Vasić, B. Bojović, T. Jovanović, Đ. Koruga, Uvod u nanotehnologije, Nauka-Don Vas, Beograd, 2011.

[20] Đ. Koruga, S. Hameroff, R. Loutfy, J. Withers, M. Sundereshan, Fullerene C60: History, Physics, Nanobiology, Nanotechnology, Elsevier (North Holland), Amsterdam, 1993.

[21] D. Stamenković, D. Kojić, L. Matija, Z. Miljković, B. Babić, Physical properties of contact lenses characterized by scanning probe microscopy and optomagnetic fingerprint, Int. J. Mod. Phys., B **24** (2010) 825–834.

[22] D. Stamenković, Istraživanje i razvoj gaspropusnih nanofotoničnih kontaktnih sočiva na bazi poli (metilmetakrilata) i fulerena, doktorska disertacija, Mašinski fakultet, Univerzitet u Beogradu, 2012.

[23] C.L. Bell, N.A. Peppas, Water, solute and protein diffusion in physiologically responsive hydrogels of poly(methacrylic acid-g-ethylene glycol), Biomaterials **17** (1996) 1203–1218.

[24] Nedeljko B. Milosavljević, Nikola Z. Milašinović, Jovanka M. Filipović, Melina T. Kalagasidis Krušić, Sinteza i karakterizacija kopolimernih hidrogelova hitozana, itakonske kiseline i *N*-izopropilakrilamida, Hem. Ind. **65** (2011) 657–666.

[25] J. Valencia, I. Pierola, Equilibrium swelling properties of poly(N-vinylimidazole-co-sodium styrenesulfonate) hydrogels, Eur. Polym. J. **37** (2001) 2345–2352.

[26] S.N. Swami, Radiation Synthesis of Polymeric Hydrogels for Swelling-Controlled Drug Release Studies, Ph.D. Thesis, University of New South Wales, 2005.

[27] S. Matsukawa, H. Yasunaga, C. Zhao, S. Kuroki, H. Kurosu, I. Ando, Prog. Polym. Sci. **24** (1999) 995–1044.

[28] L. Massaro, X.X. Zhu, Physical models of diffusion for polymer solutions, gels and solids, Prog. Polym. Sci. **24** (1999) 731–775.

[29] S.K. Bajpai, Swelling–deswelling behavior of poly(acrylamide-co-maleic acid) hydrogels, J. Appl. Polym. Sci. **80** (2001) 2782–2789.

[30] E. Karadağ, Ö.B. Üzüm, D. Saraydin, Swelling equilibria and dye adsorption studies of chemically crosslinked superabsorbent acrylamide/maleic acid hydrogels, Eur. Polym. J **38** (2002) 2133–2141.

[31] M. Torres-Lugo, N.A. Peppas, Molecular Design and in Vitro Studies of Novel pH-Sensitive Hydrogels for the Oral Delivery of Calcitonin, Macromolecules **32** (1999) 6646–6651.

[32] J. Kopeček, Smart and genetically engineered biomaterials and drug delivery systems, Eur. J. Pharm. Sci. **20** (2003) 1–16.

[33] N. Milosavljević, N. Milašinović, I. Popović, J. Filipović, M. Kalagasidis Krušić, Preparation and characterization of pH-sensitive hydrogels based on chitosan, itaconic acid and methacrylic acid, Poly. Int. **60** (2011) 443–452.

[34] F.A. Dorkoosh, J. Brusse, J.C. Verhoef, B.M. Rafiee-Thrani, H. Junginger, Preparation and NMR characterization of superporous hydrogels (SPH) and SPH composites, Polymer **41** (2000) 8213–8220.

[35] B. Narasiman, N.A.Peppas, Molecular Analysis of Drug Delivery Systems Controlled by Dissolution of the Polymer Carrier, J. Pharm. Sci. **86** (1997) 297–304.

[36] www.gatewaycoalition.org/files/NewEH/htmls/lowman.doc

[37] A. Gasson, J. Morris, The Contact Lens Manual, 2nd ed., Butterworth-Heinemann, Oxford, 1998.

SUMMARY

CHARACTERIZATION OF NANOPHOTONIC SOFT CONTACT LENSES BASED ON POLY(2-HYDROXYETHYL METHACRYLATE) AND FULLERENE

Aleksandra D. Debeljković, Lidija R. Matija, Djuro Lj. Koruga

NanoLab, Biomedical Engineering, Faculty of Mechanical Engineering, University of Belgrade, Kraljice Marije 16, 11000 Belgrade, Serbia

(Scientific paper)

This work presents a comparative study of characteristics of a basic and new nanophotonic material, the latter of which was obtained by incorporation of fullerene, C_{60}, in the base material for soft contact lenses. The basic (SL38) and nanophotonic materials (SL38-A) for soft contact lenses were obtained by radical polymerization of 2-hydroxyethyl methacrylate and 2-hydroxyethyl methacrylate and fullerene, which were derived by the technology in the production lab of the company Soleko (Milan, Italy). The materials were used for production of soft contact lenses in the company Optix (Belgrade, Serbia) for the purposes of this research. Fullerene was used due to its absorption transmission characteristics in ultraviolet, visible and near infrared spectra. For the purposes of material characterization for potential application as soft contact lenses, network parameters were calculated and SEM analysis of the materials was performed, while the optical properties of the soft contact lenses were measured by a Rotlex device. The values of the diffusion exponent, *n*, close to 0.5 indicated Fick's kinetics corresponding to diffusion. The investigated hydrogels could be classified as nonporous hydrogels. Values of optical power and map of defects, determined using a Rotlex device, showed that the optical power of the synthesized nanophotonic soft contact lens was identical to the nominal value, while this was not the case for the basic lens. In addition, the quality of the nanophotonic soft contact lens was better than the basic soft contact lens. Hence, it is possible to synthesize new nanophotonic soft contact lenses of desired optical characteristics, implying possibilities for their application in this field.

Keywords: Nanophotonic soft contact lenses • PHEMA • Fullerenes • Optical power

Study on the morphology and thermomechanical properties of poly(urethane-siloxane) networks based on hyperbranched polyester

Marija V. Pergal[1], Jasna V. Džunuzović[1], Milena Špírková[2], Rafal Poręba[2], Miloš Steinhart[3], Miodrag M. Pergal[4], Sanja Ostojić[5]

[1]*Institute of Chemistry, Technology and Metallurgy (ICTM) – Center of Chemistry, University of Belgrade, Belgrade, Serbia*
[2]*Institute of Macromolecular Chemistry AS CR, v.v.i. (IMC), Nanostructured Polymers and Composites Department, Prague, Czech Republic*
[3]*Institute of Macromolecular Chemistry AS CR, v.v.i. (IMC), Supramolecular Polymer Systems Department, Prague, Czech Republic*
[4]*Faculty of Chemistry, University of Belgrade, Belgrade, Serbia*
[5]*Institute of General and Physical Chemistry, University of Belgrade, Belgrade, Serbia*

Abstract

Two series of polyurethane films based on hyperbranched polyester of the second pseudo-generation (Boltorn®), 4,4'-methylenediphenyl diisocyanate and two different siloxane prepolymers, α,ω-dihydroxy-(ethylene oxide-poly(dimethylsiloxane)-ethylene oxide) (EO--PDMS-EO) and α,ω-dihydroxypropyl-poly(dimethylsiloxane) (HP-PDMS), were prepared by two-step polymerization in solution. The influence of the type and content of soft segment on the morphology, thermomechanical and surface properties of the synthesized polyurethanes was studied by atomic force microscopy (AFM), small-angle X-ray scattering (SAXS), scanning electron microscopy (SEM), dynamic mechanical thermal analysis (DMTA) and water absorption measurements. It was found that these techniques confirmed existence of microphase separated morphology. Synthesized polyurethanes exhibited two glass transition temperatures and one second relaxation process. The results showed that polyurethanes based on HP-PDMS had higher surface roughness, better microphase separation and waterproof performances. Samples synthesized with lower PDMS content had less hydrophobic surface, but higher crosslinking density and better thermomechanical properties.

Keywords: polyurethane networks, poly(dimethylsiloxane), hyperbranched polyester, morphology, thermomechanical properties.

Available online at the Journal website: http://www.ache.org.rs/HI/

Polymers

SCIENTIFIC PAPER

UDC 678.664:678.674:66

Hem. Ind. **67** (6) 871–879 (2013)

doi: 10.2298/HEMIND130225022P

Polyurethane (PU) networks have different applications, especially in the coatings industry, because of their specific properties such as good mechanical flexibility, toughness, chemical resistance, high gloss and high abrasion resistance [1,2]. The properties of PU networks are remarkably affected by the content, type and molecular weight of the soft segments and type of the crosslinking agent. Generally, mixed or special types of macrodiols as soft segments are used to impart specific physical properties of PU networks.

Poly(dimethylsiloxane) (PDMS) has a unique combination of properties, such as low-temperature flexibility, high thermal and thermo-oxidative stabilities, good biocompatibility, low surface energy, ultraviolet resistance and high permeability to many gases [3,4]. However, pure PDMS has weak mechanical properties, which limit its application, except in the case when PDMS is crosslinked and reinforced with adequate fillers. The non-polar nature of the PDMS structure combined with very low intermolecular interactions is responsible for its thermodynamical incompatibity with almost all organic polymers. This is reflected by the very low value of the solubility parameters of PDMSs (δ ranges 14.9–15.3 $(J/cm^3)^{1/2}$), when compared with other polymers (δ ranges 17.5–28.6 $(J/cm^3)^{1/2}$). This is the most important driving force in the formation of microphase separated morphology of PDMS containing polyurethanes. Furthermore, the low glass transition temperature of PDMS also provides ideal conditions for the formation of phase-segregated polymer morphologies [3]. In many cases, a siloxane molecular weight as low as 500–600 g/mol (6–8 siloxane repeat units) and an organic segment having only a single repeat unit is sufficient to obtain microphase separated morphology. The morphology of multiphase polymer system plays an important role in the final properties of the PU

Correspondence: M.V. Pergal, Institute of Chemistry, Technology and Metallurgy – Center of Chemistry, University of Belgrade, Njegoševa 12, 11000 Belgrade, Serbia.
E-mail: marijav@chem.bg.ac.rs
Paper received: 25 February, 2013
Paper accepted: 21 March, 2013

networks based on PDMS. In the last few years, PDMS has been used in PUs synthesis to improve the properties such as thermal stability, adhesive strength, shape memory properties and water resistance of PUs [5–8]. In addition, it has been shown that the adequate incorporation of the PDMS into PUs can impart some good properties, simultaneously avoiding appearance of unwanted macroscopic phase separation during the polymerization, without significant altering the good mechanical properties of PU networks [6–10].

Hyperbranched polyesters (HBPs) have recently attracted considerable attention as crosslinkers for PU networks preparation due to their specific three-dimensional structure, large number of end functional groups and interesting properties such as high solubility in different solvents, low degree of chain entanglements in melt, low viscosity in solution and in melt and good compatibility with other materials [11–14]. In our previous works, it has been shown that a combination of commercially available hydroxyl-functional HBPs (Boltorn®), PDMS macrodiol and aromatic diisocyanate can be used for the synthesis of PUs with good thermal and mechanical properties [15–18]. During the synthesis of PU samples, HBP with its numerous end –OH groups provides fast curing and formation of the highly crosslinked material with good mechanical properties and chemical resistance. On the other hand, the presence of PDMS improves thermal and surface properties and brings elasticity in this highly crosslinked material. The aim of this paper is to examine the effects of the type and content of PDMS on the morphology, surface and thermomechanical properties of the prepared materials using atomic force microscopy (AFM), small-angle X-ray scattering (SAXS), scanning electron microscopy (SEM), water absorption measurement and dynamic mechanical thermal analysis (DMTA).

EXPERIMENTAL PART

Materials

α,*ω*-Dihydroxy-(ethylene oxide-poly(dimethylsiloxane)-ethylene oxide) (EO-PDMS-EO) and *α*,*ω*-dihydroxypropyl-poly(dimethylsiloxane) (HP-PDMS) were supplied by ABCR and dried over molecular sieves (0.4 nm) before use. The number average molecular weights, M_n, of the EO-PDMS-EO and HP-PDMS were calculated from the ^{1}H-NMR spectroscopy results. The M_n of the prepolymer EO-PDMS-EO was 1200 g/mol, and the terminal ethylene oxide sequences consisted of one unit. The M_n of the prepolymer HP-PDMS was 960 g/mol. 4,4'-Methylenediphenyl diisocyanate (MDI), purchased from Aldrich, with an isocyanate content 33.6 wt.%, was used as received [9]. Commercially available Boltorn® hydroxy-functional aliphatic hyperbranched polyester of the second (BH-20) pseudo-generation was kindly supplied by Perstorp Specialty Chemicals AB (Sweden) and dried at 50 °C under vacuum for two days prior to use. BH-20 was synthesized in an acid-catalyzed polyesterification from the 2,2-bis(hydroxymethyl)propionic acid and a tetrafunctional ethoxylated pentaerythrytol, using pseudo one-step procedure [19]. From the number average molecular weight, determined by vapor pressure osmometry (M_n = 1340 g/mol), and hydroxyl number, determined by titration method (501.1 mg KOH/g), functionality of BH-20 was calculated (f = 12) [20]. The catalyst stannous octanoate ($Sn(Oct)_2$, from Aldrich) was used as diluted solution in anhydrous *N*-methyl-2-pyrrolidone (NMP). NMP was supplied by Acros, distilled under vacuum before use. Tetrahydrofuran (THF) was purchased from J. T. Baker, dried over lithium aluminum hydride and distilled before use.

Synthesis of polyurethane films

Two series of polyurethanes (series PUS-EO and PUS-HP) were synthesized by a two-step polymerization in solution, using mixture NMP/THF as solvent and stannous octanoate as catalyst. For the samples of the series PUS-EO, the prepolymer was EO-PDMS-EO, while for the samples of the series PUS-HP it was HP-PDMS. Crosslinking agent for both series was BH-20. Series PUS-EO (PUS-EO15, PUS-EO30 and PUS-EO60), and series PUS-HP (PUS-HP15, PUS-HP30 and PUS-HP70) were consisted of three samples of different soft segment content. The last two numbers in the name of the PUs denote the weight percent of the soft segment (EO-PDMS-EO or PDMS-HP).

All PU networks were synthesized in the similar manner under the optimal polymerization conditions [9]: the molar ratio of NCO/OH groups was 1.05/1, the amount of the catalyst $Sn(Oct)_2$ was 0.15 mol.% calculated on the amount of prepolymer (*i.e.*, ca. 0.02 wt.% in the polyurethane), while a mixture of NMP/THF (7/1, v/v) was employed as the solvent. Reactions were carried out in a four-neck round-bottom flask equipped with a mechanical stirrer, an argon inlet, a reflux condenser and an addition funnel. Calculated amounts of prepolymer and MDI were weighted into the reaction flask at room temperature, dissolved in the mixture of NMP/THF and then heated up to 40 °C under an argon atmosphere. The reaction was started by the introduction of $Sn(Oct)_2$. The reaction mixture was stirred for 30 min (for PUS-EO series) or 20 min (for PUS-HP series) at 40 °C to prepare the NCO-terminated prepolymer, when the theoretical NCO content was attained [9]. The NCO content was controlled by dibutylamine back-titration method [21]. In the second stage of reaction, dilute solution of BH-20 in NMP was added drop-wise to the NCO-terminated prepolymer and reaction was continued at 40 °C for 10 min. Finally, the obtained reaction mixture was cast into a Teflon®

mold. The crosslinking reaction was continued in a force-draft oven during 40 h at 80 °C and 1 h at 110 °C, and finally 10 h at 50 °C in a vacuum oven. The thickness of the obtained yellow films was about 1 mm.

Characterization

Dynamic mechanical thermal analyses (DMTA) of the PU films were performed on an ARES G2 rheometer (TA Instruments) at a frequency of 1 Hz, strain 0.1%, with a heating rate of 3 °C/min and in the temperature range from –135 to 180 °C. The measurements were carried out using rectangular specimens (16.6 mm×7.5 mm×1.0 mm±0.2 mm), under torsion mode, using torsion fixture (rectangle) geometry. Density of the PUs was measured at 20.1 °C, using a pycnometer and distilled water as medium. The average of four measurements was used. The hardness measurements of the PU films were performed on a Shore A apparatus (Hildebrand, Germany). The average of at least five measurements was used.

Atomic force microscopy (AFM) was used for the evaluation of the surface topography and phase images of the fracture areas after previous freeze-fracturing of PU films at the temperature of liquid nitrogen. A commercial atomic force microscope (MultiMode Digital Instruments NanoScopeTM Dimension IIIa), equipped with the SSS-NCL probe, Super Sharp Silicon^{TM}-SPM--Sensor (NanoSensors^{TM} Switzerland; spring constant, ≈ 35 N/m, resonant frequency, ≈ 170 kHz) was used. Measurements were performed under ambient conditions using the tapping mode AFM technique.

Small-angle X-ray scattering (SAXS) experiments were performed using a 3 pinhole camera (Molmet/Rigaku), attached to a multilayer aspherical optics (Osmic Confocal Max-Flux), which monochromatizes and concentrates the beam of a microfocus X-ray tube (Bede) operating at 45 kV and 0.66 mA (30 W). The camera had a multiwire, gas-filled 2D detector with 0.2 m diameter of an active area (Gabriel design).

Scanning electron microscopy (SEM) micrographs of the PUs were obtained on a JEOL JSM-6610 microscope.

Water absorption (*WA*) of the PUs was determined by immersing the films in distilled water for 48 h at room temperature. The water absorption of the films was calculated as follows: $(w - w_0)\times100 / w_0$, where w is the weight of wet and w_0 is the weight of the dry sample.

RESULTS AND DISCUSSION

Two series of PU networks based on ethylene oxide-poly(dimethylsiloxane)-ethylene oxide or hydroxypropyl-poly(dimethylsiloxane) as the soft segments, 4,4'--methylenediphenyl diisocyanate and hyperbranched polyester of the second pseudogeneration as the hard segment, were synthesized by two-step polymerization in solution. Two-step polymerization in solution was applied to improve the compatibility between reactants during the synthesis of PUs, using the mixture NMP/ /THF as a reaction medium. The content and type of soft segment were varied in order to investigate the influence of these variables on the morphology and properties of the synthesized PU networks.

The influences of the type and content of soft segments on the viscoelastic properties of PU networks were investigated by dynamic mechanical thermal analysis of samples. The storage shear modulus, G', and the mechanical loss factor, tan δ, of PU samples as function of temperature are displayed in Figure 1. DMTA results

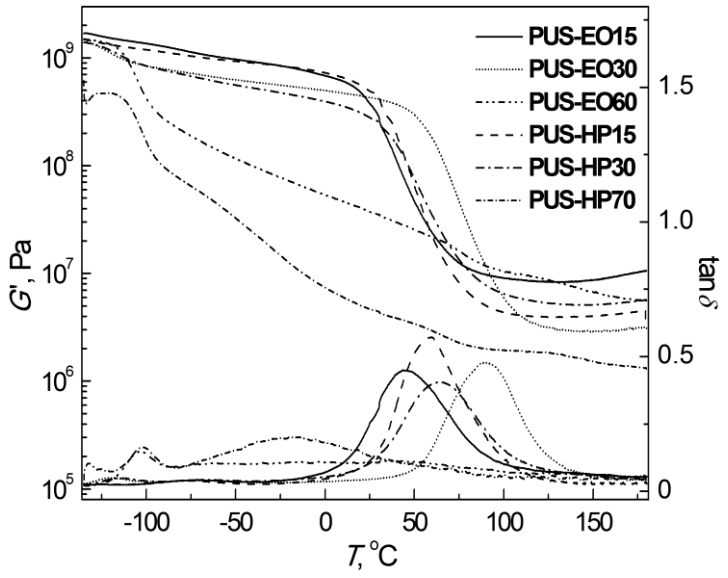

Figure 1. Storage modulus (G') and tan δ of the synthesized PUs versus temperature.

are summarized in Table 1. The dynamic mechanical behavior illustrates the microphase separated morphology of the synthesized PUs. The PU networks have two glass transition temperatures, of the soft and hard segments, and one secondary relaxation process. Tan δ *vs*. temperature dependences of samples show glass transition in the temperature region from –126 to –102 °C for samples of both series, associated with the soft PDMS segment (T_{gSS}). This peak does not change its position by changing the type of PDMS macrodiols, while T_{gSS} decreases with decreasing PDMS content, indicating better microphase separation with decreasing PDMS content. The obtained results showed a relatively small increase of T_{gSS} for samples with higher PDMS content in comparison to the PDMS prepolymer (–123 °C) [3], indicating a certain degree of segmental mixing in PUs. In addition to this, the sample PUS-EO60 has aditional relaxation peak at –9 °C assigned to the movement of etoxypropyl end PDMS groups [22]. For other investigated PUs this transition was not visible, indicating that movement of PDMS end groups is restricted by the presence of crosslinks and hard MDI-HBP segments. DMTA results show that dynamic mechanical properties of PUS-EO60 and PUS-HP70 are different in comparison with other investigated PUs (Figure 1). As shown in Figure 1, the storage modulus of PUS-EO60 and PUS-HP70 gradually decreases, due to the very low degree of chemical crosslinking of these two PU samples. The DMTA curves show a small maximum in tan δ (T_2) in the temperature region from –74 to –59 °C (PUS-EO series) and from –79 to –17 °C (PUS-HP series), which corresponds to the subglass relaxation process. This is probably a consequence of the movement of the part of chain which contains urethane groups connected to the Boltorn® HBP [13]. Due to the steric hindrance, these urethane groups are not involved in the formation of hydrogen bonds and are therefore more mobile. The temperatures associated with the second relaxation process increase with increasing PDMS content in both series and values of T_2 are higher for samples of PUS-HP series. The glass transition temperature of the hard (MDI-HBP) segment (T_{gHS}) was detected from tan δ curves in the temperature region from 40 to 90 °C (PUS-EO series) and from 58 to 60 °C (PUS-HP series). Generally, the values of T_{gHS} are higher for samples in PUS-HP series. From the obtained DMTA results, it can be concluded that, the change in the T_{gHS} values of the synthesized PUs indicates changes in the degree of phase separation. It can be concluded that PU samples of PUS-HP series have higher degree of microphase separation than samples of PUS-EO series, as a result of higher incompatibility between the hydroxypropyl terminated PDMS and the urethane components (MDI and BH-20). During the synthesis of PU samples based on EO-PDMS-EO, EO blocks act as compatibilizers between non-polar PDMS prepolymer and urethane reactants. Therefore, the presence of terminal EO blocks in PDMS prepolymer improves miscibility between reactants and PU samples based on EO-PDMS-EO have lower T_{gHS} values and consequently lower degree of microphase separation. In the tan δ temperature dependence of PUS-EO60 and PUS-HP70, the presence of broader peaks also implies that miscibility of the network components is better than in other synthesized samples. Samples PUS-EO30 and PUS-HP30 have the highest values of T_{gHS} in both series, due to the highest crosslinking density (Table 1). The reason for higher crosslinking density of samples with 30 wt.% of soft segment in both series in comparison with samples containing 15 wt.% of soft segment may be steric hindrance caused by HBP molecules, which is more pronounced in samples with 15 wt.% of soft segment because of higher amount of BH-20. Therefore, instead of participating in the reaction of crosslinking, –OH groups of the HBPs may be hydrogen bonded. It can be concluded that the glass transition temperature of the PU networks is influenced by the crosslinking density, the content and type of soft segments and by mutual miscibility between components.

DMTA analysis is a quick and direct method for the determination of crosslinking density of the synthesized PUs. The crosslinking density of the synthesized PU networks can be calculated from the rubber elasticity theory using equation (1), by assuming the absence of entanglements and that the synthesized PUs exhibit affine behavior where chains and crosslinks

Table 1. Temperatures corresponding to the tan δ maximum, cross-linking density, v, molecular weight of polymer chain between cross-links, Mc, values of the ratio Ts/TgH(tan δ), hardness and water absorption, WA, of the synthesized PUs

Sample	tan δ			$v\times10^4$	M_c	T_s/T_{gHS}	Hardness Shore A	*WA* / %
	T_{gSS} / °C	T_2 / °C	T_{gHS} / °C	mol/cm^3	g/mol	(tan δ)		
PUS-EO15	–126	–74	46	26.23	415	0.414	91	5.7
PUS-EO30	–120	–69	90	8.19	1280	0.572	88	3.0
PUS-EO60	–102	–59	40	–	–	–	85	1.3
PUS-HP15	–126	–79	60	11.85	937	0.463	93	7.2
PUS-HP30	–114	–63	65	15.33	732	0.486	91	2.3
PUS-HP70	–102	–17	58	4.92	2368	0.883	88	1.6

move proportionally to the macroscopic deformation, due to the high functionality and presence of the steric hindrance [23,24].

$$\nu = \frac{G'}{RT} \quad (1)$$

where G' represents the rubbery plateau modulus at $T = (T_{gH})_{G''} + 90$ °C and $(T_{gH})_{G''}$ is the glass transition temperature of the hard segments determined from the loss modulus (G'') maximum. Value of the molecular weight of polymer chain between crosslinks, M_c, was evaluated as:

$$M_c = \frac{\rho_{PU}}{\nu} \quad (2)$$

where ρ_{PU} is the density of PU samples, which is between 1.050 and 1.096 g/cm^3 for PUS-EO samples, and between 1.110 and 1.165 g/cm^3 for PUS-HP samples.

The estimated values for ν, given in Table 1, generally decrease with an increase of the soft segment content, except for PUS-EO30 and PUS-HP30 samples, which have the highest crosslinking density. The values of the M_c, listed in Table 1, are inversely proportional to the crosslinking density. The increase of the crosslinking density increased hardness from 85 to 91 Shore A (PUS-EO series), and from 88 to 93 Shore A (PUS-HP series). Hardness of PU samples of PUS-HP series is higher than for PU samples of PUS-EO series.

Value of the ratio between softening point, determined as the onset of the log G' drop in the glass transition region of the MDI-HBP segments (Figure 1), and T_{gH}(tan δ), represents a measure of the width of tan δ peak which corresponds to the glass transition of the hard segments [14]. From Table 1 it can be observed that, as the soft segment content decreases, value of T_s/T_{gH} (tan δ) also decreases and a broadening of tan δ peak occurs, indicating that different lengths of the chains between crosslinks are formed.

From DMTA results, values of G' for PU networks are higher than values of the loss modulus (not presented) in the whole investigated temperature region. This observation indicates that cohesion and stability of the PU networks is not destroyed and that PU samples show elastic properties under investigated experimental conditions. At lower temperatures, the value of G' increases with increasing hard segment content, while in the temperature region from 20 to 100 °C there is reduction in G' values due to the increased mobility of chains caused by the glass transition of hard segments. After that, the value of G' again increases in the rubbery plateau region at around 150 °C with increasing hard segment content, indicating a simultaneous increase of crosslinking density. It can be observed (Figure 1) that the rubbery plateau modulus of the investigated PU networks is higher than the values obtained for other crosslinked polyurethane based on hydroxybutyl-PDMS [25] and for PUs based on poly(propylene oxide) and Boltron® HBP [14]. Therefore, the incorporation of the EO-PDMS-EO or HP-PDMS into PU networks based on BH-20 as crosslinker improved the thermomechanical properties of the polymer.

PU samples containing different amount of soft segments and synthesized with different PDMS type were analyzed by AFM. In order to obtain the "bulk" information, surface areas of freeze-frozen samples were studied. The results are given in Figures 2 (3D height images) and 3 (2D phase images). Based on prior studies, it is known that the bright regions represent the hard phase (hard ordered domains in a polyurethane), while the darker regions represent the soft phase. Height images, showing surface topography, substantially differ for PUs containing different soft segment content: PUS-EO30 and PUS-HP15 sample have smooth "chain-like" relief (PUS-HP15 is the smoothest one), while the topographies of PUS-EO60 and PUS-HP30 samples show agglomerates of μm size (PUS-EO60 is the roughest one). Roughness, R_q, values for all samples are given in Table 2. The samples with higher R_q values have rougher surface. Therefore, the sample PUS-HP30 has rougher surface than PUS-EO30.

Phase images (*i.e.*, maps of tip-sample interactions) enable qualitative insight into the sample homogeneity relief. 2D AFM pictures of phase images are given in Figure 3. It is evident that the PU samples are distinguished by heterogeneous character, apparently connected with strong microphase separation. Sample PUS-HP15 is the most homogeneous, and samples PUS--EO30, PUS-EO60 and PUS-HP30 are heterogeneous either on nm (PUS-EO30) or even on μm level (PUS--EO60 and PUS-HP30).

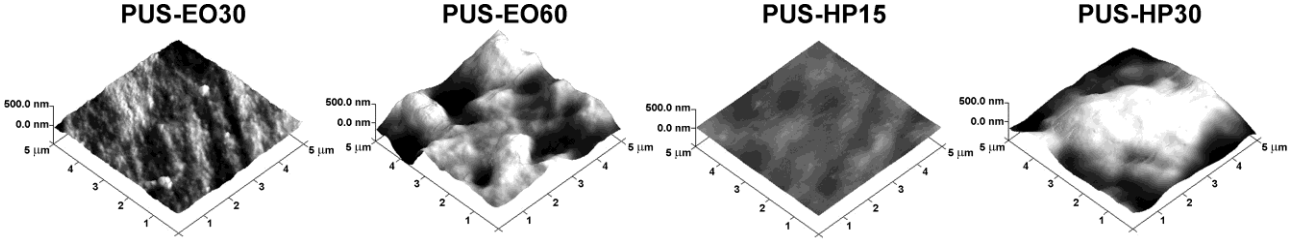

Figure 2. 3D AFM images of frozen PU samples (scans 5×5 μm^2, z-scale 500 nm in all cases).

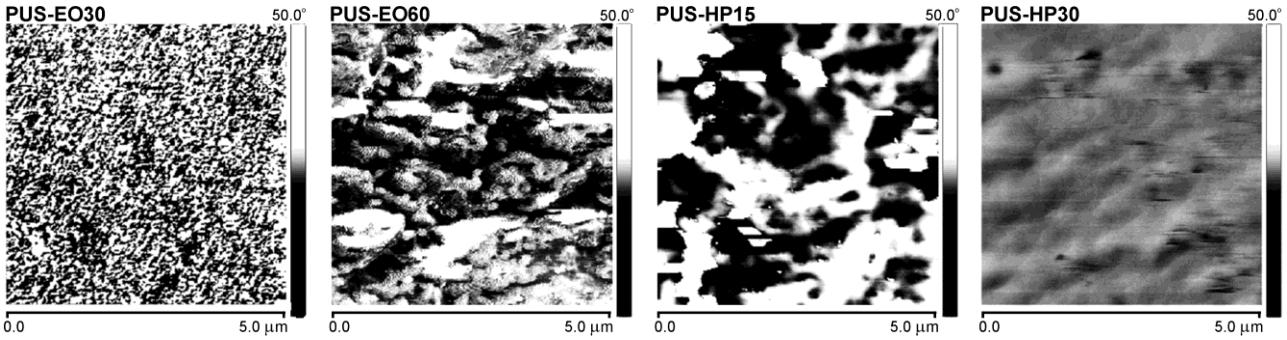

Figure 3. 2D AFM phase images of frozen PU samples (scans 5×5 µm^2, z-scale 50 ° in all cases).

Table 2. Roughness values and SAXS interdomain spacing, D, of PU samples; Surface area: the total area of examined sample surface (the three-dimensioned area ofa given region expressed as the sum of the area of all the triangles formed by three adjacent data points)

Sample	Surface area, µm^2	R_q[a] / nm	R_a[b] / nm	R_{max}[c] / nm	D[d] / nm
PUS-EO30	26.2	25	20	213	10.5
PUS-EO60	29.0	141	108	829	8.1
PUS-HP15	25.1	6	5	44	12.1
PUS-HP30	26.8	161	133	741	11.0

[a](RMS) The standard deviation of the *Z* values within the given area.; [b](mean roughness): the mean value of the surface relative to the center place; [c](max height): the difference in height between the highest and lowest points on the surface relative to the mean plane; mean: the average of all *Z* values within the enclosed area; [d]interdomain spacing of PUS-HP70 is 5.9 nm

The microphase separated morphology of the synthesized PU networks was confirmed by SAXS analysis. SAXS profiles of PU samples are shown in Figure 4. The results (except for the sample PUS-HP70) showed the presence of well-defined scattering peaks, indicating the presence of a microphase separated morphology under ambient conditions. According to the SAXS data, sample PUS-HP70 exhibits a broad scattering peak, suggesting the greater phase-mixing in comparison with other synthesized PUs. The average interdomain spacings in the PU samples were calculated from the position of the interference peaks in the respective scattering intensity profiles of the samples according to Bragg's law, $D = 2\pi/q$, where q is the scattering vector. The values of interdomain spacing are listed in Table 2. As expected, the interdomain spacing was found to decrease with an increase of the soft segment content. As the hard segment content increases, while keeping the soft segment length constant, the center-to-center distance between the hard domains increases as shown by the SAXS results. The value of interdomain spacing of hard segments is 10.5 nm for PUS-EO30 and 11.0 nm for PUS-HP30. The obtained results showed that interdomain spacing of hard segments depend on the soft segment content but not on the soft segment structure (Table 2). The interdomain spacing of hard segments is of the same order as those often found for polyurethanes presented in literature [26]. According to the Figure 4, the larger increase of the scattering intensity for PUS-HP30 can be related to the presence of better microphase separated structures in comparison with the sample PUS-EO30. Analysis of the SAXS profiles at higher values of scattering vector ($q > q_{max}$) shows that the scattering intensity, $I(q)$, changes as follows: $I(q) \sim q^{-n}$. For the PUS-EO30, PUS-HP15 and PUS-HP30, scattering intensity follows Porod's law, *i.e*., $I(q) \sim q^{-4}$, which is typical of well-microphase separated structures with clear boundaries between phases [27,28]. On the other hand, for samples PUS-EO60 and PUS-HP70 values of the exponent n are 1.7 and 1.1, respectively, indicating that scattering intensity for these samples decreases slower than q^{-4} at high q [28]. PUs which have n lower than 4 have also lower degree of microphase separation according to the Velankar *et al*. [28].

The surface morphology of prepared films was investigated by SEM and the SEM microphotographs of the "air" surface of PU samples are shown in Figure 5. The obtained results reveal existence of microphase separated morphology of PU materials. As shown in Figure 5, on the surface of sample PUS-EO30, in contrast to the PUS-HP30, the PDMS soft segments form spherical phase of about 4.5 µm in diameter. According to the literature, it is possible that small amounts of polyurethane components are trapped inside the PDMS spheres [8]. The SEM microphotographs of other synthesized PUs in both series showed that the hard segments were unequally distributed in the PDMS soft segment. Microdomains of hard segments, hydrogen-bonded in aggregates, irregular in shape and surrounded by EO-PDMS-EO matrix, are visible on the surface of PUS-EO60 (Figure 5). SEM results of the samples PUS-EO15 and PUS-HP15 indicate increased homoge-

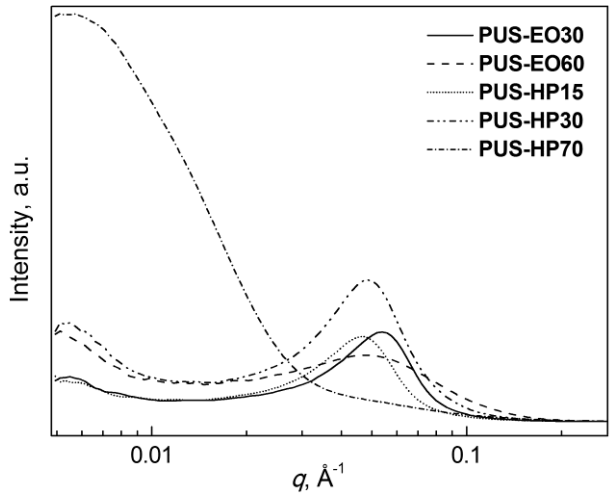

Figure 4. SAXS profiles of the synthesized PU materials.

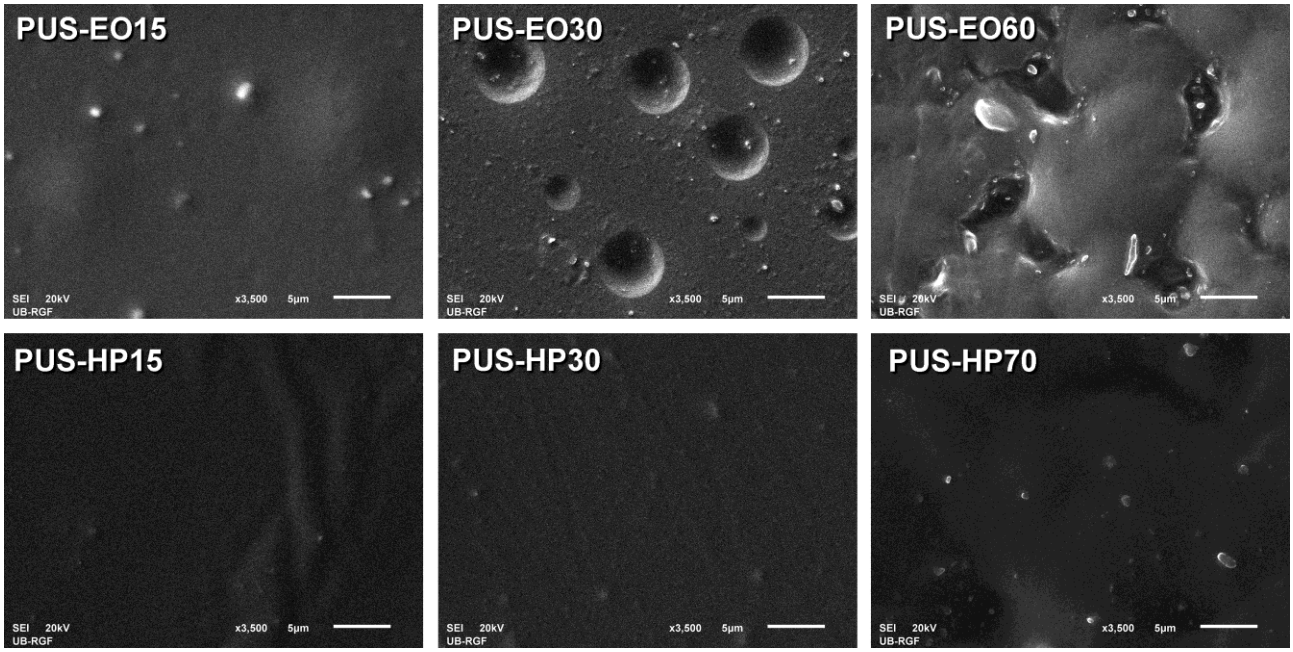

Figure 5. SEM Microphotographs of "air" surface of PU samples.

neity in samples and improved compatibility of all components. Therefore, the surface morphology of PU samples is strongly affected by the type and content of soft segments.

Water absorption was measured to determine the bulk hydrophobicity of the synthesized PUs and the obtained results are presented in Table 1. The water absorption after 48 h increases with decreasing soft segment content in both series. This may be attributed to the hydrophobic character of PDMS and its surface activity. Namely, PDMS in PU networks can migrate to the surface of samples due to its lower surface energy in comparison to the surface energy of polyurethane [3,29]. The PUs with higher soft segment content have a more hydrophobic surface and better water resistance. The weight percent of the absorbed water is lower for PUS-HP samples in comparison with samples in PUS-EO series. Therefore, samples based on PDMS-HP prepolymer are more hydrophobic. The water absorption in the synthesized PUs was lower than the values obtained for other PDMS based polyurethanes with comparable soft segment content [30].

CONCLUSION

Two series of polyurethane films were synthesized by two-step polymerization in NMP/THF mixture in order to investigate the effect of the type and content of PDMS soft segment on the morphology and properties of PUs. The investigated series differ in the type of functionality of terminated PDMS, which was incor-

porated into the PU networks based on HBP as the flexible segments. In the first series, ethoxypropyl terminated PDMS was employed, while in the second hydroxypropyl terminated PDMS was used. Dynamic mechanical thermal analysis revealed existence of two glass transitions, of the soft and hard segments, and also the presence of subglass relaxation process. AFM, SAXS and SEM experiments supported DMTA results and confirmed the presence of microphase separated morphology of the synthesized PUs. The results showed that the microphase separation was more pronounced in the PU networks based on HP-PDMS, as a result of the higher incompatibility between the hydroxypropyl--PDMS prepolymer and the polar reactants, MDI and HBP. Compared with EO-PDMS-EO containing polyurethanes, samples synthesized based on HP-PDMS have higher surface roughness coefficient, increased hardness, more hydrophobic surface and better waterproof performance. The results showed increase of crosslinking density, improvement of thermomechanical properties and less hydrophobicity with decreasing the soft segment content. The obtained results indicate that the synthesis of poly(urethane-siloxane) based on HBP leads to creation of materials with good thermomechanical and surface properties, which can be easily tailored by changing the type of PDMS prepolymer or the content of soft segments.

Acknowledgements

This work was financially supported by the Ministry of Education, Science and Technological Development of the Republic of Serbia (Project No. 172062) and Czech Science Foundation (GACR, Project No. P108/10/0195).

REFERENCES

[1] J. Dodge, in: M.E. Rogers, T.E. Long (Eds.), Synthesis Methods in Step-Growth Polymers, Wiley, Hoboken, NJ, 2003, pp. 197–214.

[2] D.K. Chattopadhyay, K.V.S.N. Raju, Structural engineering of polyurethane coatings for high performance applications, Prog. Polym. Sci. **32** (2007) 352–418.

[3] I. Yilgör, J. McGrath, Polysiloxane Containing Copolymers: A Survey of Recent Developments, Adv. Polym. Sci. **86** (1988) 1–86.

[4] P.R. Dvornić, R.W. Lenz, High Temperature Siloxane Elastomers, Hüthing Wepf, Heidelberg, New York, 1990.

[5] M.V. Pergal, V.V. Antić, S. Ostojić, M. Marinović-Cincović, J. Djonlagić, Influence of the content of hard segments on the properties of novel urethane-siloxane copolymers based on a poly(*ε*-caprolactone)-*b*-poly(dimethylsiloxane)-*b*-poly(*ε*-caprolactone) triblock copolymer, J. Serb. Chem. Soc. **76** (2011) 1703–1723.

[6] M.V. Pergal, V.V. Antić, G. Tovilović, J. Nestorov, D. Vasiljević-Radović, J. Djonlagić, In vitro biocompatibility evaluation of novel urethane–siloxane copolymers based on poly(*ε*-caprolactone)-*block*-poly(dimethylsiloxane)-*block*-poly(*ε*-caprolactone), J. Biomater. Sci. Polym., E **23** (2012) 1629–1657.

[7] J.P. Sheth, A. Aneja, G.L. Wilkes, E. Yilgor, G.E. Atilla, I. Yilgor, F.L. Beyer, Influence of system variables on the morphological and dynamic mechanical behavior of polydimethylsiloxane based segmented polyurethane and polyurea copolymers: a comparative perspective. Polymer **45** (2004) 6919–6932.

[8] P. Majumdar, D.C. Webster, Preparation of siloxane-urethane coatings having spontaneously formed stable biphasic microtopograpical surfaces, Macromolecules **38** (2005) 5857–5859.

[9] M.V. Pergal, V.V. Antic, M.N. Govedarica, D. Gođevac, S. Ostojić, J. Djonlagic, Synthesis and characterization of novel urethane-siloxane copolymers with a high content of PCL-PDMS-PCL segments, J. Appl. Polym. Sci. **122** (2011) 2715–2730.

[10] A. Stanciu, V. Bulacovschi, V. Condratov, C. Fadei, A. Stoleriu, S. Balint, Thermal stability and the tensile properties of some segmented poly(ester-siloxane)urethanes, Polym. Degrad. Stab. **64** (1999) 259–265.

[11] E. Žagar, M. Žigon, Aliphatic Hyperbranched polyesters based on 2,2-bis(methylol)propionic acid – Determination of structure, solution and bulk properties, Prog. Polym. Sci. (Oxford) **36** (2011) 53–88.

[12] P.K. Maji, A.K. Bhowmick, Influence of number of functional groups of hyperbranched polyol on cure kinetics and physical properties of polyurethanes, J. Polym. Sci. Part A Polym. Chem. **47** (2009) 731–745.

[13] P. Czech, L. Okrasa, J. Ulanski, G. Boiteux, F. Mechin, P. Cassagnau, Studies of the molecular dynamics in polyurethane networks with hyperbranched crosslinkers of different coordination numbers, J. Appl. Polym. Sci. **105** (2007) 89–98.

[14] A. Asif, W. Shi, X. Shen, K. Nie, Physical and thermal properties of UV curable waterborne polyurethane dispersions incorporating hyperbranched aliphatic polyester of varying generation number, Polymer **46** (2005) 11066–11078.

[15] M.V. Pergal, J.V. Džunuzović, M. Kićanović, V. Vodnik, M.M. Pergal, S. Jovanović, Thermal properties of poly(urethane-ester-siloxane)s based on hyperbranched polyester, Russ. J. Phys. Chem., A **85** (2011) 2251–2256.

[16] M.V. Pergal, J.V. Džunuzović, S. Ostojić, M.M. Pergal, A. Radulović, S. Jovanović, Poly(urethane-siloxane)s based on hyperbranched polyester as crosslinking agent: synthesis and characterization, J. Serb. Chem. Soc. **77** (2012) 919–935.

[17] J.V. Džunuzović, M.V. Pergal, R. Poręba, S. Ostojić, N. Lazić, M. Špírková, S. Jovanović, Studies of the thermal and mechanical properties of poly(urethane–siloxane)s cross-linked by hyperbranched polyesters, Ind. Eng. Chem. Res. **51** (2012) 10824–10832.

[18] J.V. Džunuzović, M.V. Pergal, R. Poręba, V.V. Vodnik, B.R. Simonović, M. Špírková, S. Jovanović, Analysis of dynamic mechanical, thermal and surface properties of poly(urethane-ester-siloxane) networks based on hyper-

branched polyester, J. Non-Cryst. Solids **358** (2012) 3161.

[19] E. Malmström, M. Johansson, A. Hult, Hyperbranched aliphatic polyesters, Macromolecules **28** (1995) 1698–1703.

[20] J. Vuković, Synthesis and characterization of aliphatic hyperbranched polyesters, PhD thesis, Univerzitet u Osnabrück-u, Nemačka, 2006., http://www.dart-europe.eu/full.php?id=36706

[21] Å. Marand, J. Dahlin, D. Karlsson, G. Skarping, M. Dalene, Determination of technical grade isocyanates used in the production of polyurethane plastics, J. Environ. Monit. **6** (2004) 606–614.

[22] R. Hernandez, J. Weksler, A. Padsalgikar, J. Runt, Microstructural organization of three-phase polydimethylsiloxane-based segmented polyurethanes, Macromolecules **40** (2007) 5441–5449.

[23] B.S. Chiou, P.E. Schoen, Effects of crosslinking on thermal and mechanical properties of polyurethanes, J. Appl. Polym. Sci. **83** (2002) 212–223.

[24] L. Vallete, C.-P. Hsu, Polyurethane and unsaturated polyester hybrid networks: 2. Influence of harddomains on mechanical properties, Polymer **40** (1999) 2059–2070.

[25] M. Alexandru, M. Cazacu, M. Cristea, A. Nistor, C. Grigoras, B.C. Simionescu, Poly(siloxane-urethane) crosslinked structures obtained by sol-gel technique, J. Polym. Sci., B **49** (2011) 1708–1718.

[26] J.T. Koberstein, R.S. Stein, Small-angle X-ray scattering studies of microdomain structure in segmented polyurethane elastomers, J. Polym. Sci., B **21** (1983) 1439–1472.

[27] I. Krakovský, Z. Bubeníková, H. Urakawa, K. Kajiwara, Inhomogeneous structure of polyurethane networks based on poly(butadiene)diol: 1. The effect of the poly(butadiene)diol content, Polymer **38** (1997) 3637–3643.

[28] S. Velankar, S.L. Cooper, Microphase separation and rheological properties of polyurethane melts. 2. Effect of block incompatibility on the microstructure, Macromolecules **33** (2000) 382–394.

[29] H.D. Hwang, H.J. Kim, Enhanced thermal and surface properties of waterborne UV-curable polycarbonate-based polyurethane (meth)acrylate dispersion by incurporation of polydimethylsiloxane, React. Funct. Polym. **71** (2011) 655–665.

[30] Y.H. Lee, E.J. Kim, H.D. Kim, Synthesis and properties of waterborne poly(urethane urea)s containing polydimethylsiloxane, J. Appl. Polym. Sci. **120** (2011) 212–219.

IZVOD

PROUČAVANJE MORFOLOGIJE I TERMOMEHANIČKIH SVOJSTAVA UMREŽENIH POLI(URETAN-SILOKSANA) NA BAZI HIPERRAZGRANATOG POLIESTRA

Marija V. Pergal[1], Jasna V. Džunuzović[1], Milena Špírková[2], Rafał Poręba[2], Miloš Steinhart[3], Miodrag M. Pergal[4], Sanja Ostojić[5]

[1]*Institut za hemiju, tehnologiju i metalurgiju (IHTM)-Centar za hemiju, Univerzitet u Beogradu, Beograd, Srbija*
[2]*Institute of Macromolecular Chemistry AS CR, v.v.i. (IMC), Nanostructured Polymers and Composites Department, Prague, Czech Republic*
[3]*Institute of Macromolecular Chemistry AS CR, v.v.i. (IMC), Supramolecular Polymer Systems Department, Prague, Czech Republic*
[4]*Hemijski fakultet, Univerzitet u Beogradu, Beograd, Srbija*
[5]*Institut za opštu i fizičku hemiju, Univerzitet u Beogradu, Beograd, Srbija*

(Naučni rad)

U ovom radu pripremane su dve serije poliuretanskih filmova na bazi hiperrazgranatog poliestra druge pseudo generacije (Boltron®), 4,4′-metilendifenildiizocijanata i dva različita siloksanska pretpolimera kao što su α,ω-dihidroksi-(etilenoksid-poli(dimetilsiloksan)-etilenoksid) (EO-PDMS-EO) i α,ω-dihidroksipropil-poli(dimetilsiloksan) (HP-PDMS), dvostepenom polimerizacijom u rastvoru. Uticaj vrste i sadržaja mekog segmenta na morfologiju, termomehanička i površinska svojstva sintetisanih poliuretana je proučavan pomoću mikroskopije atomske sila (AFM), rasipanja X-zraka pod malim uglovima (SAXS), skenirajuće elektronske mikroskopije (SEM), dinamičko mehaničke termičke analize (DMTA) i merenja količine apsorbovane vode. Nađeno je da primenjene tehnike potvrđuju postojanje morfologije mikrofaznog razdvajanja. Sintetisani poliuretani pokazivali su dve temperature ostakljivanja i jedan sekundarni relaksacioni proces. Rezultati su pokazali da poliuretani na bazi HP-PDMS su imali veći koeficijent hrapavosti, bolje mikrofazno razdvajanje i bolju otpornost prema vodi. Uzorci sintetisani sa nižim sadržajem PDMS-a su imali manju hidrofobnost, ali veću gustinu umrežavanja i bolja termomehanička svojstva.

Ključne reči: Umreženi poliuretani • Poli(dimetilsiloksan)• Hiperrazgranati poliestar • Morfologija • Termomehanička svojstva

Adsorption of azo dyes on polymer materials

Vesna V. Panić[1], Sanja I. Šešlija[1], Aleksandra R. Nešić[2], Sava J. Veličković[3]

[1]*Innovation Center of the Faculty of Technology and Metallurgy, University of Belgrade, 11000 Belgrade, Serbia*
[2]*Vinca Institute of Nuclear Science, University of Belgrade, 11000, Belgrade, Serbia*
[3]*Faculty of Technology and Metallurgy, University of Belgrade, 11000, Belgrade, Serbia*

Abstract

The use of polymeric adsorbents for the removal of azo dyes from solution has been reviewed. Adsorption techniques are widely used to remove certain classes of pollutants from waters, especially those which are not easily biodegradable. The removal of azo dyes as pollutants from wastewaters of textile, paper, printing, leather, pharmaceutical and other industries has been addressed by the researchers. The wider use of already available adsorbents is restricted due to their high costs which lead to investigation and development of new materials that can be cheaper, eficient and easy regenerated. The aim of this article is to present to the readers the widespread investigations in recent years of synthetic and natural polymers as adsorbents and potential replacement of conventional adsorbents. This review presents only the data obtained using raw, hydrogel, grafted and crosslinked forms of synthetic and nature based polymers, and the discussion is limited to these polymer-based materials and their adsorption properties.

Keywords: adsorption, azo dyes, synthetic polymers, hydrogels, natural polymers.

Available online at the Journal website: http://www.ache.org.rs/HI/

Polymers

REVIEW PAPER

UDC 66.081.3:667.281:678.7/.8

Hem. Ind. **67** (6) 881–900 (2013)

doi: 10.2298/HEMIND121203020P

The intensive development of industrial production throughout the world has been followed by ever increasing formation of wastewaters, demanding improvement of the existing, and introduction of new processes for their treatment. The presence of dyes in wastewaters from industrial effluents and water supplies and their removal has received much attention in recent years due to the fact that many of them exhibit toxicity. Pollution by dyes is a serious threat to the aquatic ecosystem, which affects the quality of life and human health as well. Among the unwanted properties of dyes, resistance to natural degradation, allergenicity, carcinogenity, and mutagenicity are all significant. They can also cause severe damage to human beings, such as dysfunction of kidneys, reproductive system, liver, brain and central nervous system [1–4]. Even in very small quantities, dyes can be very toxic and lead to changes in salinity and visible coloration of the water, reducing sunlight penetration and thus hindering the process of photosynthesis [5–7]. Very strict laws regarding elimination of dyes from wastewaters before their discharge into water streams, together with the variety and minuscule concentrations of dye molecules make their satisfactory level of removing very difficult, requiring development of various technologies for dye elimination.

Correspondence: A.R. Nešić, Vinča Institute of Nuclear Science, University of Belgrade, 11000, Belgrade, Serbia.
E-mail: anesic@vin.bg.ac.rs
Paper received: 3 December, 2012
Paper accepted: 12 February, 2013

Therefore, decolorization of dyes is another important aspect of wastewater treatment before discharge into environment.

In this review, the use of polymer materials, both synthetic and natural by origin, for removal of azo dyes from aqueous solutions is presented. Polymeric adsorbents show increasing advantages over conventional adsorbents because of their simple processing, relatively easy regeneration and the possibility to shape them into most suitable form (*e.g.*, sheets, beads, membranes). This review presents only the data obtained using raw, hydrogel, grafted and crosslinked forms of synthetic and naturally based polymers, and the discussion will be limited to these polymer-based materials and their adsorption properties. The effects of various parameters such as polymer characteristics and the activation conditions on biosorption are presented and discussed.

CLASSIFICATION OF DYES

Dyes exhibit considerable structural diversity, and can be classified by their chemical structure or their application to the fiber type. Dyes must carry one or more functionalities giving the dye color, called chromophores, as well as an electron withdrawing or donating substituents that cause or intensify the color of the chromophores, called auxochrom. The chromophore group can be a base for dye classification. The most important chromophores are azo (–N=N–), carbonyl (–C=O), methine (–CH=), nitro ($–NO_2$) and quinoid groups. The most important auxochromes are amine ($–NH_3$), carboxyl (–COOH), sulfonate ($–SO_3H$) and hydro-

xyl (–OH) groups. Dyes may also be classified according to their solubility: soluble dyes like acid, basic, metal complex, direct, mordant and reactive dyes or insoluble dyes including sulfur, azoic, vat and disperse dyes.

Almost 10^9 kg of dyes are produced annually in the world, of which azo dyes represent about 70% by weight [8]. Because such large quantities of azodyes are being produced and used daily by leather tanning, textile, paper production, food industry, etc. and since they are known to transform to carcinogenic aromatic amines in the environment, their incorrect disposal is a major environmental concern and can affect human and animal health [9]. As removal of azo dyes is of a particular interest for this revew, some typical azo dyes are represented in Figure 1.

As can be seen from the presented structures, azo dyes possess a lot of reactive groups that enables good bonding to the substrate (for example: silk, wool, cotton, nylon fibers, etc.) through formation of covalent and physical bonds with–OH, –NH, or –SH groups in its structure.

COMMON WATER-TREATMENT METHODS FOR REMOVAL OF DYES

A vast array of processes are currently in use for removal of dyes from wastewaters such as: biological treatments [11–13], flocculation and coagulation [14––16], advanced oxidation [17–19], adsorption processes [20–23], etc. Table 1 presents the most widely

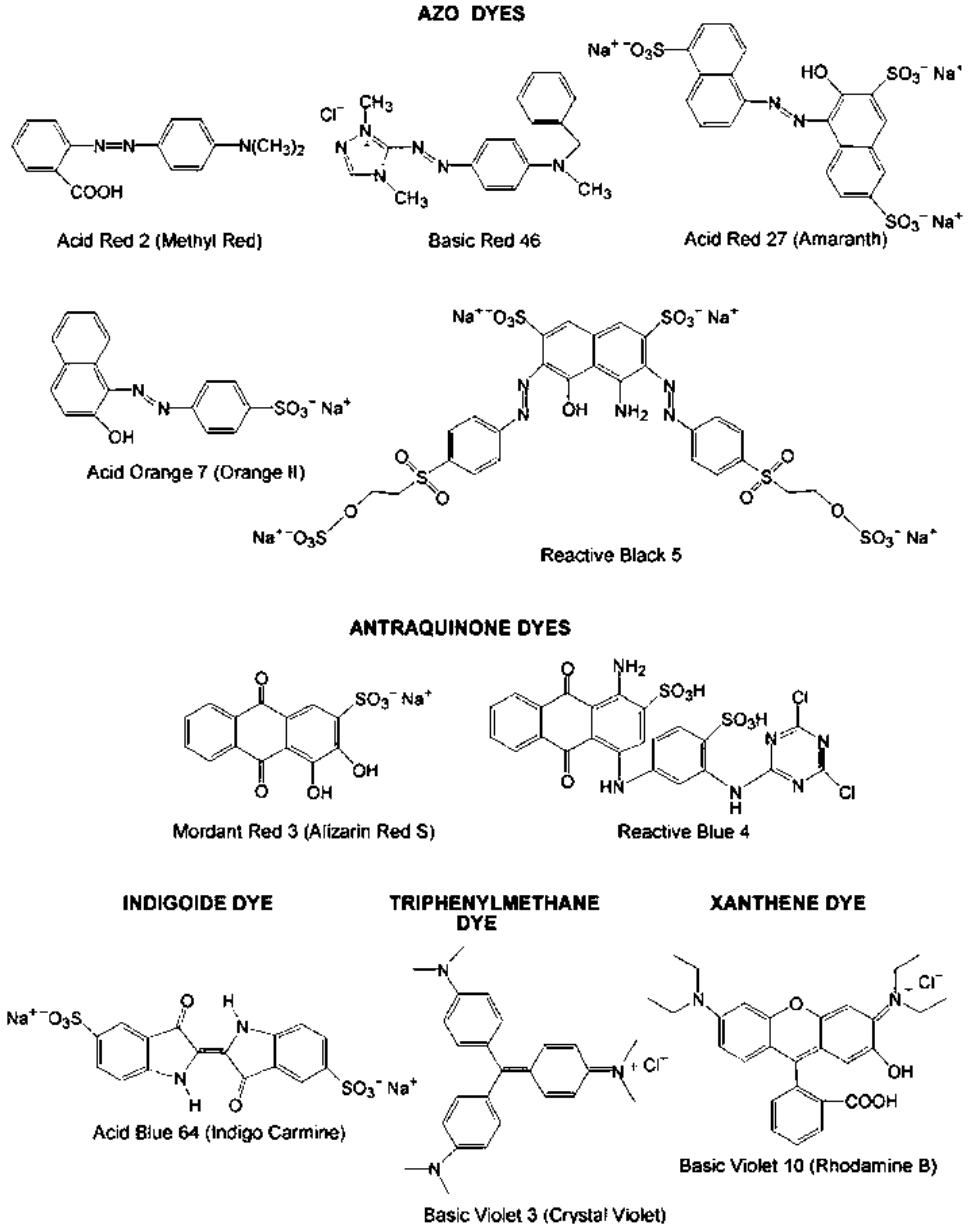

Figure 1. Chemical structures of typical synthetic azo dyes.

Table 1. Advantages and drawbacks of commonly used methods for removal of pollutants from wastewaters

Methods	Advantages	Drawbacks
Ozonation	No sludge production	Short half-life of ozone (20 min)
Oxidative process (H_2O_2)	Simplicity of application	H_2O_2 should be first activated
Fenton reagents, H_2O_2+Fe (II) salt	High efficiency of water-soluble and non water-soluble pollutants	Big sludge production
Photochemical degradation (UV/H_2O_2)	No sludge production	Formation of side products, high cost
Adsorption	High efficiency for removal of different types of dyes and metal ions	Regeneration of adsorbents
Ionic exchange (resin)	Regeneration-no adsorbent loss	Low adsorption capacity
Electrokinetic coagulation	Low cost	High sludge production
Irradiation	Effective oxidation at lab scale	High cost, requires a lot of dissolved O_2
Biological process	Ecological feasible	Slow process, low range of operated temperature
Coagulation/flocculation	Low cost	Heavy chemical consumption, high sludge production

used methods for removal of dyes from wastewater, along with their advantages and drawbacks.

Despite the large number of methods, the application of most of them is often limited by costs of the process itself (especially when applied in small plants), inefficiency and the need to remove the sludge after treatment [24]. Another limiting factor is the formation of toxic degradation products that may happen in some cases. Adsorption processes are becoming increasingly popular as a way of treatment not only of colored effluents but of various other kinds of wastewaters as well, because of their economical feasibility, simplicity and a high level of efficiency.

ADSORPTION OF DYES ON POLYMER MATERIALS

Interest in finding adequate, cost-effective adsorbents with sufficient adsorption capacity, adsorption rate and mechanical properties has increased extensively in recent times. Different types of activated carbon are generally used, and therefore these are the most often investigated sorbents for removal of dyes from wastewaters [25–27]. However, their use is limited because they are expensive sorbents with high-cost regeneration, and taking into account the cost of treatment of polluted water is increasingly important.

Often suggested alternatives are natural materials [28,29] that are renewable or plentiful, usually used without or with minimal pretreatment; waste and by-products in various industries, agriculture and households [30] whose use reduces the cost of sorption process and contributes to preservation of the environment, and low-cost synthetic materials, such as polymer materials, with tailor-made properties for removal of particular pollutant and /or suitable to be applied in specific conditions [31,32].

Polymeric adsorbents show increasing advantages over conventional adsorbents (activated carbon, ion--exchangers, etc.) because of their simple processing, the possibility to be tailor-made and that their adsorption is generally a reversible process, i.e. the adsorbed dyes from waste streams could be effectively desorbed under mild conditions for resource recovery or further treatment. The desorption reagents required depend mainly on the properties of the adsorbed dye, the typical ones being inorganic acids (*e.g.*, HCl or H_2SO_4), alkaline (NaOH or Na_2CO_3), or organic solvents (methanol, alcohol or acetone) [33–36].

The separation of dyes is mainly achieved from aqueous solutions, where the driving force for the adsorption is very strong and enables a fast process.

Various molecular and especially functional groups along polymer chains can form different interactions with dye molecules. Depending on the dominant type of interactions between dye and adsorbent, the adsorption can be physical or chemical by nature. If the adsorbate (dye) molecules are attracted by weak van der Waals forces towards the adsorbent molecules, the adsorption is known as physical adsorption or physisorption, whereas when the dye molecules are bound to the surface of adsorbent by chemical bonds, the adsorption is known as chemical adsorption or chemisorption. Some features which are useful in recognizing physisorption and chemisorption are presented in Table 2.

Adsorption of azo dyes on synthetic polymer materials

In recent years, functional polymers have been increasingly tested as a potential alternative to traditional adsorbents due to their vast surface area, perfect mechanical rigidity, adjustable surface chemistry and feasible regeneration under mild conditions [37]. Synthetic polymers have few more significant advantages

Table 2. General characteristics of physisorption and chemisorption

Physisoprtion	Chemisoprtion
Low heat of adsorption (<2 or 3 times the latent heat of evaporation)	High heat of adsorption (>2 or 3 times the latent heat of evaporation)
Relatively low temperature, always under the critical temperature of the adsorbate	High temperatures
Non-specific	Type of interaction: strong; covalent bond between adsorbate and surface
Adsorption takes place in monolayer or multilayer	Adsorption takes place only in a monolayer
Low activation energy	High activation energy
Rapid, non-activated, reversible	Reversible only at high temperature
No dissociation of adsorbed species	Increase in electron density in the adsorbent-adsorbate interface

over other adsorbent materials; for example, they can be readily manufactured in a wide range of physico-chemical properties (form, size, size distribution, porosity, hydrophobicity, etc.) and they are tunable by inserting various ligands into the structure in order to produce specific sorbents [38–40]. A wide range of polymerization techniques (conventional free-radical polymerization, γ-radiation polymerization, ring opening metathesis polymerization (ROMP), atom transfer radical polymerization (ATRP), single-electron transfer living radical polymerization (SET-LRP), reversible addition fragmentation chain transfer (RAFT) polymerization, etc. [41] enable various architectures of polymer materials (linear free chains in solution, permanently and physically cross-linked hydrogels, amphiphillic block and graft copolymers (micelles) and modified surfaces (polymer brushes) and membranes), each of them having characteristic adsorption properties. Additionally, this type of adsorbents can be easily and completely regenerated with no significant decrease in sorption capacities [42], while by choosing the appropriate monomer or comonomers, environmental friendly adsorbents causing neither direct nor indirect adversity to nature can be obtained. A list of synthetic polymer materials recently used for removal of azo-dyes is given in Table 3.

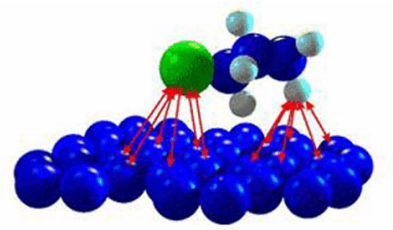

Figure 2. Illustration of adsorption process.

One of the most used forms of polymer materials in the adsorption field are hydrogels – a special type of polymeric materials with three-dimensional, cross-linked structure, able to uptake and retain large amounts of water or aqueous solutions without dissolving due to the presence of physical or chemical crosslinks [57]. During the swelling process of "smart" hydrogels, which could be tailored by external stimuli changes, the network expansion allows access of dye molecules to active centers in the interior of the material, making these materials very interesting to be used as adsorbents.

Poly(*N*-isopropylacrylamide-*co*-acrylic acid) (poly(NIPAAm-*co*-AAc)) microgels and their assemblies were tested as adsorbents for the removal of an azo-dye Orange 2 from aqueous solutions [54]. It has been shown that removal efficiency critically depended on the concentration of AAc, the size of microgels and operating temperature, yielding a maximum removal efficiency of 56.6% by the microgels system with 10% AAc and a diameter of about 1.1 mm at elevated temperature. Microgel aggregates formed from those microgels using various concentrations of *N*,*N*-methylenebisacrylamide (MBA), were found to significantly improve the removal efficiency, because of the structure (*i.e*,. hydrophobicity and internal volume) of the aggregates. The aggregates with 500 mg MBA were able to remove 73.1% of Orange 2, which is a significant enhancement compared with the unaggregated microgels. It was found that the concentration of MBA, as well as the size of microgels in the aggregates affects the percent uptake of the dye. Aggregates with large microgels resulted in notably higher removal of dye, comparing to aggregates of small microgels.

Poor mechanical properties of highly swollen polymer hydrogels can be enhanced through the preparation of interpenetrating polymer networks (IPNs), which are defined as a combination of two polymers in network form without any covalent bonds between them, or semi-IPN, when one of the components has a linear instead of network structure.

Üzüm and Karadag have investigated adsorption properties of a series of acrylamide based hydrogels modified with hydrophobic comonomers and semi-IPNs with poly(ethylene glycol) (PEG) as linear interpenetrant. They have shown that poly(acrylamide-*co*-sodium

Table 3. Some synthetic polymer adsorbents, targeted dyes and corresponding adsorption capacities

Polymeric adsorbent	Dye	Maximal adsorption capacity	Reference
Poly(glycidyl methacrylate) grafted sulfonamide based polystyrene resin with tertiary amine	Everzol black	980 mg g^{-1}	[43]
Poly(glycidyl methacrylate) grafted sulfonamide based polystyrene resin with tertiary amine	Everzol red	1000 mg g^{-1}	[41]
Poly(glycidyl methacrylate) grafted sulfonamide based polystyrene resin with tertiary amine	Calcon	1000 mg g^{-1}	[41]
Poly(ether sulfones)/poly(ethyleneimine) (PES/PEI) nanofibrous membrane	Sunset Yellow FCF	1000 mg g^{-1}	[44]
Poly(ether sulfones)/poly(ethyleneimine) (PES/PEI) nanofibrous membrane	Amaranth	454 mg g^{-1}	[42]
Porous poly(vinyl alcohol) gels	Congo red	35%	[45]
Porous poly(vinyl alcohol) gels	Methyl Orange	Not available	[43]
Poly (amidoamine-co-acrylic acid) copolymer	Direct Red 31	3400 mg g^{-1}	[46]
Poly (amidoamine-co-acrylic acid) copolymer	Direct Red 80	3448 mg g^{-1}	[44]
Macroporous polystyrene cross-linked with divinylbenzene (Purolite A-520E)	Acid Blue 29	48.2 mg g^{-1}	[47]
Poly(1-naphthylamine)	Acid Orange 10 (Orange G)	328 mg g^{-1}	[45]
Poly(1-naphthylamine)–camphorsulphonic acid	Acid Orange 10 (Orange G)	315 mg g^{-1}	[45]
Poly(*N*-vinyl-2-pyrrolidone)	Congo red	Not available	[48]
Poly(*N*-vinyl-2-pyrrolidone)	Methyl orange	Not available	[46]
Cross-linked poly(styrene) resins	Acid red 14	Not available	[49]
Poly(*N*,*N*-dimethylacrylamide-*co*-sodium acrylate) hydrogel	Basic Blue 41	710 mg g^{-1}	[50]
Poly(*N*-vinyl-2-pyrrolidone-*co*-acrylonitrile) treated with hydroxylamine–hydrochloride	Acid fast yellow G	7.6 mg g^{-1}	[51]
Poly(*N*-vinyl-2-pyrrolidone-*co*-acrylonitrile) treated with hydroxylamine–hydrochloride	Direct blue 3B	7 mg g^{-1}	[49]
Poly(*N*-vinyl-2-pyrrolidone-*co*-acrylonitrile) treated with hydroxylamine–hydrochloride	Reactive red SH	7.4 mg g^{-1}	[49]
Poly(acrylamide-*co*-acrylic acid) hydrogels	Janus Green B	44 mg g^{-1}	[52]
Poly(acrylamide-co-sodium acrylate) hydrogels	Janus green B	7×10^{-4} mol g^{-1}	[53]
Poly(acrylamide-*co*-sodium acrylate)/poly(ethylene glycol) semi-IPN	Janus green B	6.33×10^{-4} mol g^{-1}	[51]
Poly(acrylamide-*co*-sodium 4-styrenesulfonate)	Janus green B	67%	[54]
Poly(acrylamide-*co*-sodium 4-styrenesulfonate)/poly(ethylene glycol) semi-IPN	Janus green B	62%	[52]
Poly(acrylamide-*co*-sodium methacrylate) hydrogels	Janus green B	90%	[55]
Poly(acrylamide-*co*-sodium methacrylate)/poly(ethylene glycol) semi-IPN	Janus green B	87%	[53]
Poly(*N*-isopropylacrylamide-*co*-acrylic acid) microgel assemblies	Orange 2	73%	[56]

acrylate) (poly(AAm-*co*-SA)), poly(acrylamide-*co*-sodium-4-styrenesulfonate) (poly(AAm-co-NaSS)) and poly(acrylamide-*co*-sodium methacrylate) (poly(AAm-*co*--SMA) hydrogels and (poly(AAm-*co*-SA)/PEG, poly(AAm-co-NaSS)/PEG and semi-IPNs have ability to adsorbe the monovalent cationic dyes, such as Janus green B (JGB), whereas poly(acrylamide) (PAAm) does not [51––53]. The incorporation of hydrophilic groups such as sodium acrylate (SA) or 4-styrenesulfonic acid sodium salt and a polymer such as poly(ethylene glycol) in PAAm hydrogels was obtained successfully by free radical solution polymerization. The amount of JGB adsorbed onto unit dry mass of the gel increased with the content of SA, together with equilibrium swelling degree, reaching maximal value when AAm/SA weight ratio was 12.5:1, while there was no important change

of the dye removal capacity of AAm/SA/PEG semi-IPN systems when PEG has been added. Similar behavior was noticed for the system with NaSS and SMA instead of SA. Swelling and adsorption capability of corresponding hydrogels and semi-IPNs are increased with increasing NaSS, *i.e*., SMA, content in copolymeric structure due to the increased hydrophilicity of network and number of possible interactions in binding of JGB by investigated adsorbents. Among the three above-mentioned hydrophilic comonomers, introduction of sodium methacrylate is found to provide the best adsorption characteristics, as can be seen from the data listed in Table 3.

The same group has shown that poly(acrylamide-*co*--itaconic acid) hydrogels prepared by irradiating with γ radiation were also able to remove azo dyes from wastewater [58].

Therefore, the adsorption capacity of a polymeric adsorbent toward specified dye or group of dyes can be improved by introduction of monomers that have different functional groups due to the specific interaction of functional groups bound to the polymeric matrixes with the target pollutants, but also by modification of existing groups on polymer chains [59,60].

Linear polymers grafted onto crosslinked polymer resin particles offer numerous potential applications due to the combination of the non-solubility resin and the flexibility of the graft polymer side-chains as the functional group carrier. The flexible side-chains can provide pseudo-homogeneous reaction conditions and better accessibility of involved active centers. Senkal *et al.* have synthesized poly(glycidyl methacrylate) grafted sulfonamide based polystyrene resin with tertiary amine which has been shown to be an efficient adsorbent for removal of azo dyes from water as a result of tertiary amine group's affinity towards dye molecules [41]. A beaded polymer with a poly(glycidyl methacrylate) (PGMA) surface shell was prepared in three steps, starting from poly(styrene-divinyl benzene) based beads. The synthetic protocol included chlorosulfonation, sulfamidation with 2-chloroethylamine hydrochloride and grafting reaction of PGMA. Graft polymerization of GMA from polystyrene resin-supported 2-chloroethyl sulfonamide groups was carried out using atom transfer radical polymerization (ATRP). When graft chains were attached to the resin with stable sulfonamide linkages, this material could be modified via epoxy groups to impart any desired functionality in mild reaction conditions. The polymeric resin was subsequently modified with diethyl amine to introduce tertiary amine groups that enable very good adsorption properties. Even though obtained adsorption capacities for removal of employed azo dyes were very high over a wide pH range, it is determined that increase in pH from 2 to 8, leads to increase in adsorption capacities from 600 to 890 mg g^{-1}, 580 to 910 mg g^{-1} and 620 to 850 mg g^{-1}, for Everzol black, Everzol red and Calcon, respectively. This adsorbent has also shown to be easily regenerated by using basic methanol and 0.1 M HCl, recovering about 94.4% of dye.

Copolymer hydrogels based on *N*-vinyl-2-pyrrolidone (NVP) and methyl methacrylate (MMA) or acrylonitrile (AN) were prepared by γ-irrradiation copolymerization [49]. The nitrile groups (–CN) in the prepared copolymer were subsequently treated with hydroxylamine-hydrochloride and converted into amidoxime groups that have an affinity for the anions of the reactive, acid and direct dye molecules. Such a process resulted in improving both the swelling behavior and adsorption capacity, thus in all experiments treated poly(NVP-*co*-AN) hydrogel showed higher affinity toward dye uptake compared to poly(NVP-*co*-MMA) and untreated poly(NVP-*co*-AN). The adsorption of the pollutants on prepared hydrogels was investigated at various pH values. The uptake of decreases with increasing pH, until it reaches its minimum value at pH 10. For acid dye, the dye uptake decreases with increasing pH, up to pH 7, then starts to increase at a faster rate beyond pH 7.

A few possible ways of bonding are usually involved in dye adsorption on polymer materials: hydrogen bonding, ion exchange, electrostatic and hydrophobic interactions [61]. Analyzing the composition of treated poly(NVP-*co*-AN) and the structure of used dyes, it was concluded that electrostatic interactions together with hydrophobic interactions and hydrogen bonding could occur between cationic groups of NVP and anionic groups of the dyes. Hydrophobic effects, which are specifically aqueous solution interactions, in the present case would involve the aromatic rings and the methyl and methine groups on the dye molecules and methine groups on the gel. Hydrogen bonding could be expected to occur between amine groups of the oxygen atom on the dye molecules and the carbonyl groups on the monomer units of the crosslinked copolymer.

In case of many listed synthetic polymer adsorbents, it is proven that they show strong pH-dependent behavior. Bearing in mind that most of the used polymer materials, as well as azo dyes, are ionic in nature, it is expected that the solution pH affects the structure of the dye as well as the structure of the polymeric material itself, has significant influence on the surface changes of the adsorbents, the degree of ionization of present functional groups, and as a consequence, onto the investigated adsorption process [62]. If mechanism of dye uptake is attributed to the electrostatic attraction force between the dye and the polymeric material, at adequate pH, charged groups on polymer chains would be free to promote electrostatic interactions with dye ions. Any change in either charge would affect the

uptake percentage. Novel micro-nano structure poly(ether sulfones)/poly(ethyleneimine) (PES/PEI) nanofibrous membranes have been synthesized and utilized as adsorbents for removal of anionic azo-dyes Sunset Yellow FCF Amaranth [42] . A series of adsorption experiments were carried out to investigate the influence of membrane dosage, initial solution pH value, contact time, initial solution concentration and adsorption temperature on the adsorption performance. Polyethyleneimine (PEI) has a large amount of amino and imino groups in its polymer chain. The experimental results showed that the removal of the anionic dyes on this PES/PEI nanofibrous membrane was a pH-dependent process with the maximum adsorption capacity at the initial solution pH of 1. The adsorption equilibrium data were all fitted well to the Langmuir isotherm equation, with maximum adsorption capacity values of 1000 mg g^{-1} and 454.4 mg g^{-1}, for Sunset Yellow FCF and Amaranth, respectively. Solution pH had shown a significant effect on the uptake of dyes, since it determined the surface charge of the adsorbent and the degree of ionization and speciation of the dyes. At low pH solution a relatively high concentration of protons was available to protonate amine and imino groups ($–NH_2$ and –NH-) on PEI, forming $–NH_3^+$ and $–NH_2^+–$ groups capable to attract dye anions. The electrostatic interactions between the PES/PEI nanofibrous membrane and the anionic dyes were proven by x-ray photoelectron spectroscopy (XPS). The results have also shown that the adsorption capacity of of PES/PEI nanofibrous toward tested dyes increased with increasing initial dye concentrations because of the increase in the driving force of concentration gradient with an increase in the initial concentration, but then tended to level off when complexes between the chelating sites and the absorbates reached saturation.

In order to prove the outstanding effect of PEI component in PES/PEI nanofibrous affinity membranes, the pure PES nanofibrous membrane was also used for removal the anionic dyes. The maximum adsorption capacity of pure PES nanofibrous membranes for SY FCF and AM were very low (4.2 and 3 mg g^{-1}, respectively) indicating that PES functioned mainly as a matrix.

As can be seen from Table 3, by far the best results regarding adsorption capacities of synthetic polymer materials for azo-dyes are reported for poly(amido-amine-*co*-acrylic acid) copolymer use for removal of direct dyes, Direct Red 31 and Direct Red 80 [44]. The adsorption capacity increases when the pH is decreased. Maximum adsorption of anionic dyes occured at acidic pH 2, where significantly high electrostatic attraction existed between the positively charged ($–NH_3^+$) surface of the PAC and negatively charged anionic dye. As the pH of the system increases, the number of positively charged sites decreased, as well as the adsorption efficiency of PAC. An important limitation resulting from the high reactivity and non-selectivity of adsorbent that reacts with non-target compounds was noticed in the presence of inorganic salts, because these salts have small molecules and compete with dyes for the same adsorption sites on PAC. It results in a higher adsorbent dosage demand to accomplish the desired degree of dye removal efficiency.

In literature are also reported pH independent polymer adsorbents, such as poly(1-naphthylamine) (PNA) and PNA doped with camphor-sulphonic acid (CSA) used for sulphonate azo dye Acid Orange 10 removal from acidic and basic medium [45]. In that case adsorption predominantly occurs through hydrophobic interactions, i.e. strong van der Waals attraction between naphthalene groups of PNA and Acid Orange 10 dye.

It could be concluded that some of proposed adsorbents have shown limited ability to remove the employed dye, while with the others the ability of potential development and application was noted.

NATURAL POLYMERS

Natural polymers represent an interesting and attractive alternative as adsorbents because of their particular structure, physico-chemical characteristics, chemical stability, high reactivity and excellent selectivity towards heavy metal ions and dyes, resulting from the presence of reactive chemical groups in polymer chains. Much attention has recently been focused on polysacharides such as starch, alginate, cyclodextrin, cellulose and chitosan. It is well known that polysaccharides which are abundant, renewable and biodegradable resources have a capacity to associate by physical and chemical interactions with a wide variety of molecules. Hence adsorption onto polysaccharide derivatives can be a low-cost and feasible procedure of choice in water decontamination. Compared with conventional sorbents for removing pollutants from solution, such as commercial activated carbons and synthetic ion-exchange resins, the advantage of polysaccharide based adsorbent is possibility of easy regeneration if its required. The main disadvanteges of polysaccharide adsorbents are their low porosity, pH dependence and dependence of different sources of raw materials, so there is increasing interest in modification of these materials to enhance adsorption capacity.

Starch

Next to cellulose, starch is the most abundant carbohydrate in the world and is present in living plants as energy storage material. Starches are mixtures of two polyglucans, amylopectin and amylose, but they contain only a single type of carbohydrate, glucose (Figure 3).

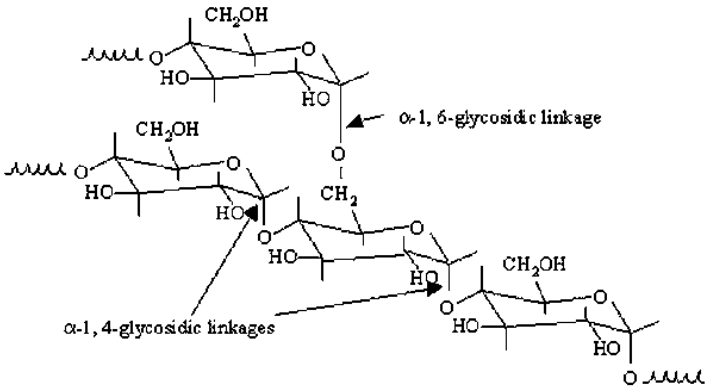

Figure 3. Starch structure.

Amylose is nearly unbranched, while amylopectin is highly branched with the branches connected in α-1,6 position of the anhydroglucose unit [63].

Starches are unique raw materials, inexpensive and widely available in many countries. They possess several other advantages which make them excellent materials for industrial use. However, the hydrophilic nature of starch is a major constraint which seriously limits the development of starch-based materials. Chemical derivatisation has been proposed as a way to solve this problem and to produce water resistant adsorbents.

Very important feature is the possibility of starch to adsorb water. This ability comes from interaction of free –OH groups on the glucose units and the water molecules (Figure 4) [64,65].

The hydroxyl groups interact with water molecules by hydrogen bonding. Van den Berg *et al*. proposed that the Brunauer, Emmett and Teller equation (BET) could be related to the number of adsorption sites on starch, because the monolayer capacity is found to be strongly related to the number of polar groups that are able to adsorb water on the starch surface [66].

Both types of starch chains, amylose and amylopectin, establish hydrogen bonds with water molecules. Amylopectin structures also physically trap water molecules in the matrix of chain branches in the amorphous portion of the starch. When the water molecules are trapped in this way, some of the nearby –OH groups hydrogen bond with the trapped water molecule and become unavailable for additional hydrogen bonding. The amylopectin branched structure has overlapping hydroxyl groups which are proposed to correspond to more hydroxyl groups per unit area of the starch surface. Thus an adsorbent high in amylopectin is hypothesized to have a greater adsorption capacity [64].

As a biodegradable biomass, starch has attracted considerable attention since it can be modified to remove heavy metal ions and dyes [67–70]. In order to test the dye adsorption numerous modifications of starch were investigated. Cationic starch derivatives containing primary, secondary, and tertiary amino groups and quaternary ammonium salt and etherified and grafted cationic starch derivatives were treated with three types of dyes – an acid dye, a hydrolyzed reactive dye, and a direct dye in order to determinate

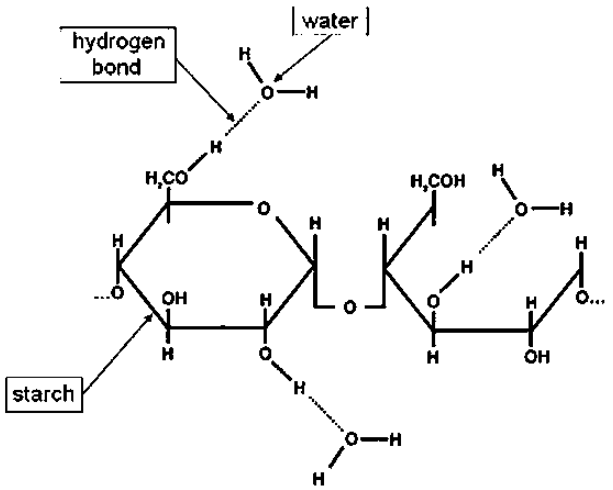

Figure 4. Hydrogen bonding of water to starch molecules.

factors affecting the dye sorption value [71]. The dye sorption value increased with increasing amine content to a maximum value and then decreased for all amine types. The maximum sorption depends on the dye type: acid dye >hydrolyzed reactive dye > direct dye. The cationic starch ethers were better adsorbents for dyes than the grafted cationic starch derivatives. The dye sorption value increased with increasing pH; the maximum dye sorption value of the direct dye was at pH 4, whereas those for the acid and hydrolyzed reactive dyes were at pH 5 [72].

Crosslinked starch-based adsorbents are an important class of starch derivatives. The crosslinked polymeric materials have a three-dimensional network structure and can swell in aqueous medium without dissolution [73].

Klimaviciute *et al*. studied the adsorption of anionic dyes Acid Yellow 36, Acid Orange 7, Acid Orange 52, Acid Red 151 on the crosslinked materials with epichlorohydrin starches containing quaternary ammonium groups. The adsorption of all investigated dyes by the cationic starches with different groups increased in the following order: primary amino < secondary amino < < tertiary amino < quaternary ammonium groups. The adsorption of the dyes by the cationic starches having primary, secondary and tertiary amino groups can be effectively only in the acid solution. In alkaline and acid solutions of dyes only quaternary ammonium groups can effectively work. It is shown that starches crosslinked with epichlorohydrin containing quaternary ammonium groups are more suitable for the anionic dye adsorption from a textile dyeing solution compared with modified starches containing only quaternary ammonium groups [74]. Crosslinked amphoteric starch with carboxymethyl and quaternary ammonium groups was investigated for removal of Acid Light Yellow 2G and Acid Red G, by Xu *et al*. [75]. It was noticed that the residual concentration of the Acid Red G decreased abruptly when the pH value was above 10 due to the presence of negatively charged phenolic hydroxyl groups which can become potentially active sites and could attracted by the ammonium groups in the absorbents. The maximum adsorption capacity was 113,6 and 135,6 mg g^{-1} for Acid Yellow 2G and Acid Red G dye, respectively.

Ju studied the discoloration of cationic starch with different degrees of substitution (DS) for C.I. Reactive Red 2 and C.I. Reactive Yellow 145 [76]. It was found that cationic starch with a higher DS had high adsorption capacity. When DS increased from 0.37 to 0.70, dye uptake increased from 45.9 and 53.4% to 59.2 and 67.1% for C.I. Reactive Red 2 and C.I. Reactive Yellow 145, respectively.

Delvala *et al*. used crosslinked polysaccharides derivatives containing tertiary amine groups to recover various textile dyes in aqueous solutions. The crosslinked polymers have been prepared in one step by reticulation of starch-enriched flour using only epichlorohydrin as cross-linking agent in the presence of NH_4OH. Polysaccharides form insoluble gels on reaction with epichlorohydrin (EPI) under alkaline conditions and in this way weakly basic anion-exchange groups were introduced into polymer matrices. Among others, the adsorption of two azo dyes: Acid Red 1 and Acid Red 40 was studied. The result shows that the presence of amino groups and the nature of the dye could influence the adsorption capacity. This adsorbent can be applied on both acid and basic dyes. For acid dyes, the active sites are the quaternary ammonium groups, while for basic dyes, they are carboxymethyl groups. The adsorption processes are exothermic for acid dyes, which mean that low temperature will facilitate the adsorption, while the basic dyes have the highest adsorption capacity at 303 K [77].

Cheng *et al*. investigated starch modified with etylenediamine for removal of Acid Orange 10 (AO10), Acid Green 25 (AG25) and Amido Black 10B (AB10B) [78]. The maximum capacity for each dye at pH value of 4 was achieved. The adsorption of AG25 and AB10B followed pseudo-second-order model, whereas adsorption of AO10 could be adequately described by both models. According to the Langmuir equation the capacities followed the sequence AB10B (1.1 mmol/g) > AG25 (0.8 mmol/g) > AO10 (0.6 mmol/g). Wang *et al*. investigated native and enzymatic hydrolyzed starch modified with diethylenetriamine for removal of Acid Orange 7 (AO7), AO10, AG25 and Acid Red 18 (AR18) [79]. In all cases the modified hydrolyzed starch had higher adsorption capability than modified native starch. With increase of grafting groups, the adsorption of dyes increased on modified hydrolyzed starch. Increments of the sorption capacities for the four acid dyes was higher than values obtained by Cheng et al. and the sequence of AO7 (2,5 mmol g^{-1}) > AO10 (1,2 mmol g^{-1}) > AR18 (1,6 mmol g^{-1}) > AG25 (1,8 mmol g^{-1}). Cheng *et al*. also investigated dithiocarbamate-modified starch (DTCS) for removal of AO7, AO10, AR18, AG25, Acid Black 1 (AB1) [80]. With the increase of pH value, the adsorption capacity for each dye decreased dramatically. The authors suggested that in acidic medium, positive surface charge is developed due to protonation of dithiocarbamate which increased with in decrease in pH of dye solution. The capacities for individual dyes follow the sequence AO 7 (0.8 mmol/g) > AO 10 (0.4 mmol/g) > AB 1 (0.38 mmol/g) > AR 18 (0.37 mmol/g) > AG 25 (0.31 mmol/g).

Alginate

Alginates are unbranched polysaccharides consisting of 1-4 linked β-D-mannuronic acid (M) and its C-5 epimer α-L-guluronic acid (G) (Figure 5). It is comprised

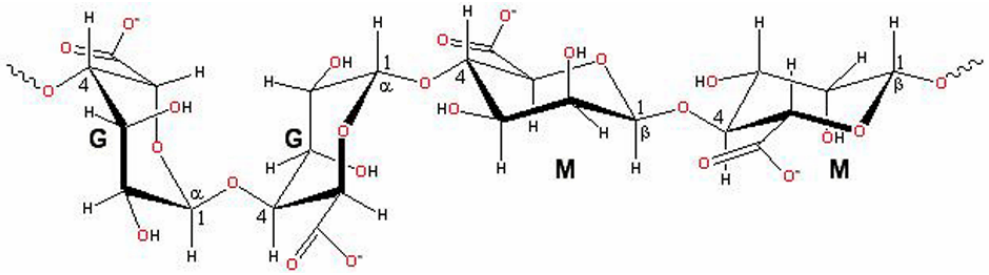

Figure 5. Alginate structure.

of sequences of M (M-blocks) and G (G-blocks) residues interspersed with MG sequences (MG-blocks). While it is possible to obtain alginates from both algal and bacterial sources, commercially available alginates currently come only from algae. The copolymer composition, sequence and molecular weights vary with the source and species that produce the copolymer. The combination of chemical and biochemical techniques provides considerable potential for creating modified alginic acid derivatives with control over monosaccharide sequence and nature, location and quantity of substituents [81].

One of the important properties of alginate is the ability to form hydrogels and has the capacity to remove toxic pollutants [82,83]. An aqueous solution of alginate is readily transformed into a hydrogel on addition of metallic divalent cations. Calcium alginate immobilized microbial cultures have been used to remove dyes, Reactive Black 22 and Direct Black 22 [84]. The beads from 0.05M concentration of the $CaCl_2$ solution had the lowest resistance to compression compared to those cross-linked in $CaCl_2$ solutions with higher concentrations. Decoloration rate of the softer beads was higer probably because lower $CaCl_2$ concentrations resulted in fewer cross-links at the guluronic acid binding sites leading to weaker cohesion in the alginate matrix to allow better diffusion through the bead. Decoloration has been shown to follow first-order kinetics with respect to dye concentration.

Alginate could be effectively used as a biosorbent for the removal of cationic dyes. The alginate biosorbent exhibited high sorption capacities toward Basic Red 18 and Basic Blue 41 which were used as model compounds in single and binary systems. Adsorption is increased with increase in adsorbent dosage and this can be attributed to reduced availability of adsorption sites. The equilibrium capacity depends on initial dye concentration and decreases with an increase in this values. At low initial dye concentrations, the adsorption of dyes by alginate is very intense and reaches equilibrium very quickly which indicates the possibility of the formation of monolayer coverage of the molecules at the outer interface of the alginate. When the pH increases the adsorption capacity increases and the maximum adsorption of basic dyes occurs at pH 8. This pH value provides a considerably high electrostatic attraction exists between the negatively charged surface of the adsorbent, due to the ionization of functional groups of the adsorbent and positively charged cationic dye molecules [85].

Cyclodextrin

Cyclodextrins (CDs) comprise a family of three well-known industrially produced substances. The practically important, industrially produced CDs are the α-, β-, and γ-cyclodextrins (Figure 6). The three major cyclodextrins are crystalline, homogeneous, nonhygroscopic substances, built up from glucopyranose units. The α-cyclodextrin comprises six glucopyranose units,

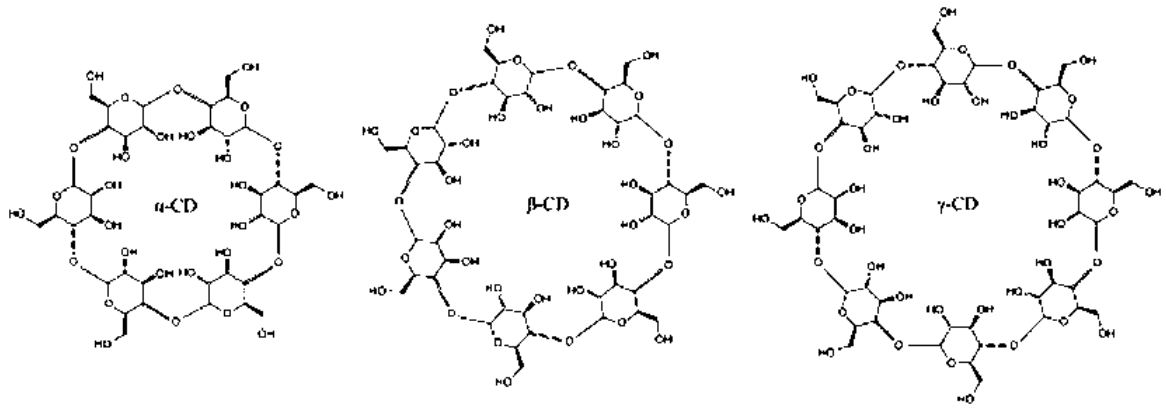

Figure 6. α-, β-, and γ-cyclodextrin structures.

β-cyclodextrin comprises seven such units, and γ-cyclodextrin comprises eight such units. Cyclodextrins can be obtained by enzymatic degradation of starch. In this process compounds with six to twelve glucopyranose units per ring are produced. Depending on the enzyme and the way thereaction is controlled, the main product is α-, β- or γ-cyclodextrin (6, 7 and 8 glucopyranose units, respectively).

The most notable feature of cyclodextrins is their ability to form solid inclusion complexes ("host–guest" complexes) with a very wide range of solid, liquid and gaseous compoundsby a molecular complexation. In these complexes a guest molecule is held within the cavity of the cyclodextrin host molecule. Cyclodextrin inclusion is a stoichiometric molecular phenomenon in which usual only one guest molecule interacts with the cavity of the cyclodextrin molecules to become entrapped. 1:1 complex is the simplest and most frequent case. However, 2:1, 1:2, 2:2, or even more complicated associations, and higher order equilibrium exist almost always simultaneously. The ring structure of cyclodextrins allows them to act as hosts and form inclusion compounds with various small molecules which provides them good application in textile industry for removing of certain dyes [86].

Cyclodextrin polymers were modified using hexamethylene diisocyanate (HMDI) as a cross-linking agent in dry dimethylformamide and used as a sorbent for the removal of some selected azo dyes from aqueous solutions. Cyclodextrin based materials were used to remove the following dyes: direct violent 51 (DV-51), methyl orange (MO), and tropaeolin 000 (TP). These materials exhibit approximately same sorption capacity toward all the azodyes except DV-51 which contains more sulfonates and azogroups than the others. This is due to establishment of intermolecular hydrogen bonds between hydroxyl and amide groups in the polymer and between sulfonate groups of DV-51 [87]. These results were in agreement with the literature data published by using β-CD based polymers with epichlorohydrin [21]. The values of the adsorption capacity for DV-51 increased with increasing of the pH as always in the case of the inclusion complex with β-CD and aromatic derivatives [88]. The sorption was dependent on the presence of amide and sulfonate groups and according to this, it assumed that in the adsorption mechanism, hydrogen bonding, hydrophobic interactions (pollutant–polymer and pollutant–pollutant interactions), complexation and acid–base interactions between the sorbent and the pollutant, physical adsorption due to the polymer network and chemical interactions of solute dyes via ion exchange are all involved. The same modification of cyclodextrin using HMDI was reported for efficiently removal of Titanium Yellow (TY) and Direct Blue 71 (DB 71) [89]. The maximum sorption capacity these materials had shown for the removal of Titanium Yellow from an aqueous solution (52%). Cyclodextrin cross-linked using 4,4'-methylene bisphenyldiisocyanate (MDI) was also used for removal of azo dyes (Evans Blue and Chicago Sky Blue) and is turned to be efficient extractant. It is shown that cyclodextrin modified with MDI has higher values of adsorption capacity compare to cyclodextrin modified with HMDI. According to Langmuir sorption equation, maximum capacity of 12.09 mmol g^{-1}, was determined for the adsorption of Evans Blue [23].

Cellulose

Cellulose is a renewable resource and one of the most abundant organic materials on the planet. Cellulose is mostly obtained from wood pulp and cotton. Cellulose content in cotton can be up to 94%, while this content in wood pulp is lower due to presence of lignin, but it's still above 50%. Cellulose can also be made by bacteria and is thus called microbial or bacterial cellulose.

The molecular structure of cellulose comprises of repeating β-D-glucopyranose units which are covalently linked through acetal functions between the OH group of the C4 and C1 carbon atoms (β-1,4-glucan) (Figure 7). Cellulose is a large, linear-chain polymer with a large number of hydroxyl groups (three per anhydroglucose (AGU) unit) and present in the preferred 4C1 conformation. To accommodate the preferred bond angles, every second AGU unit is rotated 180 in the plane. The length of the polymeric cellulose chain depends on the number of constituent AGU units (degree of polymerisation, DP) and varies with the origin and treatment of the cellulose raw material [90].

There are four different polymorphs of cellulose: cellulose I, II, III and IV (Figure 8). Cellulose I, native cellulose, is the form found in nature, and it occurs in two allomorphs, Iα and Iβ. Cellulose II, or regenerated

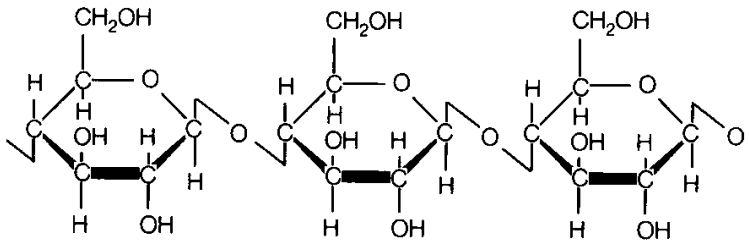

Figure 7. Chemical structure of cellulose.

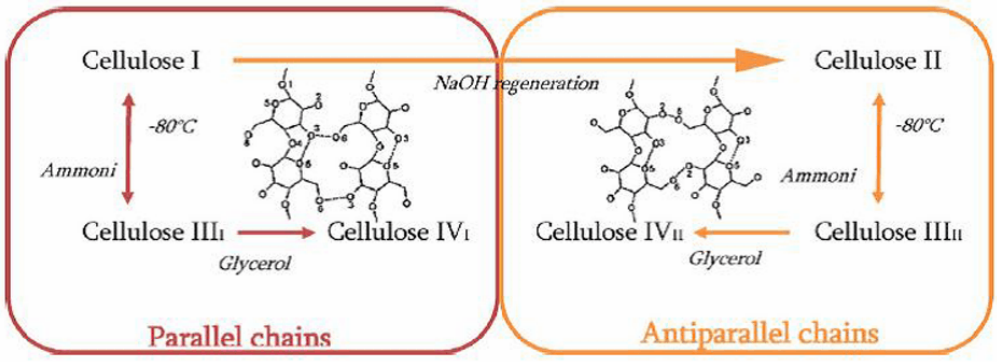

Figure 8. Polymorphs of cellulose.

cellulose, emerges after re-crystallization or mercerization with aqueous sodium hydroxide. It is the most stable crystalline form. The major distinction between these two forms of cellulose lies in the layout of their atoms: cellulose II has antiparallel packing, whereas the chains in cellulose I are in a parallel direction. Cellulose III is obtained by ammonia treatment of cellulose I or II, and cellulose IV is finally produced from cellulose III by treatment with glycerol [91,92]. Three hydroxyl groups in each β-D-glucopyranose units are able to interact with one another forming intra and intermolecular hydrogen bonds.

Cellulose in its form as a polymer raw material have been used mainly in two general areas: one being the use in constructing materials based on wood and cotton and also paper and board. The accessibility of cellulose depends on its origin, processing condition, and composition, *i.e.*, index of crystallinity (*Ic*), degree of polymerization (*DP*), and contents of cellulose, hemicellulose, and lignin. Also cellulose has been widely used as a starting material for chemical reactions in attempt of create cellulose based artifacts that can be used in a medicine, pharmacy, bioenergy and wastewater applications [94–97]. The utilization of cellulose as a bioaffinity carrier material should enhance the adsorption of organic wastes due to its abundant hydroxyl groups, which give cationic nature to the biopolymer. The beads, films and resins based on natural cellulose were used to adsorb heavy metals and hazardous azo dyes. However, conventional bioadsorbents based on cellulose are difficult to be separated and recovered except by high speed centrifugation or filter. Also, as the molecular structure of cellulose itself is compact and inactive, it is inefficient for dye removal without any modification. Thus, proper treatment is required to introduce reactive sites and activate the sorption ability.

Buvaneswari *et al*. investigated the adsorption of Methyl Orange onto cellulose surface. The influence of different parameters such as pH, temperature and concentration of dye solution on adsorption capacity was studied [98]. The optimum value of pH for adsorption of Methyl Orange was 6, while with further increase of pH of dye solution percentage of adsorption decreased. The adsorption of Methyl Orange slightly increased up to 40 °C and further increase of temperature decreased the adsorption due to the collapse of hydrogen bonds.

Siroky *et al*. investigated the effect of alkali treatment in range of NaOH from 0–7.2 mol dm^{-3} on CI Reactive Red 120 sorption behaviour onto cellulose II [99]. It was observed that greatest adsorption of dye onto cellulose II occured for samples treated with 3.3 and 2.5 mol dm^{-3} aqueous NaOH solution and reached adsorption capacity up to 80 mg g^{-1}. With further increase of NaOH concentration, the adsorption capacity decreased. Pores in the celullose II significantly affected by alkali treatment (< 2 nm diameter) and accessibility of dye (1.4 nm) sorption into those pores account the differences observed herein.

The adsorption of the anionic dyes CI Reactive Red 120, Yellow and CI Direct Blue 1 on cellulose fixed with reactive dyes having six and eight sulfonate groups was investigated to elucidate the *co*-ion repulsion effect on the adsorption of anionic dyes [100]. The amounts of dye adsorption on reactively dyed cellulose decreased by the repulsive effect of the sulfonate groups of the reactive dyes fixed previously. The larger amounts of fixed dye and lower ionic strength influenced decreasing of the adsorption, compared with the case of undyed cellulose. Although the apparent substantivity of CI Direct Blue 1 decreased with an increase in the amount of fixed dye, this dye showed the same saturation value on reactively-dyed cellulose as that on original cellulose. CI Reactive Red 120 and Yellow had no different influence on the adsorption of CI Direct Blue 1 on cellulose reactively-dyed with them, in spite of the number of sulfonate groups. With increase in the pH of the dye-bath, the hydroxyl groups of cellulose and dyes dissociated and led tothe reduction of reactive dyes adsorption. A decrease due to the dissociation of cellulose occured at pH > 10.5.

The pH-dependence of three vinylsulfonyl reactive dye solutions, C.I. Reactive Red 22, Black 5, and Blue-

-Cu, on decolorization by cellulose immersed in an aqueous solution was examined under anaerobic and aerobic conditions by Okada *et al*. [101]. The results showed that with an increase in pH in the acid region, the rates of decolorization for Red 22 and Black 5 under anaerobic conditions and oxidative decolorization for Blue-Cu under aerobic ones decreased, whereas those of oxidative decolorization for Red 22 increased under aerobic conditions. The rates of decolorization for the three dyes under anaerobic conditions in the alkaline region showed little pH-dependence. The rates of oxidative decolorization under aerobic conditions increased with increasing pH in the alkaline region.

Cellulose gels regenerated from aqueous alkali–urea solvent for adsorption of Congo Red were investigated by Isobe *et al*. [102]. In spite of the apparent similarity in pore structures, adsorption of Congo Red by cellulose gels showed striking difference depending on the coagulant types. The adsorption level was significantly higher for organic solvents than for aqueous solutions used as coagulant. The order was: MeOH > > EtOH > acetone > Na_2SO_4 ≥ H_2SO_4. The authors suggested that the difference in affinity with Congo Red was due to diffrent polarity of the coagulant. The maximum adsorption capacity was 180 mg g^{-1} for MeOH-regenerated cellulose.

A novel hybrid hydrogel of IPN was synthesized by the graft copolymerization reaction among cellulose (Cell), polymethacrylic acid (PMAA) and bentonite (Bent), in the presence of MBA as a crosslinker and potassium peroxydisulphate ($K_2S_2O_8$) as an initiator by Anirudhan *et al.* [103]. The resulting IPN was used as an adsorbent for studying the effectiveness in the removal of methylene blue. The adsorption loading reached the maximum at pH 6.5 with maximum monolayer capacity of 317.7 mg g^{-1}. Batch recycling of PMAA-g-Cell/Bent was conducted and the results confirmed that the sorption capacity of the IPNs was unaffected by the regeneration process.

In order to enhance the sorption capacity of anionic dyes Acid Green, Ismative Violet 2R and Direct Pink 3B, Taleb *et al*. investigated copolymer hydrogels composed of poly(vinyl alcohol) (PVA) and carboxymethyl cellulose (CMC) prepared by using electron beam irradiation as crosslinking agent [104]. Results showed that the sorption capacity of dyes onto PVA/CMC hydrogel decreased significantly with increase of pH. At lower pH values (below the pK of carboxylic groups, approximately 4.6), the –COO– groups in CMC are protonated to –COOH groups and the negatively charged molecules of dyes cause the increase in dye adsorption. As the pH increased, the sorbent surface became negatively charged which didn't favor the adsorption of anionic dye molecules due to the electrostatic repulsion between the negatively charged surface and the dye anions. The adsorption capacities varied as direct pink 3B > acid green B > ismative 2R and the maximum sorption capacity was 140 mg g^{-1}.

Chitosan

Chitosan is the *N*-deacetylated derivative of chitin, which is a naturally abundant polysaccharide and the supporting material of crustaceans, insects, etc. and is easily obtained from crustacean shells (such as prawns and crabs), insects and fungi. Chitosan could be produced by alkaline deacetylation of chitin.

The molecular structure of chitosan comprises of β (1-4) linked D-glucosamine residues with a variable number of randomly located *N*-acetyl-glucosamine groups. In spite of the presence of acetamide groups at the C2-positions, chitosan is structurally very similar to cellulose. Celulose has hydroxyl groups at C2-positions in place of acetomaide groups (Figure 9).

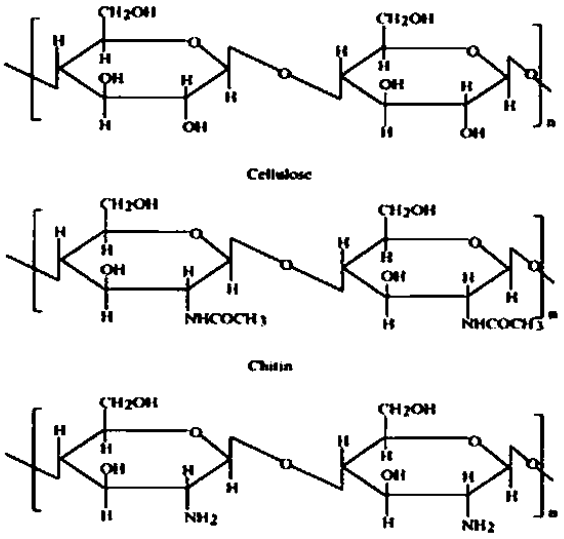

Figure 9. Structure of chitin and chitosan.

Chitosan has a wide range of applications that depend on its physical, chemical, and biological properties. The principal areas are agriculture, wastewater treatment, food and beverages, cosmetics and toiletries, biomedics and pharmaceutics, fibers and textiles and paper technology [106].

Chitosan has excellent properties for the adsorption of heavy metals and dyes, principally due to high hydrophillicity, presence of amine and hydroxyl groups which can serve as active sites and flexible structure of the polymeric chains. However, chitosan is easy to dissolve at low pH, resulting in the limitation of its applications. On the other side, chitosan has very poor sorption capability in alkaline solution. Another problem with chitosan is its poor physicochemical characteristics, in particular porosity, as with most of the other polysaccharides as well. Beside nonporosity,

chitosan possesses very low specific area ranging between 2 and 30 $m^2 g^{-1}$, so there is a need to modify natural chitosan physically or chemically in order to improve sorption capability.

The adsorption capacity of chitosan depends on physical parameters such as: crystallinty, porosity and particle size. Generally, with increase of porosity and decrease of particle size and crystallinity, the adsorption capacity increases. Trung *et al*. determined that decrystallized chitosan could be better than crystalline chitosan for adsorption of azo dyes [107]. The gel formation procedure, freeze drying procedure and crosslinking can decrease the crystallinity and enhance porosity. The main chemical parameters that affect the adsorption capacity are molecular weight, degree of deacetylation, solubility and ionic strength. When comparing the chitosan samples with different degree of deacetylation, adsorption capacity of azo dye increases with increase of degree of deacetylation, as reported by Sasha *et al*. [108].

Chitosan can be modeled in several shapes: gels, flakes, powders, beads, membranes and particles [109]. There are only a few articles in the literature related to the flake and powder forms of chitosan because of their low surface activity and porosity. Mahmoodi *et al*. investigated the removal of Direct Red 23 (DR23) and Acid Green 25 (AG25) by raw chitosan from textile effluent in single and binary systems was investigated. The maximum adsorption capacity was in single system, 178 and 155 mg g^{-1} for removal the AG25 and DR23, respectively. Iqbal *et al*. used chitosan flakes, extracted from prawns and labeo rohita scales to remove acid yellow dye from water [110]. Prawn scales showed greater adsorption capacity than the labeo rohita scales and reached its maximum at 0.168 mg g^{-1}.

The most widely investigated types of chitosan as adsorbents are beads and gels. Chitosan beads can be formed by precipitation in alkaline solution, or in alkaline bath containing usually glutaraldehyde (GLA), tripolyphosphate (TPP) or epichlorhydrin (EPI) as crosslinker. Crosslinked chitosan have been studied recently to improve its chemical stability in any acidic media. The adsorption capacity depends on degree of crosslinking. In general way, the adsorption capacity can increase or decrease with the extent of cross-linking depending on the functional groups. Chitosan can form crosslinked networks by reaction between the amino or hydroxyl group of the chains with crosslinking agents.

Concerning the specific azo dyes, Chatterjee et al. investigated the chitosan beads for removal of the Congo Red dye [111]. The maximum adsorption capacity was 93 mg g^{-1} at pH 6. The presence of sodium chloride at the concentration of 0.5 and 1 M in dye solution reduced the adsorption by 14.4 and 28.0%, respectively. Sodium dodecyl sulphate also inhibited adsorption of Congo red. The ability of chitosan beads, derived from deacetylated crab shell chitin, to remove acid dyes – Acid Green 25 (AG25), Acid Orange 10 (AO10), Acid Orange 12 (AO12), Acid Red 18 (AR18) and Acid Red 73 (AR73) from effluent solution by adsorption has been studied [112]. Based on the Langmuir isotherm analysis, the extremely high monolayer adsorption capacities were determined to be 645, 923, 973, 693.2 and 728 mg g^{-1} chitosan for AG25, AO10, AO12, AR18 and AR73, respectively. The differences in capacities may be due to the difference in the molecular size of dye molecules and the number of sulphonate groups of each dye. The results demonstrated that monovalent and smaller dye particle have superior capacities due to increase in dye/chitosan ratio in the system, enabling deeper penetration of dye molecules to the internal pore structure of chitosan.

The chitosan beads crosslinked by TPP and GLA were used as barriers to the transport of Reactive Black 5 dye in soil column experiments by Lazaridis *et al*. [113]. The solution of chitosan was added dropwise from a pipette into an aqueous solution of glutaraldehyde 5 g/L, which also contained 5 g tripoly phosphate at pH 6, adjusted with an aqueous HCl solution, so the beads were prepared. The maximum adsorption capacity of Reactive Black 5 by TPP crosslinked chitosan beads was 238 mg g^{-1}. The sorption capacity of Methylene Orange by GLA crosslinked chitosan particles was 140 mg g^{-1} according Morais *et al.* [114]. Chen *et al*. also investigated the adsorption of Reactive Black 5 dye onto GLA crosslinked chitosan beads [115]. The crosslinked chitosan microparticles were prepared through homogeneous coupling reaction and microparticle formation using a sodium hydroxide solution. The maximum adsorption capacity according to Chen *et al*. was 1680 mg g^{-1}. The significantly higher adsorption capacity obtained by Chen *et al*. indicated that the sorption depends on the procedure for the preparation of the crosslinked beads [116]. Chitosan beads crosslinked with EPI showed the maximum Red dye adsorption capacity of 52.7 mg g^{-1}. The adsorption of dye decreased in the presence of surfactant dodecylbenzenesulfonate as a result of competitive adsorption for the same sites between the same charged dye and surfactant molecules. The adsorption properties of non-crosslinked and crosslinked chitosan beads with ethylene glycol diglycidyl ether (EGDE) for removal of Acid Red 37 (AC 37) and Acid Blue 25 (AB 25) were compared [117]. It was shown that the adsorption capacities of chitosan for both acid dyes were comparatively higher than those of chitosan-EGDE. The authors explained that the adsorption capacity was lower for crosslinked chitosan beads because of decreasing of the number of free amine groups after crosslinking with EGDE. Adsorption capacities of AB 25 were higher then of AC 37 for both

cases, non-crosslinked and crosslinked chitosan beads. The maximum adsorption capacities were followed: 128 mg g^{-1} for adsorption of AC 37 onto chitosan beads, 59.5 mg g^{-1} for adsorption the same dye onto chitosan corsslinked with EGDE, 263 mg g^{-1} for adsorption of AB 25 onto chitosan beads and 142.8 mg g^{-1} for adsorption AB 25 onto chitosan crosslinked with EGDE.

Improving chitosan properties such as increasing chelating or complexation properties was attempted by graft copolymerization. Chitosan has two types of reactive groups that can be grafted: a) free amino groups on deacetylated units and b) the hydroxyl groups on the C3 and C6 carbons on acetylated or deacetylated units. The new functional groups incorporated as grafts on chitosan may increase the density of sorption sites, change the pH range for dye sorption and increase sorption selectivity for the target dye.

Poly(methyl methacrylate) grafted chitosan (Ch-g--PMMA) was used for removal of anionic dyes Procion Yellow MX 8G (PY) and Remazol Brilliant Violet 5R (RV 5R) by Singh *et al*. [118]. Degree of grafting had big influence on adsorption capacity and with increase in degree of grafting (%) from 50 to 250, there was an increase in the adsorption for all dyes. It was observed that percentage removal of dye by Ch-g-PMMA was almost constant for a wide pH range. According to the Langmuir isotherms, the maximum adsorption capacities of dyes onto Ch-g-PMMA were as for PY and RV 5R 250 and 357 mg g^{-1}, respectively. The same authors investigated removal of the same dyes by chitosan grafted with poly(acrylamide) [119]. The maximum adsorption capacities were significantly higher than capacities obtained by chitosan grafted with PMMA, and reached its maximum 1000 and 1428.6 mg g^{-1} for PY and RV 5R dye, respectively. Chitosan was also grafted with other methacrylates. Konaganti *et al*. investigated chitosan grafted with different poly(alkyl methacrylate)s: chitosan grafted poly(methyl methacrylate) (Ch-g-PMMA), chitosan grafted poly(ethyl methacrylate) (Ch-g-PEMA), chitosan grafted poly(butyl methacrylate) (Ch-g-PBMA) and chitosan grafted poly-(hexyl methacrylate) (Ch-g-PHMA), for removal of anionic dye Orange G [120]. Also, adsorption capacity of anionic sulfonated dyes –Orange G (Acid Orange 10-AO10) and Congo Redonto (CR) Ch-g-PBMA were investigated. The grafted chitosan possessed higher adsorption capacities compared to the values of ungrafted chitosan. Also, the adsorption capacities in all cases increased with increasing the percentage of grafting. The adsorption capacity of these dyes on Ch-g-PBMA followed the order CR>AO10. The adsorption capacity follows the order: Ch-g-PMMA>Ch-g-PEMA >Ch-g-PBMA > Ch-g-PHMA > chitosan, with the adsorption equilibrium capacity of Ch-g-PMMA being 4.5 times that of chitosan.

It could be concluded that some of proposed adsorbents have shown limited ability as raw natural materials to remove the employed dye, while the derivatives of natural polymers could be effectively used in place of commercial adsorbents due to biodegradabillity, easier regenaration, high eficiency and low cost.

CONCLUSIONS

Intensive industrial development is accompanied by an increasing volume of wastewater, which in terms of environmental protection and sustainable development requires the need to enhance the existing and introduce new processes for wastewater treatment. Azo dyes, which are toxic and naturally very difficult to degrade, require special scientific and technological attention. Considerable efforts are now being made in the research and development of polymeric materials and derivatives as basic materials for new applications because of increasing cost of conventional adsorbents. This review has attempted to cover a wide range of polymeric adsorbents so that the reader can get an idea about the various types and forms of polymeric materials used for the removal of azo dyes from the wastewater. Polymeric adsorbents show increasing advantages over conventional adsorbents because of their simple processing, relatively easy regeneration and the possibility to shape them into most suitable form. The literature reveals that in some cases the modification of the adsorbent increased the removal efficiency. Many of the reported materials can be regenerated conveniently, which can further reduce the cost of the water treatment process.

Acknowledgement

The authors acknowledge funding from the Ministry of Education, Science and Technological Development of the Republic of Serbia, Projects No. 43009 and 172062.

REFERENCES

[1] K. Kadirvelu, M. Kavipriya, C. Karthika, M. Radhika, N. Vennilamani, S. Pattabhi, Utilization of various agricultural wastes for activated carbon preparation and application for the removal of dyes and metal ions from aqueous solutions, Biores. Technol. **87** (2003) 129–132.

[2] A.R. Dinçer, Y. Günes, N. Karakaya, E. Günes, Comparison of activated carbon and bottom ash for removal of reactive dye from aqueous solution, Biores. Technol. **98** (2007) 834–839.

[3] D. Shen, J. Fan, W. Zhou, B. Gao, Q. Yue, Q. Kang, Adsorption kinetics and isotherm of anionic dyes onto organo-bentonite from single and multisolute systems, J. Hazard. Mater. **172** (2009) 99–107.

[4] J.O. Duruibe, M.D.C. Ogwuegbu, J.N. Egwurugwu, Heavy metal pollution and human biotoxic effects , Internat. J. Physi. Sci. **2**(5) (2007) 112–118.

[5] D.K. Mahmoud, M.A.M. Salleh, W.A.W.A. Karim, A. Idris, Z.Z. Abidin, Batch adsorption of basic dye using acid treated kenaf fibre char: Equilibrium, kinetic and thermodynamic studies, Chem. Eng. J. **181–182** (2012) 449––457.

[6] L. Fan, C. Luo, X. Li, F. Lu, H. Qiu, M. Sun, Fabrication of novel magnetic chitosan grafted with graphene oxide to enhance adsorption properties for methyl blue, J. Hazard. Mater. **215–216** (2012) 272–279.

[7] M. Asgher, H.N. Bhatti, Evaluation of thermodynamics and effect of chemical treatments on sorption potential of Citrus waste biomass for removal of anionic dyes from aqueous solutions, Ecol. Eng. **38** (2012) 79–85.

[8] K.Z. Elwakeel, Removal of Reactive Black 5 from aqueous solutions using magnetic chitosan resins, J. Hazard. Mater. **167** (2009) 383–392.

[9] E. Forgacs, T. Cserhati, G. Oros, Removal of synthetic dyes from wastewaters: a review, Environ. Int. **30** (2004) 953–971.

[10] C.A.M. Huitle, E. Brillas, Decontamination of wastewaters containing synthetic organic dyes by electrochemical methods: A general review, Appl. Catalysis. **87** (2009) 105–145.

[11] N. Masoudzadeha, F. Zakeria, T. B. Lotfabada, H. Sharafi, F. Masoomi, H. S. Zahiri, G. Ahmadian, K. A. Noghabi, Biosorption of cadmium by Brevundimonas sp. ZF12 strain, a novel biosorbent isolated from hot-spring waters in high background radiation areas, J. Hazard. Mater. **197** (2011) 190–198.

[12] T. Robinson, G. McMullan, R. Marchant, P. Nigam, Remediation of dyes in textile effluent: a critical review on current treatment technologies with a proposed alternative, Biores. Technol. **77** (2001) 247–255.

[13] V. Venugopal, K. Mohanty, Biosorptive uptake of Cr(VI) from aqueous solutions by Parthenium hysterophorus weed: Equilibrium, kinetics and thermodynamic Studies, Chem. Eng. J. **174** (2011) 151–158.

[14] Z.B. Wu, W.M. Ni, B.H. Guan, Application of chitosan as flocculant for coprecipitation of Mn(II) and suspended solids from dual-alkali FGD regenerating process, J. Hazard. Mater. **152** (2008) 757–764.

[15] M.F. Chong, K.P. Lee, H.J. Chieng, I. Ramli, Removal of boron from ceramic industry wastewater by adsorption-flocculation mechanism using palm oil mill boiler (POMB) bottom ash and polymer, Water Res. **43** (2009) 3326–3334.

[16] S. Song, A. Lopez-Valdivieso, D.J. Hernandez-Campos, C. Peng, M.G. Monroy-Fernandez, I. Razo-Soto, Arsenic removal from high-arsenic water by enhanced coagulation with ferric ions and coarse calcite, Water Res. **40** (2006) 364–372.

[17] H. Dong, X. Guan, D. Wang, C. Li, X. Yang, X. Dou, A novel application of H2O2-Fe(II) process for arsenate removal from synthetic acid mine drainage (AMD) water, Chemosphere **85** (2011) 1115–1121.

[18] S.G. Segura, E. Brillas, Mineralization of the recalcitrant oxalic and oxamic acids by electrochemical advanced oxidation processes using a boron-doped diamond anode, Water Res. **45** (2011) 2975–2984.

[19] X. Zhao, B. Zhang, H. Liu, J. Qu, Removal of Arsenite by Simultaneous Electro-Oxidation and Electro-Coagulation Process," J. Hazard. Mater. **184** (2010) 472–476.

[20] S.A. Kosa, G. A. Zhrani, M. A. Salam, Removal of heavy metals from aqueous solutions by multi-walled carbon nanotubes modified with 8-hydroxyquinoline, Chem. Eng. J. **181–182** (2012) 159–168.

[21] E. Dana, A. Sayari, Adsorption of heavy metals on amine-functionalized SBA-15 prepared by co-condensation: Applications to real water samples, Desalination **285** (2012) 62–67.

[22] A. Bée, D. Talbot, S. Abramson, V. Dupuis, Magnetic alginate beads for Pb(II) ions removal from wastewater, J. Colloid. Interf. Sci. **362** (2011) 486–492.

[23] H. Tang, C. Chang, L. Zhang, Efficient adsorption of Hg(II) ion on chitin/cellulose composite membranes prepared via environmentally friendly pathway, Chem. Eng. J. **173** (2011) 689–697.

[24] K. Xie, W. Zhao, X. He, Adsorption properties of nanocellulose hybrid containing polyhedral oligomeric silsesquioxane and removal of reactive dyes from aqueous solution, Carbohydr. Polym. **83** (2011) 1516–1520.

[25] N. Amin, Removal of direct blue-106 dye from aqueous solution using new activated carbons developed from pomegranate peel: Adsorption equilibrium and kinetics, J. Hazard. Mater. **165** (2009) 52–62.

[26] V.Gómez, M. Larrechi, M. Callao, Kinetic and adsorption study of acid dye removal using activated carbon, Chemosphere **69** (2007) 1151–1158.

[27] R. Tovar-Gómez, D. Rivera-Ramírez, V. Hernández-Montoya, A. Bonilla-Petriciolet, C. Durán-Valle, M. Montes-Morán, Synergic adsorption in the simultaneous removal of acid blue 25 and heavy metals from water using a Ca(PO3)2-modified carbon, J. Hazard. Mater. **199–200** (2012) 290–300.

[28] A. Nesic, S. Velickovic, D. Antonovic, Characterization of chitosan/montmorillonite membranes as adsorbents for Bezactiv Orange V-3R dye, J. Hazard. Mater. **209–210** (2012) 256–263.

[29] S. Dawood,T. Kanti Sen, Removal of anionic dye Congo red from aqueous solution by raw pine and acid-treated pine cone powder as adsorbent: Equilibrium, thermodynamic, kinetics, mechanism and process design, Water Res. **46** (2012) 1933–1946.

[30] S.Deng,Y. Peng Ting, Polyethylenimine-modified fungal biomass as a high-capacity biosorbent for Cr(VI) anions: Sorption capacity and uptake mechanisms, Environ. Sci. Technol. **39** (2005) 8490–8496.

[31] V.V. Panic, Z.P. Madzarevic, T. Volkov-Husovic, S.J. Velickovic, Poly(methacrylic acid) Based Hydrogels as Sorbents for Removal of Cationic Dye Basic Yellow 28: Kinetics, Equilibrium Study and Image Analysis, Chem. Eng. J. **217** (2013) 192–204.

[32] M. Min, L. Shen, G. Hong, M. Zhu, Y. Zhang, X. Wang, Y. Chen, B. Hsiao, Micro-nano structure poly(ether sulfones)/poly(ethyleneimine) nanofibrous affinity membranes for adsorption of anionic dyes and heavy metal ions in aqueous solution, Chem. Eng. J. **197** (2012) 88–100.

[33] B.C. Pan, J.L. Chen, Q.X. Zhang, Y.Wang, Treatment and resource reuse of industrial wastewater from production process of phenyl acetic acid, Chin. J. React. Polym. **8** (1999) 82–89.

[34] B.J. Pan, B.C. Pan, W.M. Zhang, Q.R. Zhang, Q.X. Zhang, S.R. Zheng, Adsorptive removal of phenol fromaqueous phase by using a porous acrylic ester polymer, J. Hazard. Mater. **157** (2008) 293–299.

[35] W.G. Feng, Q.X. Zhang, J.L. Chen, Z.Y. Xu, B.C. Pan, X. Su, Treatment of wastewater From production process of 2,3-acid, Chin. J. React. Polym. **8** (1999) 68–75.

[36] L. Lv, B.C. Pan, W.M. Zhang, J.L. Chen, Q.X. Zhang, Study on the treatment of industrial wastewater containing triethylamine with polymeric adsorbents, Chin. J. React. Polym. **9** (2000) 174–180.

[37] B. Pan, B.Pan,W. Zhang, L. Lv, Q. Zhang, S. Zheng, Development of polymeric and polymer-based hybrid adsorbents for pollutants removal from waters. Chem. Eng. J. **151** (2009) 19–29.

[38] F. An, X. Feng, B. Gao, Adsorption property and mechanism of composite adsorbent PMAA/SiO2 for aniline, J. Hazard. Mater. **178** (2010) 499–504.

[39] D. Maksin, A. Nastasović, A. Milutinović-Nikolić, Lj. Suručić, Z. Sandić, R. Hercigonja, A. Onjia, Equilibrium and kinetics study on hexavalent chromium adsorption onto diethylene triamine grafted glycidyl methacrylate based copolymers, J. Hazard. Mater. **209**–**210** (2012) 99–110.

[40] G. Azhgozhinova, O. Güven, N. Pekel, A. Dubolazov, G. Mun, Z. Nurkeeva, Complex formation of linear poly-(methacrylic acid) with uranyl ions in aqueoussolutions, J. Colloid. Interface. Sci. **278** (2004) 155–159.

[41] O. Azzaroni, Polymer brushes here, there, and everywhere: Recent advances in their practical applications and emerging opportunities in multiple research fields. J. Polym. Sci. A Polym. Chem. **50** (2012) 3225–3258.

[42] A. Nastasović, S. Jovanović, D. DJordević, A. Onjia, D. Jakovljević, T. Novaković, Metal sorption on macroporous poly(GMA-co-EGDMA) modified with ethylene diamine, React. Funct. Polym. **58** (2004) 139–147.

[43] B.F. Senkal, F. Bildik, E. Yavuz, A. Sarac, Preparation of poly(glycidyl methacrylate) grafted sulfonamide based polystyrene resin with tertiary amine for the removal of dye from water, React. Funct. Polym. **67** (2007) 1471––1477.

[44] M. Min, L.Shen, G. Hong, M. Zhu, Y. Zhang, X. Wang, Y. Chen, B. S. Hsiao, Micro-nano structure poly(ether sulfones)/poly(ethyleneimine) nanofibrous affinity membranes for adsorption of anionic dyes and heavy metal ions in aqueous solution, Chem. Eng. J. **197** (2012) 88–100.

[45] S.R. Sandeman, V.M. Gunko, O.M. Bakalinska, C.A. Howell, Y. Zheng, M.T. Kartel, G.J. Phillips, S.V. Mikhalovsky, Adsorption of anionic and cationic dyes by activated carbons, PVA hydrogels, and PVA/AC composite, J. Colloid Interface Sci. **358** (2011) 582–592.

[46] N.M. Mahmoodi, F. Najafi, A.Neshat, Poly(amidoamine-co-acrylic acid) copolymer: Synthesis, characterization and dye removal ability, Ind. Crops. Prod. **42** (2013) 119–125.

[47] U. Riaz, S.M. Ashraf, Semi-conducting poly(1-naphthylamine) nanotubes: A pH independent adsorbent of sulphonate dyes, Chem. Eng. J. **174** (2011) 546–555.

[48] H.K. Can, B. Kirci, S. Kavlak, A.Güner, Removal of some textile dyes from aqueous solutions by poly(*N*-vinyl-2-pyrrolidone) and poly(*N*-vinyl-2-pyrrolidone)/K2S2O8 hydrogels, Radiat. Phys. Chem. **68** (2003) 811–818.

[49] C. Valderrama, J.L. Cortina, A. Farran, X. Gamisans, F.X. de las Heras, Kinetic study of acid red "dye" removal by activated carbon and hyper-cross-linked polymeric sorbents Macronet Hypersol MN200 and MN300, React. Funct. Polym. **68** (2008) 718–731.

[50] V. Bekiari, M. Sotiropoulou, G. Bokias, P. Lianos, Use of poly(N,N-dimethylacrylamide-co-sodium acrylate) hydrogel to extract cationic dyes and metals from water, Colloids Surfaces, A **312** (2008) 214–218.

[51] S.E. Abd El-Aal, E.-S.A. Hegazy, M.F. AbuTaleb, A.M. Dessouki, Radiation synthesis of copolymers for adsorption of dyes from their industrial wastes. J. Appl. Polym. Sci. **96** (2005) 753–763.

[52] S. Duran, D. Şolpan, O. Güven, Synthesis and characterization of acrylamide–acrylic acid hydrogels and adsorption of some textile dyes, Nucl. Instrum. Methods Phys. Res., B **151** (1999) 196–199.

[53] Ö.B. Üzüm, E. Karadağ, Equilibrium swelling studies and dye sorption characterization of AAm/SA hydrogels cross-linked by PEGDMA and semi-IPNs with PEG, Adv. Polym. Technol. **31** (2012) 141–153.

[54] Ö.B. Üzüm, E. Karadağ, Water and dye sorption studies of novel semi IPNs: Acrylamide/4-styrenesulfonic acid sodium salt/peg hydrogels. Polym Eng Sci. (2012), doi: 10.1002/pen.23378

[55] Ö.B. Üzüm, E. Karadağ, Behavior of semi IPN hydrogels composed of PEG and AAm/SMA copolymers in swelling and uptake of Janus Green B from aqueous solutions, J. Appl. Polym. Sci. **125** (2012) 3318–3328.

[56] D. Parasuraman, A.K. Sarker, M.J. Serpe, Poly(N-Isopropylacrylamide)-based microgels and their assemblies for organic-molecule removal from water, Chem. Phys. Chem. **13** (2012) 2507–2515.

[57] N. Peppas, P. Bures, W. Leobandung, H. Ichikawa, Hydrogels in pharmaceutical formulations, Eur. J. Pharm. Biopharm. **50** (2000) 27–46.

[58] E. Karadag, D.Saraydin, O.Güven, Interaction of some cationic dyes with acrylamide/itaconic acid hydrogels. J. Appl. Polym. Sci. **61** (1996) 2367–2372.

[59] B. Pan, B. Pan, W. Zhang, L. Lv, Q. Zhang, S. Zheng, Development of polymeric and polymer-based hybrid adsorbents for pollutants removal from waters, Chem. Eng. J. **151** (2009) 19–29.

[60] K. Zheng, B.C. Pan, Q.J. Zhang, W.M. Zhang, B.J. Pan, Y.H. Han, Q.R. Zhang, W. Du, Z.W. Xu, Q.X. Zhang, Enhanced adsorption of p-nitroaniline from water by a carboxylated polymeric adsorbent, Sep. Purif. Technol. **57** (2007) 250–256.

[61] Q.H. Hu, S.Z. Qiao, F. Haghseresht, M.A. Wilson, G.Q.Lu, Adadsorption study for removal of basic red dye using bentonite, Ind. Eng. Chem. Res. **45** (2006) 733–738.

[62] D.Sun, X. Zhang, Y. Wu, X. Liu, Adsorption of anionic dyes from aqueous solution on fly ash. J. Hazard. Mater. **181** (2010) 335–342.

[63] L. Sair, W.R. Fetzer, Water sorption by starches, Ind. Eng. Chem. **36** (1944) 205–208.

[64] V. Rebar, E.R. Fischbach, D. Apostolopoulos, J.L. Kokini, Thermodynamics of water and ethanol adsorption on four starches as model biomass separation systems, Biotechnol. Bioeng. **26** (1984) 513–517.

[65] A.S. Kulik, J.R. Chris de Costa, J. Haverkamp, Water organization and molecular mobility in maize starch investigated by two-dimensional solid-state NMR, J. Agric. Food Chem. **42** (1994) 2803–2807.

[66] C. van den Berg, F.S. Kaper, J.A.G. Weldring, I. Wolters, Water binding by potato starch, J. Food Technol. **10** (1975) 589–602.

[67] D.K. Kweon, J.K. Choi, E.K. Kim, S.T. Lim, Adsorption of divalent metal ions by succinylated and oxidized corn starches, Carbohydr. Polym. **46** (2001) 171–177.

[68] W.C. Chan, T.P. Fu, Mechanism of removing chlorophenolic compounds from solution by a water-insoluble cationic starch, J. Polym. Res. **1** (1997) 47–55.

[69] W.C. Chan, J.Y. Wu, Dynamic adsorption behaviors between Cu^{2+} ion and water-insoluble amphoteric starch in aqueous solutions, J. Appl. Polym. Sci. **81** (2001) 2849–2855.

[70] W.C. Chan, J.C. Ferng, Mass transport process for the adsorption of Cr(VI) onto water-insoluble cationic starch synthetic polymers in aqueous systems, J. Appl. Polym. Sci. **71** (1999) 2409–2418.

[71] M.I. Khalil, A.A. Aly, Use of Cationic Starch Derivatives for the Removal of Anionic Dyes from Textile Effluents, J. Appl. Polym. Sci. **93** (2004) 227–234.

[72] B.Z. Ju, Preparation and application of cationic starch with high degree of substitution, PhD Thesis, 2000, pp. 105–126.

[73] F. Renault, N. Morin-Crini, F.Gimbert, P.M. Badot, G. Crini, Cationized starch-based material as a new ion-exchanger adsorbent for the removal of C.I. Acid Blue 25 from aqueous solutions, Biores. Technol. **99** (2008) 7573–7586.

[74] R. Klimaviciute, A. Riauka, A. Zemaitaitis, The binding of anionic dyes by cross-linked cationic starches, J. Polym. Res. **14** (2007) 67–73.

[75] S. Xu, J. Wang , R. Wu, J. Wang , H. Li, Adsorption behaviors of acid and basic dyes on crosslinked amphoteric starch, Chem. Eng. J. **117** (2006) 161–167.

[76] M. Zhang, B.Z. Ju, S.F. Zhang, W. Ma, J.Z. Yang, Synthesis of cationic hydrolyzed starch with high DS by dry process and use in salt-free dyeing, Carbohydr. Polym. **69** (2007) 123–129.

[77] F. Delvala, G. Crinib, N. Morinc, J. Vebrel, S. Bertini, G. Torri, The sorption of several types of dye on crosslinked polysaccharides derivatives, Dyes Pigments **53** (2002) 79–92.

[78] R. Cheng, Sh. Ou, M. Li , Y. Li , B. Xiang, Ethylenediamine modified starch as biosorbent for acid dyes, J. Hazard. Mater. **172** (2009) 1665–1670.

[79] Z. Wang, B. Xian, R. Cheng, Y. Li, Behaviors and mechanism of acid dyes sorption onto diethylenetriamine-modified native and enzymatic hydrolysis starch, J. Hazard. Mater. **183** (2010) 224–232.

[80] R. Cheng, B. Xiang, Y. Li, M. Zhang, Application of dithiocarbamate-modified starch for dyes removal from aqueous solutions, J. Hazard. Mater. **188** (2011) 254––260.

[81] S.N. Pawar, K.J. Edgar, A review of chemistry, properties and applications, Biomaterials **33** (2012) 3279–3305.

[82] A. Martinse, A. Skijak-Braek, O. Smidsrod, Alginate as immobilization material: I. Correlation between chemical and physical properties of alginate gel beads, Biotechnol. Bioeng. **33** (1989) 79–89.

[83] E. W.Shin, R.M. Rowell, Cadmium ion sorption onto lignocellulosic biosorbent modified by sulfonation: the origin of sorption capacity improvement, Chemosphere **60** (2005) 1054–1061.

[84] J.A. Ramsay, W.H.W. Mok, Y.S. Luu, M. Savage, Decoloration of textile dyes by alginate-immobilized Trametes versicolor, Chemosphere **61** (2005) 956–964.

[85] N.M. Mahmoodi, Equilibrium, kinetic and thermodynamic of dye removal using alginate from binary system, J. Chem. Eng. Data **56** (2011) 2802–2828.

[86] B. Voncina, Application of cyclodextrins in textile dyeing, Textile dyeing, P. Hauser (Ed.), InTech, 2011, available from: http://www.intechopen.com/books/textile-dyeing/applicationof-cyclodextrins-in-textile-dyeing.

[87] E.Y. Ozmen, M. Sezgin, A. Yilmaz, M. Yilmaz, Synthesis of β-cyclodextrin and starch based polymers for sorption of azo dyes from aqueous solutions, Biores. Technol. **99** (2008) 526–531.

[88] G. Crini, Studies on adsorption of dyes on beta-cyclodextrin polymer, Biores. Technol. **90** (2003) 193–198.

[89] E.Yilmaza, S. Memonb, M. Yilmaza, Removal of direct azo dyes and aromatic amines from aqueous solutions using two β-cyclodextrin-based polymers, J. Hazard. Mater. **174** (2010) 592–597.

[90] D. Klemm, H.P. Schmauder, T.Heinze, Cellulose, in: S. De Baets, E.J. Vandamme, A. Steinbuchel, (Eds.), Polysaccharides. II.Polysaccharides from eukaryotes, Vol. 6. Wiley-VCH, Weinheim, pp. 275–320.

[91] C. Aulin, S. Ahola, P. Josefsson, T. Nishino, Y. Hirose, M. Österberg, L. Wagberg, Nanoscale cellulose films with different crystallinities and mesostructures – Their surface properties and interaction with water, Langmuir **25**(13) (2009)7675–7685.

[92] G. Siqueira, J. Bras, A. Dufresne, Cellulosic bionanocomposites: A review of preparation, properties and applications, Polymer **2**(4) (2010) 728–765.

[93] N. Lavoine, I. Desloges, A. Dufresne, J. Bras, Microfibrillated cellulose – Its barrier properties and applications in cellulosic materials: A review, Carbohydr. Polym. **90** (2012) 735–764.

[94] O. Chambin, D. Champion,, C. Debray, M.H. Rochat-Gonthier,M. Le Meste, Y. Pourcelot, Effects of different

cellulose derivatives on drug release mechanism studied at a preformulation stage, J. Controll. Rel. **95** (2004) 101–108.

[95] K. Zih-Perényi, A. Lásztity, S. Pusztai, Study of interference of pharmaceuticals with complexing characteristics in solid phase microextraction of lead on chelating celluloses, Microchem. J. **85** (2007) 149–156.

[96] K.P. Gregoire, J.G. Becker, Design and characterization of a microbial fuel cell for the conversion of a lingocellulosic crop residue to electricity, Biores. Technol. **119** (2012) 208–215.

[97] D.W. O'Connell, C. Birkinshaw, T.F. O'Dwyer, Heavy metal adsorbents prepared from the modification of cellulose: A review, Biores. Technol. **99** (2008) 6709–6724.

[98] N. Buvaneswari, C. Kannan, Plant toxic and non-toxic nature of organic dyes through adsorption mechanism on cellulose surface, J. Hazard. Mater. **189** (2011) 294––300.

[99] J. Siroky, R.S. Blackburn, T. Bechtold, J. Taylor, P. White, Alkali treatment of cellulose II fibres and effect on dye sorption, Carbohydr. Polym. **84** (2011) 299–307.

[100] S.H. Bae, H. Motomura, Z. Morita, Effect of anionic groups in cellulose on the adsorption of reactive dyes on cellulose, Dyes Pigments **34** (1997)37–55.

[101] Y. Okada, M. Sakai, I. Takahashi, Effect of pH on the fading behavior of vinylsulfonyl azo dyes on cellulose in aqueous solutions, Dyes Pigments **24** (1994) 1–10.

[102] N. Isobe, U.J. Kim, S. Kimura, M. Wada, S. Kuga, Internal surface polarity of regenerated cellulose gel depends on the species used as coagulant, J. Colloid Interf. Sci. **359** (2011) 194–201.

[103] T.S. Anirudhan, A.R. Tharun, Preparation and adsorption properties of a novel interpenetrating polymer network (IPN) containing carboxyl groups for basic dye from aqueous media, Chem. Eng. J. **181**–**182** (2012) 761–769.

[104] M.F. Abou Taleb, H.L. Abd El-Mohdy, H.A. Abd El-Rehim, Radiation preparation of PVA/CMC copolymers and their application in removal of dyes, J. Hazard. Mater. **168** (2009) 68–75.

[105] N. Majeti V.R. Kumar, A review of chitin and chitosan applications, React. Funct. Polym. **46** (2000) 1–27.

[106] M. Rinaudo, Chitin and chitosan: Properties and applications, Prog. Polym. Sci. **31** (2006) 603–632.

[107] T.S. Trung, C.H. Ng, W.F. Stevens, Characterization of decrystallized chitosan and its application in biosorption of textile dyes, Biotechnol. Lett. **25** (2003) 1185–1190.

[108] T.K. Saha, S. Karmaker, H. Ichikawa, Y.J. Fukumori, Mechanisms and kinetics of trisodium 2-hydroxy-1,1'--azonaphthalene-3,4',6-trisulfonate adsorption onto chitosan, J. Colloid Interf. Sci. **286** (2005) 433–439.

[109] N.M. Mahmoodi, R. Salehi, M. Arami, H. Bahrami, Dye removal from colored textile wastewater using chitosan in binary system, Desalination **267** (2011) 64–72.

[110] J. Iqbal , F.H. Wattoo, M.H.S. Wattoo, R. Malik, S.A. Tirmizi, M. Imran, A.B. Ghangro, Adsorption of acid yellow dye on flakes of chitosan prepared from fishery wastes, Arabian J. Chem. **4** (2011) 389–395.

[111] S. Chatterjee, B.P. Chatterjee, A.K. Guha, Adsorptive removal of Congo Red, a carcinogenic textile dye by chitosan hydrobeads: Binding mechanism, equilibrium and kinetics, Colloids Surfaces, A **299** (2007) 146–152.

[112] Y.C. Wong, Y.S. Szeto, W.H. Cheung, G. McKay, Biosorption of acid dyes on chitosan-equilibrium isotherm analyses, Process Biochem. **39** (2004) 693–702.

[113] N.K. Lazaridis, H. Keenan, Chitosan beads as barriers to the transport of azo dye in soil column, J. Hazard. Mater. **173** (2010) 144–150.

[114] W.A. Morais, A.L.P. Fernandes, T.N.C. Dantas, M.R. Pereira, J.L.C. Fonseca, Sorption studies of a model anionic dye on crosslinked chitosan, Colloids Surfaces, A **310** (2007) 20–31.

[115] A.H. Chen, S.M. Chen, Biosorption of azo dyes from aqueous solution by glutaraldehyde-crosslinked chitosans, J. Hazard. Mater. **172** (2009) 1111–1121.

[116] A.R. Cestari, E.F.S. Vieira, J.A. Mota, The removal of the indigo carmine dye from aqueous solutions using crosslinked chitosan–evaluation of adsorption thermodynamics using a full factorial design, J. Hazard. Mater. **160** (2008) 337–343.

[117] A. Kamari, W.S.W. Ngah, L.K. Liew, Chitosan and chemically modified chitosan beads for acid dyes sorption, J. Environment. Sci. **21** (2009) 296–302.

[118] V. Singh, A.K. Sharma, D.N. Tripathi, R. Sanghi, Poly-(methylmethacrylate) grafted chitosan: An efficient adsorbent for anionic azo dyes, J. Hazard. Mater. **161** (2009) 955–966.

[119] V. Singh, A.K.Sharma, R.Sanghi, Poly(acrylamide) functionalized chitosan: an efficient adsorbent for azo dyes from aqueous solutions, J. Hazard. Mater. **166** (2009) 327–335.

[120] V.K. Konaganti, R. Kota, S. Patil, G. Madras, Adsorption of anionic dyes on chitosan grafted poly(alkyl methacrylate)s, Chem. Eng. J. **158** (2010) 393–401.

IZVOD

ADSORPCIJA AZO BOJA NA POLIMERNIM MATERIJALIMA

Vesna V. Panić[1], Sanja I. Šešlija[1], Aleksandra R. Nešić[2], Sava J. Veličković[3]

[1]*Inovacioni centar, Tehnološko–metalurški fakultet, Univerzitet u Beogradu, 11000 Beograd, Srbija*
[2]*Institut za Nuklearne nauke Vinča, Univerzitet u Beogradu, 11000, Beograd, Srbija*
[3]*Tehnološko–metalurški fakultet, Univerzitet u Beogradu, 11000 Beograd, Srbija*

(Pregledni rad)

Intenzivan industrijski razvoj praćen je sve većom količinom otpadnih voda, što u smislu zaštite životne sredine i održivog razvoja nalaže potrebu poboljšanja postojećih i uvodjenje novih postupaka obrade otpadnih voda. Posebnu naučno-tehnološku pažnju zahtevaju azo boje, koje su veoma toksične i u prirodi veoma teško razgradive. Azo boje su podložne bioakumulaciji, a zbog kancerogenih i mutagenih svojstava neretko su pretnja zdravlju ljudi i očuvanju okoline. Primenu fizičko-hemijskih metoda za uklanjanje azo-boja iz otpadnih voda često ograničavaju visoke cene, potrebe za odlaganjem nastalog štetnog mulja ili nastanak toksičnih sastojaka razgradnje. Adsorpcija je jedna od najzastupljenijih metoda za uklanjanje raznih zagadjivača iz otpadnih voda zbog jednostavnosti, ekonomičnosti i efikasnosti ove metode. S obzirom da su konvencionalni adsorbenti, kao što je aktivni ugalj, veoma skupi, u poslednje vreme se sve više ulaže u ispitivanja i razvoj novih materijala za uklanjanje zagadjivača iz otpadnih voda koji će biti lako razgradivi, netoksični, jeftini i efikasni u njihovom uklanjanju. U ovom radu biće prikazan pregled iz literature polimernih materijala za uklanjanje azo boja iz otpadnih voda. Polimerni materijali pokazuju prednosti u odnosu na konvencionalne adsrobente zbog jednostavne upotrebe i rukovanja s njima i mogućnosti oblikovanja u pogodne i željene forme. Adsorpcija na polimernim materijalima je najčešće reverzibilan proces, što nije slučaj kod konvencionalnih adsorbenta. Adsorbovana boja na polimernim materijalima, u zavisnosti od tipa boje, se lako može desorbovati u kiseloj ili alkalnoj sredini, kao i u acetonu, tako da se materijal može regenerisati i ponovo koristiti za uklanjanje boja iz otpadnih voda. U ovom radu će biti prikazani sintetički i prirodni polimeri u formi hidrogela, umreženih i kalemljenih sistema za uklanjanje azo boja. Takodje, prikazan je efekat različitih parametara kao što su koncentracija, pH i temperatura rastvora boje, na adsorpciju na polimernim materijalima.

Ključne reči: Adsorpcija • Azo boje • Sintetički polimeri • Hidrogelovi • Prirodni polimeri

Synthesis and characterization of thermosensitive hydrogels and the investigation of modified release of ibuprofen

Snežana S. Ilić-Stojanović[1], Ljubiša B. Nikolić[1], Vesna D. Nikolić[1], Jela R. Milić[2], Jakov Stamenković[1], Goran M. Nikolić[3], Slobodan D. Petrović[4]

[1]*University of Niš, Faculty of Technology, Leskovac, Serbia*
[2]*University of Belgrade, Faculty of Pharmacy, Belgrade, Serbia*
[3]*University of Niš, Faculty of Medicine, Niš, Serbia*
[4]*University of Belgrade, Faculty of Technology and Metallurgy, Belgrade, Serbia*

Abstract

The method of the synthesis of poly(*N*-isopropylacrylamide-*co*-2-hydroxypropyl methacrylate) hydrogels obtained by radical polymerization is described. Their characterization was carried out by the determination of the quantity of residual monomers and by investigating their structure using FTIR. Three glass transitions were detected by DSC method. The porous surfaces of hydrogels with incorporated ibuprofen were shown in SEM micrographs. The swelling ratio of hydrogels decreased with the temperature increase and the swelling transport mechanism changed from non-Fickian to Fickian. Ibuprofen was incorporated in the hydrogel as a drug carrier and the released quantity depending on the temperature was monitored by HPLC. The hydrogel with the lower cross-linker content had the highest swelling degree (α = 34.72) at 10 °C and released the largest amount of ibuprofen (64.21 mg/$g_{xerogel}$) at 40 °C.

Keywords: *N*-isopropylacrylamide, copolymer hydrogel, thermal properties, swelling, ibuprofen.

Available online at the Journal website: http://www.ache.org.rs/HI/

Polymers

SCIENTIFIC PAPER

UDC 678–13:66.095.26:547.057

Hem. Ind. **67** (6) 901–912 (2013)

doi: 10.2298/HEMIND130119038I

Hydrogels are polymer materials that have the ability to swell in water and to absorb great quantities of water or other physiological fluids within their structures, whereby their structure remains unchanged. Due to large water content, soft and elastic consistency, hydrogels, more than any other class of synthesized biomaterials, resemble living tissue [1]. They have the ability to respond to different environmental changes and show a dramatic change in properties such as the change of swelling degree; because of this they are named ”smart” or “intelligent” gels.

In the last twenty years, hydrogels, and especially poly(*N*-isopropylacrylamide), pNIPAM, have drawn great attention of researchers with respect to their application in medicine and pharmaceuticals [2]. Poly(*N*-isopropylacrylamide) is a biocompatible and non-biodegradable temperature-responsive hydrogel which has both hydrophilic and hydrophobic groups. The ability of hydrogels to absorb and release molecules of different size has enabled their use as carriers in the systems for the controlled release of drugs [3]. *N*-Isopropylacrylamide (NIPAM) was first synthesized by Coover and Shearer in 1953 [4]. The effects of external stimuli on some polymers were investigated in the 1960’s by Heskins and Guillet [5]. They found that under standard conditions, the lower critical solution temperature (LCST) at which pNIPAM passed through the phase transition was 32 °C. At temperatures below LCST, it exhibits a hydrophilic nature because the interaction of polymer chains with water molecules is dominant and hydration of hydrophobic groups of the polymer chain occurs, hydrogen bonds are formed and the gel swells. The conformation changes are primarily the result of releasing water molecules from the polymer structure [6].

To achieve the required temperature and pH sensitivity of a hydrogel during the synthesis, it is common to copolymerize the thermo-sensitive component, most often NIPAM, with a certain quantity of anionic monomer–acrylic, methacrylic, maleic, or itaconic acid [7–11]. By adjusting the composition of copolymer it is possible to bring the LCST value closer to physiological temperature (36–38 °C), which is especially important for the controlled release of drugs [12–13]. There are many published works which report the use of thermal analysis, study the phase transition of pNIPAM gels and measure LCST by using differential scanning calorimetry (DSC) [14–17]. The glass transition temperature (*T*g) of pNIPAM and copolymers of poly(*N*-isopropylacrylamide)-*co*-acrylamide was determined by using DSC [18]. At higher temperatures, the structure of the gel wrapper is controlled by introducing hydrophilic acrylamide as the functional temperature-sensitive intelli-

Correspondence: S. Ilić-Stojanović, University of Niš, Faculty of Technology, Bulevar oslobođenja 124, 16000 Leskovac, Serbia.
E-mail: ilic.s.snezana@gmail.com
Paper received: 19 January, 2013
Paper accepted: 19 April, 2013

gent system with the controlled drug release rate [19––21]. NIPAM gel is used for the design of the positive thermosensitive pulsing drug release system so that the drug release is triggered by the temperature increase and stopped by the temperature decrease [22–25].

Hydrophilic 2-hydroxypropyl methacrylate (HPMet) is a convenient biocompatible material with living tissues and satisfactory tolerance by cells [26]. It can copolymerize with other monomers to produce copolymers with a hydroxyl group at the chain end. It has the ability to preserve living tissues and antigens against various enzymes and reagents, and presents an excellent choice for various immunocytochemical procedures [27]. The controlled polymerization of two industrially relevant hydroxy-functional monomers, glycerol monomethacrylate and HPMet was investigated [28]. The isolation of lignin from the water mixture by using copolymer of NIPAM and HPMet was studied [14]. The synthesis of hydrogels based on NIPAM with HPMet obtained by gamma irradiation, their characterization and the investigation of caffeine release properties was investigated [29]. Unlike the corresponding copolymers, thermosensitive hydrogels based on NIPAM with HPMet have not been studied to great extent.

The aims of this paper were: the synthesis of poly(*N*-isopropylacrylamide-*co*-2-hydroxypropyl methacrylate) hydrogels, p(NIPAM-*co*-HPMet) by radical polymerization, their characterization and investigation of their application as a drug carrier. The structures of the obtained copolymers were characterized using FTIR, SEM and DSC techniques and by analyzing the residual monomer content and swelling behavior. From the standpoint of safety ibuprofen, 2-(4-isobutylphenyl) propionic acid was selected as a model drug. Ever since clinical tests in 1966 proved the activity of ibuprofen in the treatment of rheumatoid arthritis, and the first commercialization in 1969, ibuprofen has become one of the most important non-steroidal anti-inflammatory drugs (NSAID) [30,31]. The influence of monomer and cross-linker molar ratio on their swelling behavior was already published [32]. The presented results are one part of an extensive research concerning the possibility of application of p(NIPAM-*co*-HPMet) hydrogels as potential carriers for modified delivery of NSAID [33].

EXPERIMENTAL

Reagents

N-Isopropylacrylamide (NIPAM) 99%, 2-hydroxypropyl methacrylate (HPMet) 96.5% and 2,2'-azobis(2-methylpropionitrile) (AZDN) 98% by Acros Organics, New Jersey, US; ethylene glycol dimethacylate (EGDM) 97% by Fluka Chemical Corp., CH; acetone by Centrohem, Belgrade, RS; methanol by Unichem, Belgrade, RS; ibuprofen 98% by Sigma-Aldrich Co., US.

Synthesis of p(NIPAM-*co*-HPMet) hydrogel

Cross-linked copolymers of NIPAM with 5 mol% of HPMet, in reference to the amount of NIPAM monomer, were obtained by radical polymerization using EGDM as a cross-linker and AZDN as the initiator in acetone as the solvent. EGDM concentration in the reaction mixture varied: 0.5, 1, 1.5, 2 and 3 mol% compared to the total comonomer mass. After homogenization and the monomer dilution, the reaction mixture was injected into glass tubes which were then fused, and subjected to polymerization under the temperature regime: 70 °C 2 h, 80 °C 1 h, and 85 °C 0.5 h to activate the initiator and the polymerization process, and for the full utilization of the initiator. After cooling, the obtained gels were separated from the glass tubes. Gels were extracted by methanol to remove all non-reacted water-insoluble compounds, monomers and oligomers. Methanol was changed daily for three days. Then, they were submerged into methanol/distilled water solutions in 75/25, 50/50, 25/75 and 0/100% ratios and kept for a day in the order to effect flushing of methanol from the hydrogel. The extracts were analyzed by HPLC method to determine the amount of a residual monomer. Swollen gels were dried to constant mass at 20 to 40 °C to pass into the xerogel stage for further testing.

Characterization of p(NIPAM-*co*-HPMet) hydrogel

Fourier transform infrared spectroscopy (FTIR)

Samples of 1 mg of synthesized copolymers were pressed into a pellet with 150 mg of KBr of spectrophotometric purity and FTIR spectra were recorded on a BOMEM MB-100 (Hartmann & Braun, Canada) in the wavelength range of 4000–400 cm^{-1}.

Scanning electron microscopy (SEM)

Samples of swollen p(NIPAM-*co*-HPMet) hydrogel, one pure and one with loaded ibuprofen, were first lyophylised for SEM microscopy and then metalized by gold-palladium alloy (15/85) and then recorded on a JEOL scanning microscope JSM-5300.

Differential scanning calorimetry (DSC)

Thermal properties of samples were investigated by differential scanning calorimetry (DSC) by using a DSC Q100 (TA instruments). The samples were heated at ramping rate of 10 °C min^{-1}, with the gas flow (nitrogen) 50 cm^3 min^{-1} and the weight of the tested samples was about 3 mg. Standard calibration was performed by using indium, the melting temperature of which was 157 °C. The sensitivity of the instrument was 10 mV cm^{-1}.

Residual monomers analysis

The solutions obtained by the extraction of polymerized gels were analyzed by HPLC method on the

device: Agilent 1100 Series, column: ZORBAX XDB-C18 250 mm×4.6 mm, 5 µm, eluent: methanol, flow rate: 1 cm^3 min^{-1}, injected sample volume: 10 µl, temperature: 25 °C, detector: DAD 1A, detection wavelength: 220 nm.

Swelling behavior

Xerogels were immersed in distilled water and swelling was monitored gravimetrically at temperatures from 10 to 50 °C. The swelling ratio, α, was calculated as:

$$\alpha = \frac{m - m_0}{m_0} \quad (1)$$

where m_0 is the mass of xerogel and m is the mass of swollen gel at the time t.

Loading and release of ibuprofen studies

In order to investigate the possibilities of the application of synthesized hydrogels as carriers for the modified release, ibuprofen was used as the model drug. The xerogel was swollen in the ibuprofen solution in methanol/distilled water mixture (80/20), 40 mg cm^{-3} for 48 h.

The swollen gel was soaked with 7 cm^3 of distilled water and the amount of the released ibuprofen was monitored for 24 h at the temperatures of 20 and 40 °C. The content and amount of the released ibuprofen was performed by HPLC an Agilent 1100 Series device, under the following conditions: detector: DAD 1200; detection wavelength: 225 nm, column: Zorbax XDB-C18, 250 mm×4.6 mm, 5 µm, eluent: methanol/distilled water, 80/20; eluent flow: 1 cm^3 min^{-1}; injected sample volume: 20 µl, temperature: 25 °C.

RESULTS AND DISCUSSION

Synthesis of p(NIPAM-co-HPMet) hydrogel

The synthesis of p(NIPAM-*co*-HPMet) hydrogel was performed with 0.5, 1, 2 and 3 mol% of EGDM. The obtained product with cross-linker content below 1 mol% of EGDM remained in solution state after polymerization without required hydrogel consistency, and as such it was not used for further analysis.

Characterization of p(NIPAM-co-HPMet) hydrogel

Fourier transform infrared spectroscopy (FTIR)

The nature of bonding and the structure of obtained hydrogels were characterized by FTIR. Figure 1 shows FTIR spectra of NIPAM and HPMet monomers and EGDM cross-linker.

In FTIR spectra of NIPAM the following bands were observed: $\nu_s(CH_3)$ at 2875 cm^{-1}, $\nu_{as}(CH_3)$ at 2970 cm^{-1}, $\nu_{as}(CH_2)$ at 2933 cm^{-1}, $\nu_{as}(CH)$ from the vinyl group at 3072 cm^{-1} where the typical absorption amounts are between 3000–3100 cm^{-1}. The valence absorption of N–H bond from the amide structure was observed at 3284 cm^{-1}, while the amide band I was observed at 1658 cm^{-1}. The band at 1622 cm^{-1} originated from the valence vibrations of the C=C double bond.

The FTIR spectrum of HPMet monomer showed a wide band originating from the valence vibration of the O–H group and was present between 3100–3600 cm^{-1} with a peak at 3450 cm^{-1}. Symmetrical and asymmetrical bands from C–H vibrations were also present: $\nu_s(CH_3)$ at 2894 cm^{-1} and $\nu_{as}(CH_3)$ at 2980 cm^{-1}. Valence vibrations of the C=C double bond were observed at 1638 cm^{-1}.

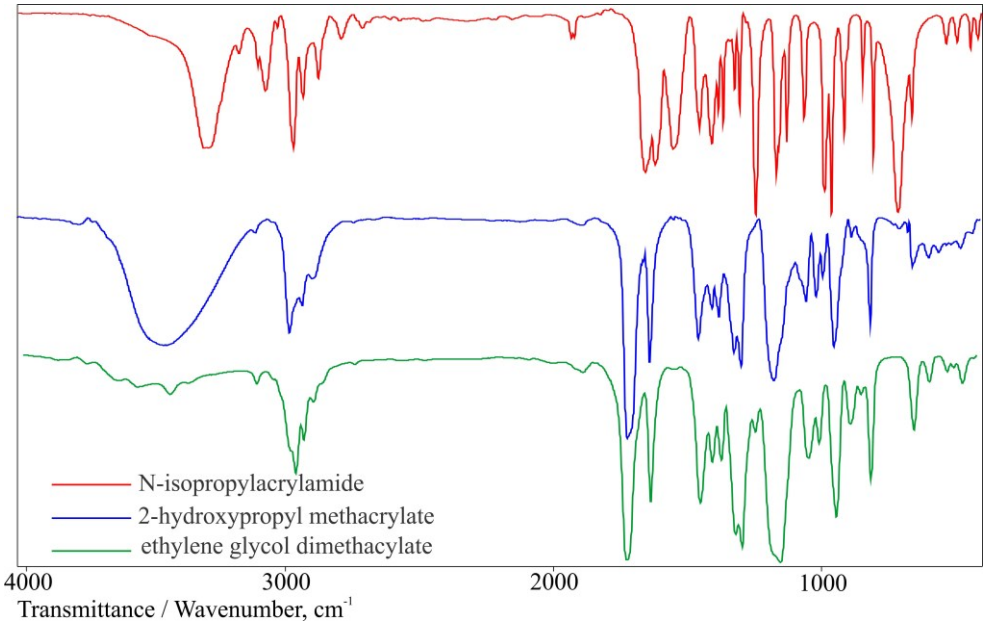

Figure 1. FTIR Spectra of NIPAM, HPMet and EGDM.

In the FTIR spectrum of EGDM a band from the valence vibrations of the C=O ester group were present, conjugated with double C=C bond, with a peak at 1725 cm^{-1}. There are peaks originating from valence vibrations of C–O bond, reflected by wide peaks at about 1150 to 1180 cm^{-1}. The peak at 1636 cm^{-1} originated from the absorption of the double bond. Also, the bands: $\nu_s(CH_3)$ at 2894 cm^{-1}, $\nu_{as}(CH_3)$ at 2960 cm^{-1}, $\nu_{as}(CH_2)$ at 2930 cm^{-1}, ν_{as}(CH) from the vinyl group at 3105 cm^{-1} were observed.

Figure 2 shows FTIR spectra of synthesized p(NIPAM-*co*-HPMet) xerogels with: 1, 1.5, 2 and 3 mol% of EGDM. Since the hydrogel synthesis was carried out by the initiation using radicals formed by decomposition of AZDN, there appeared to be no absorption in gel FTIR spectra that could originate from the double C=C bond. N–H and O–H groups in the polymer chains were observed as lateral groups. In FTIR spectra, wide bands in the range from 3100 to 3600 cm^{-1} were observed, with clearly indicated peaks at about 3282 cm^{-1} and 3431 cm^{-1}, originating from valence vibrations of N–H and O–H groups, respectively. Also, there was a band originating from amide band I from C=O amide at 1648 cm^{-1}, C=O valence from ester at 1716 cm^{-1}, as well as the bands originating from valence vibrations of C-H bonds of methyl and methylene groups in the range 2800-3000 cm^{-1}. FTIR spectra of p(NIPAM-*co*--HPMet) with different molar ratio of EGDM cross-linker had a similar aspect since the concentration of EGDM was too low to be noticed in FTIR spectra. On the other hand, the monomer ratio in the copolymer was identical.

Scanning electron microscopy (SEM)

SEM was used to investigate the morphology of obtained hydrogel. In Figure 3a, the SEM micrograph of hydrogel of p(NIPAM-*co*-HPMet) is given, showing the structure of hydrogel with the characteristic porous surface. The hydrogel morphology has a structure with spherical and ellipsoidal surfaces that probably facilitate and accelerate the absorption of water into the gel. All hydrogel samples with different cross-linker ratios show a similar surface structure. Figure 3b presents the surface structure of hydrogel with the loaded particle of ibuprofen.

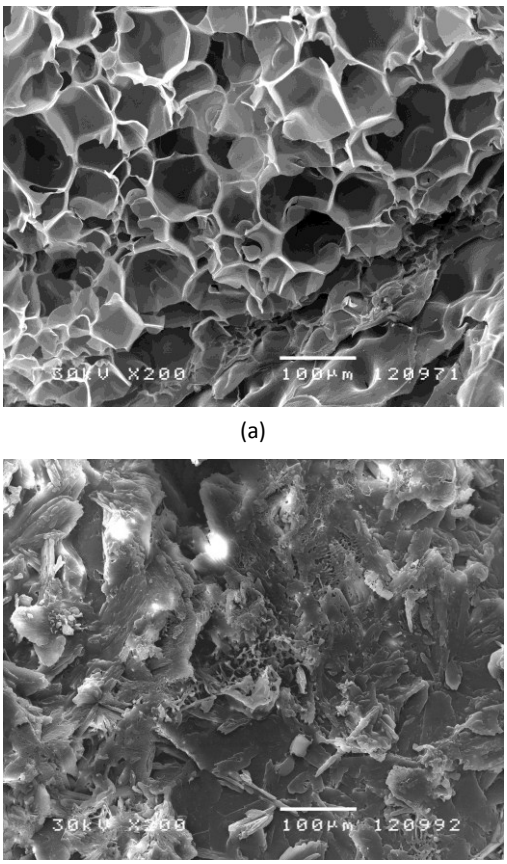

Figure 3. SEM Micrographs of p(NIPAM-co-HPMet): a) pure and b) with loaded ibuprofen.

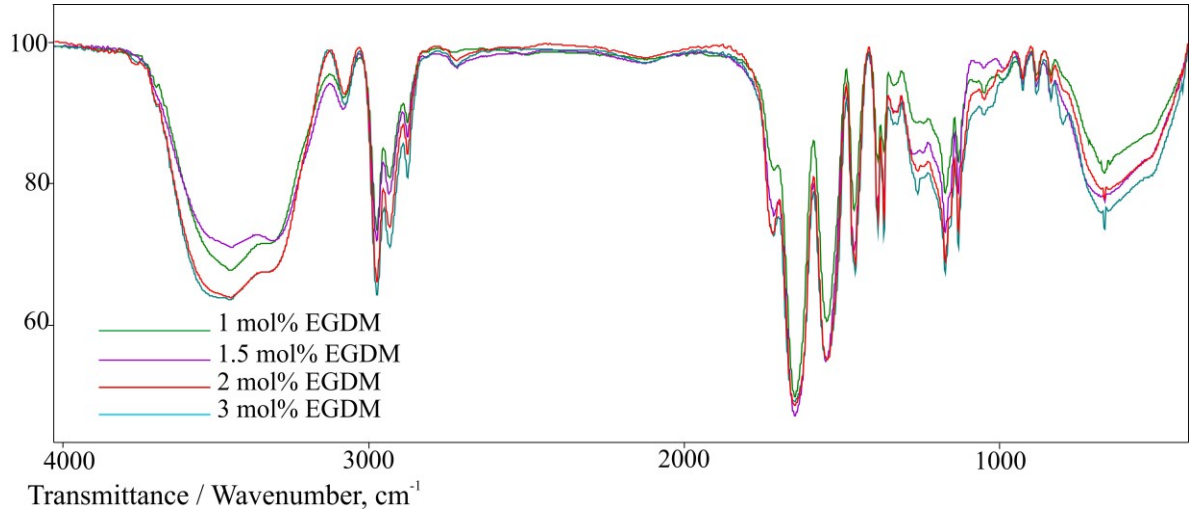

Figure 2. FTIR Spectra of p(NIPAM-co-HPMet) xerogels with 1, 1.5, 2 and 3 mol% of EGDM.

Differential scanning calorimetry (DSC)

The glass transition temperature of copolymerized xerogels was investigated. DSC thermograms obtained for p(NIPAM-*co*-HPMet) copolymers with 1, 2 and 3 mol% of EGDM in the themperature range 50–100 °C and 100–150 °C are showed in Figure 4a and b, respectively, as well as Table 1. As it can be seen, p(NIPAM-*co*-HPMet) has three glass transition temperatures determined with the endothermic peaks of weak intensity. The result analysis showed that thermal properties of p(NIPAM-*co*-HPMet) xerogels do not show a sharp phase transition to glassy state. The occurrence of 3 glass transitions may be due to structural irregularities of polymer networks with different crosslinking ratio and the presence of retained traces of unreacted monomers in the polymer network. According to available literature data, the pNIPAM xerogel has two glass transition temperatures T_g at 85 and 135 °C [18,34–36], while pHPMet has a T_g at 95 °C [37]. The first and the third glass transition temperature (T_{g1} and T_{g3}) may be due to pNIPAM, and the second one T_{g2}, in the temperature range 75–85 °C is due to pHPMet.

The values of T_{g1} and T_{g2} indicated the increasing trend when the cross-linker content increased, as it can be seen in Table 1. This was obvious because the increase in the crosslinker content in p(NIPAM-*co*-HPMet) xerogels resulted in higher dense networks

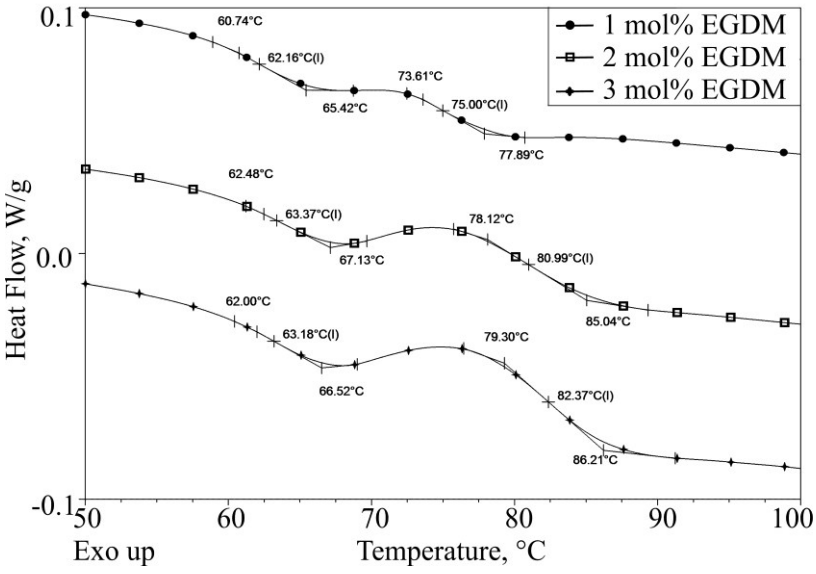

(a)

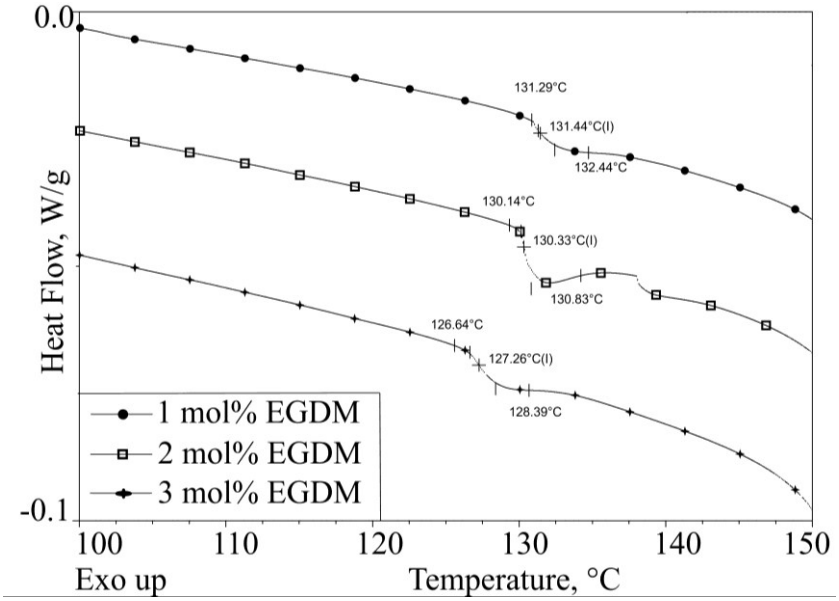

(b)

Figure 4. DSC Thermograms of p(NIPAM-co-HPMet) in temperature range: a) 50–100 °C and b) 100–150 °C.

that lead to higher T_g values. It can be noticed that the values of T_{g3} of copolymers p(NIPAM-*co*-HPMet) were decreased in comparison to pNIPAM homopolymer, when adding a certain amount of HPMet monomer. The p(NIPAM-*co*-HPMet) copolymers reached the third phase transition to glassy state at lower temperature values, proportionally to mole ratio of the cross-linker. The decrease of cross-linking ratio in copolymer leads to less crystalline structure, because the crystalline domains which occur in pure pNIPAM disappear. All xerogels were synthesized under the same conditions and with the same HPMet monomer content (5 mol%) and the only difference was the cross-linker content. It can be seen that small differences in T_g were caused by differences in the density of the polymer network, which is directly related to polymer-polymer interactions.

Table 1. Glass transition temperatures of p(NIPAM-co-HPMet) xerogels

EGDM content, mol%	T_{g1} / °C	T_{g2} / °C	T_{g3} / °C
1	62.16	75.00	131.44
2	63.37	80.99	130.33
3	63.18	80.37	127.26

Residual monomer analysis

HPLC Chromatographs of NIPAM and HPMet hydrogels monomers were made on DAD detector. The monomer concentration was determined based on the calibration curve.

The dependence of the peak area on NIPAM concentration was linear for concentration range of 1 mg cm^{-3}, for which the following equation applies:

$$C = \frac{A - 113}{26652.8} \quad (2)$$

where A is the peak area (mAUs), and C is the concentration of NIPAM (mg cm^{-3}).

The dependence of the peak area on HPMet concentration was linear for concentration range of 1 mg cm^{-3}, for which the following equation applies:

$$C = \frac{A - 435.3}{10164.7} \quad (3)$$

where A is the peak area (mAUs), and C is concentration of HPMet (mg cm^{-3}). The amounts of residual monomers in synthesized copolymer hydrogels are given in Table 2.

The calculation regarding the quantity of monomer in the reaction mixture at the beginning of the reaction shows that the values were from 0.55 to 1.05% for NIPAM, and from 1.37 to 1.62% for HPMet. The content of residual monomers leads to the conclusion that the conversion of monomers was almost complete.

Table 2. Amount of residual monomers in xerogel

p(NIPAM-*co*-HPMet)	EGDM content, mol%			
	1	1.5	2	3
	Residual monomer, mg g^{-1}			
NIPAM	8.006	8.109	9.675	5.076
HPMet	1.079	1.088	1.273	1.056

Swelling behavior

The time dependence of hydrogels swelling ratio, α, for p(NIPAM-*co*-HPMet) observed at temperatures of 10 °C is given in Figure 5. As it can be seen, the swelling ratio increases extensively during the first 6 h.

At the temperature of 10 °C the swelling ratio is about 20% higher compared to the values obtained for swelling ratio at 20 °C [32]. The highest swelling ratio was noted in the hydrogel with the lowest EGDM cross-

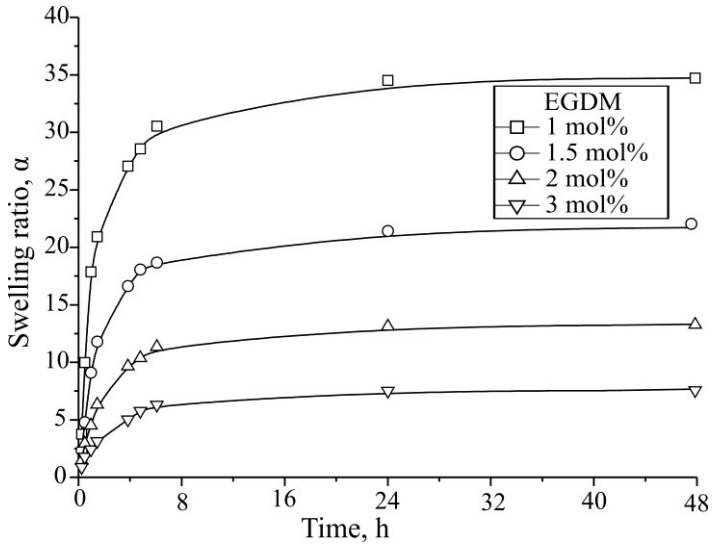

Figure 5. Swelling ratio, α, at 10 °C for p(NIPAM-co-HPMet) hydrogels with different EGDM content.

linker content at 10 °C, *i.e.*, 1 g of gel with 1 mol% EGDM can absorb about 35 g of water. The swelling ratio decreases at both temperatures with the increase of the cross-linking degree, as expected, because the higher cross-linker content increases the density of cross-linking, thus reducing the mobility of polymer chains. The reason for the reduction of the swelling ratio at all temperatures when the amount of cross-linker is increased is the formation of a thicker cross-linking in the polymer gel. Then, the polymer chains have less space to expand, they are more fixed and, as a consequence the water absorption is lower. By adjusting the cross-linker content, the internal free volume that can be filled with water molecules can be changed. On the contrary, when the amount of cross-linker is lower, the length of polymer chains between two nodes is greater and the chains can expand and absorb more water. Great internal free volume allows a greater amount of water to be placed inside the gel, which favors the swelling [32].

The water transport into p(NIPAM-*co*-HPMet) polymer networks may be analyzed based on the nature of the sorption kinetics of the initial swelling data fitted to the exponential Ficks equation, only valid for the first 60% of the fractional uptake:

$$F = M_t/M_e = kt^n \quad (4)$$

where F is the fractional sorption, M_t/M_e; M_t and M_e are the amounts of he absorbed solvent at time t and equilibrium, respectively; k is a kinetic constant incurporating characteristic of the network structure, n is the diffusion exponent which is indicative of the transport mechanism.

The logarithmic form of Eq. (4) was used to determine the values of n and k, from slope and intercept the plots of ln F *versus* ln t for hydrogels at different EGDM contents:

$$\ln F = \ln (M_t/M_e) = \ln k + n \ln t \quad (5)$$

If $n < 0.5$ the swelling process is controlled by the Fickian diffusion mechanism, whereas a value of $0.5 < n < 1$ indicates an anomalous non-Fickian type diffusion and contributes to the water-sorption process. The calculated values for equilibrium swelling ratios and for the linear dependence of ln (M_t/M_e) on ln t of p(NIPAM-*co*-HPMet) hydrogels for hydrogel samples with different compositions at 20 and 40 °C are shown in Table 3.

The obtained values for diffusion exponents, *n,* at the temperature of 20 °C increases from 0.602 to 0.793, so p(NIPAM-*co*-HPMet) is classified as a hydrogel with anomalous transport behavior, which is intermediate between Fickian and Case II (n = 1), also known as non-Fickian behavior. Their swelling process is controlled by the diffusion of liquids and the relaxation of the polymer chains. Different calculated diffusion exponents for the swelling at 40 °C (n is between 0.303 and 0.311) suggests that the swelling process is controlled by diffusion only. This indicates that the p(NIPAM-*co*-HPMet) hydrogels are submitted to the Fickian diffusion for all EGDM molar ratio. This evidence also shows that the swelling transport mechanism was transferred from Fickian to non-Fickian transport with the decreasing themperature. The results in Table 3 indicate that as the EGDM content increases, the water fractional uptake at the same absorption time decreases, but the kinetic constant, k, and diffusion exponents, n, increase. The kinetic constants are higher at 40 °C and this fact suggests that the diffusion rate decreases at the temperature upper LCST, due to the decrease in size of free spaces in the network.

Comparing the obtained swelling results with the p(NIPAM-*co*-HPMet) hydrogels swelling ratio results obtained by gamma irradiation and described in the published work of Nizam El-Din, certain differences in the swelling ratio are noted [29]. The gels obtained by gamma irradiation have a lower swelling ratio compared to the gels obtained by radical copolymerization in the presence of EGDM cross-linker. By using gamma irradiation, the cross-linking intensity of copolymer depended on the intensity of gamma rays, and p(NIPAM-*co*-HPMet) hydrogel with lower molar ratio of HPMet (2 mol%), obtained by using 20 kGy gamma rays at 25 ºC in water had a swelling ratio of about 6. Similar result were obtained for p(NIPAM-*co*-HPMet) hydrogel with a higher molar ratio of HPMet monomer (10 mol%) produced by the polymerization method of Wensheng Cai and collaborators [14], which also achieved the swelling ratio of 6.

The thermosensitive nature of p(NIPAM-*co*-HPMet) was investigated by monitoring volume changes of swollen hydrogels with the increase of temperature.

Table 3. Equilibrium swelling ratio, α, and kinetic parameters of water diffusion into p(NIPAM-co-HPMet) hydrogels

EGDM, mol%	20 °C				40 °C			
	α	n	$k\times10^2$ / min$^{-1/2}$	R^2	α	n	$k\times10^2$ / min$^{-1/2}$	R^2
1	29.589	0.793	0.959	0.973	5.79	0.303	1.705	0.913
1.5	18.002	0.751	1.230	0.953	4.29	0.304	1.708	0.913
2	11.043	0.669	1.825	0.962	2.36	0.306	1.709	0.913
3	6.244	0.602	3.016	0.984	1.60	0.311	1.749	0.957

The swelling ratios as dependent on the temperature and EGDM cross-linker content are shown in Figure 6a and b, respectively.

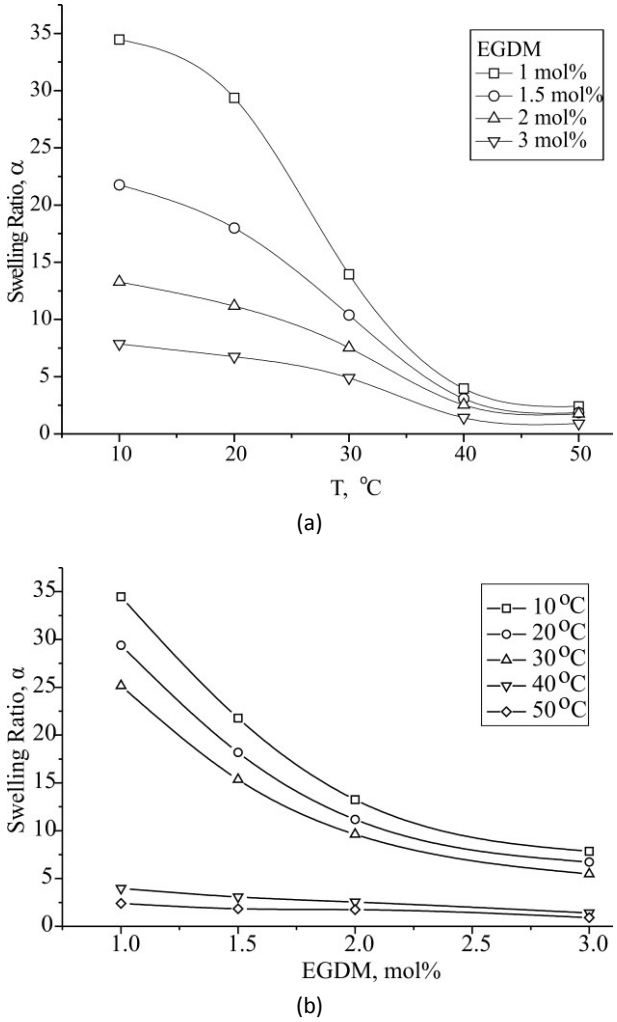

Figure 6. Swelling ratio, α, of p(NIPAM-co-HPMet) hydrogels in dependents on: a) temperature and b) EGDM content.

The decrease of the swelling ratio with the temperature increase is noted as an important characteristic of p(NIPAM-*co*-HPMet). As it can be seen, the highest swelling ratio values of the hydrogel were reached at the temperatures of 10 and 20 °C began to decrease, passing through the phase transition and intensive decrease at 40 °C, and above 50 °C reach asymptotic values (α = 0.7 for hydrogel with 3 mol% EGDM at 50 °C). Phase transition can be noted at temperature range 30–40 °C. These results are consistent with published literature data [29]. The LCST of p(NIPAM-*co*--HPMet) hydrogels was determined at 34 °C using DSC [14]. The pure pNIPAM hydrogel has LCST at 32 °C [6]. By copolymerization of NIPAM with hydrophilic HPMet monomer, it was achieved that LCST of p(NIPAM-*co*--HPMet) copolymer had slightly higher LCST than pNIPAM hydrogel and became closer to the physiological temperature. Visual monitoring of hydrogels at the phase transition temperature shows that they become opaque, milky white in color, and their collapse occurs, i.e. the contraction. The phase transition of hydrogel is determined by a delicate balance between the hydrophilic and hydrophobic groups inside the hydrogels. Because of the presence of hydrophilic HPMet monomer, the influence of hydrophobic NIPAM monomer groups is reduced and LCST of p(NIPAM-*co*-HPMet) copolymer is increased compared to pure pNIPAM. During the phase transition the breaking of hydrogen bonds and water molecules between polymer chains and the domination of hydrophobic interactions between polymer chains occur, which causes the elimination of water molecules from hydrogel. As it was published earlier, the number of hydrogen bonds in the hydrogel increases the collapse of the gel. They can further be built from the terminal OH group of HPMet with electronegative O atom from the ester functional groups (HPMet and EGDM), or with N from NIPAM [32].

All noted characteristics of p(NIPAM-*co*-HPMet) hydrogel are very important for their potential application as a carrier for the controlled release of NSAID. For the intelligent delivery of antipyretics responding to the raised body temperature in a state, a thermosensitive release system is required. This is the reason for further studying of p(NIPAM-*co*-HPMet) as an "intelligent gel", a material that reacts to the stimulus of the temperature change.

Loading and release of ibuprofen studies

The investigation of the content and amount of the released ibuprofen from thermosensitive hydrogels depending of temperature was carried out by HPLC. A calibration curve was drawn using a characteristic intensive peak with maximum absorption wavelength (λ_{max}) at 225 nm from DAD detector and the HPLC chromatogram (R_t = 2.97 min) for ibuprofen. The dependence of the peak area on the ibuprofen amount is linear for the concentration range to 1 mg cm^{-3}. For linear dependence, the following equation applies:

$$C = \frac{A - 201.2}{34952.1} \tag{4}$$

where A is the peak area (mAUs), and C is the the amount of ibuprofen (mg cm^{-3}). From this equation the unknown released concentration from the samples was calculated. The amount of ibuprofen loaded in the hydrogels was measured before the release experiment. The loading process was carried out in the saturated solution of ibuprofen and the amounts measured for hydrogels with different cross-linker ratio are shown in Table 4.

It was found that the amount of loaded ibuprofen depended on the hydrogel composition, according to

their swelling properties described in the previous part. The results for the released ibuprofen from hydrogels at room temperatures of 20 and 40 °C, similar to the body fever temperature, are shown in Figure 7a and 7b, respectively.

Table 4. The amount of loaded ibuprofen into p(NIPAM-co-HPMet)

EGDM, mol%	Loaded ibuprofen	
	$mg/g_{xerogel}$	%
1	481.77	97.32
1.5	396.35	84.74
2	337.49	61.29
3	241.79	51.36

The analysis of the obtained results in the first 24 h shows that higher ibuprofen concentration release from hydrogel is achieved when the system is exposed to higher temperature. It can be observed that at 40 °C the hydrogel with the lowest cross-linker content released the largest amount of ibuprofen (64.21 $mg/g_{xerogel}$, or 13.33% of the total loaded mass). Therefore, different temperatures may be responsible for different release behaviors. Namely, at room temperature, when the hydrogel containing ibuprofen is immersed into the water medium, the drug is transferred from the gel into water by free diffusion. If the temperature is increased, besides the free diffusion, there is an active drug extrusion of incorporated ibuprofen due to the collapse of swollen hydrogel as a consequence of the temperature increase and phase transition occurrence. This higher release rate may be related to the higher swelling ratio of the hydrogel and the weak H-bonding interaction between ibuprofen and the polymer network. At the temperature higher

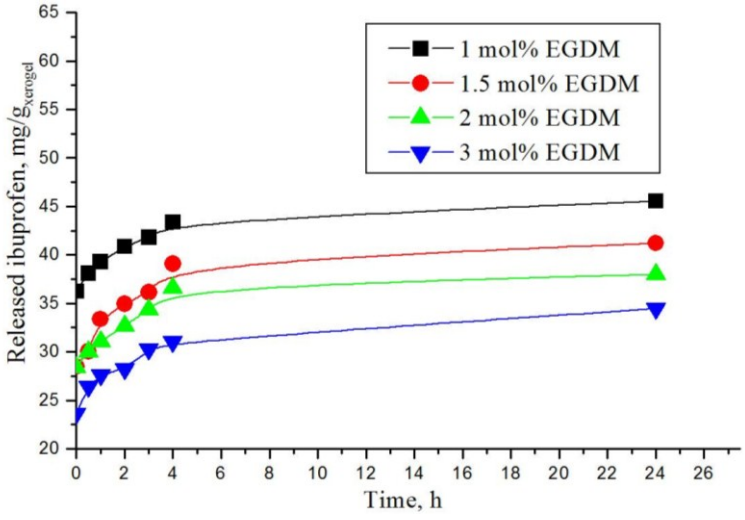

(a)

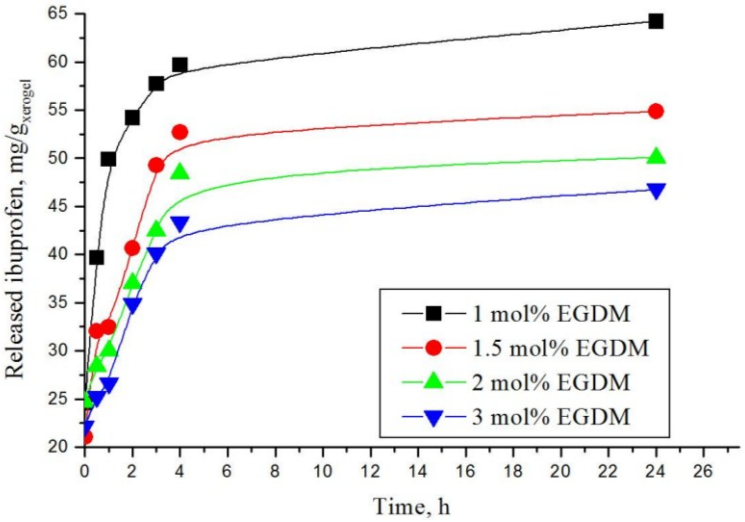

(b)

Figure 7. Ibuprofen release from p(NIPAM-co-HPMet) hydrogels at: a) 20 and b) 40 °C.

than LCST, the intermolecular hydrogen bonding between ibuprofen and hydrogel chains was broken and the drug releases from the hydrogel. The phase transition occurrence is leads to p(NIPAM-*co*-HPMet) hydrogel deswell with the increase of temperature, which leads to the decrease of the swelling degree. Thus the results are consistent with the achieved equilibrium swelling degrees of synthesized hydrogels. The kinetic parameters of the ibuprofen release mechanism from hydrogel were assessed by fitting experimental release data to Fick's equation (5) and presented in Table 5.

Table 5. Kinetic parameters of released ibuprofen from p(NIPAM-co-HPMet) at 20 and 40 °C

EGDM, mol%	Released ibuprofen			
	20 °C		40 °C	
	n	$k\times10^2$ $min^{-1/2}$	n	$k\times10^2$ $min^{-1/2}$
1	0.099	0.959	0.362	1.705
1.5	0.073	1.230	0.233	1.708
2	0.068	1.825	0.225	1.709
3	0.052	3.016	0.194	1.749

The obtained results indicate that the release process is controlled by the Fickian diffusion mechanism (n < 0.5) at both temperatures. The release profiles showed a reduction in the released amount of ibuprofen at both temperatures as the EGDM concentration was increased owing to the higher network density and small available free volume between the chains. On the other hand, as the EGDM content decreased, more ibuprofen was released from the hydrogel, which could be explained by the swelling behavior of hydrogels, as a function of EGDM content.

One of the most attractive features of these hydrogels as drug carriers is their intelligent property to external temperature changes. It is important and practical to examine the drug release data from those hydrogels at the temperature higher than LCST like the fever body temperature (40 °C). A potential application of p(NIPAM-*co*-HPMet) hydrogel in the drug delivery systems modified by temperature can be expected.

CONCLUSIONS

A new method of the preparation of thermosensitive hydrogels based on NIPAM with 5 mol% of HPMet monomer, using various concentrations of cross-linker was described. When analyzing the FTIR spectra of the obtained p(NIPAM-*co*-HPMet) hydrogels containing different amounts of EGDM cross-linker, no significant difference in the structure was observed. SEM microscopy confirmed the porous structure of hydrogels and the changed structure with incorporated ibuprofen. Three-glass transition temperatures were determined by the DSC method. The content of residual monomers showed that the conversion of NIPAM and HPMet monomers was almost complete. The swelling ratio of hydrogels decreased at all temperatures with the increase of cross-linker content, and also with the increase of the temperature. The swelling transport mechanism was transferred from Fickian at 40 °C to non-Fickian transport with the decreasing temperature at 20 °C. p(NIPAM-*co*-HPMet) are used as drug carriers for testing the ibuprofen modified release. The hydrogel with the highest swelling degree released the largest amount of ibuprofen at 40 °C. This may be explained by the incorporation of more OH groups of ibuprofen that form hydrogen bonds in the polymer network. During the phase transition, they break because of the hydrogel collapse due to the increase of the temperature upper LCST. In fact, this gives an opportunity for a wider investigation of pharmaceutical application of these hydrogels, for the modified release of NSAID.

Acknowledgement

Financial support provided by the Ministry of Education, Science and Technological Development of the Republic of Serbia, for project No. TR-34012 is gratefully acknowledged.

REFERENCES

[1] N.A. Peppas, P. Bures, W. Leobandung, H. Ichikawa, Hydrogels in pharmaceutical formulations, Eur. J. Pharm. Biopharm. **50** (2000) 27–46.

[2] J.F. Mano, Stimuli-responsive polymeric systems for biomedical applications, Adv. Eng. Mater. **10** (2008) 515––527.

[3] Y. Qiu, K. Park, Environment-sensitive hydrogels for drug delivery, Adv. Drug Delivery Rev. **53** (2001) 321–339.

[4] H.W. Coover, N.H. Shearer, *N*-substitued acrylamides by vapor phase method using acrylic acid, US 2,719,177 (1955).

[5] M. Heskins, J. Guillet, Solution properties of poly(*N*-isopropylacrylamide), J. Macromol. Sci., A **2** (1968) 1441––1455.

[6] Y.H. Bae, S.W. Kim, L.I. Valuev, Pulsatile drug delivery device using stimuli sensitive hydrogel, US 5,226,902 (1993).

[7] M.T. Garay, M.C. Llamas, E. Iglesias, Study of polymer-polymer complexes and blends of poly(N-isopropylacrylamide) with poly(carboxylic acid): 1. Poly(acrylic acid) and poly(methacrylic acid), Polymer **38** (1997) 5091–5096.

[8] J.E. Chung, M. Yokoyama, M. Yamato, T. Aoyagi, Y. Sakurai, T. Okano, Thermo-responsive drug delivery from polymeric micelles constructed using block copolymers of poly(N-isopropylacrylamide) and poly(butylmethacrylate), J. Controlled Release **62** (1999) 115–127.

[9] Z. Shen, K. Terao, Y. Maki, T. Dobashi, G. Ma, T. Yamamoto, Synthesis and phase behavior of aqueous poly(*N*-isopropylacrylamide-co-acrylamide), poly(*N*-isopropylacrylamide-*co*-*N*,*N*-dimethylacrylamide) and poly*(N*-isopropylacrylamide-co-2-hydroxyethyl methacrylate), Colloid Polym. Sci. **284** (2006) 1001–1007.

[10] T. Gan, Y. Zhang, Y. Guan, *In situ* gelation of P(NIPAM-HEMA) microgel dispersion and its applications as injectable 3d cell scaffold, Biomacromolecules **10** (2009) 1410–1415.

[11] M. Kalagasidis-Krušić, S. J. Velicković, J. Filipović, Poly-[(*N*-isopropylacrylamide)-co-(itaconic acid)] hydrogels with poly(ethylene glycol), Polym. Int. **59** (2010) 256––262.

[12] C. Zhao, X. Zhuang, P. He, C. Xiao, C. He, J. Sun, X. Chen, X. Jin, Synthesis of biodegradable thermo- and pH-responsive hydrogels for controlled drug release, Polymer **50** (2009) 4308–4316.

[13] C.M. Schilli, M. Zhang, E. Rizzardo, S.H. Thang, Y.K. Chong, K. Edwards, G.A. Karlsson, H.E. Muller, A New Double-Responsive Block Copolymer Synthesized *via* RAFT Polymerization: Poly(*N*-isopropylacrylamide)-block-poly(acrylic acid, Macromolecules **37** (2004) 7861–7866.

[14] W. Cai, E.C. Anderson, R.B. Gupta, Separation of lignin from aqueous mixtures by ionic and nonionic temperature-sensitive hydrogels, Ind. Eng. Chem. Res. **40** (2001) 2283–2288.

[15] M. Shibayama, S. Mizutani, S. Nomura, Thermal properties of copolymer gels containing *N*-isopropylacrylamide, Macromolecules **29** (1996) 2019–2024.

[16] M.D.C. Topp, P.J. Dijkstra, H. Talsma, J. Feijen, Thermosensitive micelle-forming block copolymers of poly(ethylene glycol) and poly(*N*-isopropylacrylamide), Macromolecules **30** (1997) 8518–8520.

[17] H. Inomata, S. Goto, S. Saito, Phase transition of *N*-substituted acrylamide gels, Macromolecules **23** (1990) 4887–4888.

[18] R.G. Sousa, W.M. Magalhães, R.F.S. Freitas, Glass transition and thermal stability of poly(*N*-isopropylacrylamide) gels and some of their copolymers with acrylamide, Polym. Degrad. Stab. **61** (1998) 275–281.

[19] G. Grassi, R. Farra, P. Caliceti, G. Guarnieri, S. Salmaso, M. Carenza, M. Grassi, Temperature-Sensitive Hydrogels: Potential Therapeutic Applications, Am. J. Drug Delivery 3 (2005) 239–251.

[20] D.C. Coughlan, F.P. Quilty, O.I. Corrigan, Effect of drug physicochemical properties on swelling/deswelling kinetics and pulsatile drug release from thermoresponsive poly (*N*-isopropylacrylamide) hydrogels, J Control. Release **98** (2004) 97–114.

[21] C. Elvira, J.F. Mano, J.S. Roman, R.L. Reis, Starch-based biodegradable hydrogels with potential biomedical applications as drug delivery systems, Biomaterials **23** (2002) 1955–1966.

[22] R. Yoshida, Y. Kaneko, K. Sakai, T. Okano, Y. Sakurai, Y.H. Bae, S.W. Kim, Positive thermosensitive pulsatile drug release using negative thermosensitive hydrogels, J. Controlled Release **32** (1994) 97–102.

[23] Y. Shin, J.H. Chang, J. Liu, R. Williford, Y.K. Shin, G.J. Exarhos, Hybrid nanogels for sustainable positive thermosensitive drug release, J. Controlled Release **73** (2001) 1–6.

[24] T. Okano, Y.H. Bae, H. Jakobs, S.W. Kim, Thermally on-off switching polymers for drug permeation and release, J. Controlled Release **11** (1990) 255–265.

[25] Y.Y. Akiyama, A. Kikuchi, M. Yamato, T. Okano, Ultrathin poly (*N*-isopropylacrylamide) grafted layer on polystyrene surfaces for cell adhesion/detachment control, Langmuir **20** (2004) 5506–5511.

[26] J. Kopeček, L. Šprincl, H. Bažilová, J. Vacík, Biological tolerance of poly(*N*-substituted acrylamides), J. Biomed. Mat. Res. **7** (1973) 111–121.

[27] T. Rustemeyer, S. De Ligter, B.M.E. Von Blomberg, P.J. Frosch, R.J. Scheper, Human T lymphocyte priming in vitro by haptenated autologous dendritic cells, Clin. Exp. Immunol. **117** (1999) 209–216.

[28] M. Save, J.V.M. Weaver. S.P. Armes, Atom transfer radical polymerization of hydroxy-functional methacrylates at ambient temperature: comparison of glycerol monomethacrylate with 2-hydroxypropyl methacrylate, Macromolecules **35** (2002) 1152–1159.

[29] H.M. Nizam El-Din, Characterization and caffeine release properties of *N*-isopropylacrylamide/hydroxypropyl methacrylate copolymer hydrogel synthesized by gamma radiation, J. Appl. Polym. Sci. **119** (2011) 577––585.

[30] WHO Model List of essential Medicines, 17th list, March 2011, World Health Organization.

[31] S.S. Adams, Discovery of Brufen, Chem. Brit. **23** (1987) 1193–1198.

[32] S.S. Ilić-Stojanović, Lj. Nikolić, V. Nikolić, M. Stanković, J. Stamenković, I. Mladenović-Ranisavljević, S.D. Petrović, Influence of monomer and crosslinker molar ratio on the swelling behaviour of thermosensitive hydrogels, Chem. Ind. Chem. Eng. Q. **18** (2012) 1–9.

[33] S.S. Ilić-Stojanović, Lj. Nikolić, V. Nikolić, J. Milić, J. Stamenković, G.M. Nikolić, S.D. Petrović, Potential application of thermosensitive hydrogels for controlled release of phenacetin, Hem. Ind. **66** (2012) 831–839.

[34] A. Allı, B. Hazer, Poly(N-isopropylacrylamide) thermoresponsive cross-linked conjugates containing polymeric soybean oil and/or polypropylene glycol, Eur. Polym. J. **44** (2008) 1701–1713.

[35] M.Y. Mohan, K. Lee, T. Premkumar, K.E. Geckeler, Hydrogel networks as nanoreactors: A novel approach to silver nanoparticles for antibacterial applications, Polymer **48** (2007) 158–164.

[36] J. Brandrup, E. H. Immergut, Polymer Handbook, John Wiley, New York, 1975, p. III-147.

[37] J. Dai, S.H. Goh, S.Y. Lee, K.S. Slow, Complexation between poly(2-hydroxypropyl methacrylate) and three tertiary amide polymers, J. Appl. Polym. Sci. **53** (1994) 837–845.

IZVOD

SINTEZA I KARAKTERIZACIJA TERMOOSETLJIVIH HIDROGELOVA I ISPITIVANJE MODIFIKOVANOG OSLOBAĐANJA IBUPROFENA

Snežana S. Ilić-Stojanović[1], Ljubiša B. Nikolić[1], Vesna D. Nikolić[1], Jela R. Milić[2], Jakov Stamenković[1], Goran M. Nikolić[3], Slobodan D. Petrović[4]

[1]*Univerzitet u Nišu, Tehnološki fakultet, Leskovac, Republika Srbija*
[2]*Univerzitet u Beogradu, Farmaceutski fakultet, Beograd, Republika Srbija*
[3]*Univerzitet u Nišu, Medicinski fakultet, Niš, Republika Srbija*
[4]*Univerzitet u Beogradu, Tehnološko-metalurški fakultet, Beograd, Republika Srbija*

(Naučni rad)

Prikazan je metod sinteze hidrogelova poli(*N*-izopropilakrilamid-*ko*-2-hidroksipropilmetakrilata), p(NIPAM-*ko*-HPMet), sa 5 mol% monomera HPMet-a dobijenih radikalnom polimerizacijom. Karakterizacija sintetisanih hidrogelova je izvedena određivanjem količine rezidualnih monomera i izvršena je njihova strukturna analiza pomoću infracrvene spektroskopije (FTIR), diferencijalne skenirajuće kalorimetrije (DSC) i skenirajuće elektronske mikroskopije (SEM). FTIR spektri sintetisanih hidrogelova p(NIPAM-*ko*-HPMet)-a sa različitim sadržajem umreživača EGDM-a pokazuju uzajamnu sličnost u strukturi. Površinska struktura liofilizovanih hidrogelova je porozna i uočavaju se čestice uklopljenog ibuprofena. Termička svojstva kserogelova p(NIPAM-*ko*-HPMet)-a pokazuju tri staklasta prelaza sa endotermnim pikovima slabog intenziteta. Sadržaj rezidualnih monomera dovodi do zaključka da je konverzija monomera tokom sinteze gotovo kompletna. Kinetika bubrenja hidrogelova pokazuje da se pri povećanju temperature od 20 na 40 °C mehanizam transporta tečnosti menja iz ne-Fikovog (proces bubrenja kontroliše difuzija tečnosti i relaksacija polimernih lanaca) u Fikov (kontrolisan samo difuzijom tečnosti). Mogućnost primene hidrogelova p(NIPAM-*ko*-HPMet)-a kao nosača lekova ispitivana je u zavisnosti od temperature. Ibuprofen, korišćen kao model lekovita supstanca, uklopljen je u hidrogel i količina oslobođene aktivne supstance određena je HPLC metodom. Utvrđeno je da uzorak hidrogela p(NIPAM-*ko*-HPMet)-a sa sadržajem umreživača od 1 mol% EGDM-a dostiže najveći stepen bubrenja (α = 34,72) na 10 °C i otpušta najveću količinu ibuprofena na 40 °C (64,21 mg/$g_{kserogel}$). Ispitana svojstva predstavljaju dobru osnovu za potencijalnu primenu hidrogelova kao nosača lekovitih supstanci sa modifikovanim oslobađanjem.

Ključne reči: *N*-Izopropilakrilamid • Kopolimerni hidrogel • Termičke osobine • Bubrenje • Ibuprofen

Mechanical properties of composites based on unsaturated polyester resins obtained by chemical recycling of poly(ethylene terephthalate)

Aleksandar D. Marinković[1], Tijana Radoman[2], Enis S. Džunuzović[1], Jasna V. Džunuzović[3], Pavle Spasojević[1], Bojana Isailović[1], Branko Bugarski[1]

[1]*Faculty of Technology and Metallurgy, University of Belgrade, Belgrade, Serbia*
[2]*Innovation center, Faculty of Technology and Metallurgy, University of Belgrade, Belgrade, Serbia*
[3]*Institute of Chemistry, Technology and Metallurgy (ICTM) – Center of Chemistry, University of Belgrade, Belgrade, Serbia*

Abstract

Composites based on unsaturated polyester (UPe) resins and fumed silica AEROSIL® RY 50, NY 50, RX 50 and NAX 50, as well as graphite, TiO_2 or organically modified clay CLOISITE 30B were prepared in order to investigate the influence of reinforcing agents on the mechanical properties of composites. Unsaturated polyester resins were synthesized from maleic anhydride and products of glycolysis, obtained by depolymerization of poly(ethylene terephthalate) with dipropylene glycol (UPe1 resin) and triethylene glycol (UPe2 resin) in the presence of tetrabutyl titanate catalyst. The obtained unsaturated polyesters were characterized by FTIR spectroscopy, acid and hydroxyl values, and their mechanical properties were also examined. Significant increase of the tensile modulus, tensile strength and decrease of the elongation at break was observed for composites prepared after addition of 10 wt.% of graphite or 10 wt.% of TiO_2 to the UPe resins, indicating strong interaction between matrix and filler particles. On the other hand, nanocomposites prepared using UPe2 and hydrophobically modified silica nanoparticles showed lower tensile strength and tensile modulus than polymer matrix. The presence of CLOISITE 30B had no significant influence on the mechanical properties of UPe1, while tensile strength and tensile modulus of UPe2 increased after adding 10 wt.% of clay.

Keywords: poly(ethylene terephthalate), chemical recycling; composites, mechanical properties.

Available online at the Journal website: http://www.ache.org.rs/HI/

Polymers

SCIENTIFIC PAPER

UDC 678.7–19:66.095.26:620.1/.2

Hem. Ind. **67** (6) 913–922 (2013)

doi: 10.2298/HEMIND130930077M

Poly(ethylene terephthalate) (PET) is a semi-crystalline, thermoplastic polyester that exhibits very good mechanical properties, good barrier properties and high transparency. Because of this, it is used for the production of packaging materials for soft drinks, food and pharmaceuticals, synthetic textile, photo-paper and for engineering plastics (usually reinforced with glass fibers). The production and consumption of PET products recorded the fastest growth rate in the global plastics market, but the current consumption of plastic containers is generating a huge amount of polymer waste. PET accounts for more than 8 wt.% and 12 vol.% of the world's solid waste generation [1].

The wide application and permanent increase in consumption of PET based products caused unavoidable generation of large volume of PET waste (rapid growing), which created a major environmental problem because PET is very resistant to biodegradation. Increased environmental awareness, legislative measures and public need for the sustainable development, increased interest in recycling of plastics. Plastic recycling is important from several aspects, such as energy conservation, reduced oil consumption, saving space in landfills, reduced greenhouse gas emissions and the benefits of reuse [1]. Recycling of plastic materials is divided into four categories: primary (re-extrusion), secondary (mechanical), tertiary (chemical) and quaternary (energy recovery – incineration) [2]. Chemical processing of PET and reuse of the obtained products are the most important strategy for PET recycling. PET has ester groups that can degrade using a variety of reagents such as acids, bases or water (hydrolysis of PET) [3,4], alcohols (PET alcoholysis) [5], amines (PET aminolysis) [6], glycols (PET glycolysis) [7–9], etc. In the PET glycolysis process, oligomeric products with terminal hydroxyl groups were obtained by PET depolymerization reaction with different glycol. The resulting oligomers can be used for the synthesis of various polymers, such as alkyd resins [10,11], polyurethanes [12,13] or unsaturated polyester (UPe) resins [14–16].

Unsaturated polyester resins are thermosetting polymers that are widely used in the preparation of polymer composites [17–19]. Extensive use of these materials is a consequence of their relatively low cost,

Correspondence: A.D. Marinković, Faculty of Technology and Metallurgy, University of Belgrade, Karnegijeva 4, 11120 Belgrade, Serbia.
E-mail: marinko@tmf.bg.ac.rs
Paper received: 30 September, 2013
Paper accepted: 14 October, 2013

easy of processing, good compatibility with a variety of fillers, as well as large selection of various types. However, compared with other engineering polymers, unsaturated polyesters have lower mechanical and thermal properties, which limit their use for some applications. These imperfections can be removed by adding various modified fillers [20–23]. Conventional fillers are used to improve the mechanical properties and to reduce the production costs, but their use is limited since they may lead to the phase separation and agglomeration of the filler particles, leading to a drastic deterioration of the material properties [24].

The incorporation of clay into UPe resin can result in improvements of mechanical, thermal, barrier and chemical properties, wear resistance and flame retardancy [25–29]. This can be done with less clay content than what is usually used in most conventional composites.

The most commonly used clay for polymeric composites is montmorillonite (MMT), which belongs to the general family of 2:1 layered silicates [30], and it is consisted of two fused silicate tetrahedral sheets sandwiching an edge-shared octahedral sheet of either aluminum or magnesium hydroxide. Only few works have been reported based on MMT-UPe resin derived from PET waste. Jo *et al.* [31] investigated mechanical properties and thermal stability of MMT-UPe nanocomposites and polymer concrete prepared using the MMT-UPe nanocomposite, and found that the compressive strength, elastic modulus, and splitting tensile strength of the polymer concrete based on MMT-UPe nanocomposites exceeded those of polymer concrete obtained using pure UPe resin. Also, the polymer concrete made with MMT-UPe nanocomposite showed better thermal performance than that made of pure UPe resin. Water sorption and diffusion of the MMT-UPe system was investigated by Katoch *et al.* [32]. The authors concluded that nanocomposite samples show lower diffusion coefficient than pure UPe and it decreases with increasing nanofiller content up to 4% by weight.

In this work, hybrid materials based on UPe matrix and graphite powder (GP), TiO_2, chemically modified clay CLOISITE 30B or chemically modified silica nanoparticles were prepared in order to study the influence of reinforcing agents on the mechanical properties of the obtained composite materials. Unsaturated polyesters were synthesized from di-hydroxyl functional product obtained by different methods of catalytic glycolysis of PET waste, using dipropylene glycol (DPG) and triethylene glycol (TEG), and maleic anhydride.

EXPERIMENTAL PART

Chemicals

Hydroquinone (HQ), dipropylene glycol (DPG) and triethylene glycol (TEG) were obtained from Fluka. Maleic anhydride (MA) was obtained from Sigma Aldrich. Tetrabutyl titanate (titanium (IV) butoxide; TBT) was obtained from Sigma-Aldrich. As fillers, graphite powder (GP; Dragon) and TiO_2 (Qingdao David Chemical Co., Ltd.) in the rutile crystal form (particle diameter of 0.25 μm and density of 3.9 kg dm^{-3}) were used. Four different hydrophobic nanosilica were obtained from Evonik. Aerosil® RY 50 (specific surface area of 30±15 $m^2\ g^{-1}$) and Aerosil® NY 50 (specific surface area of 30±10 $m^2\ g^{-1}$) are hydrophobic fumed silica based on Aerosil® OX 50 and Aerosil® 50, respectively, treated with silicone oil. Aerosil® RX 50 (specific surface area of 35±10 $m^2\ g^{-1}$) and Aerosil® NAX 50 (specific surface area of 40±10 $m^2\ g^{-1}$) are Aerosil® 50 nanoparticles surface modified with hexamethyldisilazan.

Organically modified clay CLOISITE 30B was obtained from Rockwood Clay Additives. CLOISITE 30B is a natural montmorillonite modified with alkyl quaternary ammonium salts, with 65% of molecules containing alkyl residue with 18 carbon atoms, 30% of the alkyl group with 16 carbon atoms and 5% of molecules containing alkyl groups with 14 carbon atoms. In the dry state, 90% of the clay particles have size below 13 μm. All chemicals were used as received without further purification.

Synthesis of UPe resins

Synthesis of UPe1

PET waste depolymerization was performed by glycolysis with DPG. In a four-necked flask of 250 ml, equipped with a mechanical stirrer, thermometer, condenser and inlet for nitrogen, 57.2 g of PET, 61.8 g of DPG and 0.2 g of TBT were placed (Table 1). The glycolysis reaction lasted for 5 hours at 210 °C, after which the reaction mixture was cooled to 90 °C. The hydroxyl value of the resulting glycolyzate was 315 mg KOH g^{-1}. Then, a Dean-Stark evaporator was added onto the flask and maleic anhydride (38.0 g) and 0.02 g of HQ were added (Table 1). The mixture was heated to 115 °C, providing constant temperature for 1 h, and then the continual temperature increase was achieved at a heating rate of 15 °C h^{-1}. When the reaction mixture temperature reached 150 °C, xylene (3 wt.%) was added to provide continual water removal by binary azeotrope, assuring in this manner a driving force for reaching the end-point of the reaction at 210 °C. After completion of the reaction, the obtained resin was cooled to 120 °C, 0.02 g of hydroquinone dissolved in 0.2 ml of ethanol was added, and then vacuum distillation (water pump) was carefully applied for 1 h to remove low boiling compounds present in the final product. Then, the resin was cooled down to 100 °C and styrene (40 wt.%) was added, followed by mixing to ensure homogeneity of the product (UPe1).

^{1}H- and ^{13}C-NMR data of UPe1 resin

^{1}H-NMR ($CDCl_3$): 1.24 (*m*, 12H, O-CH_2-CH(C$\underline{H}_3$)-O), 3.58 (*m*, 6H, O-CH_2-C$\underline{H}$(CH_3)-O-C$\underline{H}_2$-CH(CH_3)-O), 4.50 (*m*, 6H, O-C$\underline{H}_2$-CH(CH_3)-O-CH_2-C$\underline{H}$(CH_3)-O), 5.22 (*d*, 1H, styrene), 5.74 (*d*, 1H, styrene), 6.68 (*q*, 1H, styrene), 6.77 (*m*, 2H, O-(O)C-C$\underline{H}$=C$\underline{H}$-C(O)-O), 7.31 (*m*, 5H, styrene), 8.08 (*m*, 4H, H_{Ar}).

^{13}C-NMR ($CDCl_3$): 16.5 (O-CH_2-CH(CH_3)-O-CH_2--CH(C$\underline{H}_3$)-O), 18.4 (O-CH_2-CH(C$\underline{H}_3$)-O-CH_2-CH(CH_3)-O), 70.3 (O-CH_2-CH(CH_3)-O-CH_2-C$\underline{H}$(CH_3)-O), 70.7(O-C$\underline{H}_2$--CH(CH_3)-O-CH_2-CH(CH_3)-O), 73.4 (O-CH_2-CH(CH_3)-O--C$\underline{H}_2$-CH(CH_3)-O), 76.3 (O-CH_2-C$\underline{H}$(CH_3)-O-CH_2-CH(CH_3)--O), 113.7; 126.1; 127.8; 128.3 (styrene), 128.4 (O=C--HC=CH-C=O), 129.6 (CH_{Ar}), 133.6 (C_{Ar}), 136.7; 137.4 (C, styrene), 165.4 (O-C(O)-CH=CH-C(O)-C), 174.1 (O-C(O)--Ar-C(O)-O).

Synthesis of UPe2

Depolymerization of PET waste was performed by glycolysis with TEG. In a 250 ml four-necked flask, equipped with a mechanical stirrer, thermometer, condenser and inlet for nitrogen, 61.2 g of PET, 68.8 g of TEG and 0.2 g of TBT were placed (Table 1). The reaction of glycolysis lasted for 5 hours at 210 °C, after which the reaction mixture was cooled to 90 °C. The hydroxyl value of the resulting glycolyzate was 292 mg KOH g^{-1}. Then, a Dean-Stark water separator was assembled on the flask and maleic anhydride (40.4 g) and HQ (0.02 g) were added (Table 1). The synthesis of UPe2 was performed in the same manner as synthesis of UPe1.

^{1}H- and ^{13}C-NMR data for UPe2 resin (Ar is terephtaloyl moiety):

^{1}H-NMR ($CDCl_3$): 1.24 (*m*, 12H, O-CH_2-CH(C$\underline{H}_3$)-O), 2.43 (*m*, 4H, H-6, H-3, THP), 3.04 (*m*, 2H, H-1, H-2, THP), 3.58 (*m*, 6H, O-CH_2-C$\underline{H}$(CH_3)-O-C$\underline{H}_2$-CH(CH_3)-O), 4.50 (*m*, 6H, O-C$\underline{H}_2$-CH(CH_3)-O-CH_2-C$\underline{H}$(CH_3)-O), 5.22 (*d*, 1H, styrene), 5.74 (*d*, 1H, styrene), 6.68 (*q*, 1H, styrene), 6.77 (*m*, 2H, O-(O)C-C$\underline{H}$=C$\underline{H}$-C(O)-O), 7.31 (*m*, 5H, styrene), 8.08 (*m*, 4H, H_{Ar}).

^{13}C-NMR ($CDCl_3$): 16.5 (O-CH_2-CH(CH_3)-O-CH_2--CH(C$\underline{H}_3$)-O), 18.4 (O-CH_2-CH(C$\underline{H}_3$)-O-CH_2-CH(CH_3)-O), 70.3 (O-CH_2-CH(CH_3)-O-CH_2-C$\underline{H}$(CH_3)-O), 70.7(O-C$\underline{H}_2$--CH(CH_3)-O-CH_2-CH(CH_3)-O), 73.4 (O-CH_2-CH(CH_3)-O--C$\underline{H}_2$-CH(CH_3)-O), 76.3(O-CH_2-C$\underline{H}$(CH_3)-O-CH_2-CH(CH_3)-O), 113.7; 126.1; 127.8; 128.3 (styrene), 128.4 (O=C--HC=CH-C=O), 129.6 (CH_{Ar}), 133.6 (C_{Ar}), 136.7; 137.4 (C, styrene), 165.4 (O-C(O)-CH=CH-C(O)-C), 174.1 (O-C(O)--Ar-C(O)-O).

Production of composites based on UPe1 and UPe2 resins

Unsaturated polyester samples, UPe1 and UPe2, were used as the polymer matrix for the production of composite materials with addition of the following fillers: various commercial organically modified SiO_2 nanoparticles (RX50, NAX50, RY50 and NY50), organically modified clay CLOISITE 30B, rutile TiO_2 or GP. The composites (UPeN/filler) based on UPeN (where index N designates UPe resin – Upe1 and UPe2) and selected filler were obtained by mixing (grinding) appropriate amount of filler with UPeN (60 wt.% in styrene), using both modified laboratory homogenizer and ultrasonic bath. The pure UPeN and composites, (UPeN/filler), based on UPeN (60 wt.% in styrene) were cured using benzoyl peroxide (1.0 wt.%) as initiator and *N,N*-dimethylaniline (0.5 wt.%) as an accelerator.

All experiments used for the preparation of composites were conducted in three steps: weighted UPeN and filler components were carefully blended (homogenized) for 30 min using a modified laboratory homogenizer. In the second step, the sticky paste was transferred to an ultrasonic bath and treated under ultrasound for 15 min at 30 °C. The ultrasonic bath (Bandelin electronic, Berlin, Germany, power 120 W, frequency 35 kHz) was thermostated by circulating cold water through the jacket. After the addition of the accelerator and blending in a modified laboratory homogenizer at high speed (800º/min) for 1 min, the initiator was added, and the obtained uncured composite was then blended at 800 °C/min for 1 min and used for loading in PTFE mould. In this manner, UPeN/ /filler(n) were obtained, where index (*n*) designates percent of added filler (clay CLOISITE 30B: 0.25, 0.5, 1.0, 2.5, 5 and 10 wt.% and the amount of other fillers was 10 wt.%).

Characterization

The composition of the obtained product of glycolysis and the obtained unsaturated polyesters was determined using NMR and FTIR spectroscopy. ^{1}H and ^{13}C-NMR spectra were recorded on Varian Gemini 200 instrument Spectra at room temperature in deuterated chloroform ($CDCl_3$). Chemical shifts were expressed in ppm (δ) values relative to TMS (tetramethylsilane) in the ^{1}H-NMR spectra, and the residual solvent signal in ^{13}C-NMR spectra. FTIR spectra were recorded in the transmission mode, using a Bomem MB, series Hartmann & Braun, spectrometer and samples in the form of film or KBr tablet.

Table 1. Experimental conditions for UPe1 and UPe2 synthesis

Sample	PET, g	Glycol, g	Catalyst, g	Anhydride, g	Molar ratio OH/COOH	HQ, g	Styrene, g
UPe1	57.2	DPG (61.8)	TBT (0.2)	MA (38.0)	1.1	0.04	104.83
UPe2	61.2	TEG (68.8)	TBT (0.2)	MA (40.4)	1.1	0.04	113.76

The gel time of the samples was determined from the cure exotherm, measured according to ASTM D2471-99. The acid (*AV*) and hydroxyl (*HV*) values were determined according to ASTM D3644 and ASTM D2849 methods, respectively. The number average molecular weight, M_n, of the synthesized UPe was calculated as:

$$M_n = \frac{2 \times 56100}{AV + HV} \quad (1)$$

Stress-strain curves of cross-linked polyester samples and composite materials were obtained from uniaxial tensile experiments, which were carried out at room temperature by the standard method (ASTM D882). Specimens of the materials were prepared in a standard size, and subjected to testing by the use of Testing Machine, AG-Xplus HS, Shimadzu, Japan. Tensile strength, elongation at break and Young's modulus (tensile modulus) for all samples were determined as the mean of five measurements.

RESULTS AND DISCUSSION

As a starting material for unsaturated polyester resins synthesis, intermediate products obtained by depolymerization of PET waste bottles were used. Glycolysis of PET waste with dipropylene glycol or triethylene glycol in the presence of catalysts tetrabutyl titanate was performed. Hydroxyl value of the products obtained by glycolysis in the presence of DPG was 315 mg KOH g^{-1}, and 292 mg KOH g^{-1} when TEG was used. Based on the determined hydroxyl values of intermediary products, the number average molecular weight obtained by calculation according to Eq. (1) was 356 g mol^{-1} in the case of DPG and 384 g mol^{-1} when TEG was used. *AV*, *HV* and values of M_n of the synthesized UPe1 and UPe2 are given in Table 2.

Table 2. HV, AV and M_n of the synthesized UPe1 and UPe2

Sample	*AV* / mg KOH g^{-1}	*HV* / mg KOH g^{-1}	M_n / g mol^{-1}
UPe1	6.55	62.8	1620
UPe2	17.5	51.5	1630

FTIR spectra of the products of PET glycolysis with DPG and TEG are shown in Figure 1. The broad band at ≈3400 cm^{-1} originates from the stretching vibration of OH valence bond present in terminal hydroxyl groups. In the FTIR spectrum of the product of glycolysis based on TEG, the band at 2975 cm^{-1}, corresponding to the asymmetric deformation of C–H stretching vibration in the methyl group, was not observed due to the lack of methyl groups in TEG. This band is visible in the spectrum of the product of glycolysis based on DPG. Also, for the same reason there is no band at 1377 cm^{-1}, which originates from the bending vibration of C–H bonds present in the methyl group. The intense band, observed at ≈1720 cm^{-1}, originates from valence vibration of C=O present in ester group. The absorption bands between 1300 and 1100 cm^{-1} originate from C–O stretching vibrations, asymmetric and symmetric, respectively, present in ester group of terephthalic acid. The band at 879 cm^{-1} originates from the deformation vibrations of aromatic C–H out of plane connections. It is characteristic of 1,4-disubstituted benzene ring, which in this case comes from the terephthalic acid moiety.

After the reactions of glycolysis, maleic anhydride at the molar ratio of hydroxyl and carboxyl groups of 1.1, was added in the flask. Figure 1 shows also FTIR spectra of the synthesized unsaturated polyesters UPe1 and UPe2. Comparison with spectra of starting product indiates significant reduction in the intensity of band at 3400 cm^{-1}, which originates from the stretching vibration of OH groups. Also, band at 1078 cm^{-1}, which is derived from the alcoholic C–O stretching deformation vibration, is reduced. At the same time, the appearance of new bands at 1644 and 979 cm^{-1} can be observed in the FTIR spectrum of UPe1 resin, which correspond to the C=C stretching (skeletal) vibration of benzene ring and out of plane bending vibrations of 1,2-*trans* disubstituted C=CH group, present in maleic acid fragment, respectively. Aromatic C–H stretching vibration, overlapped with vinyl group, appeared in the region 3076––3010 cm^{-1} in the spectra of the synthesized UPe.

The cure exotherms of UPe1 and UPe2, cross-linked with 1.0 wt.% benzoyl peroxide and 0.5 wt.% *N,N*-dimethylaniline, are presented in Figure 2. According to these results, the maximum curing temperature of UPe1 (88 °C) was quite higher and reached earlier (13 min) than for UPe2 (41 °C after 21 min). Curing reaction of UPe1 is faster than curing reaction of UPe2, due to the better miscibility of polyester resin containing DPG with styrene than the resin containing TEG.

Results of the studies of mechanical properties are shown in Figures 3–7, and the values of tensile strength, σ_p, elongation at break, ε_b, and tensile modulus, *E*, of cured UPe1 and UPe2 resins, as well as of corresponding composites are given in Tables 3 and 4. According to the results it could be noticed that cross-linked sample UPe1 showed greater tensile strength and modulus, and lower elongation at break than the cross-linked sample UPe2 (Figure 3, Tables 3 and 4). The reason for this behavior lies in the different flexibility of polyester chain. In the case of polyester Upe2, based on TGE, the spacing between the double bonds in polyester chains is larger than in the UPe1 polyester chains causing more flexible Upe2 chains. Nanocomposites based on UPe1 and clay have no significantly different mechanical properties, *i.e.*, tensile strength and elongation at break are slightly modified, and tensile modulus decreases with increasing clay content and this

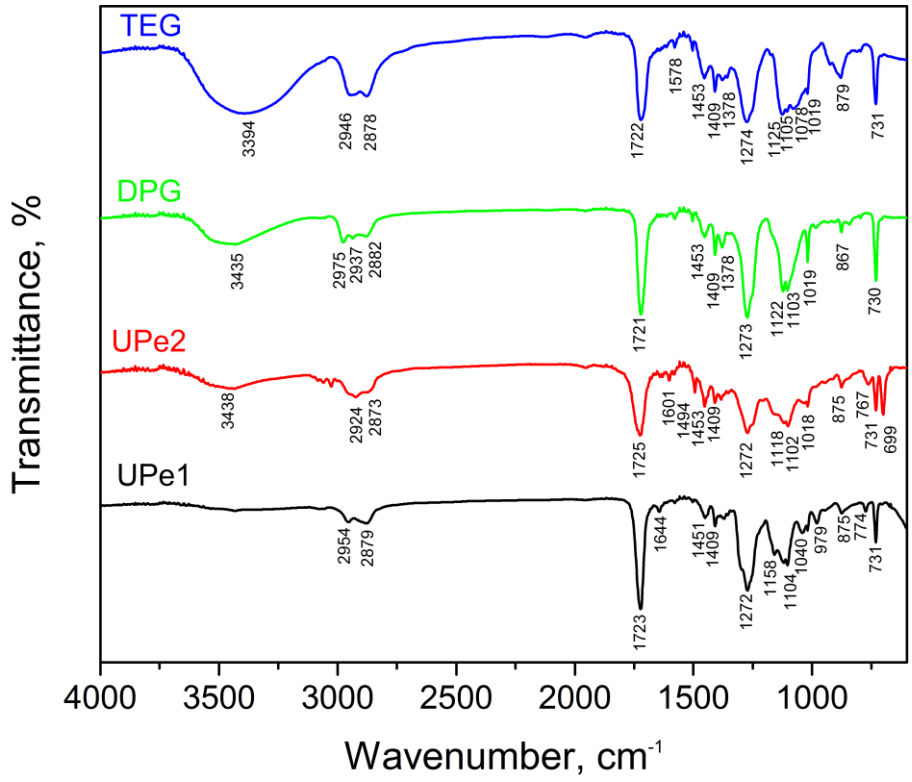

Figure 1. FTIR Spectra of UPe1, UPe2, and glycolyzed products (obtained using DPG and TEG).

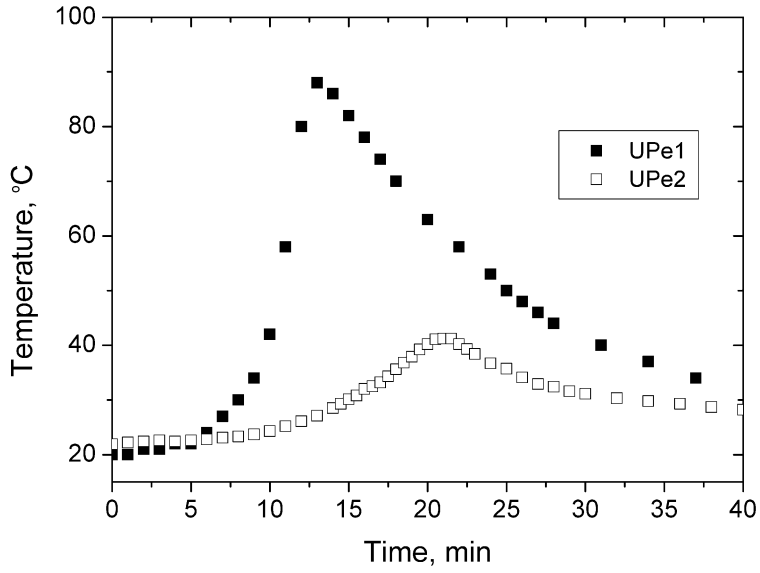

Figure 2. The cure exotherms of UPe1 and UPe2 cross-linked with 1.0 wt.% benzoyl peroxide and 0.5 wt.% N,N-dimethylaniline.

change is less than 10% compared to the pure polyester (Figure 4, Table 3).

The greatest influence on the mechanical properties of the composites was found when graphite and TiO_2 (10 wt.%) were added as fillers, which is reflected as significant increase of the tensile modulus, tensile strength and decrease of the elongation at break compared to the corresponding UPe resins (Figure 5, Table 3). In the case of nanocomposites prepared from UPe2 resin, the addition of hydrophobically modified silica nanoparticles leads to decrease of tensile strength and tensile modulus, which indicates a weak interaction between the filler particles and the polymer matrix (Figure 6, Table 4). The largest decrease in tensile strength and tensile modulus was observed in composite samples obtained after addition of nanofiller particles AEROSIL® RY50, due to low intensity of interaction between nanofiller, modified with silicone oil,

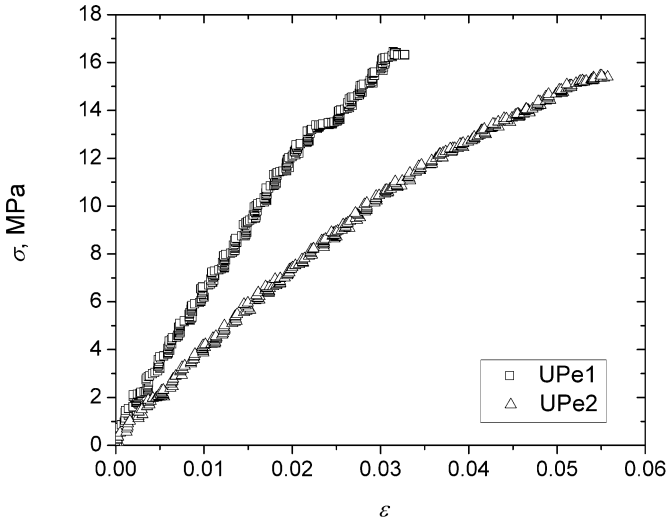

Figure 3. The stress-strain curves of the cured samples UPe1 and UPe2.

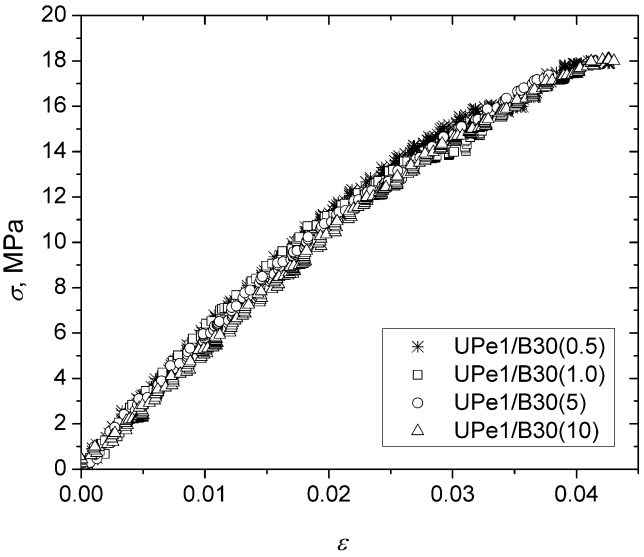

Figure 4. The stress-strain curves of the nanocomposites based on UPe1 and CLOISITE 30B.

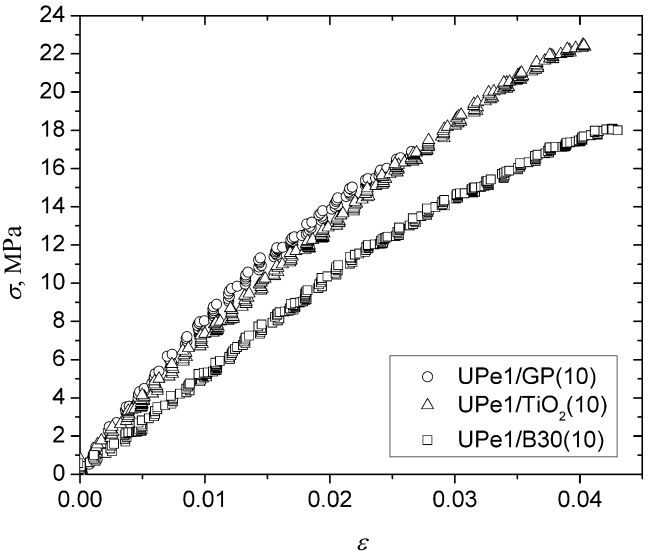

Figure 5. The stress-strain curves of the composites based on UPe1 and graphite, clay and titanium dioxide.

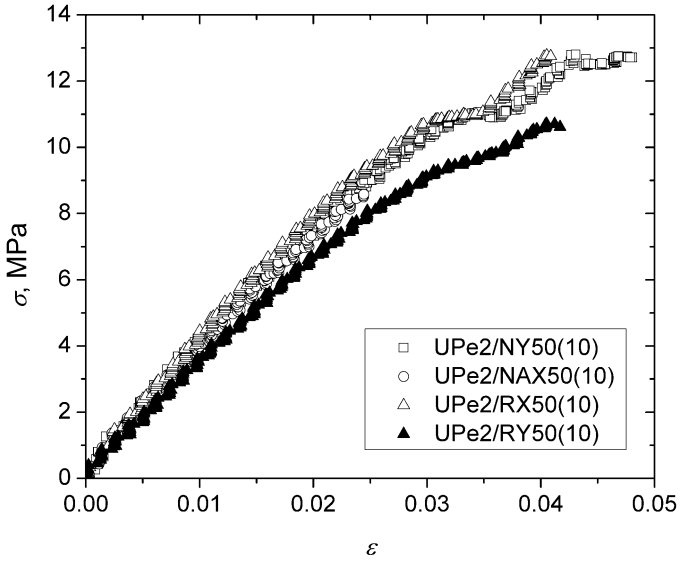

Figure 6. The stress-strain curves of the nanocomposites based on UPe2 and AEROSIL® nanofillers.

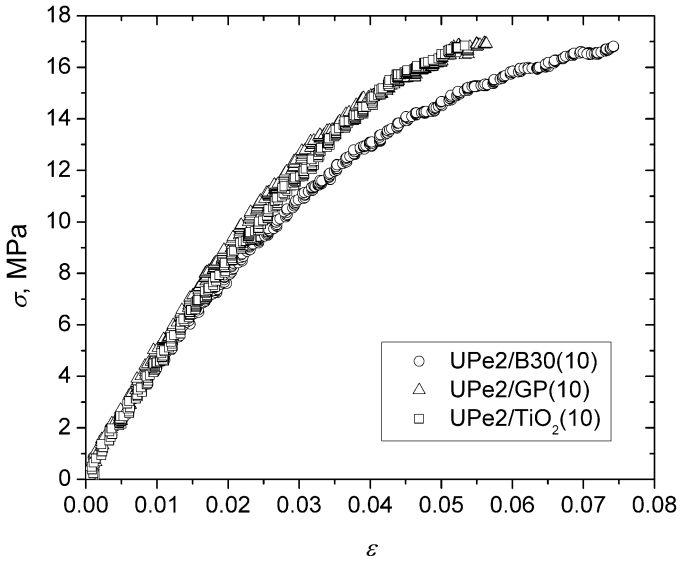

Figure 7. The stress-strain curves of the composites based on UPe2 and graphite, clay and titanium dioxide.

Table 3. Results of the mechanical testing of cured UPe1 and corresponding composites

Sample	σ_p / MPa	ε_{max} / %	E / MPa
UPe1	16.33	3.27	647
UPe1/B30(0.25)	15.96	3.44	656
UPe1/B30(0.5)	15.87	3.30	624
UPe1/B30(1.0)	14.92	3.24	606
UPe1/B30(2.5)	19.95	3.68	604
UPe1/B30(5)	17.34	3.78	597
UPe1/B30(10)	18.00	4.30	606
UPe1/GP(10)	16.90	2.65	805
UPE1/TiO_2(10)	22.45	4.03	741

Table 4. Results of mechanical testing of cured UPe2 and corresponding composites

Sample	σ_p / MPa	ε_{max} / %	E / MPa
UPe2	15.22	5.66	421
UPe2/NY50(10)	11.08	3.55	422
UPe2/NAX50(10)	14.83	6.00	408
UPe2/RX50(10)	12.79	4.39	446
UPe2/RY50(10)	10.62	4.17	363
UPe2/GP(10)	16.91	5.64	510
UPe2/B30(10)	16.82	7.42	457
UPe2/TiO_2(10)	16.57	5.36	454

and cross-linked UPe2 resin. The presence of 10 wt.% clay, graphite or TiO_2 in UPe2 resin increased tensile strength and tensile modulus, which indicates stronger interaction between filler particles themselves and matrix and filler particles (Figure 7, Table 4).

CONCLUSION

Maleic anhydride and di-hydroxyl functional products obtained after catalytic glycolysis of PET waste, using dipropylene glycol or triethylene glycol, were used for the synthesis of unsaturated polyesters. The glycolyzed products and UPe resins were characterized by FTIR spectroscopy, acid and hydroxyl value. Curing reaction of UPe1 was faster than curing reaction of UPe2 due to the better miscibility of styrene with polyester resin based on glycolyzed product which contains DPG. Due to the higher polymer chain rigidity, UPe1 showed higher tensile strength and modulus, and lower elongation at break than UPe2.

The obtained UPe resins were further used as matrix for the synthesis of composites using chemically modified silica nanoparticles or clay CLOISITE 30B, as well as graphite powder or TiO_2 as fillers. The influence of reinforcing agents on the mechanical properties of the prepared composites was investigated. It was shown that the addition of CLOISITE 30B to the UPe1 had no significant influence on the mechanical properties, while tensile strength and tensile modulus of UPe2 increased after adding 10 wt.% of clay. The greatest influence on the mechanical properties of the composites was found when graphite and TiO_2 (10 wt.%) were added as fillers to the synthesized UPe, which is reflected as significant increase of tensile modulus, tensile strength and decrease of the elongation at break, indicating strong interaction between matrix and filler particles. On the other hand, tensile strength and tensile modulus of nanocomposites prepared from UPe2 resin and hydrophobically modified silica nanoparticles decreased, while the composite prepared with AEROSIL® RY50 had the lowest mechanical properties.

Acknowledgement

The authors acknowledge financial support from Ministry of Education, Science and Technological development of Serbia, Project No. 172013.

REFERENCES

[1] S.M. Al-Salem, P. Lettieri, J. Baeyens, Recycling and recovery routes of plastic solid waste (PSW): a review, Waste Manag. **29** (2009) 2625–2643.

[2] R. López-Fonseca, I. Duque-Ingunza, B. de Rivas, L. Flores-Giraldo, J.I. Gutiérrez-Ortiz, Kinetics of catalytic glycolysis of PET wastes with sodium carbonate, Chem. Eng. J. **168** (2011) 312–320.

[3] K. Li, X. Song, D. Zhang, Depolymerization of poly(ethylene terephthalate) with catalyst under microwave radiation, J. Appl. Polym. Sci. **109** (2008) 1298–1301.

[4] R. López-Fonseca, M.P. González-Velasco, J.R. González-Velasco, J.I. Gutiérrez-Ortiz, A kinetic study of the depolymerisation of poly(ethylene terephthalate) by phase transfer catalysed alkaline hydrolysis, J. Chem. Technol. Biotechnol. **84** (2009) 92–99.

[5] M. Goto, H. Koyamoto, A. Kodama, T. Hirose, S. Nagaoka, B.J. McCoy, Degradation kinetics of polyethylene terephthalate in supercritical methanol, AIChE J. **48** (2002) 136–144.

[6] M.E. Tawfik, S.B. Eskander, Chemical recycling of poly(ethylene terephthalate) waste using ethanolamine, Sorting of the end products, Polym. Degrad. Stab. 95 (2010) 187–194.

[7] F. Pardal, G. Tersac, Kinetics of poly(terephthalate) glycolysis by diethylene glycol. I. Evolution of liquid and solid phases, Polym. Degrad. Stab. 91 (2006) 2840––2847.

[8] C.-H. Chen, C.-Y. Chen, Y.-W. Lo, C.-F. Mao, W.-T. Liao, Studies of glycolysis of poly(ethylene terephthalate) recycled from postconsumer soft-drink bottles. I. Influences of glycolysis conditions, J. Appl. Polym. Sci. **80** (2001) 943–948.

[9] R. López-Fonseca, I. Duque-Ingunza, B. de Rivas, S. Arnaiz, J.I. Gutiérrez-Ortiz, Chemical recycling of post-consumer PET wastes by glycolysis in the presence of metal salts, Polym. Degrad. Stab. **95** (2010) 1022–1028.

[10] G.P. Karayannidis, D.S. Achilias, I.D. Sideridou, D.N. Bikiaris, Alkyd resins derived from glycolized waste poly-

(ethylene terephthalate), Eur. Polym. J. **41** (2005) 201––210.

[11] A. Torlakoğlu, G. Güçlü, Alkyd–amino resins based on waste PET for coating applications, Waste Manag. **29** (2009) 350–354.

[12] M. Kathalewar, N. Dhopatkar, B. Pacharane, A. Sabnis, P. Raut, V. Bhave, Chemical recycling of PET using neopentyl glycol: Reaction kinetics and preparation of polyurethane coatings, Prog. Org. Coat. **76** (2013) 147–156.

[13] G. Güçlü, M. Orba, Alkyd resins synthesized from post-consumer PET bottles, Prog. Org. Coat. **65** (2009) 362––365.

[14] D.J Suh, O.O Park, K.H Yoon, The properties of unsaturated polyester based on the glycolyzed poly(ethylene terephthalate) with various glycol compositions, Polymer **41** (2000) 461–466.

[15] J.M.L. Reis, Effect of aging on the fracture mechanics of unsaturated polyester based on recycled PET polymer concrete, Mat. Sci. Eng., A **528** (2011) 3007–3009.

[16] A.M. Atta, M.E. Abdel-Raouf, S.M. Elsaeed, A.-A.A. Abdel-Azim, Curable resins based on recycled poly-(ethylene terephthalate) for coating applications, Prog. Org. Coat. **55** (2006) 50–59.

[17] Cs. Varga, N. Miskolczi, L. Bartha, G. Lipóczi, Improving the mechanical properties of glass-fibre-reinforced polyester composites by modification of fibre surface, Mater. Design **31** (2010) 185–193.

[18] R. Sengupta, M. Bhattacharya, S. Bandyopadhyay, A.K. Bhowmick, A review on the mechanical and electrical properties of graphite and modified graphite reinforced polymer composites, Prog. Polym. Sci. **36** (2011) 638––670.

[19] S.S. Ray, M. Okamoto, Polymer/layered silicate nanocomposites: a review from preparation to processing, Prog. Polym. Sci. **28** (2003) 1539–1641.

[20] M. Zhang, R.P. Singh, Mechanical reinforcement of unsaturated polyester by Al_2O_3 nanoparticles, Mat. Lett. **58** (2004) 408–412 .

[21] L. Tibiletti, C. Longuet, L. Ferry, P. Coutelen, A. Mas, J.-J. Robin, J.-M. Lopez-Cuesta, Thermal degradation and fire behaviour of unsaturated polyesters filled with metallic oxides, Polym. Degrad. Stab. **96** (2011) 67–75.

[22] Y.-F. Shih, Y.-T. Wang, R.-J. Jeng, K.-M. Wei, Expandable graphite systems for phosphorus-containing unsaturated polyesters. I. Enhanced thermal properties and flame retardancy, Polym. Degrad. Stab. **86** (2004) 339––348.

[23] L.B. Manfredi, E.S. Rodríguez, M. Wladyka-Przybylak, A. Vázquez, Thermal degradation and fire resistance of unsaturated polyester, modified acrylic resins and their composites with natural fibres, Polym. Degrad. Stab. **91** (2006) 255–261.

[24] K.A. Carrado, in G.A. Shonaike, S.G. Advani, (Eds.), Advanced Polymeric Materials: Structure Property Relationships, CRC Press, Boca Raton, FL, 2003, Ch. 10.

[25] X. Kornmann, L.A. Berglund, J. Sterte, E.P. Giannelis, Nanocomposites based on montmorillonite and unsaturated polyester, Polym. Eng. Sci. **38** (1998) 1351–1358.

[26] R.K. Bharadwaj, A.R. Mehrabi, C. Hamilton, C. Trujillo, M. Murga, R. Fan, A. Chavira, A.K. Thompson, Structure–property relationships in cross-linked polyester–clay nanocomposites, Polymer **43** (2002) 3699–3705.

[27] M. Chieruzzi, A. Miliozzi, J.M. Kenny, Effects of the nanoparticles on the thermal expansion and mechanical properties of unsaturated polyester/clay nanocomposites, Composites, A **45** (2013) 44–48.

[28] P. Jawahar, R. Gnanamoorthy, M. Balasubramanian, Tribological bahaviour of the clay-thermoset nanocomposites, Wear **261** (2006) 835–840.

[29] P. Kiliaris, C.D. Papaspyrides, Polymer/layered silicate (clay) nanocomposites: An overview of flame retardancy, Prog. Polym. Sci. **35** (2010) 902–958.

[30] J.C. Huang, Zk Zhu, J. Yin, X.f. Qian, Y.Y. Sun, Poly-(etherimide)/montmorillonite nanocomposites prepared by melt intercalation: morphology, solvent resistance properties and thermal properties, Polymer **42** (2001) 873–877.

[31] B.-W. Jo, S.-K. Park, D.-K. Kim, Mechanical properties of nano-MMT reinforced polymer composite and polymer concrete, Constr. Build. Mater. **22** (2008) 14–20.

[32] S. Katoch, V. Sharma, P.P. Kundu, Water sorption and diffusion through saturated polyester and their nanocomposites synthesized from glycolyzed PET waste with varied composition, Chem. Eng. Sci. **65** (2010) 4378––4387.

IZVOD

MEHANIČKA SVOJSTVA KOMPOZITA NA BAZI NEZASIĆENIH POLIESTARSKIH SMOLA DOBIJENIH HEMIJSKOM RECIKLAŽOM POLI(ETILEN-TEREFTALATA)

Aleksandar D. Marinković[1], Tijana Radoman[2], Enis S. Džunuzović[1], Jasna V. Džunuzović[3], Pavle Spasojević[1], Bojana Isailović[1], Branko Bugarski[1]

[1]*Tehnološko–metalurški fakultet, Univerzitet u Beogradu, Beograd, Srbija*
[2]*Inovacioni centar, Tehnološko-metalurški fakultet, Univerzitet u Beogradu, Beograd, Srbija*
[3]*IHTM – Centar za Hemiju, Univerzitet u Beogradu, Beograd, Srbija*

(Naučni rad)

U ovom radu sintetisani su kompoziti na bazi nezasićenih poliestarskih (UPe) smola i SiO_2 (AEROSIL®:RY 50, NY 50, RX 50 i NAX 50), grafita, TiO_2 ili organski modifikovane gline CLOISITE 30B u cilju ispitivanja uticaja punioca na mehanička svojstva kompozita. Nezasićene poliestarske smole su sintetisane polazeći od anhidrida maleinske kiseline i proizvoda glikolize dobijenih depolimerizacijom poli(etilen-tereftalata) sa dipropilen glikolom (UPe1 smola) ili trietilen glikolom (UPe2 smola) u prisustvu katalizatora tetrabutil titanata. Sintetisane nezasićene poliestarske smole su ispitane primenom FTIR spektroskopije, određen im je kiselinski i hidroksilni broj i ispitana su njihova mehanička svojstva. Molarna masa srednja po brojnoj vrednosti sintetisanih nezasićenih poliestarskih smola je između 1620–1630 g mol^{-1}. Moduli istezanja i zatezna čvrstoća kompozita pripremljenih dodavanjem 10 mas.% grafita ili TiO_2 nezasićenim poliestarskim smolama su značajno porasli u odnosu na čiste poliestre, dok se izduženje pri kidanju smanjilo, što ukazuje na postojanje jakih interakcija između matrice i čestica punioca. Sa druge strane, nanokompoziti sintetisani korišćenjem UPe2 i modifikovanih nanočestica SiO_2 su imali manju zateznu čvrstoću i module istezanja nego čista nezasićena poliestarska smola. Pokazano je da prisustvo gline CLOISITE 30B nema značajan uticaj na mehanička svojstva smole UPe1, dok su vrednosti modula istezanja i zatezne čvrstoće UPe2 porasle nakon dodavanja 10 mas.% gline.

Ključne reči: Poli(etilen-tereftalat) • Hemijska reciklaža • Kompoziti • Mehanička svojstva

Uticaj veličine nanočestica TiO_2 i njihove površinske modifikacije na reološka svojstva alkidne smole

Tijana S. Radoman[1], Jasna V. Džunuzović[2], Katarina B. Jeremić[3], Aleksandar D. Marinković[3], Pavle M. Spasojević[1], Ivanka G. Popović[3], Enis S. Džunuzović[3]

[1]*Inovacioni centar, Tehnološko-metalurški fakultet, Univerzitet u Beogradu, Beograd, Srbija*
[2]*Institut za hemiju, tehnologiju i metalurgiju (IHTM) – Centar za hemiju, Univerzitet u Beogradu, Beograd, Srbija*
[3]*Tehnološko–metalurški fakultet, Univerzitet u Beogradu, Beograd, Srbija*

Izvod

Sferne čestice TiO_2 različitih veličina dispergovane su u alkidnoj smoli. Površinska modifikacija nanočestica TiO_2 izvedena je propil galatom i lauril galatom. Ispitivan je uticaj veličine nanočestica TiO_2, koncentracije, kao i vrste površinske modifikacije na reološka svojstva alkidne smole. Dobijeno je da je viskoznost pripremljenih disperzija veća od viskoznosti čiste smole, da raste sa smanjenjem prečnika čestica i opada sa povećanjem frekvencije. Površinski modifikovane čestice imaju veći uticaj na viskoznost alkidne smole nego nemodifikovane zbog povećanja efektivnog zapreminskog udela čestica u disperziji. Za najmanju koncentraciju TiO_2 viskoznost je veća kada je modifikacija izvršena lauril galatom, dok sa povećanjem koncentracije, zbog manje disperzione stabilnosti čestica modifikovanih propil galatom, dolazi do njihove aglomerizacije i naglog povećanja viskoznosti.

Ključne reči: *TiO_2 nanočestice, površinska modifikacija, propil galat, lauril galat, alkidna smola, reologija.*

Dostupno na Internetu sa adrese časopisa: http://www.ache.org.rs/HI/

Polimeri

NAUČNI RAD

UDK 678.6:54:66

Hem. Ind. **67** (6) 923–932 (2013)

doi: 10.2298/HEMIND131106081R

Alkidi predstavljaju grupu nezasićenih poliestara, sa razgranatom molekulskom strukturom, koji se dobijaju reakcijama polikondenzacije dikarbonskih kiselina, polivalentnih alkohola i monokarbonskih masnih kiselina [1–3]. U zavisnosti da li se kao polazne komponente za sintezu alkida koriste masne kiseline ili odgovarajuća biljna ulja, postoje dva osnovna načina sinteze alkida. Ako se koriste masne kiseline, onda se alkidi dobijaju direktnom esterifikacijom dikarbonskih kiselina, višefunkcionalnih alkohola i masnih kiselina. U slučaju kada se kao polazna komponenta koristi ulje, prvo se vrši alkoholiza ulja višefunkcionalnim alkoholom, a zatim se izvodi poliesterifikacija dikarbonskih kiselina sa mono i diestrima masnih kiselina i poliola koji su dobijeni u procesu alkoholize. Prema sadržaju ulja alkidi se dele na: kratkouljne (manje od 40% ulja), srednjeuljne (od 40 do 60% ulja) i dugouljne (preko 60% ulja). U zavisnosti od toga da li sadrže ostatke nezasićenih ili zasićenih masnih kiselina, alkidi se dele na sušive i nesušive. Sušivi su oni koji sadrže ostatke nezasićenih masnih kiselina. Ove alkidne smole umrežavaju pod dejstvom svetlosti i kiseonika iz vazduha (oksidativno sušenje) [4,5]. Sam mehanizam umrežavanja uključuje otkidanje vodonika sa alilne metilenske grupe pri čemu nastaje slobodni radikal koji reaguje sa kiseonikom iz vazduha i nastaje hidroperoksid [6–8]. Razlaganjem tako nastalog hidroperoksida nastaju slobodni radikali koji dovode do umrežavanja alkidne smole. Reakciju razgradnje nastalih hidroperoksida katalizuju soli nekih metala koje se nazivaju ubrzivači (sikativi) [9]. Alkidne smole koje u sebi sadrže pretežno zasićene masne kiseline nazivaju se nesušive i ne mogu umrežiti pod dejstvom kiseonika. Umrežavanje ovih smola vrši se na povišenim temperaturama uz dodatak odgovarajućih termoreaktivnih smola [10,11].

Zahvaljujući jednostavnom načinu sinteze, mogućnosti da se svojstva alkidnih smola mogu značajno i kontrolisano menjati samo izborom reaktanata i njihovog odnosa, da su kompatibilne sa velikim brojem polimera i da sirovine za njihovo dobijanje potiču iz bioobnovljivih izvora, alkidne smole su našle široku primenu kao vezivo u najrazličitijim vrstama premaza [12––14]. Procenjuje sa da alkidne smole čine oko 45% veziva u industriji premaza. Bitno svojstvo po kome se alkidne smole razlikuju od većine ostalih polimernih veziva jeste da one dobro kvase neorganski pigment. Komercijalni neorganski pigmenti koji se danas koriste u industriji premaza su mikrometarskih dimenzija i mogu poboljšati mehanička, optička i antikoroziona svojstva premaza. Međutim, ovi pigmenti mogu imati i neželjena dejstva na svojstva umreženog premaza, pre svega na smanjenje adhezije premaza na supstrat, smanjenje elastičnosti premaza, smanjenje otpornosti na udar, smanjenje transparentnosti, smanjenje otpornosti na abraziju i grebanje i mogu dovesti do delaminacije (ljuštenja) premaza. Sem lošeg uticaja na svojstva umreženog premaza, još jedan veliki problem koji se

Prepiska: E.S. Džunuzović, Tehnološko–metalurški fakultet, Univerzitet u Beogradu, Karnegijeva 4, 11120 Beograd, Srbija.
E-pošta: edzunuzovic@tmf.bg.ac.rs
Rad primljen: 6. novembar, 2013
Rad prihvaćen: 14. novembar, 2013

javlja u toku samog skladištenja premaza jeste sedimentacija pigmenta koja dovodi do promene viskoznosti premaza, smanjuje njegovu pokrivnu moć i skraćuje vreme skladištenja [15]. Zbog svega gore navedenog, danas se sve više pažnje posvećuje ispitivanju mogućnosti upotrebe pigmenta nanometarskih dimenzija. Poznato je da zbog svojih malih dimenzija, nanočestice imaju veliku specifičnu površinu. Odgovarajućom modifikacijom površine nanopigmenta postiže se bolja interakcija sa alkidnom smolom (polimernom matricom) tako da se, u poređenju sa pigmentom mikrometarskih dimenzija, uvođenjem puno manje količine pigmenta nanometarskih dimenzija može postići isti efekat na svojstva alkidne smole. Upotrebom pigmenta nanometarskih dimenzija dobiće se bolja mehanička, optička, termička i barijerna svojstva premaza. Takođe će se smanjiti mogućnost stvaranja „plikova“ i ljuštenja premaza, što dovodi do bolje postojanosti i dužeg veka trajanja premaza [16–23].

U ovom radu ispitivan je uticaj veličine nanočestica TiO_2, koncentracije nanočestica, kao i vrste površinske modifikacije na reološka svojstva alkidne smole na bazi sojinog ulja sa sadržajem ulja od 65%. Korišćena su tri komercijalna uzorka čestica TiO_2 različitih veličina, dva uzorka submikronskih dimenzija i jedan nanometarskih dimenzija. Četvrti korišćeni uzorak su nanočestice titandioksida dobijene hidrolizom titanijum tetraizopropoksida u kiseloj sredini. Površinska modifikacija nanočestica titan-dioksida izvršena je estrima galne kiseline. Korišćena su dva *n*-alkil galata sa različitom dužinom lanca alkil grupe: propil galat i lauril galat. Ispitivan je uticaj nemodifikovanih i površinski modifikovanih čestica TiO_2 na reološka svojstva alkidne smole u zavisnosti od veličine TiO_2 čestica i dužine ugljovodoničnog lanca estarske alkil grupe galatnog liganda.

EKSPERIMENTALNI DEO

Korišćene hemikalije

Za sintezu TiO_2 koloida korišćen je titanijum tetraizopropoksid proizvođača Acros Organics. Propil galat (PG) i lauril galat (LG), korišćeni za površinsku modifikaciju TiO_2 nanočestica, dobijeni su od proizvođača Aldrich. Oznake komercijalnih uzoraka TiO_2 koji su korišćeni u ovom radu, njihova veličina i proizvođač dati su u Tabeli 1. Alkidna smola na bazi sojinog ulja CHS-ALKYD S 653, sa sadržajem ulja od 65%, dobijena je od proizvođača Spolchemie. Svi rastvarači korišćeni su bez dodatnog prečišćavanja.

Koloidni rastvor TiO_2 dobijen je hidrolizom titanijum-tetraizopropoksida u kiseloj sredini na 80 °C na način opisan u literaturi [24].

Postupak modifikacije sintetisanih TiO_2 nanočestica izveden je na isti način sa oba galata i biće opisan na primeru dobijanja površinski modifikovanih čestica TiO_2 sa lauril galatom (TiO_2–LG). U smeši hloroforma i metanola rastvoreno je 0,1136 g LG i pomešano u levku za odvajanje sa 10 ml koloidnog rastvora TiO_2. Posle energičnog mućkanja, u levku je izdvojen donji hloroformski sloj tamno crvene boje koji sadrži čestice TiO_2–LG. On je odvojen od gornjeg vodenog sloja i polako uz mešanje magnetnom mešalicom je ukapan u sto puta veću količinu metanola. Čestice TiO_2–LG su izdvojene u obliku taloga, koji je posle redispergovan u hloroformu.

Tabela 1. Komercijalni uzorci TiO_2 koji su korišćeni u ovom radu
Table 1. Commercial TiO_2 samples used in this work

Uzorak	Veličina TiO_2, nm	Proizvođač
R-2195	250	Qingdao David Chemical Co., Ltd.
A-HR	170	Tioxide
P25	21	Degussa

Površinska modifikacija komercijalnog uzorka nanočestica TiO_2 (P25) izvršena je na isti način kao i sintetisanih. U 10 ml vode dispergovano je 0,02 g P25 i pomešano u levku za odvajanje sa 7,5 ml hloroforma i 2,5 ml metanola u kome je rastvoreno 0,0170 g LG. Posle energičnog mućkanja gornji vodeni sloj se obezbojio, a površinski modifikovane P25 nanočestice (P25-LG) su prešle u donji hloroformski sloj koji je postao bledo crvene boje. P25–LG nanočestice su pretaložene dva puta u metanolu i osušene u vakuum sušnici na 40 °C do konstantne mase.

Priprema uzoraka

Praškasti uzorci TiO_2 dispergovani su u alkidnoj smoli uz pomoć ultrazvuka. Određena količina prečišćenih površinski modifikovanih nanočestica TiO_2 je dispergovana u hloroformu i dodata u alkidnu smolu nakon čega je iz smeše otparen hloroform na sobnoj temperaturi pod sniženim pritiskom.

Karakterizacija

FTIR spektri osušenih uzoraka površinski modifikovanih i nemodifikovanih čestica TiO_2, presovani u KBr pločice, snimljeni su na FTIR spektrometru BOMEM MB-102. Apsorpcioni spektri nemodifikovanog i površinski modifikovanog TiO_2 koloida snimljeni su na instrumentu Perkin-Elmer UV–Vis spektrofotometar, model Lambda-5.

Veličina i oblik sintetisanih nanočestica TiO_2 određeni su uz pomoć transmisione elektronske mikroskopije, a snimci su urađeni na transmisionom elekronskom mikroskopu JEOL-1200EX.

Kompleksna dinamička viskoznost (η^*) pripremljenih disperzija određena je na mehaničkom spektrometru Rheometrics, model RMS 605, pri dinamičkom smicanju između dve paralelne ploče, pri konstantnoj tem-

peraturi od 25 °C. Frekvencija je varirana u opsegu od 0,1 do 100 rad/s sa konstantnom deformacijom od 5%.

REZULTATI I DISKUSIJA

Oblik i veličina koloidnih nanočestica TiO_2, dobijenih hidrolizom prekursora (titanijum-tetraizopropoksida) u kiseloj sredini, određeni su uz pomoć transmisione elektronske mikroskopije (TEM). Na slici 1 prikazana je TEM mikrofotografija sintetisanog koloida sa koje se vidi da su sintetisane čestice približno sfernog oblika, prečnika oko 4 nm.

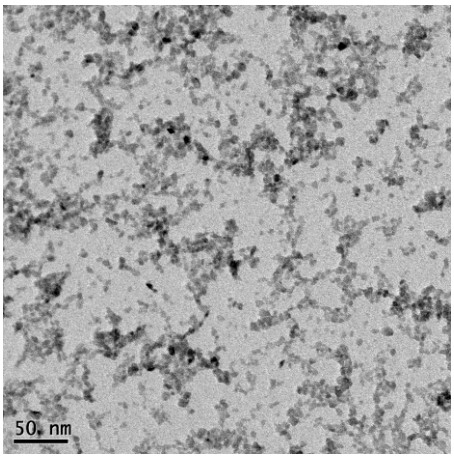

Slika 1. TEM mikrofotografija TiO_2 nanočestica.
Figure 1. TEM Micrograph of TiO_2 nanoparticles.

Površinska modifikacija sintetisanih koloidnih čestica TiO_2, tj. njihova hidrofobizacija koja je omogućila njihov prelazak iz vodene u organsku fazu, izvršena je sa PG i LG tako što je rastvor galata u smeši hloroforma i metanola pomešan sa sintetisanim vodenim koloidom TiO_2, pri čemu je gotovo trenutno došlo do izdvajanja tamno crvenog organskog sloja. To ukazuje da su se korišćeni estri galne kiseline hemijski vezali za površinu TiO_2 nanočestica, pri čemu je došlo do formiranja kompleksa uz izmenu naelektrisanja („*charge transfer complex*“ – CTC), od koga potiče ta intenzivna crvena boja, a što je i potvrđeno FTIR i UV apsorpcionom spektroskopijom. Na slici 2 prikazani su FTIR spektri LG, osušenog TiO_2 koloida i osušenih TiO_2 nanočestica, površinski modifikovanih LG-om (TiO_2–LG).

Sa slike 2 se jasno vidi da se karakteristične trake iz FTIR spektra LG na 3450 i 3350 cm^{-1}, koje odgovaraju vibracijama istezanja OH grupa na benzenovom prstenu, u potpunosti gube u FTIR spektru TiO_2–LG nanočestica, dok su trake koje potiču od vibracija istezanja estarske C=O grupe na oko 1670 cm^{-1} i trake na 2920 i 2850 cm^{-1}, koje potiču od vibracija istezanja alifatskih C–H veza iz lauril grupe prisutne i u spektru TiO_2–LG nanočestica. Na osnovu toga se može zaključiti da je koordinativna veza između površinskih atoma titana i LG ostvarena preko susednih OH grupa na benzenovom jezgru. Dobijeni rezultati su u skladu sa rezultatima objavljenim u literaturi, koji ukazuju da je dominantan način vezivanja galata za površinu TiO_2 nanočestica onaj po kome se dve susedne OH grupe vezuju za dva različita Ti atoma na površini čestice što dovodi do stvaranja „bridging“ kompleksa [25–27].

Na slici 3 prikazani su apsorpcioni spektri sintetisanog vodenog koloida TiO_2 i TiO_2–LG nanočestica disper-

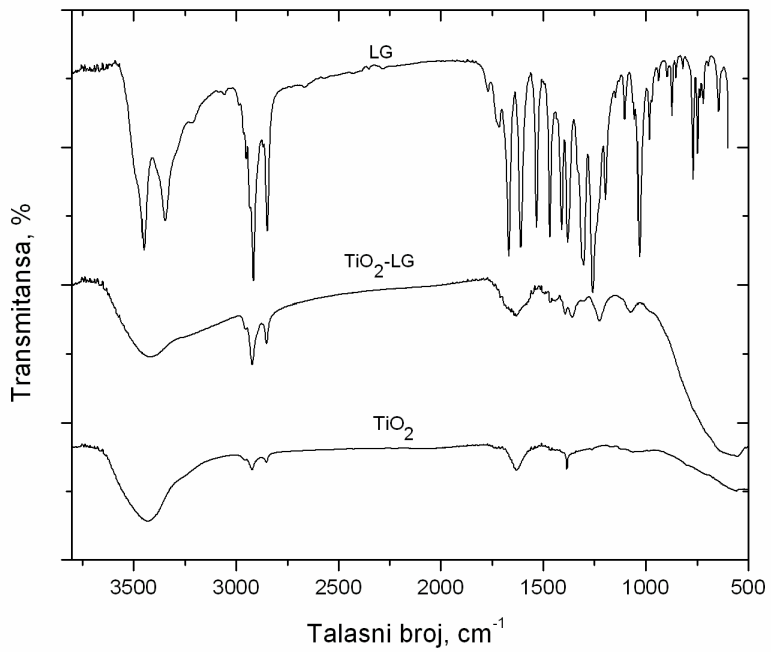

Slika 2. FTIR spektri LG i nanočestica TiO_2 i TiO_2–LG.
Figure 2. FTIR Spectra of LG and TiO_2 and TiO_2–LG nanoparticles.

govanih u hloroformu. Može se uočiti da je apsorpcioni spektar TiO_2–LG nanočestica pomeren ka većim talasnim dužinama („*red shift*“) u odnosu na spektar TiO_2 koloida. Početak apsorpcije kod modifikovanih TiO_2–LG čestica je oko 650 nm, dok je kod nemodifikovanih 380 nm. Ovo značajno pomeranje početka apsorpcije nanočestica TiO_2 posle modifikacije ukazuje da je došlo do reakcije LG sa atomima titana na površini nanočestica TiO_2 i formiranja CTC.

Površina nanočestica komercijalnog uzorka titan-dioksida, P25, je takođe modifikovana LG-om. FTIR spektri LG, nemodifikovanih nanočestica P25 i nanočestica P25 površinski modifikovanih sa LG-om (P25–LG) prikazani su na slici 4. Na FTIR spektru nanočestica P25-LG nanočestica vidi se odsustvo pikova na 3450 i 3350 cm^{-1} koje potiču od vibracija istezanja fenilnih OH grupa iz LG, a u isto vreme pojavljuju se pikovi koji potiču od istezanja CO veza u estarskoj grupi na 1228 i 1059 cm^{-1}, što ukazuje da je došlo do hemisorpcije LG na površinu nanočestica P25 čestica i da je način vezivanja LG za površinu potpuno isti u oba slučaja tj. da su molekuli LG za površinu TiO_2 vezani preko dve susedne fenilne OH grupe.

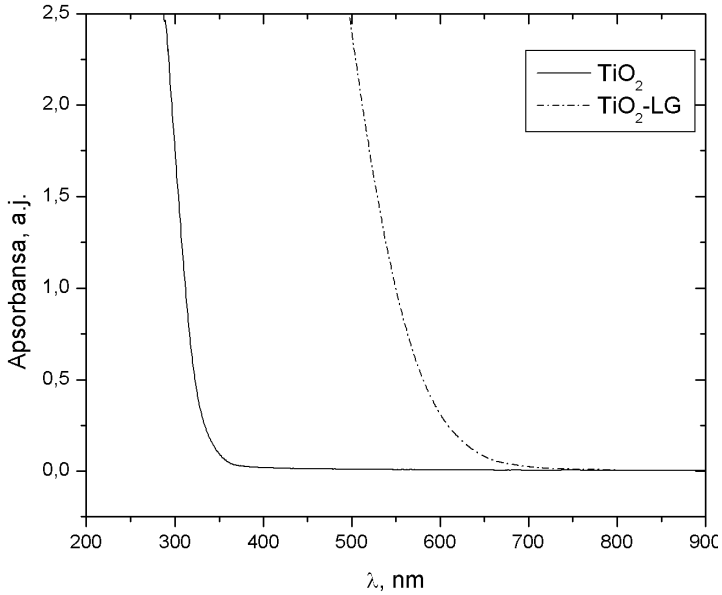

Slika 3. Apsorpcioni spektri TiO_2 koloida i nanočestica TiO_2–LG dispergovanih u hloroformu.
Figure 3. Absorption spectra of TiO_2 colloid and TiO_2–LG nanoparticles dispersed in chloroform.

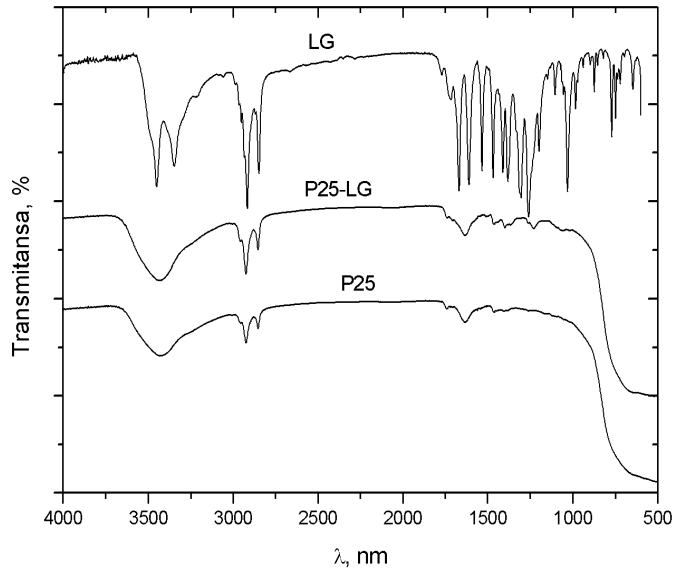

Slika 4. FTIR spektri LG i nanočestica P25 i P25–LG.
Figure 4. FTIR Spectra of LG and P25 and P25–LG nanoparticles.

Alkidne smole su jedne od najčešće korišćenih polimernih veziva u industriji premaza. U sastav premaza na bazi alkidnih smola ulaze različite vrste pigmenata, pri čemu TiO_2 predstavlja jedan od najviše korišćenih neorganskih pigmenata. Da bi se ispitao uticaj veličine čestica TiO_2 na reološka svojstva alkidne smole korišćene su tri vrste sfernih TiO_2 čestica različitih prečnika: R-2195 prečnika 250 nm, A-HR prečnika 170 nm i P25 prečnika 21 nm. Svaka od navedenih čestica TiO_2 dispergovana je u iznosu od 1 mas.% u alkidnu smolu (AS), a tako dobijene disperzije su označene sa AS/R-2195, AS/A-HR i AS/P25. Na slici 5 prikazana je zavisnost kompleksne dinamičke viskoznosti od frekvencije za uzorak čiste alkidne smole (AS) i tri pripremljene disperzije, AS/R-2195, AS/A-HR i AS/P25. Vidi se da su vrednosti viskoznosti disperzija veće od vrednosti za čistu smolu, i da rastu sa smanjenjem prečnika čestice a opadaju sa povećanjem frekvencije.

Kompleksna dinamička viskoznost je određena i za disperzije površinski modifikovanih nanočestica TiO_2 iste koncentracije (AS/TiO_2–LG i AS/TiO_2–PG), a dobijene frekvencione zavisnosti su prikazane na slici 6. Sa slika 5 i 6 se vidi da disperzija nanočestica P25–LG ima veću viskoznost nego disperzija nemodifikovanih nanočestica P25. Viskoznost AS/P25 se može predstaviti Ajnštajnovom jednačinom za slučaj nedeformabilnih

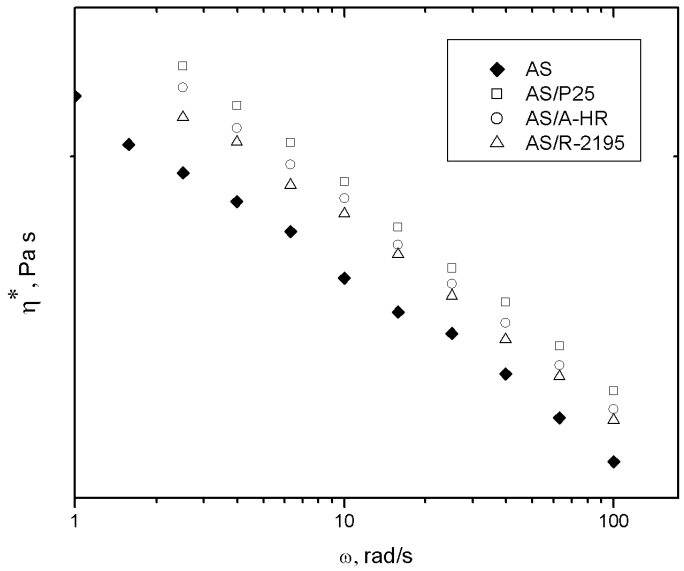

Slika 5. Zavisnost kompleksne dinamičke viskoznosti od frekvencije za AS i AS/R-2195, AS/A-HR i AS/P25 disperzije.
Figure 5. The dependence of complex dynamic viscosity vs. frequency for AS and AS/R-2195, AS/A-HR and AS/P25 dispersions.

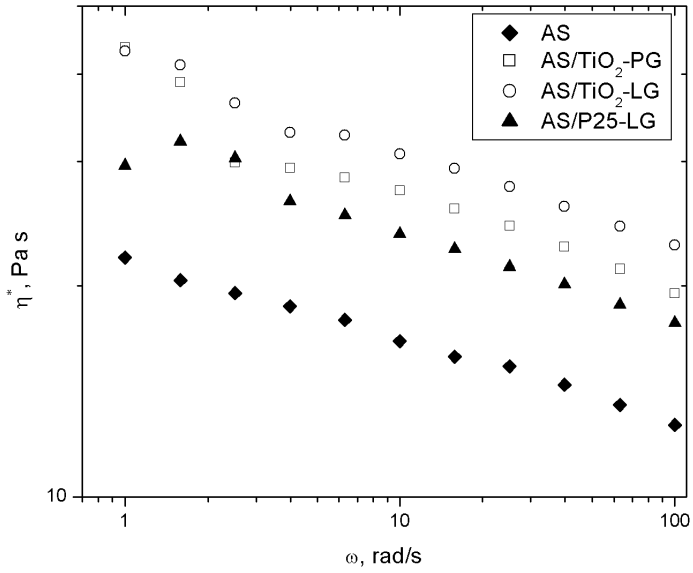

Slika 6. Zavisnost kompleksne dinamičke viskoznosti od frekvencije za AS i AS/TiO_2–PG, AS/TiO_2–LG i AS/P25–LG disperzije.
Figure 6. The dependence of complex dynamic viscosity vs. frequency for AS and AS/TiO_2–PG, AS/TiO_2–LG and AS/P25–LG dispersions.

krutih sfera, po kojoj viskoznost takvih sistema zavisi samo od zapreminskog udela dispergovane faze. Viskoznost AS/P25–LG uzorka, gde su nanočestice P25 sterno stabilisane sa LG, se takođe može aproksimirati istom jednačinom. Naime, površinski modifikovane P25–LG čestice imaju veću hidrodinamičku zapreminu nego nemodifikovane, pa se stiče utisak da je udeo dispergovane faze veći. Zbog toga se prilikom računanja zapreminskog udela dispergovane faze mora uzeti u obzir i debljina adsorbovanog sloja na površini P25 čestica. Tako određen zapreminski udeo dispergovane faze naziva se efektivni zapreminski udeo i on je veći od udela nemodifikovanih P25 čestica, pa kad se uvrsti u dati izraz dobija se da je viskoznost AS/P25–LG veća nego u slučaju uzorka AS/P25. Sa slike 6 se takođe vidi da je vrednost viskoznosti uzorka AS/P25–LG manja od vrednosti za AS/TiO_2–LG. Razlog za ovo smanjenje je isti kao i u slučaju nemodifikovanih čestica, sa smanjenjem prečnika čestica povećava se specifična površina čestica pa samim tim i intenzitet interakcija između čestica [28,29].

Sa slike 6 se može videti i da je viskoznost uzorka AS/TiO_2–LG veća od viskoznosti uzorka AS/TiO_2–PG. Zbog veće dužine ugljovodoničnog lanca lauril grupe, debljina adsorpcionog sloja je veća u slučaju TiO_2–LG čestica, samim tim je efektivni zapreminski udeo TiO_2––LG čestica u AS veći nego TiO_2–PG čestica, pa je otuda i njihov uticaj na viskoznost AS veća nego uticaj TiO_2––PG čestica [28,29].

Da bi se ispitao uticaj koncentracije nanopunila na viskoznost AS pripremljena su po tri uzorka AS/TiO_2–LG i AS/TiO_2–PG nanokompozita koncentracija 1, 2 i 3 mas.%. Zavisnost kompleksne dinamičke viskoznosti od frekvencije za ove uzorke različitih koncentracija nanočestica prikazana je na slici 7. Pri koncentraciji nanočestica od 1 mas. % vrednost viskoznosti AS/TiO_2–LG je veća od vrednosti za AS/TiO_2–PG, dok za druge dve koncentracije to nije slučaj. Za koncentraciju nanočestica od 2 mas.% viskoznost uzorka AS/TiO_2–PG je veća pri nižim frekvencijama da bi se na visokim frekvencijama izjednačila sa vrednošću za uzorak AS/TiO_2–LG. Za najveću ispitivanu koncentraciju nanočestica od 3 mas.% viskoznost uzorka koji sadrži TiO_2–PG je veća u ispitivanom opsegu frekvencija, s tim što je ta razlika mnogo više izražena pri nižim frekvencijama. Razlog za ovakvo ponašanje treba tražiti u činjenici da je disperziona stabilnost TiO_2–PG zbog kraćeg alkil lanca u galatnom ligandu manja nego TiO_2–LG nanočestica i da već pri koncentracijama od 2 mas.% dolazi do agregacije i nastanka aglomerata. Prisustvo aglomerata dovodi do povećanja viskoznosti i stiče se prividan utisak da je udeo punila veći nego što stvarno jeste. Naime, pri nastajanju aglomerata jedan deo disperzionog sredstva biva zarobljen u šupljinama između primarnih čestica koje aglomerišu, što dovodi do smanjenja zapreminskog udela disperznog sredstva oko agregata. Da postoji razlika u interakciji između čestica u ispitivanim disperzijama najbolje se vidi iz zavisnosti modula sačuvane energije (G') od frekvencije. Poznato je iz literature da sa povećanjem udela dispergovane faze opada nagib zavisnosti G' od frekvencije u odnosu na G' za čistu smolu i kada se dostigne neka kritična vrednost zapreminskog udela, G' na niskim frekvencijama ulazi u plato. Na slikama 8 i 9 prikazane su zavisnosti G'–ω za

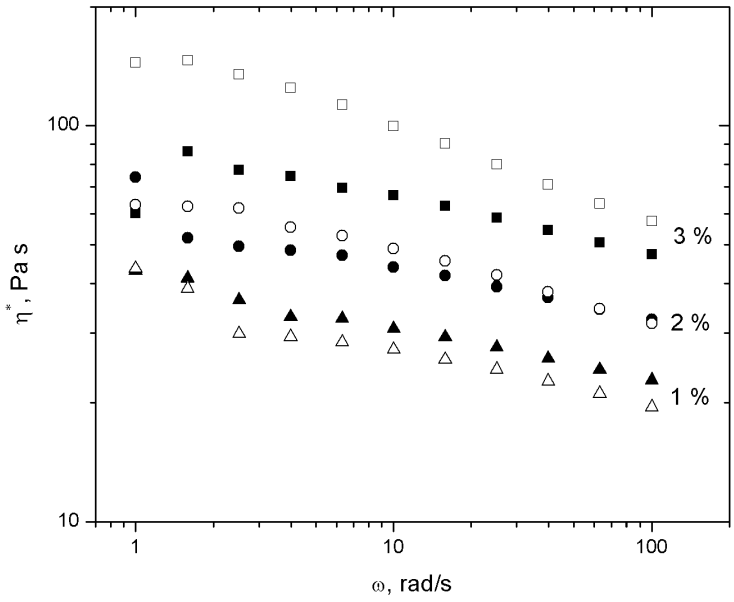

Slika 7. Zavisnost kompleksne dinamičke viskoznosti od frekvencije za uzorke AS/TiO_2–LG (puni simboli) i AS/TiO_2–PG (prazni simboli) pri različitim koncentracijama nanočestica.
Figure 7. The dependence of complex dynamic viscosity vs. frequency for samples AS/TiO_2–LG (solid symbols) and AS/TiO_2–PG (open symbols) at different concentrations of nanoparticles.

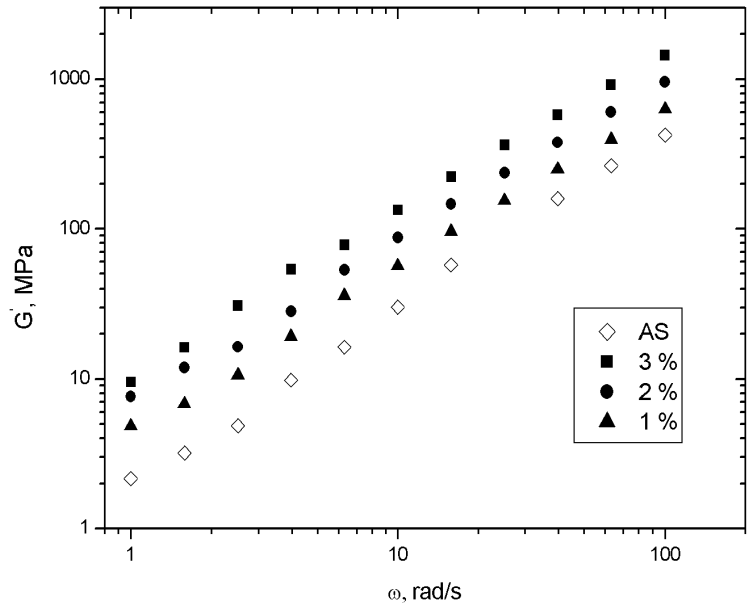

Slika 8. Zavisnost modula sačuvane energije (G') od frekvencije za uzorke AS i AS/TiO_2–LG pri različitim koncentracijama nanočestica.
Figure 8. The dependence of storage modulus (G') vs. frequency for samples AS and AS/TiO_2–LG at different concentrations of nanoparticles.

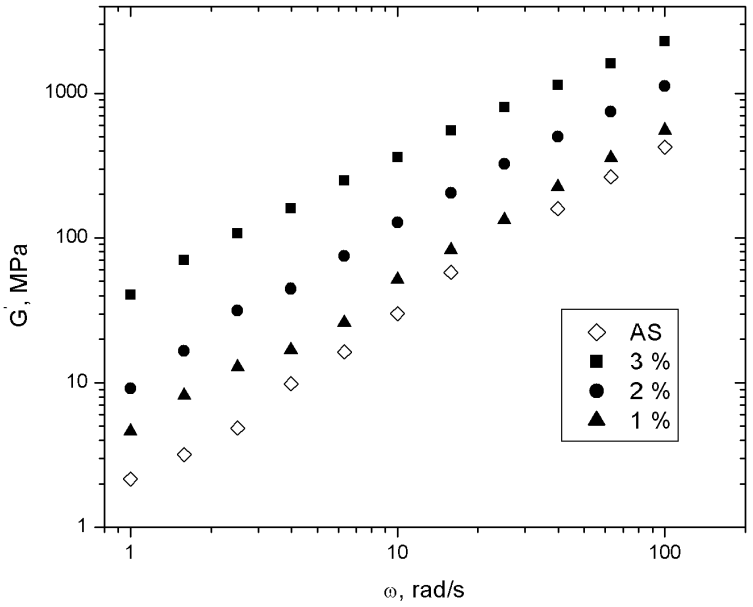

Slika 9. Zavisnost modula sačuvane energije (G') od frekvencije za uzorke AS i AS/TiO_2–PG pri različitim koncentracijama nanočestica.
Figure 9. The dependence of storage modulus (G') vs. frequency for samples AS and AS/TiO_2–PG at different concentrations of nanoparticles.

disperzije sa različitim udelom TiO_2–LG i TiO_2–PG nanočestica. Vidi se da je u slučaju TiO_2–PG nanočestica došlo do promene nagiba zavisnosti G'–ω, dok je u slučaju TiO_2-LG nanočestica nagib zavisnosti G'–ω ostao isti. Dobijeni rezultati ukazuju da su međusobne interakcija između TiO_2–PG čestica više izražene nego između TiO_2–LG [28,29].

Na slikama 10 i 11 prikazane su zavisnosti modula sačuvane energije, $G'(\omega)$, od modula izgubljene energije, $G''(\omega)$, za disperzije sa različitim udelom TiO_2–LG i TiO_2–PG nanočestica. Na osnovu ovih zavisnosti može se reći da li postoje neke mikrostrukturne razlike između ispitivanih uzoraka. Ako ne postoje mikrostrukturne razlike između uzoraka, onda se njihove zavisnosti G'–G'' moraju poklopiti sa zavisnošću za čistu smolu. Sa slike 10 se vidi da se dobijene zavisnosti G'–G'' za disperzije AS/TiO_2–LG sa različitim udelom TiO_2–LG poklapaju sa zavisnošću G'–G'' za čistu smolu, ali u slučaju AS/TiO_2–PG sa porastom koncentracije TiO_2–PG nagib G'–G'' opada u odnosu na čistu smolu što ukazuje na

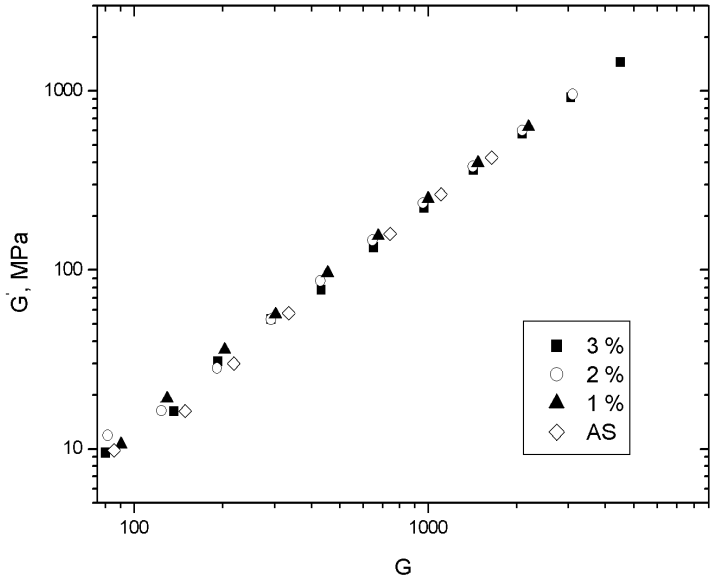

Slika 10. Zavisnost modula sačuvane energije (G') od modula izgubljene energije (G˝) za uzorke AS i AS/TiO_2–LG pri različitim koncentracijama nanočestica.
Figure 10. The dependence of storage modulus (G') vs. loss modulus (G˝) for samples AS and AS/TiO_2–LG at different concentrations of nanoparticles.

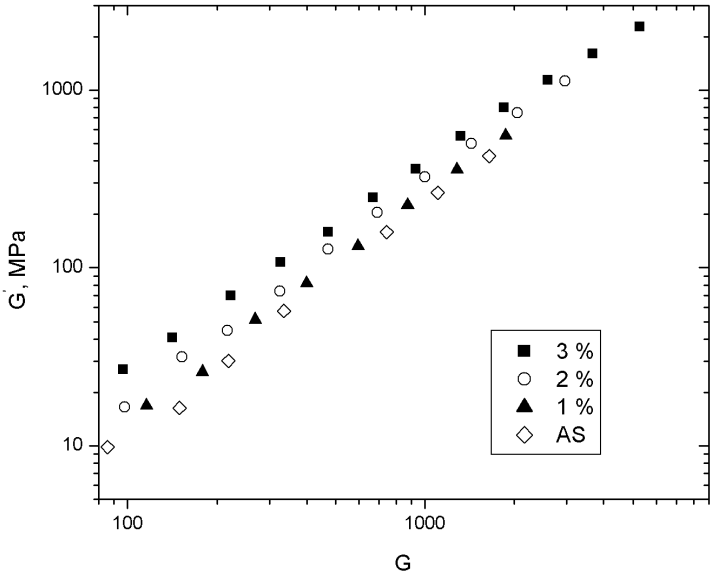

Slika 11. Zavisnost modula sačuvane energije (G') od modula izgubljene energije (G˝) za uzorke AS i AS/TiO_2–PG pri različitim koncentracijama nanočestica.
Figure 11. The dependence of storage modulus (G') vs. loss modulus (G˝) for samples AS and AS/TiO_2–PG at different concentrations of nanoparticles.

postojanje mikrostrukturnih razlika. Sa porastom koncentracije TiO_2–PG u ispitivanim disperzijama, zbog lošije disperzione stabilnosti, dolazi do stvaranja aglomerata koji predstavljaju tu strukturnu razliku [30].

ZAKLJUČAK

Pripremljene su disperzije nemodifikovanih TiO_2 čestica, kao i disperzije površinski modifikovanih nanočestica u alkidnoj smoli na bazi sojinog ulja sa sadržajem ulja od 65%. Ispitan je uticaj veličine nanočestica TiO_2, koncentracije nanočestica, kao i vrste površinske modifikacije na viskoznost pripremljenih disperzija. Utvrđeno je da sa smanjenjem prečnika nemodifikovanih TiO_2 čestica raste viskoznost disperzije, jer se sa smanjenjem prečnika čestica povećava specifična površina čestica pa samim tim i intenzitet interakcija između čestica. Površinski modifikovane čestice imaju veći uticaj na viskoznost alkidne smole nego nemodifikovane, jer one usled prisustva adsorbovanog organskog sloja

imaju veću hidrodinamičku zapreminu nego nemodifikovane. Uticaj koncentracije TiO_2 je naročito izražen kod nanočestica modifikovanih PG jer sa povećanjem koncentracije dolazi do aglomeracije TiO_2-PG nanočestica usled njihove lošije disperzione stabilnosti.

Zahvalnica

Ovaj rad je finansiralo Ministarstvo prosvete, nauke i tehnološkog razvoja Republike Srbije (Projekti br. 172062 i 45020).

LITERATURA

[1] T.C. Patton, Alkyd resin technology, Interscience Publ., New York, 1962.

[2] A. Hofland, Alkyd resins: From down and out to alive and kicking, Prog. Org. Coat. **73** (2012) 274–282.

[3] F.S. Gunera, Y. Yagci, A.T. Erciyes, Polymers from triglyceride oils, Prog. Polym. Sci. **31** (2006) 633–670.

[4] J.W. Gooch, Emulsification and Polymerization of Alkyd Resins, Kulwer Academic Publishers, New York, 2002.

[5] M.D. Soucek, T. Khattab, J. Wu, Review of autoxidation and driers, Prog. Org. Coat. **73** (2012) 435–454.

[6] J.C. Hubert, R.A.M. Venderbasch, W.J. Muizbelt, R.P. Klaasen, K.H. Zabel, Singlet oxygen drying of alkyd resins and model compounds, J. Coat. Tech. **69** (1997) 59–64.

[7] Z.O. Oyman, W. Ming, R. van der Linde, Oxidation of drying oils containing non-conjugated and conjugated double bonds catalyzed by a cobalt catalyst, Prog. Org. Coat. **54** (2005) 198–204.

[8] G. Ye, F. Courtecuisse, X. Allonas, C. Ley, C. Croutxe-Barghorn, P. Raja, P. Taylor, G. Bescond, Photoassisted oxypolymerization of alkyd resins: Kinetics and mechanisms, Prog. Org. Coat. **73** (2012) 366–373.

[9] V.D. Athawale, A.V. Chamanker, The effects of driers on film properties of alkyd resin, Pigm. Resin Technol. **26** (1997) 378–381.

[10] A. Bal, G. Güçlü, I. Acar, T.B. İyim, Effects of urea formaldehyde resin to film properties of alkyd–melamine formaldehyde resins containing organo clay, Prog. Org. Coat. **68** (2010) 363–365.

[11] D.T.C. Ang, S.N. Gan, Novel approach to convert non-self drying palm stearin alkyds into environmental friendly UV curable resins, Prog. Org. Coat. **73** (2012) 409–414.

[12] E.A. Murillo, P.P. Vallejo, B.L. López, Synthesis and characterization of hyperbranched alkyd resins based on tall oil fatty acids, Prog. Org. Coat. **69** (2010) 235–240.

[13] E.A. Murillo, B.L. López, Novel waterborne hyperbranched acrylated-maleinized alkyd resins, Prog. Org. Coat. **72** (2011) 731–738.

[14] E. Dzunuzovic, S. Tasic, B. Bozic, D. Babic, B. Dunjic, UV-curable hyperbranched urethane acrylate oligomers containing soybean fatty acids, Prog. Org. Coat. **52** (2005) 136–143.

[15] R. Bhavsar, R. Raj, R. Parmar, Studies of sedimentation behaviour of high pigmented alkyd primer: A rheological approach, Prog. Org. Coat. **76** (2013) 852–857.

[16] D.Y. Perera, Effect of pigmentation on organic coating characteristics, Prog. Org. Coat. **50** (2004) 247–262.

[17] M.V. Popa, P. Drob, E. Vasilescu, J.C. Mirza-Rosca, A. Santana Lopez, C. Vasilescu, S.I. Drob, The pigment influence on the anticorrosive performance of some alkyd films, Mater. Chem. Phys. **100** (2006) 296–303.

[18] S.J.F. Erich, H.P. Huinink, O.C.G. Adan, J. Laven, A.C. Esteves, The influence of the pigment volume concentration on the curing of alkyd coatings: A 1D MRI depth profiling study, Prog. Org. Coat. **63** (2008) 399–404.

[19] F. Cadena, L. Irusta, M.J. Fernandez-Berridi, Performance evaluation of alkyd coatings for corrosion protection in urban and industrial environments, Prog. Org. Coat. **76** (2013) 1273–1278.

[20] S.K. Dhoke, A.S. Khanna, Effect of nano-Fe_2O_3 particles on the corrosion behavior of alkyd based waterborne coatings, Corros. Sci. **51** (2009) 6–20.

[21] H. Shi, F. Liu, E. Han, Y. Wei, Effects of Nano Pigments on the Corrosion Resistance of Alkyd Coating, J. Mater. Sci. Technol. **23** (2007) 551–558.

[22] B. Ramezanzadeh, M.M. Attar, Characterization of the fracture behavior and viscoelastic properties of epoxy-polyamide coating reinforced with nanometer and micrometer sized ZnO particles, Prog. Org. Coat. **71** (2011) 242–249.

[23] B. Ramezanzadeh, M.M. Attar, M. Farzam, A study on the anticorrosion performance of the epoxy–polyamide nanocomposites containing ZnO nanoparticles, Prog. Org. Coat. **72** (2011) 410–422.

[24] B. O'Regan, J. Moser, M. Anderson, M. Grätzel, Vectorial Electron Injection into Transparent Semiconductor Membranes and Electric Field Effects on the Dynamics of Light-Induced Charge Separation J. Phys. Chem. **94** (1990) 8720–8726.

[25] I. Janković, Z. Šaponjić, E. Džunuzović, J. Nedeljković, New hybrid properties of TiO_2 nanoparticles surface modified with catecholate type ligands, Nanoscale Res. Lett. **5** (2010) 81–88.

[26] E.S. Džunuzović, J.V. Džunuzović, A.D. Marinković, M.T. Marinović-Cincović, K.B. Jeremić, J.M. Nedeljković, Influence of surface modified TiO_2 nanoparticles by gallates on the properties of PMMA/TiO_2 nanocomposites, Eur. Polym. J. **48** (2012) 1385–1393.

[27] E.S. Džunuzović, J.V. Džunuzović, T.S. Radoman, M.T. Marinović-Cincović, Lj.B. Nikolić, K.B. Jeremić, J.M. Nedeljković, Characterization of In Situ Prepared Nanocomposites of PS and TiO_2 Nanoparticles Surface Modified with Alkyl Gallates: Effect of Alkyl Chain Length, Polym. Comp. **34** (2013) 399–407.

[28] A.V. Shenoy, Rheology of Filled Polymer Systems, Kluwer Academic Publishers, Dordrecht, 1999.

[29] A. W. Macosko, Rheology Principles, Measurements and Applications, Wiley-VCH, New York, 1994.

[30] P. Pötschke, T.D. Forens, D.R. Paul, Rheological behavior of multiwalled carbon nanotube/polycarbonate composites, Polymer **43** (2002) 3247–3255.

SUMMARY

THE INFLUENCE OF THE SIZE AND SURFACE MODIFICATION OF TiO_2 NANOPARTICLES ON THE RHEOLOGICAL PROPERTIES OF ALKYD RESIN

Tijana S. Radoman[1], Jasna V. Džunuzović[2], Katarina B. Jeremić[3], Aleksandar D. Marinković[3], Pavle M. Spasojević[1], Ivanka G. Popović[3], Enis S. Džunuzović[3]

[1]*Innovation center, Faculty of Technology and Metallurgy, University of Belgrade, Karnegijeva 4, Belgrade 11120, Serbia*
[2]*Institute of Chemistry, Technology and Metallurgy (ICTM) – Department of Chemistry, University of Belgrade, Studentski trg 12–16, 11000 Belgrade, Serbia*
[3]*Faculty of Technology and Metallurgy, University of Belgrade, Karnegijeva 4, 11120 Belgrade, Serbia*

(Scientific paper)

Spherical TiO_2 particles of different size were dispersed in alkyd resin based on soybean oil. Four samples of TiO_2 particles were used, three commercial and one obtained by acid catalyzed hydrolysis of titanium tetraisopropoxide. The size of the synthesized nanoparticles was determined by transmission electron microscopy. Surface modification of TiO_2 nanoparticles was performed with propyl gallate and lauryl gallate. The influence of the size of TiO_2 nanoparticles, their concentration and type of the surface modification on the rheological properties of alkyd resin was investigated. The obtained results have shown that the viscosity of the prepared dispersions was higher than the viscosity of the pure resin, increases with decreasing particle diameter and decreases with frequency increase. Surface modified particles showed higher influence on the viscosity of alkyd resin than unmodified, because their hydrodynamic volume is higher due to the presence of the adsorbed gallates, leading to the increase of effective volume fraction of particles in dispersion. For the lowest TiO_2 concentration, the viscosity was higher for the sample modified with lauryl gallate, due to the higher thickness of the adsorbed layer. The increase of concentration, because of less dispersion stability of the particles modified with propyl gallate, leads to particle agglomeration. The presence of agglomerates, which was confirmed by a change in the slope of the functional dependence of storage modulus on loss modulus, leads to a rapid increase in viscosity.

Keywords: TiO_2 Nanoparticles • Surface modification • Propyl gallate • Lauryl gallate • Alkyd resin • Rheology

Reversed-phase HPLC retention data in correlation studies with lipophilicity molecular descriptors of carotenoids

Sanja O. Podunavac-Kuzmanović, Lidija R. Jevrić, Aleksandra N. Tepić, Zdravko Šumić

Faculty of Technology, University of Novi Sad, Bul. Cara Lazara 1, 21000 Novi Sad, Serbia

Abstract

Influence of chemical structure on the lipophilicity of isolated free carotenoids from paprika oleoresin was studied by a quantitative structure-retention relationship (QSRR) approach. The chromatographic behavior of these compounds was investigated by reversed phase high-pressure liquid chromatography (RP HPLC). The retention mechanism was determined using acetone-water as the mobile phase on a reversed-phase column (SB-C18). A variety of lipophilicity parameters (log *P*) were calculated using different software products. Based on the correlations, nonlinear structure–activity models were derived between the retention constants, t_r (retention time of investigation compounds) and log *P* values. Five high quality QSRR models were found to have a good predictive ability and close agreement between experimental and predicted values. The study showed that the retention constants can be used as a measure of lipophilicity of investigated compounds at a high significant level.

Keywords: carotenoids, RP HPLC, Lipophilicity, QSRR.

Available online at the Journal website: http://www.ache.org.rs/HI/

SCIENTIFIC PAPER

UDC 635.649:543.544.5:544.722.123

Hem. Ind. **67** (6) 933–940 (2013)

doi: 10.2298/HEMIND121015010P

Red pepper (*Capsicum annuum* L.) is one of the most important vegetable cultures in the province of Vojvodina in Serbia. There are a number of foods containing paprika or its compounds. It is especially important because of its high nutritive and biological value [1,2]. In recent years, carotenoids have been a subject of research interest as potential antioxidants, based on studies that reported that a higher consumption of carotenoids leads to lower risk of cancer and cardiovascular diseases [3,4]. The yellow, orange and red colors of paprika fruit originate from carotenoids and the pigments are synthesized during ripening. They are the most widespread group of pigments – the number of naturally occurring carotenoids continues to rise and has reached about 750 [5]. More than 25 different pigments have been identified in the fruits of paprika: green chlorophylls, yellow-orange lutein, zeaxanthin, violaxanthin, antheraxanthin, β-cryptoxanthin, β-carotene, etc. The red pigments capsanthin, capsorubin and cryptoxanthin are unique to the Capsicum species. The colour of paprika is determined by the proportion of red to yellow pigments [6,7], whereas β-, α-, γ-carotene and β-cryptoxanthin, as provitamins, contribute to its nutritive value. The quality of paprika and its oleoresins is determined primarily by their color [8-11]. Capsanthin and capsorubin, which comprise 65–80%, contribute the red colour to paprika [12–14]. In the fruits of paprika during ripening, free carotenoids esterification with fatty acids occurs [15].

Saturated fatty acids are known to be more stable and solid at room temperature. With an increase in the number of double bonds, the fluidity rises. On the other hand, unsaturated fatty acids are prone to autoxidation, which leads to the generation of free radicals and increasing risk of cancer. However, substituting saturated with unsaturated fats in diet lowers the level of total cholesterol and LDL cholesterol in blood. Also, linoleic (18:2) and α-linolenic (18:3) are essential fatty acids, which play an important role in human nutrition.

Because of their potential biological activity, for initial chemical screening of activity of investigated compounds, it is first recommended to determine their lipophilicity. The most widely accepted measure of lipophilicity is the octanol-water partition coefficient, which is expressed in its logarithmic form as log *P* [16].

Literature is rich in research articles investigating similarities/dissimilarities between log *P* and chromatographic retention. Determination of partition coefficient using the classical "shake-flask" technique has a series of disadvantages and has been successfully replaced by alternative chromatographic methods, since the partition coefficient (lipophilicity) of a compound between aqueous and organic phase determines both its permeation through biological membranes and retention in RP LC [17–24].

Quantitative structure (chromatographic) retention relationships (QSRR) have been considered a model approach to establish strategy and methods of property predictions. QSRR analysis appears especially attractive from the general chemometric point of view

Correspondence: L.R. Jevrić, Department of Applied and Engineering Chemistry, Faculty of Technology, University of Novi Sad, Bulevar Cara Lazara 1, 21000 Novi Sad, Serbia.

E-mail: lydija@uns.ac.rs

Paper received: 15 October, 2012

Paper accepted: 11 January, 2013

because it provides the best testing of the applicability of individual structural parameters for property description.

Currently, QSRR studies can be used to: identify the most useful structural descriptors, predict retention for a new analyte and to identify unknown analytes, gain insight into molecular mechanism of separation operating in a given chromatographic system, quantitatively compare separation properties of individual types of chromatographic columns, evaluate properties, other than chromatographic physicochemical properties of analytes, such as lipophilicity, estimate relative bioactivities within sets of drugs and other xenobiotics [25]. In QSRR studies, relations between molecular descriptors and retention have been explored [26]. The aim of this methodology is to derive a model to describe the chromatographic retention on a given chromatographic system, which then can be used for future retention prediction of new solutes. Thus, when a meaningful and statistically significant model is found, no additional experiments are needed to predict the retention for new solutes.

In QSRR studies, molecular descriptors are either determined from experiments or computed by molecular mechanics or even semi-empirical quantum chemical techniques. Chromatographic retention is a physical phenomenon that is primarily dependent on the interactions between the solute and the stationary phase. The compatibility of experimental and theoretical approaches for the determination of organic compound lipophilicity remains also a focus of scientific interest.

Considering the practical importance of isolated free carotenoids from paprika oleoresin, the main objective of this study was to examine the retention behavior of seven carotenoids in reversed-phase chromatographic systems (HPLC) of mobile phase (acetone-water). Obtained chromatographic data were correlated to selected lipophilicity parameters. This method includes data collection, molecular descriptor selection, correlation model development, and finally model evaluation. QSRR studies have prediction abilities.

EXPERIMENTAL

Material

Commercial ground paprika of the "Aleva N.K." variety, harvested in 2005, was obtained from the Aleva a.d. company from Novi Kneževac, the most important producer of ground pepper in Serbia. The mean diameter of the particles was 0.224 mm. Ground pepper was placed into the thimble in the middle portion of the Soxhlet apparatus, the solvent was then poured in, and the process was continued until complete discoloration of sample was achieved. Soxhlet (Sx) extract of paprika was obtained using technical grade hexane. The solvent was evaporated from extract under vacuum.

HPLC Analysis of carotenoid content

Qualitative and quantitative analysis of samples-free carotenoids (Figure 1) was performed according to a previously described method [27]. HPLC was performed using a Hewlett-Packard liquid chromatograph HP 1090 equipped with Diode Array Detector (DAD). A reversed-phase column (Zorbax SB-C18, 5 μm, 3.0×250 mm^2 i.d.), protected by a guard column (Zorbax SB-C18, 5 μm, 4.6×12 mm^2 i.d., Agilent, USA) was used throughout this research. The mixture of mobile phase acetone:water (75:25; v/v) was used and the HPLC separations were performed by the following linear gradient: 0–25% of acetone in 10 min, then until 100% of acetone by 35 min, 100% of acetone by 45 min, 0% of acetone by 65 min, post time 15 min. The flow rate of the mobile phase was set at 0.500 mL/min. The oven

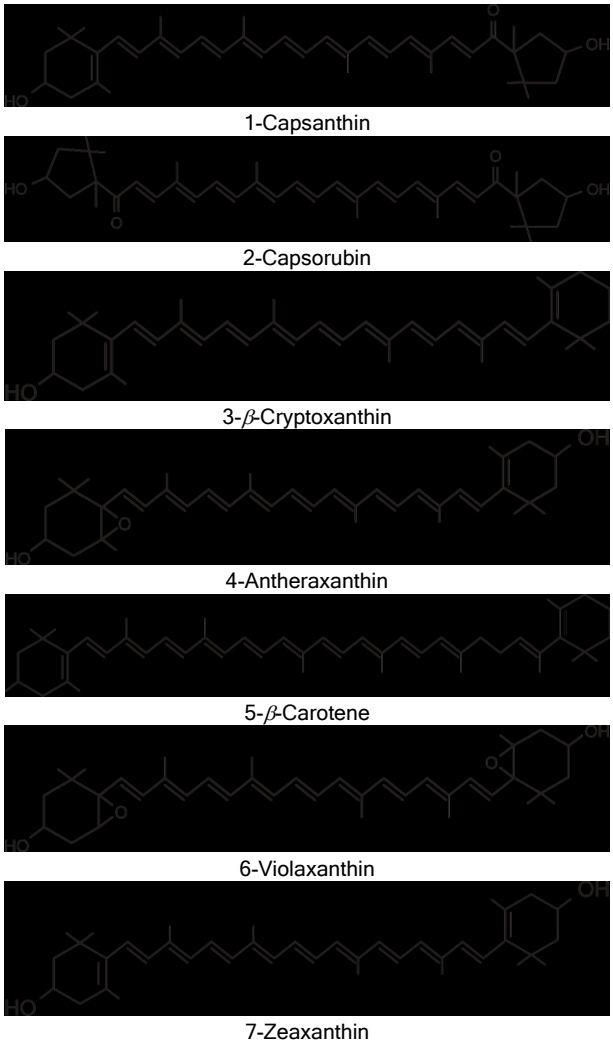

Figure 1. Chemical structures of the carotenoids from paprika studied.

was operated at room temperature (25 °C). The sample injection volume was 10 μL, and the injection was performed manually. The chromatograms were acquired in the range 460+4 nm by DAD detector; the spectra were recorded in the range of 350–550 nm. Carotenoid standards capsanthin, capsorubin, antheraxanthin, zeaxanthin, violaxanthin, β-carotene were obtained from "Carotenature", Switzerland; 80-β-apo-carotenal was obtained from Fluka, Germany. All reagents used were HPLC grade.

Molecular modelling and calculations of lipophilicity parameters

Molecular modelling studies were performed using CS Chem-Office Software version 7.0 (Cambridge software) running on a P-III processor [28]. All molecules were constructed by using Chem Draw Ultra 7.0 and saved as the template structures. For every compound, the template structure was suitably changed considering its structural features, copied to Chem 3D 7.0 to create a 3-D model and, finally, the model was cleaned up and subjected to energy minimization using molecular mechanics (MM_2). The minimization was executed until the root mean square (RMS) gradient value reached a value smaller than 0.1 kcal/mol·A. The Austin Model-1 (AM-1) method was used for re-optimization until the RMS gradient attained a value smaller than 0.0001 kcal/mol·A using MOPAC. Partition coefficients and aqueous solubility values were calculated with different theoretical bases (atomic based prediction, fragment based prediction): Alog P_s, AClog *P*, Alog *P*, Mlog *P*, log P_{Kowin}, Xlog *P*2, and Xlog *P*3 by applying different theoretical procedures (Table 1) [29,30].

Statistical methods

The complete regression analysis was carried out by PASS 2005, GESS 2006, NCSS Statistical Softwares [31].

RESULTS AND DISCUSSION

Lipophilicity determination

Lipophilicity is one of the important physico-chemical parameters that determine the activity. Hence, the estimation of the lipophilic character of new, potentially biologically active compounds is regarded as one of the first parameters to be determined at the earliest possible opportunity. It has been recognized that the retention of a compound in reversed-phase liquid chromatography (RP-LC) is governed by its lipophilicity and thus chromatography may be successfully used for the determination of lipophilicity. Although HPLC is a relatively new LC technique, it offers several practical advantages compared to the traditional shake-flask method, including a rapid and simple way of lipophilicity determination, reproducibility, broader dynamic range, insensitivity to impurities or degradation products, and a wide choice of adsorbents and solvents.

The main purpose of this study was to use chromatographic data – retention time (t_r) as a descriptor of the lipophilic character for carotenoids studied.

Correlation of retention time, t_r, and log *P*

To investigate the quantitative effects of the structural parameters of free carotenoids from paprika oleoresin retention time, QSRR analysis with seven different partition coefficients (log *P*) was employed. First, the correlation of each one of the log *P* values with each other was calculated. The resulting correlation matrix is shown in Table 2. The correlation matrix was constructed to find the interrelationship among the parameters, which shows that all the lipophilicity descriptors selected in the study are highly mutually correlated ($r > 0.85$). Therefore, any combination of these descriptors in multiple regression analysis may result with a model suffering from multi-colinearity.

Usually, lipophilicity parameters are linearly related to retention time, but in the more general case this relationship is not linear. Therefore, a complete regression analysis was performed, using linear, quadratic and cubic relationships. It is apparent from the data presented in Table 3 that the fit quality improved with higher (second or third) order polynomials.

Among the presented lipophilicity parameters, log*P* values that had the highest correlation with t_r were retained and used to find a nonlinear monoparametric models. The resulting models were:

Table 1. Partition coefficients calculated by different theoretical methods

Compd.	*A*log P_s	*AC*log *P*	*A*log *P*	*M*log *P*	log P_{Kowin}	*X*log *P*2	*X*log *P*3
1	8.37	9.91	8.26	6.30	13.46	7.05	10.34
2	10.46	15.99	14.99	10.29	21.65	12.62	16.97
3	9.08	11.94	10.76	7.94	16.08	8.63	12.25
4	8.20	9.95	8.81	6.22	13.18	6.93	10.60
5	7.43	8.78	8.10	5.42	11.41	6.68	10.29
6	8.77	9.27	7.70	6.37	13.27	7.87	11.08
7	8.30	11.11	9.52	7.06	14.95	7.18	10.91

Table 2. Correlation (r) matrix for lipophilicity descriptors used in this study

r	Alog *P*s	AClog *P*	Alog *P*	Mlog *P*	log P_{Kowin}	Xlog *P*2	Xlog *P*3
Alog *P*s	1	0.911	0.876	0.952	0.947	0.951	0.929
AClog *P*		1	0.990	0.989	0.903	0.942	0.958
Alog *P*			1	0.971	0.973	0.943	0.965
Mlog *P*				1	0.996	0.956	0.960
log P_{Kowin}					1	0.957	0.963
Xlog *P*2						1	0.995
Xlog *P*3							1

Table 3. Correlation coefficients (r) calculated for relationship between retention time and different log P values

Parameter	$t_r = a\log P + b$	$t_r = a\log P^2 + b\log P + c$	$t_r = a\log P^3 + b\log P^2 + c\log P + d$
*A*log*P*s	0.8869	0.8979	0.9179
*AC*log*P*	0.9371	0.9426	**0.9658**
*A*log*P*	0.9361	0.9470	**0.9798**
*M*log*P*	0.9488	0.9494	**0.9775**
logP_{Kowin}	0.9303	0.9325	**0.9667**
*X*log*P*2	0.8974	0.9184	0.9484
*X*log*P*3	0.8984	0.9387	**0.9795**

$$t_r = -0.457AC\log P^3 + 15.689AC\log P^2 - \\ -177.703AC\log P + 652.919$$
$$r^2 = 0.9328,\ s = 17.7960 \quad (1)$$

$$t_r = -0.561A\log P^3 + 18.276A\log P^2 - \\ -186.718A\log P + 617.785$$
$$r^2 = 0.9600,\ s = 10.5843 \quad (2)$$

$$t_r = -1.128M\log P^3 + 26.012M\log P^2 - \\ -187.286M\log P + 436.234$$
$$r^2 = 0.9555,\ s = 11.7775 \quad (3)$$

$$t_r = -0.159\log P_{Kow}{}^3 + 7.669\log P_{Kow}{}^2 - \\ -115.682\log P_{Kow} + 564.124$$
$$r^2 = 0.9345,\ s = 17.3226 \quad (4)$$

$$t_r = -1.423X\log P3^3 + 55.120X\log P3^2 - \\ -689.682X\log P3 + 2818.871$$
$$r^2 = 0.9594,\ s = 10.7601 \quad (5)$$

where r^2 is the square of the correlation coefficient and *s* is the standard deviation.

It is obvious that the obtained regression equations have high statistical quality and these models can be used to predict the retention time for free carotenoids from paprika oleoresin. To confirm the predictive power of the models, the retention times were calculated by the theoretical models 1–5. From the data presented in Table 4, it can be concluded that the observed and the estimated t_r are very close to each other. This indicates the good predictability of the established models.

Figure 2 shows the linear plots of predicted *vs.* experimental values of the retention constants. To investigate the existence of a systemic error in developed model, the residuals of predicted values of t_r were plotted against the experimental values in Figure 3. The propagation of the residuals on both sides of zero indicates that no systemic error exists in the deve-

Table 4. Experimental and predicted retention parameters (t_r / min) of investigated carotenoids

Compd.	Experimental	Prediction by									
		Eq. (1)	Residue	Eq. (2)	Residue	Eq. (3)	Residue	Eq. (4)	Residue	Eq. (5)	Residue
1	10.665	6.9842	3.6808	6.0261	4.6389	6.7628	3.9021	7.2504	3.4146	7.6669	2.9981
2	34.442	34.5153	–0.0733	34.4753	–0.0333	34.5376	–0.0957	34.5131	–0.0711	34.4452	–0.0032
3	26.177	23.2777	2.8993	25.2463	0.9307	24.5539	1.6231	23.2998	2.8772	25.9499	0.2271
4	6.928	7.1637	–0.2356	7.4108	–0.4828	6.2990	0.6289	6.2253	0.7027	6.7700	0.1580
5	4.883	6.0926	–1.2096	6.0941	–1.2111	5.7292	–0.8462	5.5344	–0.6514	8.0049	–3.1220
6	5.788	5.3947	0.3933	7.3322	–1.5442	7.2181	–1.4301	6.5326	–0.7446	8.5088	–2.7209
7	9.895	15.3498	–5.4548	12.1932	–2.2982	13.6773	–3.7823	15.4224	–5.5274	7.4321	2.4629

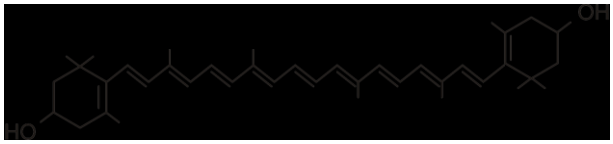

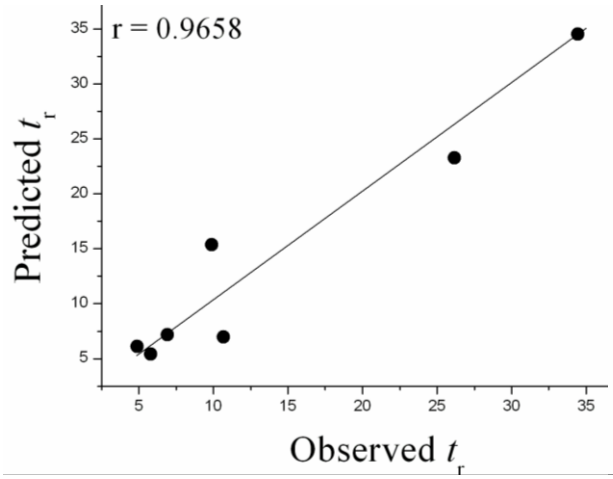

Eq. (1)

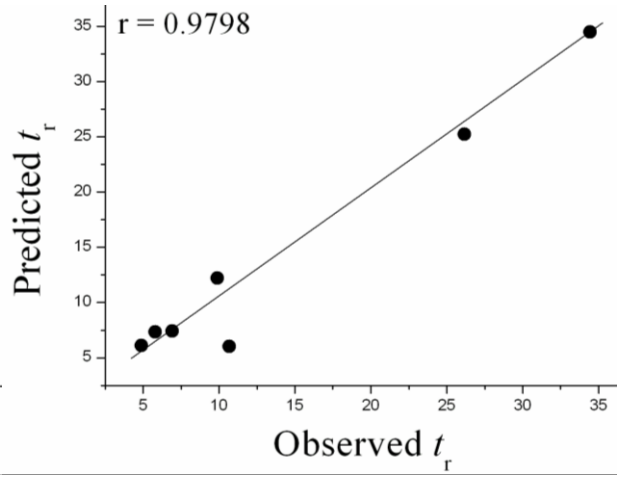

Eq. (2)

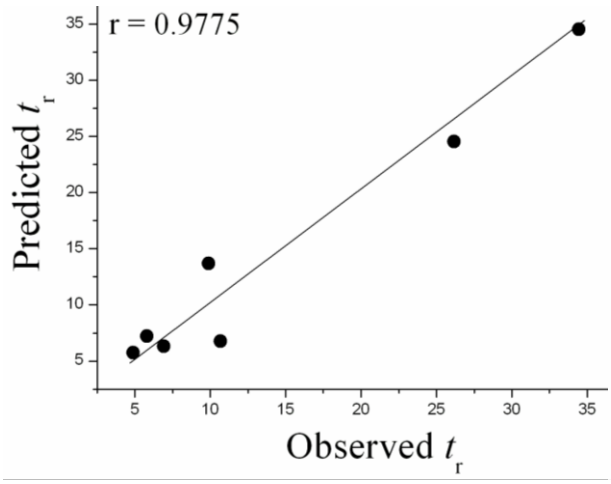

Eq. (3)

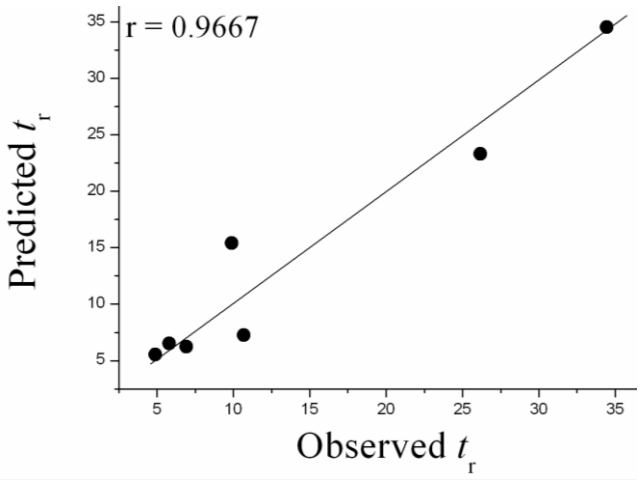

Eq. (4)

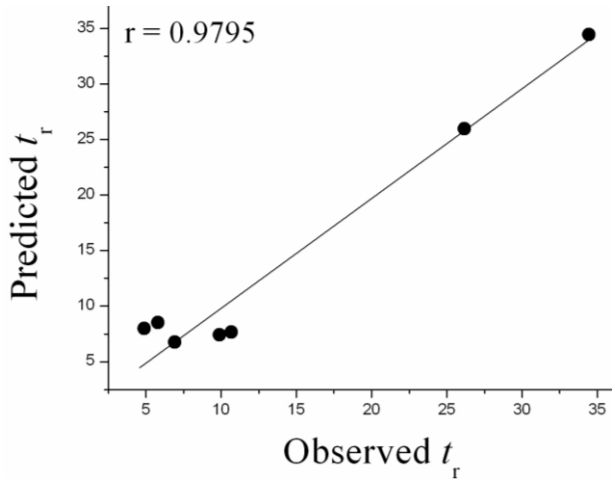

Eq. (5)

Figure 2. Plot of predicted versus experimentally observed values retention parameters of investigated carotenoids obtained using HPLC.

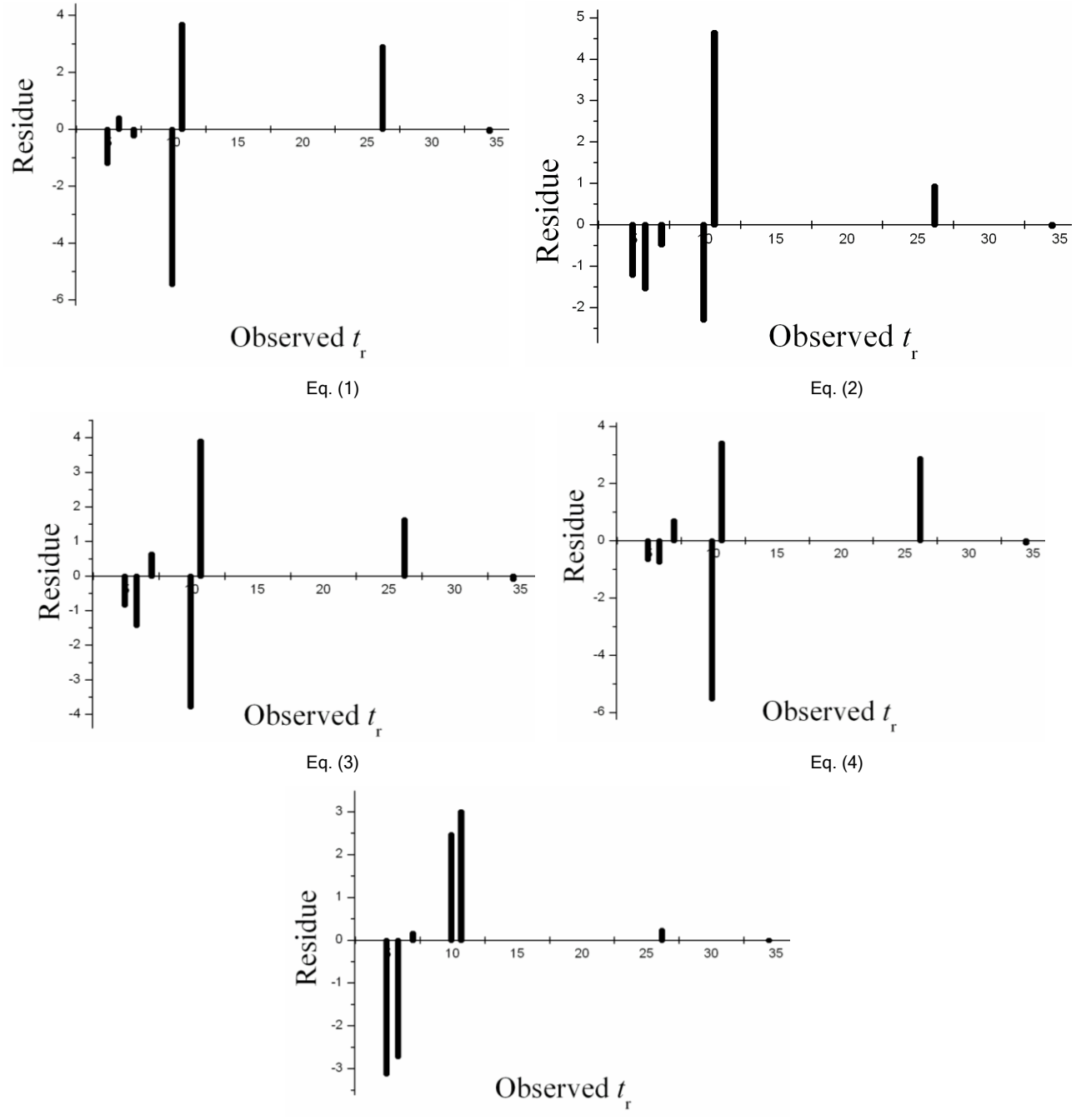

Figure 3. Plot of the residual values against the experimentally observed retention time (t_r) values.

lopment of regression models, as suggested by Jalali-Heravi *et al.* [32].

These results illustrated that the chemometric analysis combined with a successful variable selection procedure is adequate to generate an efficient QSRR model for predicting the retention time of free carotenoids from paprika oleoresin. All the present results suggest a dependence of the lipophilicity parameters on retention constant of compounds investigated. By knowing the exact values for these parameters and correlations, we can accurately predict the retention behaviour of free carotenoids from paprika oleoresin.

CONCLUSION

It is well known that mechanisms of chromatographic separation are very complex and depend of many factors such as type of chromatographic system, physicochemical characteristics of analytes, experimental conditions, etc. Therefore, in order to under-

stand chromatographic processes, it is very useful to establish mathematical models that can predict the retention behavior of analytes based on their structural characteristics in the applied chromatographic system. Determination of the correlations between molecular structure and retention behavior of molecules in different chromatographic systems is the main task of quantitative structure–retention relationships (QSRR) chemometric method. Chemometric processing of chromatographic data can reveal systematic information both about the analytes (retention, physicochemical properties, etc.) and about the stationary phases studied (the molecular mechanism of separation). In QSRR models, the retention (*e.g.*, the retention parameter, t_r) of solutes in specific chromatographic system is presented as a function of molecular descriptors of the analytes. The main parameters used in QSRR studies are physicochemical parameters. QSRR analysis was performed to find the quantitative effects of the molecular structure of isolated free carotenoids from paprika oleoresin on their retention time. Different lipophilicity parameters were calculated for each molecule using different software products. The obtained partition coefficients had good correlation among each other. A complete regression analysis was performed, using linear, quadratic and cubic relationships between the retention constants and lipophilicity parameters. The fit quality improved with higher (second or third) order polynomials. Five high quality nonlinear structure–activity models were derived between the retention constants and lipophilicity parameters of isolated free carotenoids from paprika oleoresin. The best QSRR mathematical models were used to predict retention time and close agreement between experimental and predicted values was obtained, indicating that these models can be successfully applied to predict the retention constants for this class of molecules.

Acknowledgement

These results are part of the projects No. 114-451--2707/2012-01, financially supported by the Provincial Secretariat for Science and Technological Development of Vojvodina and projects No. 172012, 172014 and 31055 supported by the Ministry of Education, Science and Technological Development of the Republic of Serbia, 2011–2014.

REFERENCES

[1] H. Daood, V. Illés, M. Gnayfeed, B. Mézáros, G. Horváth, P. Biach, Extraction of pungent spice pepper by supercritical carbon dioxide and subcritical propane, J. Supercrit. Fluid. **23** (2002) 143–152.

[2] T. El-Adawy, K. Taha, Characteristics and composition of watermelon, pumpkin, and paprika seed oils and flours, J. Agric. Food Chem. **49** (2001) 1253–1259.

[3] A. El-Agamey, G. Lowe, D. McGarvey, A. Mortensen, D. Phillip, T. Truscott, Carotenoid radical chemistry and antioxidant/pro-oxidant properties, Arch. Biochem. Biophys. **430** (2004) 37–48.

[4] T. Maoka, K. Mochida, M. Kozuka, Y. Ito, Y. Fujiwara, K. Hashimoto, Cancer chemopreventive activity of carotenoids in the fruits of red paprika *Capsicum annuum* L., Cancer Lett. **172** (2001) 103–109.

[5] G. Britton, S. Liaaen-Jensen, H. Pfander, In Carotenoids handbook, Birkha user Verlag, Basel, 2004, p. 5–33.

[6] D. Hornero-Méndez, R. de Guevara, M. Mínguez-Mosquera, Carotenoid biosynthesis changes in five red pepper (*Capsicum annuum* L.) cultivars during ripening, Cultivar selection for breeding, J. Food Agric. Chem. **48** (2000) 3857–3864.

[7] M. Jarén-Galán, M. Mínguez-Mosquera, Quantitative and qualitative changes associated with heat treatments in the carotenoid content of paprika oleoresin, .J. Agri. Food Chem. **47** (1999) 4379–4383.

[8] Lj. Vračar, A. Tepić, B. Vujičić, S. Šolaja, Influence of the heat treatment on the colour of ground pepper (*Capsicum annuum*), Acta Period. Technol. **38** (2007) 53–58.

[9] A. Tepić, G. Dimić, B. Vujičić, Ž. Kevrešan, M. Varga, Z. Šumić, Quality of commercial ground paprika and its oleoresins, Acta Period. Technol. **39** (2008) 77–83.

[10] A. Tepić, B. Vujičić, Colour change in pepper (*Capsicum annuum*) during storage, Acta Period. Technol. **35** (2004) 59–64.

[11] A. Tepić, Z. Šumić, M. Vukan, Influence of particle diameter on the colour of ground pepper (*Capsicum annuum* L.), Acta Period. Technol. **41** (2010) 87–93.

[12] A. Tepić, Z. Zeković, S. Kravić, A. Mandil, Pigment content and fatty acid composition of paprika oleoresins obtained by conventional and supercritical carbon dioxide extraction, CyTA – J. Food **7** (2009) 95–102.

[13] M. Jarén-Galán, U. Nienaber, S. Schwartz, Paprika (*Capsicum annuum*) oleoresin extraction with supercritical carbon dioxide, J. Agric. Food Chem. **47** (1999) 3558–3564.

[14] M. Weissenberg, I. Schaeffler, E. Menagem, M. Barzilai, A. Levy, Isocratic non-aqueous reversed-phase high-performance liquid chromatographic separation of capsanthin and capsorubin in red peppers (*Capsicum annuum* L.), paprika and oleoresin, J. Chromatogr., A **757** (1997) 89–95.

[15] M. Mínguez-Mosquera, D. Hornero-Méndez, D, Changes in carotenoid esterfication during the fruit ripening of *Capsicum annuun* cv Bola, J. Agric. Food Chem. **42** (1994) 640–644.

[16] R. Todeschini, V. Consonni, Handbook of Molecular Descriptors, Wiley VCH, New York, 2000.

[17] L. Jevrić, B. Jovanović, S. Velimirović, A. Tepić, G. Koprivica, N. Mišljenović, Application of Lipophilicity Parameters in QSRR Analysis of Newly Synthesized s-Triazine Derivatives Prediction of the Retention Behaviour, Hem. Ind. **65** (2011) 533–540.

[18] L. Jevrić, S. Velimirović, G. Koprivica, N. Mišljenović, T. Kuljanin, A. Tepić, Prediction of s-triazine components

lipophilicity of total herbicides, Rom. Biotehnolog. Lett. **17** (2012) 6882–6892.

[19] R. Kaliszan, QSRR: Quantitative Structure-(Chromatographic) Retention Relationships, Chem. Rev. **107** (2007) 3212–3246.

[20] A. Pyka, W. Klimczok, Study of Lipophilicity and Application of Selected Structural Descriptors in QSAR Analysis of Nicotinic Acid Derivatives. Investigations on RP18, J. Planar Chromatogr. **18** (2005) 300–304.

[21] N.U. Perišić-Janjić, S.O. Podunavac-Kuzmanović, J.S. Balaž, Đ.Vlaović, Chromatographic behaviour and lipophilicity of some benzimidazole derivatives, J. Planar. Chromatogr. **13** (2000) 123–129.

[22] N.U. Perišić-Janjić, S.O. Podunavac-Kuzmanović, RPTLC study of QSRR and QSAR for some benzimidazole derivatives, J. Planar. Chromatogr. **21** (2008) 135–141.

[23] S.O. Podunavac-Kuzmanović, D.D. Cvetković, Lipophilicity and antifungal activity of some 2-substituted benzimidazole derivatives, Chem. Ind. Chem. Eng. Q. **17** (2011) 9–15.

[24] S.O. Podunavac-Kuzmanović, D.D. Cvetković, D.J. Barna, The effect of lipophilicity on the antibacterial activity of some 1-benzylbenzimidazole derivatives, J. Serb. Chem. Soc. **73** (2008) 967–978.

[25] J. Ghasemi, S. Saaidpour, QSRR prediction of the chromatographic retention behavior of painkiller drugs, J. Chromatogr. Sci. **47** (2009) 156–163.

[26] J. Chou, P. Jurs, Computer-assisted computation of partition coefficients from molecular structures using fragment constants, J. Chem. Inf. Comput. Sci. **19** (1979) 172–178.

[27] H. Morais, A. Ramos, T. Cserháti, E. Forgács, Effects of fluorescent light and vacuum packaging on the rate of decomposition of pigments in paprika (*Capsicum annuum*) powder determined by reversed-phase high-performance liquid chromatography, J. Chromatogr., A. **936** (2001) 139–144.

[28] CS. Chem. Office, Version 7.0, Cambridge Soft Corporation, 100 Cambridge Park Drive, Cambridge, MA, 02140-2317, 2001.

[29] http://www.vcclab.org/lab/alogps/start.html

[30] http://www.chemsilico.com

[31] http://www.ncss.com

[32] M. Jalali-Heravi, A. Kyani, A quantitative structure- property relationship of gas chromatographic/mass spectrometric retention data of 85 volatile organic compounds as air pollutant materials by multivariate methods, J. Chem. Inf. Comput. Sci. **44** (2004) 1328–1335.

IZVOD

RETENCIONI PARAMETRI RP HPLC U KORELACIJI SA MOLEKULSKIM DESKRIPTORIMA LIPOFILNOSTI KAROTENOIDA

Sanja O. Podunavac-Kuzmanović, Lidija R. Jevrić, Aleksandra N. Tepić, Zdravko Šumić

Univerzitet u Novom Sadu, Tehnološki fakultet, Novi Sad, Srbija

(Naučni rad)

Paprika (*Capsicum annuum* L.) je jedna od najznačajnijih povrtarskih kultura u svetu i kod nas. Osnovno merilo kvaliteta mlevene začinske paprike je njena ekstrahovana boja, površinska boja i kvalitativni i kvantitativni sastav karotenoida. Karotenoidi su grupa jedinjenja od velikog interesa, pre svega zbog svoje karakteristične crvene boje, provitamina i antioksidativnog delovanja. Visoko-pritisna tečna hromatografija (HPLC), je jedna od najmoćnijih metoda za analizu organskih jedinjenja. U tom kontekstu, u ovom radu je upotrebom HPLC-a na obrnutim fazama ispitan uticaj hemijske strukture na lipofilnost izolovanih slobodnih karotenoida paprike primenom QSRR analize. Kao pokretna faza je bila primenjena smeša vode i acetona sa različitim zapreminskim udelima acetona u ukupnoj zapremini pokretne faze dok je nepokretna faza bila obrnuto-fazna SB-C18 kolona. Odabrani parametri lipofilnosti (log*P*) su izračunati primenom različitih softverskih programa. U osnovi ovih korelacija izvedeni su nelinearni modeli između retencionih konstanti, t_r (retenciono vreme ispitivanih karotenoida) i log *P* vrednosti. Definisano je pet kvalitetnih QSRR modela, čija je validnost potvrđena visokim statističkim parametrima korelacije. Sposobnost izvedenih predikcionih modela se ogleda u dobrom slaganju između eksperimentalnih i predikcionih vrednosti retencionog vremena. Rezultati ovih ispitivanja ukazuju da retencione konstante mogu biti mera lipofilnosti ispitivanih karotenoida i to na visokom i značajnom nivou.

Ključne reči: Karotenoidi • RP HPLC • Lipofilnost • QSRR

Thermal resistance testing of standard and protective filtering military garment on the burning napalm mixture

Dusan S. Rajic[1], Zeljko J. Kamberovic[1], Radovan M. Karkalic[2], Negovan D. Ivankovic[3], Zeljko B. Senic[4]

[1]*University of Belgrade, Innovation Center of Faculty of Technology and Metallurgy, Belgrade, Serbia*
[2]*Technical Test Center, Belgrade, Serbia*
[3]*University of Defence, Military Academy, Belgrade, Serbia*
[4]*Military Technical Institute, Belgrade, Serbia*

Abstract

Fires are an accompanying manifestation in modern weaponry use and in various accidents in peacetime. The standard military uniform is a primary barrier in protection of a soldier's body from all external influences, including the thermal ones which can cause burns. The minimum thermal resistance to the effect of burning napalm mixture (BNM) in individual uniform garment materials was determined, and found to be higher for simultaneous use of more materials one over another (the so-called sandwich materials), where the best thermal protection was exhibited by sandwich materials with an air interspace. The requirement for the thermal resistance of the material of the filtrating protective suit (FPS) to the effect of BNM (≥ 15 s) was fully met. The highest thermal resistance was demonstrated by the FPS whose inner layer was made of polyurethane foam with active carbon. The FPS thermal resistance to the effect of BNM was found to be proportional to water vapor permeability through this garment mean, and inversely proportional to air permeability.

Keywords: thermal resistance, RCB protection, physiological suitability, burning napalm mixture.

Available online at the Journal website: http://www.ache.org.rs/HI/

SCIENTIFIC PAPER

UDC 623.4:355:66

Hem. Ind. **67** (6) 941–950 (2013)

doi: 10.2298/HEMIND120817011R

Fires are a side effect of the use of conventional weapons. They frequently occur in different types of accidents. Extreme cases of thermal effects occurring during nuclear explosions and in the moment of projectile (laborated with napalm mixture) explosion, where the incendiary napalm jellied mixture disperses through the space in the form of different size drops. Although the use of napalm and nuclear weapons is forbidden by international conventions, these weapons are still in the arsenals of many armies in the world, so the possibility of their use is not excluded in practice [1].

Soldier uniforms are made of the highest quality fabrics combined with flame retardants. Most flame retardant textiles are designed to reduce the ease of ignition and also reduce the flame propagation rates. Conventional textiles can be rendered flame retardant by chemical after-treatments as co-monomers in their structures, or by use of flame retardant additives during extrusion. High performance fibers with inherently high levels of flame and heat resistance require the synthesis of all aromatic structures, but these are expensive and used only when performance requirements justify cost [2].

Correspondence: N.D. Ivankovic, MA, University of Defence, Military Academy, Pavla Jurisica-Sturma 33, 11000 Belgrade, Serbia.
E-mail: negovan.ivankovic@gmail.com
Paper received: 17 August, 2012
Paper accepted: 25 January, 2013

During the burning napalm mixture (BNM) effects, the soldier's clothing, which is supposed to protect his body, is exposed to thermal effects which causes it to burn through, thus leaving the skin burnt. Military burn injuries on the battlefield can be attributed to three causes: flame and thermal threats, incidental or secondary hazards and accidents. Threat-generated burns result from the direct employment of a flame and thermal weapons. Incidental or secondary burns result from flame and thermal weapons or other threats (*i.e.*, ballistic, blast, directed energy) that ignite battlefield combustibles, including clothing or equipment that can also present a burn hazard. Accidents comprise the remaining burn hazard. The degree of skin damage depends on many factors, such as the heat source strength, time of heat exposure, affected skin surface, heat transfer mode, age and health condition of an injured person, and the anatomical structures of the skin that has been exposed to the effect of heat [1]. However, it is generally considered that the first degree burns can be expected in humans in temperature zones of 40 to 45 °C, second degree burns between 45 and 60 °C, and third degree above 60 °C. Burns of the second and third degree directly disable soldiers to continue fighting and perform other activities, and they require treatment. It is considered that, in a possible world war in the future, burns would take between 40 and 50% of

all injuries, which indicates the considerable importance of studying this problem.

Burns are a significant cause of morbidity and mortality in the military environment in combat and peacetime, but the impact of clothing on burns is not addressed adequately in the medical literature. Historically, even in combat, burn injuries more often result from the ignition of battlefield combustibles due to accidents or secondary flame effects in the environment, than from direct flame and thermal threats [3]. In addition, the specific cause of casualties and fatalities has been difficult to characterize in terms of burn injuries because many were documented as involving multiple trauma and explosions. Until recently the flame threat had generally been categorized as relatively low for the individual soldier, and due to the increased use and exposure to fuels, burn injuries had been more prevalent for both Navy and Air Force personnel. However, during Operation Iraqi Freedom, the use of improvised explosive devices (IEDs) against USA ground forces has become prevalent. The IEDs serve not only as ignition points for battlefield combustibles, but have been enhanced to include fuels, making them a direct battlefield threat to the soldier and increasing the likelihood of burn injuries. Kim [4] has reviewed the characteristics of several battlefield threats and combustibles, estimating that the values of the heat flux of thermobaric, incendiary and flame weapons, and JP-8 fuel converge to a common heat flux of about 2.0 cal cm^{-2} s^{-1} over time. Since the likelihood of survival of a direct hit from a flame and thermal weapon is low based on the initial ignition temperatures and known blast effects, and the fact that many burn injuries result from the secondary effects of the environment, a thermal flux of 2.0 cal cm^{-2} s^{-1} was selected as most representative of a military fire hazard that is survivable if exposure time is short. Appropriately developed protective clothing should provide critical seconds of increased escape time to distance oneself from the flame hazard and thereby provide a lesser, but survivable exposure time [4].

The first line of defense against flame assault is the clothing system outer-layer, which in every configuration tested is flame resistant. Each additional clothing under-layer adds insulation and increases protection time [5]. It is assumed that thermal energy is absorbed as latent heat of fusion when the material melts. When melted onto the skin, this heat will then be delivered to the skin and superficial tissues in a continuing manner as it solidifies again, potentially increasing the thermal dose delivered and tissue damaged in heating and cooling phases. Although the physical processes will undoubtedly occur, there is little quantitative information in the literature to support the view that this is a notable contributor to the burn – the rate of heat release to the tissues in the solidifying process may be quite slow and capable of being dissipated by conduction and blood flow.

Most clothing materials will ignite if the temperature is high enough and potentially deliver thermal energy from this process to the skin and underlying layers. The total energy liberated by combustion of material will not necessarily be transferred to the skin and the proportion of energy transferred will depend on the material, undergarment, air gaps and any pretreatment.

Viscose rayon is formed from wood pulp and is a filamentous form of cellulose. Cotton, wool and viscose rayon, are not thermoplastic and will not shrink in response to heat. At 245 °C for untreated wool and 350 °C for cotton and viscose rayon, a carbonaceous “char” is formed, with volatile liquids and gases generated, before combustion at 600, 350 and 420 °C, respectively.

Synthetic material fibers are stronger than most natural fibers and clothing manufactured from them can be made lighter and warmer by incorporating air spaces. This characteristic enables wet synthetic clothing to dry more quickly but, when burning, is a more open structure and may burn rapidly and completely. Mixtures of synthetic and natural materials can behave detrimentally – the non-thermoplastic material may support the burning of thermoplastic material within its char and propagate the combustion. This is termed “scaffolding” and although demonstrated experimentally with clothing samples, appears to be unusual in combat burn simulations. The favorable qualities of lightness, warmth, permeability to moisture vapour, quick drying and durability, mean that these materials are ideal for combat personnel in adverse conditions. Specialized fabrics such as Nomex™ or Kevlar™ are thermoplastic, but will not soften until 275 and 340 °C and they melt at 375 and 560 °C, respectively. These materials will not burn until temperatures reach more than 500 and 550 °C, respectively, but their action as sole protection against burns is limited by other factors such as thermal conductivity. A fire retardant material with high thermal conductivity such as Nomex™ will require an effective inner insulating layer to prevent conduction through the materials to the skin surface. Nomex™ as an outer layer with an equal mixture of wool and cotton as undergarment was found to be significantly better protection than Nomex™ as outer and inner layers against flame exposure over 1.75 s duration. The extent of any air gap is not made clear, but a two-layer Nomex™ system is also significantly better than a single layer of Nomex™ for any tested duration.

The fire retardance of textiles can be enhanced by additives or coatings. The mechanisms of action can

differ, but the aim is to prevent combustion or to increase the magnitude of the thermal energy required to cause combustion. These mechanisms may include the production of a barrier to oxygen, or stabilizing intermediate pyrolysis products and forming a char, thus preventing the formation of flammable, volatile products.

A well trained army, equipped with quality means for personal protection, could reduce losses to a minimum and provide functional operability at the shortest possible time, even after a surprise attack, using nuclear weapons or napalm. It is therefore necessary to study the thermal resistance of various protective materials, with constant requirements for the improvement of utility performance. Depending on the degree of radioactive, chemical and biological (RCB) contamination, tactical tasks, the need for easier movement, performing tasks of different difficulty and other important factors, the selection of the appropriate personal protective means of isolating or filtering type is being done. Isolating means have good protective properties and bad physiological properties. Their purpose is to protect the body, legs and arms from RCB contamination. A number of means for body protection is based on isolating materials. These include protective coveralls, light protective overgarments, protective gloves, protective boots and protective socks. They are made of different materials: elastomers (*e.g*., butyl rubber) and thermoplastics (Tyvek®, polyethylene, etc.). They are used in conditions of RCB weapons usage, in the process of decontamination, reconnaissance, stay on the contaminated soil, etc. when it is necessary to remain protected for a few hours [6–10].

Garments based on filtrosorption materials are physiologically better suited than those based on isolating materials. They provide much longer stays in contaminated zones, and beyond, as well as performing tasks of higher physical and mental level. In addittion to this, these means have good protective properties in respect to the effect of RCB agents. When it comes to personal body protection during long stay on the land and in an atmosphere contaminated with RCB agents, as well as during carrying out difficult tasks in a warm environment, the filtering protective suit (FPS) has no alternative [11]. The materials of which FPS is made, as opposed to the materials of isolating means, are permeable to air and water vapor, which means that they are physiologically more suitable, which reduces the possibility of heat stress in carrying out assigned tasks [12–15].

Protective garment means, even in the phase of their development, need to meet a whole series of tactical-technical requirements that must be fulfilled before their adoption in armaments and military equipment. When it comes to protective thermal characteristics of protection means for bodies, they are required to protect the user from burning napalm mixture (BNM) for at least 15 s [16].

The aim of this study is to determine which type of standard military clothing and FPS, as a representative of filtering type protective RCB clothing, will best consolidate in itself an acceptable level of effective thermal protection of BNM, and at the same time provide satisfactory functional characteristics, *i.e.*, adequate physiological response of human organism. All these activities are carried out in respect to the relevant requirements in the field of standardization of test conditions [17].

EXPERIMENTAL

Investigation of thermal characteristics of suit materials

The method of testing BNM effects [15] was based on an apparatus consisting of:

- Material sample holders
- Ring for fixing the material sample
- Ring for separation of the material
- Tripod on which the sample holder is mounted
- Metal pans for the protection from BNM which burns the sample
- Measuring head with temperature sensors
- Amplifier assembly
- Power supplies
- Computer, printer, plotter
- Chronometer.

The measuring head had the following characteristics:

- Temperature measurement range: 0–100 °C
- Allowed overdraft (no damage) to 200 °C
- Decomposition within the measurment range: 0.5 °C
- Accuracy of the measured values: 1% of range
- The time constant of response: 2 s
- The number of sensors (measuring points): 7.

The test method for resistance of materials to the effect of BNM involves three test procedures:

- Timing of burning through sample material
- Temperature measurement on the opposite side of the material exposed to the effect of BNM
- Visual evaluations of material behavior.

Time of sample material burning through

Napalm mixture (about 2 cm^3) is applied by syringe in the middle of the sample material. Then the mixture is being burned and time of burning measured. Time of burning represents the time from the moment of ignition of the applied napalm mixture to the face of material, to the point of its appearance on the opposite side.

Testing time of burning is monitored visually and measured by chronometer.

Measurement of temperature

The purpose of this method is to determine the thermal properties of materials, *i.e*., measuring the temperature on the opposite side of the sample material exposed to the effects of 2 cm^3 of BNM (temperature is measured on the side of the body). Seven sensors of the measuring head measure temperature as a function of time – during the effects of BNM and cooling of the materials once the effect of flame is over (Figure 1).

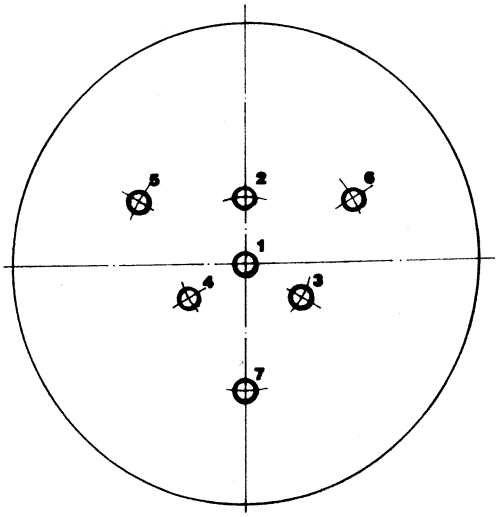

Figure 1. Layout and identification of measurement sensor.

The measurement head is first set on the sample holder according to Figure 2, and then test material of selected variant (single or sandwich materials with and without an air space between layers) is set on the head. It is particularly important to point out the materials used in this study were previously exposed to different climatic influences [17–19]. When testing the sandwich materials, the measuring head is placed respectively: a sample of one soldiers' garment material, the ring for material samples separation (if sandwich materials are tested), a sample of the second material of outer garment or protective RCB means (Figure 2). The number of samples and the ring are in the desired and realistic range. A drop of a previously made napalm mixture (volume of 2 cm^3) is applied to the outer material sample by syringe and it is then ignited. At the time of napalm mixture ignition, the temperature sensors are activated and software data processing is performed. After 200 s (or any other time in the interval time from 0 to 300 s, which is governed by the software package) the curves for all temperature sensors, or for the temperature sensor that detects the highest temperature, are drawn on the screen.

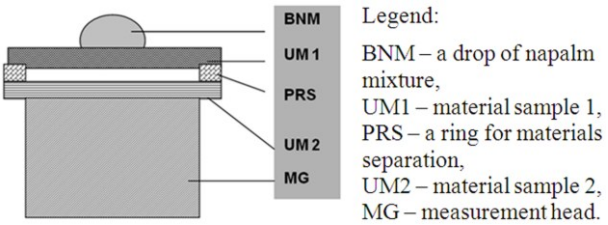

Figure 2. Procedure for testing of sandwich materials on effect of BNM.

The obtained temperature data are processed by computer and reported in tabular or graphic form. Tabular data and obtained curves of temperatures in function of time for each of the seven sensors, define the thermal characteristics of tested material and offer the possibility of determining the time until appearance damage of skin in form of 1^{st}, 2^{nd} or 3^{rd} degree burns [11], *i.e*., give the opportunity to define the procedures and time that are at disposal to a soldier to neutralize the effects of BNM.

Visual evaluations of material behavior

Visual evaluations of material behavior during effect of BNM refer primarily to the assessment of material self-extinguishing (do the material extinguish after the cessation of firing effect). The characteristics of flame, combustion products (fumes, gases, particles, etc.), as well as burning behavior of materials and degree of material degradation after effects of BNM are visually monitored.

Tested samples of means for the body protection

In experiments the following FPS means are used: filtering protective suit – model 2 (OFZ-M2), manufacturer „Trayal“, Kruševac, Serbia, filtering protective suit, model 2 PUR (OFZ-M2PUR), manufacturer „Trayal“, Kruševac, Serbia, and filtering protective suit, model 00 (OFZ-M00), manufacturer „Mile Dragic Production“, Zrenjanin, Serbia.

The tested materials

In the experimental study of thermal characteristics the materials used for production of a set of the uniform M03, manufacturer "Mile Dragic Production", Zrenjanin, Serbia, were as follows: camouflage undershirt (hereinafter referred to as an undershirt), camouflage shirt (hereinafter referred to as a shirt), camouflage jacket (hereinafter: blouse) and different variants of the material testing (Table 1).

Test variations of material resistance to the effects of BNM, *i.e*., their thermal performances, refer to the real image of wearing the soldier garment and FPS as representative means for personal RCB body protection. Testing variants of individual materials, sandwich materials and sandwich materials with air interspace are given in Table 2.

Table 1. Material characteristics; $\overline{X}$ – mean value, SD – standard deviation

No.	Material of garment and protective means	Raw material composition	Thickness, mm ($\overline{X} \pm SD$)	Surface mass, g/m^2 ($\overline{X} \pm SD$)
1	Undershirt	Cotton 100%	0.55±0.03	168±0.2
2	Shirt	Cotton 67%, polyester 33%	0.42±0.02	212±0.4
3	Blouse	Cotton 50%, polyester 50%	0.47±0.04	263±0.3
4	FPS-M2	Outer layer: cotton 67%, polyester 33%	0.45±0.08	185.3±0.4
		Inner layer: the spheres of active carbon material (AUM) on the fabric	0.85±0.04	300.7±0.2
5	FPS-M2PUR	Outer layer: cotton 67%, polyester 33%	0.48±0.03	190.1±0.3
		Inner layer: activated carbon powder traped into PUR and sandwich of two light fabrics	0.8±0.04	340.1±0.5
6	FPS-M00	Outer layer: cotton 67%, polyester 33%	0.42±0.05	215.3±0.6
		Inner layer: AUM glued to the fabric and covered with another cloth	0.78±0.05	380.2±0.5

Table 2. Variations of test materials

No.	Materials	Test variant
1	Individual materials	Camouflage undershirt (undershirt)
2		Camouflage shirt (shirt)
3		Camouflage jacket (blouse)
4		FPS M2
5	Sandwich materials	Undershirt + FPS-M2
6		Undershirt + shirt + FPS-M2
7		Undershirt + shirt + blouse + FPS-M2
8	Sandwich materials with air interspaces (AI)	Undershirt + AI + FPS-M2
9		Undershirt + shirt + AI + FPS-M2
10		Undershirt + AI + shirt + blouse + FPS-M2
11		Undershirt + shirt + AI + blouse + FPS-M2
12		Undershirt + shirt + blouse + AI + FPS-M2
13		Undershirt + AI + shirt + AI + blouse + FPS-M2
14		Undershirt + AI + shirt + blouse + AI + FPS-M2
15		Undershirt + shirt + AI + blouse + AI + FPS-M2
16	Sandwich materials with three air interspaces (AI)	Undershirt + AI + shirt + AI + blouse + AI + FPS-M2

RESULTS AND DISCUSION

The air permeability refers to the amount of air (expressed in cubic meters) that is let through a square meter of fabric per min ($m^3\ m^{-2}\ min^{-1}$). This is measured at the prescribed pressure difference, in standard environmental conditions. The permeability of air through clothing is one of its most important functional characteristics. It is affiliated with the size and distribution of pores of textile materials. In terms of higher outer temperature and at higher body loads, it creates a large amount of heat and sweat, so a higher air permeability of the clothing material is needed to improve the physiological suitability. This is in contrast with the increasing degree of protection against RCB agents, where the lower air permeability is desirable. The results of air permeability of standard war uniform are shown in Table 3.

It can be seen that the uniform undershirt has the highest air permeability in the standard military kit, and military pants have the lowest air permeability. Table 4 shows the results of air permeability through an FPS sandwich of materials.

All FPS sandwich materials have higher air permeability of the blouse and pants, which is a very important fact considering that the FPS can be used as a standard war uniform. The highest air permeability was exhibited by FPS-M00. 1.2 times greater than the permeability of FPS-M2 and 1.8 times greater than the permeability of FPS-M2PUR.

Analysis of the obtained results of air permeability testing (Tables 3 and 4) on one hand, and the thermal resistance on BNM effect (Figure 3) in FPS and 16 test

Table 3. Air permeability of standard war uniform

Part of uniform	Air permeability, $m^3\ m^{-2}\ min^{-1}$							
	From the face side to the reverse side of the face			$\bar{X} \pm SD$	From the reverse side of the face to the face side			$\bar{X} \pm S$
Blouse	2.51	2.47	2.48	2.48±0.02	2.57	2.61	2.60	2.59±0.02
	2.47	2.50	2.48		2.60	2.58	2.58	
Pants	2.09	2.09	2.08	2.09±0.01	1.42	1.34	1.36	1.36±0.03
	2.11	2.08	2.11		1.38	1.40	1.35	
Shirt	11.96	11.98	11.92	11.94±0.03	11.75	11.81	11.78	11.76±0.03
	11.94	11.92	11.98		11.72	11.74	11.75	
Undershirt	184.17	185.21	184.72	184.82±0.6	182.45	182.56	182.29	182.38±0.2
	185.25	184.13	185.49		181.98	182.55	182.47	

Table 4. Air permeability of sandwich materials; VT – a type of treatment (I – untreated, II – after exposure to climate and after test-exploitation investigations); A – from the face side to the reverse side of the face; B – from the reverse side of the face to the face side

Model FPS	Air permeability, $m^3\ m^{-2}\ min^{-1}$		
	VT	A ($\bar{X} \pm SD$)	B ($\bar{X} \pm SD$)
FPS-M2	I	7.2±0.8	7.2±0.8
	II	7.1±0.7	7.1±0.8
FPS-M2PUR	I	4.9±0.4	4.9±0.6
	II	4±0.5	4.9±0.5
FPS-M00	I	8.3±0.7	8.8±0.7
	II	8.2±0.7	8.7±0.8

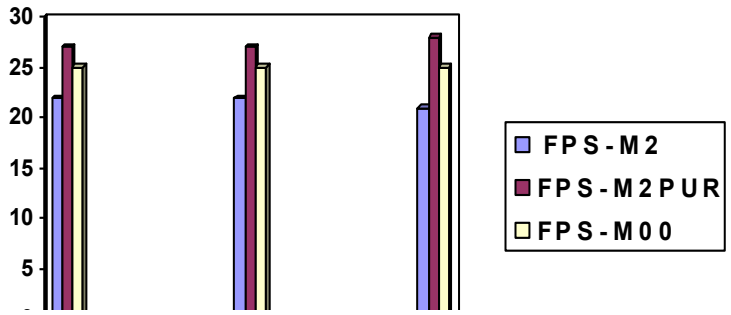

Figure 3. Burning through time (s) at the effect of BNM on the outer and inner layer of the FPS sample after three types of treatment: a – untreated samples, b – samples after the climate impact and c – samples after exploitation.

combinations of materials and garment means (Figure 4) on the other, established that these two parameters are inversely proportional.

The flow of steam or sweat from the surface of human skin to the surroundings is one of the most important parameters for prediction of the use value of a protective garment. The human body uses a very efficient cooling mechanism, which activates when there is no sufficient heat release, physiologically by respiration and dry heat stream. This is particularly expressed during great physical exertion or high temperature environment conditions, which occur in the case of BNM effects. In this case, the sweat glands of the skin surface begin to exude sweat along with the water which evaporates and thus the skin pushes away excess heat into the environment. The water vapor travels from the skin through garment in ambient air due to vapor pressure difference on the skin surface and the partial pressure of water vapor in the surrounding air. The results of the examination of water vapor permeability of FPS sandwich materials are shown in Table 5.

The obtained values for water vapor permeability of FPS suit materials indicate that all materials were of satisfactory quality in terms of sweat removal from the user's body. FPS-M00 had the highest water vapor permeability, 1.2 times more than water vapor permeability of the FPS-M2 and FPS-M2PUR.

Table 5. The water vapor permeability of sandwich materials

Model FPS		Water vapor permeability, g/m^2·24 h ($\overline{X}$ ±*SD*)
FPS-M2	I	3131.5±0.8
	II	3129.2±0.7
FPS-M2PUR	I	3125.5±0.9
	II	3120.3±0.9
FPS-M00	I	3825.6±0.7
	II	3820.3±0.6

Analyzing the test results of water vapor permeability (Table 5) on one hand, and the FPS thermal resistance at BNM effect (Figure 3) on the other hand, their proportional interdependence could be determined. It can be concluded that the materials of all three FPS models are permeable to water vapor, which contributes to a better exchange of heat generated in the body with the surroundings and a better transfer of sweat fluid compared to the isolating materials and the materials of less water vapor permeability. Results of FPS materials resistance testing to the effects of BMN are shown in Figure 3.

From Figure 3 it can be noticed that the time of burning through the outer and inner layer of untreated FPS was highest for FPS-M2PUR (27 s) and lowest for FPS-M2 (22 s). Exposed to BNM effects, material samples of all three FPSs burned and there was intense smoke.

Time of burning through the outer and inner layer of samples exposed to climatic influences [13,14,16] at all three FPSs samples is the same as at untreated samples, from which it can be concluded that climate changes do not negatively affect the thermal resistance of the FPS samples.

The time of burning through the outer and inner layer of exploited FPS samples is the largest for FPS M2PUR (28 s), and lowest for FPS-M2 (21 s). Exposed to BNM effects, material samples of all three FPSs burn and there is intense smoke.

Since the tactical-technical requirements for FPS--M2 indicated that this mean must not be burnt through for at least 15 s during BNM effects, the results in Figure 3 show that this requirement is satisfying for all three FPS models. Figure 3 shows that in all test conditions (untreated samples, after climate change and after exploitation) the highest thermal resistance during BNM effect was found for FPS-M2PUR, then FPS-M00 and finally FPS-M2. This is logical, because the lowest air permeability was found for FPS-M2PUR.

The FPS materials are made to have some protective properties in respect to the effect of BNM which is defined through the regulations on the quality of this mean. However, processing of flame retardants considerably increases the costs, because it is more difficult to meet some other tactical-technical requirements, for example camouflaging.

Figure 4 shows the results of determining material resistance to the effects of BNM by measuring temperature on the opposite side of the material regarding the side of BNM effects: individual materials, sandwich materials and sandwich materials with an air interspace. The obtained temperatures have been correlated with the appropriate degree of burns. Figure 4 shows an overview of temperature rise on the opposite side of the specimen from the moment of the critical temperature (40 °C), when burns occur for the time base of 7 cycles of measurements of each sensor.

Based on the obtained results (Figure 4) it can be seen that in all tested variants of individual materials, the time before 1st degree burns appear was very short (1 s), which means that the structural characteristics of the materials of soldiers' garments and FPS-M2 (primarily raw composition, thickness and porosity) do not influence protection. The time elapsed until 2nd degree burns appear was different compared to the test version and it is longest for FPS-M2 (9 s), followed by undershirt and blouse (4 s) and at the end shirt (2 s). The longest protection time of the variation with FPS--M2 is caused by the maximum thickness of this material, and the shortest time of the shirt variation is related to the minimum thickness. Variations of mate-

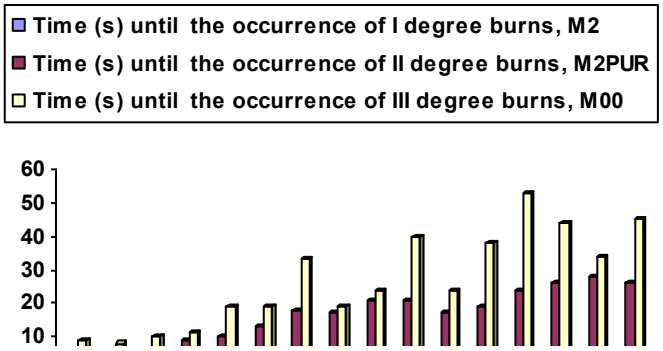

Figure 4. Occurrence time of 1st, 2nd and 3rd degree burns at the effect of BNM on 16 types of test materials and their combinations.

rial of undershirt and blouse have the same time protection which is 4 s. Cotton fibers, of which undershirt is made, give the same resistance to the effects of BNM as a mixture of polyester/cotton, which is built into the blouse, due to better thermal properties of cotton relative to polyester fiber, and because of the structural characteristics of these two variants (thickness, surface mass and porosity). Thelapsed time before the occurrence of 3rd degree burns is slightly larger than the elapsed time of before the occurrence of 2nd degree burns. It can be said that the individual materials of undershirt, shirt and blouse do not have good thermal protection. A soldier affected by the influence of BNM, would get 2nd degree burns in a short period of time (4 s) and would be unable to fight.

As for the results of sandwich combination resistance to the effects of BNM, the time before 1st degree burns occur remained at the level of 1 s, but the time before the occurrence of 2nd degree burns was significantly longer than the time of the individual materials (Figure 4). Also, the time before the occurrence of 3rd degree burns was significantly longer than the time of protection responsible for the burns of 2nd degree. Each additional layer extends the time of protection. For variants: undershirt + FPS-M2, undershirt + shirt + + FPS-M2 and undershirt + shirt + blouse + FPS-M2, the elapsed times before the occurrence of 2nd degree burns were 10, 13 and 18 s respectively, and the elapsed times before the occurrence of 3rd degree burns for the same variants were 19, 19 and 33 s. The results clearly show that the blouse, as an additional layer, significantly increases the resistance of the sandwich material to the effect of BNM. Based on it, it can be concluded that the overall thickness of the layers of garment over a certain thickness significantly increases the time of protection.

Since it is known that the air interspace (AI) is an insulator which represents a barrier to the heat passing through, it is expected that the existence of air spaces increases the resistance of the sandwich material to the heat passing through (*i.e.*, to the effect of BNM). Figure 4 shows that variations of the test material with AI show a longer time of protection until the occurrence of the 2nd and 3rd degree burns in relation to variations of the sandwich material without AI. Also, Figure 4 shows that the time elapsed until the occurrence of the 2nd degree burns in variants with and without AI, or variant 5 (undershirt + FPS-M2) and 8 (undershirt + AI + FPS-M2) was 10 and 17 s, respectively. In variant 6 (undershirt + shirt + FPS-M2) and variant 9 (undershirt + shirt + AI + FPS-M2) the amount of time was 13 and 15 s, and for variant 7 (undershirt + shirt + + blouse + FPS -M2) and variant 9 (undershirt + AI + + shirt + blouse + FPS -M2) 18 and 21 s. A similar difference is observed in the analysis of time elapsed until occurrence of the 2nd degree burns. Results of the resistance testing of sandwich materials with two AI on BNM effect suggests further increased resistance to heat transmission and better protective properties than the presence of only one AI. Comparison of variants of the same sandwich materials with one and two AI shows that additional AI extends the times before the occurrence of 2nd degree burns for 7 to 11 s (variants 9 and 10 with an AI and variants 13 and 14 with two AI). Differences in the obtained times are higher when looking at the occurrence of burns of 3rd degree. The results show that variants of sandwich materials with three AI do not lead to increased resistance in relation to variants of sandwich materials with two AI, which should be checked in future. It is noteworthy that in the present study, AI was always of the same thickness (1 mm) and that this was a constant thickness along the entire surface of the test material variants.

Although it is said that 2nd degree burns disable soldiers for any action, it should be understood conditionally. The BNM drops that reach the human body have different distribution, density and size. Also, there are differences depending on which body parts are affected by BNM, and differences in percentage involvement. The size of the affected body area is very important, as well as whether the vital organs are in those areas or not. Despite these facts, the obtained elapsed times until the occurrence of 2nd degree burns, give chance to an affected person (on a lesser or greater extent by BNM drops), to react adequately and eliminate or reduce the risk of injuries caused by BNM effects.

CONCLUSION

Each additional clothing under-layer adds insulation and increases protection time. Tests performed with various samples show differences in performance that are likely due to differences in material type and garment construction.

Testing the thermal resistance of three FPS models when affected by a burning napalm mixture in a set time of at least 15 s was carried out, where it was determined that this requirement is fully met in all models. The highest thermal resistance was demonstrated by FPS-M2PUR (produced from polyurethane foam and activated carbon), then FPS-M00 (woven fabric and spherical carbon adsorbent), and finally FPS--M2 (fabric and spherical carbon adsorbent). A proportional relationship between the thermal resistance of FPS to the effect of BNM and water vapor permeability through this garment mean has been determined, and inverse proportionality in relation to air permeability, which had been expected.

This study determined the thermal resistance of soldiers garment (undershirt, shirt and blouse) and FPS--M2 during the effect of BNM, by measuring the tem-

perature on the opposite side from that which has been treated by a drop of BNM, and by measuring the time before occurrence of burns of 1st, 2nd and 3rd degree. The thermal resistance of single and sandwich materials (more garment means worn one over the other at once) with one, two and three air interspaces was determined.

Individual materials show the lowest thermal resistance to the effects of BNM, followed by sandwich materials. Sandwich materials with air interspace provide the best thermal protection because the air presents the insulation to heat passing through. When exposed to the effect of a BNM, all variants of test materials experience a short time (1 s) until temperature causes the 1st degree burns. However, the critical time at which materials protect a user from the effects of BNM is the elapsed time before the 2nd degree burns appear, because the garment user is disabled to perform any task at that very time. When wearing sandwich materials, the time before the 2nd degree burns occur is long enough for the user to take appropriate steps to eliminate or minimize the harmful consequences caused by the influence of BNM. This critical time may be longer if an amount of BNM affects a smaller area of a body or if vital organs stay intact.

Acknowledgements

Ministry of Education, Science and Technological Development of the Republic of Serbia support this work, Grant No. TR34034 (2011–2014).

REFERENCES

[1] A.D. McLean, Burns and Military Clothing, J. R. Army Med. Corps **147** (2001) 97–106.

[2] F. Hull, J. Gambill, A. Hansche, G. Agni, J. Evangelista, C. Powell, M. Auerbach, J. Dillon, Ö. Arnas, Engineering an undergarment for flash/flame protection, Proceedings, ASME-IMECE 2011-63888, Denver, CO, 2011.

[3] D.W. Tucker, S.A. Rei, Soldier Flame/Thermal Hazard Assessment, Natick/TR-99/039L, U.S. Army Soldier and Biological Chemical Command, Natick, MA, 01760-5020.

[4] I.L. Kim, Battlefield Flame/Thermal Threats or Hazards and Thermal Performance Criteria, TR-00/015L, U.S. Army Soldier and Biological Chemical Command, Natick, MA, 01760-5020.

[5] G. Song, R.L. Barker, H. Hamouda, A. V. Kuznetsov, P. Chitrphiromsri, R.V. Grimes, Modeling the Thermal Protective Performance of Heat Resistant Garments in Flash Fire Exposures, Textile Res. J. **74** (2004) 1033–1040.

[6] The Military Medicine Series, Part I. Warfare, Weaponry, and the Casualty, Volume 5: Conventional Warfare: Ballistic, Blast, and Burn, Office of the Surgeon General, U.S. Department of the Army, Washington, DC, 1990.

[7] T.E. Bowen, R.F. Bellamy (Eds.), Ch. 3, Burn Injury, Emergency War Surgery, 2nd US Rev. of The Emergency War Surgery NATO Handbook, U.S. Department of Defense, Washington, DC, 1989, pp. 35–56.

[8] A Report on the Thermal Protective Performance (TPP) and the Pyroman Evaluation for the U.S. Army Soldier Systems Command, Center for Research on Textile Protection and Comfort (T-PACC), College of Textiles, North Carolina State University, Raleigh, NC, 1999.

[9] D. Jackson, An overview of thermal protection, Protective Clothing Conference, Clemson University, SC, 1998.

[10] A.R. Horrocks, Developments in flame retardants for heat and fire resistant textiles – the role of char formation and intumescences, Polym. Degrad. Stability **54** (1996) 143–154.

[11] Z. Senic, M. Jevremovic, R. Karkalic, Determination of the resistance of soldiers garment means to the effect of burning napalm mixture, OTEH, 2007.

[12] R. Karkalic, Optimization of thin film sorption carbon materials built into the CBRN means in function of the protective characteristics and physiological fitness, Ph.D. Thesis, Military Academy, 2006.

[13] EN ISO 12894:2001, Ergonomics of the thermal environment – Medical supervision of individuals exposed to extreme hot or cold environments, CEN-European Committee for Standardization.

[14] EN ISO 9886:2004, Ergonomics – Evaluation of thermal strain by physiological measurements. CEN-European Committee for Standardization.

[15] SORS 6704:1988, RCB body protection – Test method for resistance of materials to the effects of napalm mixture, Direction for Standardization, Codification and Metrology, Ministry of Defense, Republic of Serbia.

[16] I. Mekjavic, E. Banister, J. Morrison, Environmental Ergonomics, Taylor & Francis, London, 1987.

[17] SORS 0187:1979, Testing of external influences on the armament and military equipment, Raised temperature, Method 102. Direction for Standardization, Codification and Metrology, Ministry of Defense, Republic of Serbia.

[18] SORS 0188:1991, Testing of external influences on the armament and military equipment, Lowered temperature, Method 103. Direction for Standardization, Codification and Metrology, Ministry of Defense, Republic of Serbia.

[19] SORS 0186:1991, Testing of external influences on the armament and military equipment, Sudden temperature changes, Method 101. Direction for Standardization, Codification and Metrology, Ministry of Defense, Republic of Serbia.

IZVOD

TESTIRANJE TERMIČKE OTPORNOSTI STANDARDNE I FILTRIRAJUĆE ZAŠTITNE VOJNIČKE UNIFORME NA GORUĆU NAPALM SMEŠU

Dušan S. Rajić[1], Željko J. Kamberović[1], Radovan M. Karkalić[2], Negovan D. Ivanković[3], Željko B. Senić[4]

[1]*Univerzitet u Beogradu, Inovacioni centar Tehnološko-metalurškog fakulteta, Beograd, Srbija*
[2]*Tehnički opitni centar, Beograd, Srbija*
[3]*Univerzitet odbrane, Vojna akademija, Beograd, Srbija*
[4]*Vojnotehnički institut, Beograd, Srbija*

(Naučni rad)

Požari su prateća manifestacija kod upotrebe naoružanja u savremenom ratu i u slučajevima nastanka različitih akcidenata u mirnodopskim uslovima. Standardna vojnička uniforma predstavlja primarnu prepreku u zaštiti tela vojnika od svih spoljnih uticaja, uključujući i termičke koji mogu da izazovu opekotine. Cilj ovog rada je da utvrdi koja vrsta standardne vojničke odeće i odela filtrirajućeg zaštitnog (OFZ) kao predstavnika zaštitne RHB odeće filtracionog tipa će u sebi najbolje da objedini prihvatljivi nivo efikasne termičke zaštite od goruće napalm smeše (GNS) uz istovremeno obezbeđenje zadovoljavajućih funkcionalnih karakteristika tj. adekvatnog fiziološkog odgovora organizma čoveka. Sve ove aktivnosti su sprovedene uz poštovanje relevantnih zahteva na polju standardizacije uslova ispitivanja. Utvrđena je najmanja termička otpornost na delovanje GNS kod pojedinačnih odevnih materijala uniforme, veća kod istovremenog korišćenja više materijala jednih preko drugih (tzv. sendvič materijala), a najbolju termičku zaštitu pružaju sendvič materijali sa vazdušnim međuprostorom (VP). Taktičko–tehnički zahtev za termičku otpornost materijala OFZ na dejstvo GNS (≥ 15s) kod sva tri ispitivana modela u potpunosti je ispunjen. Najveću termičku otpornost je pokazao OFZ-M2PUR koji je urađen na bazi poliuretanske pene i aktivnog uglja, zatim OFZ-M00 na bazi tkane tkanine i sferičnog ugljeničnog adsorbenta i konačno OFZ--M2 na bazi tkane tkanine i sferičnog ugljeničnog adsorbenta. Utvrđena je proporcionalna zavisnost između termičke otpornosti OFZ na dejstvo GNS i propustljivosti vodene pare kroz ovo odevno sredstvo, a obrnuta u odnosu na propustljivost vazduha.

Ključne reči: Termička otpornost • RHB zaštita • Fiziološka podobnost • Goruća napalm smeša

Analiza značaja kvaliteta ambalaže lekova za krajnje korisnike i farmaceutsku industriju u sklopu sistema upravljanja kvalitetom

Irma M. Lončar[1], Janko M. Cvijanović[2]

[1]*Galenika a.d. Beograd, Srbija*
[2]*Ekonomski institut Beograd, Srbija*

Izvod

U radu su prikupljene i analizirane informacije o značaju kvaliteta ambalaže lekova, kao pokazatelja procesa sledljivosti u lancu snabdevanja i originalnosti leka, za krajnje korisnike i za farmaceutsku industriju. Sprovedene su dve ankete: jedna među korisnicima lekova (252 ispitanika) a druga među stručnjacima zaposlenim u 7 farmaceutskih kompanija u Srbiji. Većina korisnika (82,5%), smatra da je kvalitet ambalaže važan, ali samo 41,8% od njih misli da izgled ambalaže može biti pokazatelj originalnosti leka. Postojanje kontrolne markice (KM) na ambalažnom pakovanju leka za korisnike nema velikog značaja: većina (86,9%) zna njenu funkciju, ali bi se 60,2% od njih ipak odlučilo da kupi lek i bez KM. Više od dve trećine stručnjaka iz farmaceutske industrije (68,4%) smatra da uvođenje KM ne doprinosi efikasnijem poslovanju. Iako većina proizvođača (84,2%) smatra da bi uvođenje GS1 Datamatrix-a omogućilo kompletnu sledljivost leka od proizvođača do krajnjeg korisnika, samo 22,2 % od njih je počelo sa primenom ovog sistema, a samo 15,8% ima na svojim proizvodima neku dodatnu zaštitu od falsifikovanja. Svi ispitanici su u visokom procentu zadovoljni funkcionisanjem sistema sledljivosti u svojim kompanijama, a poboljšanje kvaliteta ambalažnog pakovanja lekova vide kao deo unapređenja kvaliteta procesa sledljivosti unutar kompanije u ukupnom procesu sistema menadžmenta kvalitetom.

Ključne reči: *kvalitet ambalažnog pakovanja, sledljivost, farmaceutska industrija.*

Dostupno na Internetu sa adrese časopisa: http://www.ache.org.rs/HI/

NAUČNI RAD

UDK 615.014.8:615.012

Hem. Ind. **67** (6) 951–959 (2013)

doi: 10.2298/HEMIND121221013L

Upravljanje sistemom kvaliteta (QMS, eng. *quality management system*) ima suštinski značaj u proizvodnji lekova, prvenstveno zbog toga što je lek specifičan proizvod čiji kvalitet ima direktan uticaj na zdravlje ljudi. U okviru QMS izuzetno je važno kontinuirano poboljšanje svih organizacionih procesa i sistema, uključujući i proces upravljanja kvalitetom ambalažnog materijala za pakovanje lekova, kako bi se unapredile vrednosti za krajnjeg korisnika/kupca. Do pre dvadesetak godina, ambalaži za pakovanje lekova se nije pridavao veliki značaj. Danas se, obzirom na novija saznanja o značaju ambalaže, posebno poklanja pažnja funkciji pakovanja, počev od razvoja proizvoda, pa sve do kraja isteka roka trajanja leka, kao i posle toga (zbrinjavanje farmaceutskog otpada). Sledljivost robe u lancu snabdevanja postaje sve značajnija za farmaceutsku industriju, jer se povećana količina robe distribuira širom sveta povećavajući mogućnost zloupotreba, falsifikovanja i nelegalne trgovine. Upravo ovaj lanac praćenja podataka o kvalitetu u današnje vreme dobija zasluženu pažnju i postaje zakonska obaveza, pogotovo u farmaceutskoj industriji. Ustanovljavanje i uvođenje sledljivosti je interes svakog proizvođača jer se na taj način povećava kvalitet poslovanja i pruža dodatna sigurnost tržištu i krajnjem kupcu. Potrebe tržišta su sve zahtevnije, a visoki standardi koji se nameću u farmaceutskoj industriji diktiraju uspešnoj kompaniji da stalno radi na unapredjenju sistema upravljanja kvalitetom. Upravljanje lancima snabdevanja, pored aspekta pakovanja, manipulacije, transporta i skladištenja lekova [1], podrazumeva i aspekt sledljivosti podataka o leku od proizvođača do krajnjeg korisnika. Analiza uticaja uspostavljenog sistema menadžmenta kvaliteta na performanse poslovanja u farmaceutsko-hemijskoj industriji Srbije, pokazuje da postoji pozitivan uticaj primene tehnika analize rizika i upravljanja znanjem [2].

U lancu snabdevanja pojavljuju se brojni sigurnosni i bezbednosni problemi koji mogu da dovedu do rizika za pacijente, materijalne štete i gubitka ugleda za brend proizvođače [3]. Ovi problemi mogu se okvirno podeliti u tri grupe. U prvoj grupi su problemi koji mogu nastati kao posledica trenda globalizacije svih aktivnosti u farmaceutskoj industriji, kao što je nabavka sirovina i izmeštanje proizvodnje generičkih lekova ili onih koji izlaze iz patentne zaštite u zemlje u razvoju zbog nižih troškova proizvodnje [4]. Kontrola rizika kroz zakonsku regulativu i inspekcije može biti neefikasna u otkrivanju svih rizika koji se mogu javiti u svakom trenutku u ogromnom broju lanaca snabdevanja, posebno kada je kontaminacija namerna ili kada postoji lažni sertifikat

Prepiska: I. Lončar, Galenika a.d. Batajnički drum b.b., 11000 Beograd, Srbija.
E-pošta: irma.loncar@gmail.com
Rad primljen: 21. decembar, 2012
Rad prihvaćen: 29. januar, 2013

da proizvod ispunjava sve propise i da je prošao inspekciju [5]. U drugu grupu problema spada falsifikovanje lekova [6], koje se suptilno razlikuje od kontaminacije, jer se odnosi na namernu lažnu proizvodnju lekova za ekonomsku dobit, a treću grupu problema čine sekundarni distribucioni kanali koji povećavaju složenost lanca snabdevanja.

Grupe lekova koje se najčešće falsifikuju su lekovi za kardiovaskularne bolesti, za gojaznost i antihiperlipidemici. Zabrinjavajući događaji vezani za falsifikovanje lekova, kao na primer igle za insulinske olovke u Holandiji, lek za malariju u Gani i inhalator u Velikoj Britaniji prisiljavaju farmaceutske proizvođače da se stalno usavršavaju u borbi protiv falsifikatora. U SAD je u 2008. godini prijavljeno više od 80 smrtnih slučajeva, kao i stotine alergijskih reakcija, koji su bili povezani sa falsifikovanom heparinom [7].

Za sprečavanje falsifikovanja postoje vidljivi (bar-kodovi, hologrami, zaptivne trake, uređaji – radio frekventni identidikatori (RFID) i tajni (nevidljivi) sistemi kako bi se očuvao integritet farmaceutskog proizvoda. Navedene tehnike, iako pružaju značajnu zaštitu od falsifikovanja, imaju određena ograničenja koja se mogu prevazići primenom principa nanotehnologija [8]. Smartfon je proizveo sredstvo za autentifikaciju proizvoda i njegovu verifikaciju putem telekomunikacione mreže, koje je postalo sredstvo izbora za borbu protiv falsifikovanja. Pomoću smart telefona može se potvrditi autentičnost prizvoda u realnom vremenu u trenutku kupovine ili kod kuće. Još jedna od novijih tehnologija za zaštitu od falsifikovanja su mikro oznake na filmu za oblaganje čvrstih formi lekova. Ove mikro oznake mogu sadržati razne šifrovane informacije o vlasniku brenda, o serijskom broju, logotip ili neki drugi tekst, dezen, oblik i simbol u česticama manjim od prečnika ljudske kose. Proizvođači lekova mogu da uvedu ovu tehnologiju mikrooznaka na svoje proizvode bez prethodnog odobrenja regulatornih agencija. Ostale metode za zaštitu od falsifikovanja podrazumevaju ugradnju malih identifikatora u pakovanje, etiketu ili sam proizvod. Neki od tih tajnih alata oslanjaju se na smartfone skenere, dok drugi zahtevaju uređaje kao što su prenosivi uređaji za uvećanje. Jedna od nanotehnologija bazira se na tajnoj slučajnoj distribuciji mikro- i nanočestica u materijalu koja stvara mašinski čitljive otiske [9]. Novi fizičko–hemijski identifikatori na nivou tablete, koji omogućavaju autentičost jedne doze, kao i autentičnost nivoa pakovanja mogu efikasnije pomoći u odbrani od falsifikatora [7].

U literaturi postoje podaci o istraživanjima sledljivosti u farmaceutskom lancu snabdevanja [10] u kojima je pokazano kako informaciona infrastruktura auto ID centara i tehnologija RFID-a, mogu da unaprede sledljivost lekova. Pored upotrebe RFID etiketa, mnogi proizvođači koriste hologrami ili skrivena mastila koja nisu vidljiva golim okom. Dati su prikazi [11] novih rešenja koja su našla primenu, kao na primer upotreba čestica (od celuloze i želatina) koje se mogu detektovati samo pomoću posebnog mikro čitača i softvera. Ove čestice mogu biti uključene u pakovanje na razne načine, stavljanjem u lepak, premazivanjem etikete ili neke druge podloge na etiketi, stavljanjem na unutrašnju stranu poklopca ili kombinovanjem sa desikantom. Praćenje svake ambalažne jedinice u toku pakovanja nudi veliki potencijal za smanjenje neusaglašenosti i time minimizira ljudske greške koje mogu dovesti do zamene i nudi farmaceutskim kompanijama način za dugoročnu lojalnost brendu i povećanje tržišnog udela [12,13]. Za inovativne farmaceutske proizvode sa povoljnim cenama, predstaviljeni su predlozi za tri nova propisa o bezbednosti i istaknut je značaj sledljivosti, a takođe i predlog u cilju jačanja sistema farmakovigilanse [14]. Jedan od alata za serijalizaciju i omogućavanje sledljivosti u lancu snabdevanja su nova tipografska rešenja za upotrebne sisteme bar kodiranih lekova koji mogu da se koriste za potvrdu identiteta proizvoda i omogućavaju njegovo praćenje i pronalaženje [15,16].

Upravljanje lancem snabdevanja pored značaja za bezbednost pacijenata ima i komercijalnu važnost u proširenju tržišta i kontroli tržišnog učešća. Mnoge farmaceutske kompanije imaju strateški fokus popunjavanja rupa u lancu snabdevanja lekovima izvan granica SAD i zapadne Evrope. Da bi smanjile troškove, kompanije okreću svoje proizvodne kapacitete ka „*offshore*" lokacijama. Preko studijskih prognoza prihoda korišćenjem RFID-a, farmaceutskog obeležavanja, holograma, bezbednosnih mastila i vatermark tehnologija (vodeni žig) mogu se videti potencijali celokupnog svetskog tržišta do 2021.godine. Ovi izveštaji predstavljaju zbir opsežnih istraživanja, uključujući intervjue sa kompanijama koje primenjuju RFID i rešenja provajdera u različitim tržišnim aplikacijama RFID, dajući izuzetan nivo uvida u ukupnu RFID industriju [17–22].

Upravljanje lancem snabdevanja ima poseban značaj kod temperaturno kontrolisanih isporuka. Postoje brojne logističke aktivnosti, kao i veliki izbor raznovrsnosnih zaštitnih pakovanja i sistema za nadgledanje i praćenje za temperaturno osetljive farmaceutske proizvode kao što su biološki lekovi i krvni derivati. Opisana je druga generacija sistema za monitoring temperature u toku transporta (data logeri) koji predstavlju jedinicu sličnu etiketi sa integrisanim temperaturnim senzorom i USB priključkom koji može da se direktno uključi u računar, za preuzimanje podataka hladnog lanca. Prikazane su i najnovije RFID tehnologije, oznake sa satelitskim modemom i GPS prijemnikom. Da bi zaštitili proizvode od „temperaturnog zlostavljanja" proizvođači lekova se oslanjaju na širi spektar alata za održavanje pošiljke u odgovarajućim uslovima. Ovi alati takođe identifikuju odstupanja od optimalnog temperaturnog opsega. Raz-

vijeni su i ekološki termalni kontejneri za višekratnu upotrebu dizajnirani da zauzimaju mnogo manje prostora od predhodnih, a njihov sadržaj se može reciklirati [23]. Neka termalna pakovanja, razvijena i testirana u skladu sa ISTA standardima, osmišljena su da pojednostave procese praćenja i obezbede poverenje u njegove performance [24].

Rezultati objavljenih pilot studija sledljivosti leka [25–27] dali su temelje za sisteme koji još više povećavaju bezbednost pacijenta i efikasnost lanca snabdevanja na duži rok. Sa danas dostupnim tehnologijama može se obezbediti ispravna identifikacija proizvoda i sprečiti distribucija falsifikovanih lekova. Pokazano je da sistem sledljivosti ima dodirnih tačaka sa svakim aspektom poslovanja u farmaceutskoj industriji. Kod nas je takođe pokrenut pilot projekat pod koordinacijom asocijacije GS1 Srbija „Sledljivost u lancu snabdevanja u zdravstvu" [28] koji ukazuje na značaj postizanja efikasne eksterne sledljivosti i bolje raspoloživosti informacija o stanju i kretanju zaliha duž lanca snabdevanja, upravljanja rokovima upotrebe, efikasnom povlačenju serije leka sa tržišta i dr.

U Srbiji dosadašnja nestandardizovana praksa označavanja lekova može da dovede do povećanog rizika za pacijente, čija zaštita mora biti na prvom mestu. Iz tog razloga je fond INOVIA (u skladu sa preporukama Evropske komisije), ukazao na neophodnost uvođenja elektronske identifikacije lekova u Srbiji, počev od njihove proizvodnje, preko skladištenja i distribucije do upotrebe od strane krajnjih korisnika [29]. Kao rešenje, GS1 je ponudio novu bar-kod simbologiju – GS1 DataMatrix (Data Matrix ECC200), kojom na veoma maloj površini može da se kodira veliki broj podataka (i do 2335 alfanumeričkih znakova) [30].

U ovom radu su prikupljene i analizirane informacije o percepciji značaja kvaliteta ambalaže lekova kao pokazatelja procesa sledljivosti u lancu snabdevanja i originalnosti, koji su elementi značajni za kvalitet leka, a samim tim i za povećanje zadovoljstva korisnika (pacijenata). Cilj rada bio je da se ispita koliki značaj za korisnike i proizvođače ima kvalitet ambalažnog pakovanja, koji ukazuje na sledljivost i originalnost lekova koji se nalaze u prometu na tržištu Srbije. Dodatni značaj ove studije je taj, što je ovo prva studija ove vrste koja je sprovedena na teritoriji Srbije. Hipoteza koju smo postavili je da će poboljšanje procesa sledljivosti, kao značajnog alata upravljanja sistemom kvaliteta u lancu snabdevanja lekovima, povećati zadovoljstvo korisnika lekova.

METODOLOGIJA ISTRAŽIVANJA

Definisani model za ispitivanje značaja sledljivosti i kvaliteta ambalažnog pakovanja za povećanje zadovoljstva korisnika u farmaceutskoj industriji u Srbiji, bazira se na predhodno navedenim istraživanjima. U cilju prikupljanja empirijskih podataka, sprovedene su dve ankete: jedna među krajnjim korisnicima lekova (252), a druga među stručnjacima (19) (menadžeri u sektoru proizvodnje, kontrole i obezbeđenja kvaliteta, razvoja i registacije) u 7 farmaceutskih kompanija u Srbiji. Prvi deo upitnika za krajnje korisnike odnosio se na opšte podatke (pol, starost, učestalost terapije u poslednjih godinu dana, obrazovanje, prirodu bolesti i posebne potrebe), a drugi deo je obuhvatio pitanja vezana za aspekt originalnosti i sledljivosti u lancu snabdevanja lekovima. Anketa koja je sprovedena među stručnim osobama zaposlenim u farmaceutskoj industriji imala je takođe dva dela: prvi se odnosio na pitanja vezana za opšte podatke o kompaniji (tip organizacije, broj zaposlenih i broj poslovnih jedinica u okviru organizacije) a drugi deo na kvalitet ambalaže i kontrolu kvaliteta procesa sledljivosti u lancu snabdevanja lekovima.

Svi prikupljeni podaci obrađeni su savremenim metodama deskriptivne i analitičke statistike uz podršku softver paketa SPSS 20.0. Od deskriptivnih metoda korišćene su sledeće: tabelarni i grafički prikazi, izračunavanje parametara istraživačkog skupa, određivanje empirijske učestalosti, njihovo izražavanje u apsolutnim i relativim brojevima. Izvršeno je izračunavanje mera centralne tendencije (standardna devijacija i koeficijent korelacije). Od analitičkih metoda (pošto je najpre svuda testirana priroda raspodele), korišćeni su adekvatni analitički metodi za testiranje značajnosti razlika (Hi-kvadrat test) i za testiranje značajnosti povezanosti (Spirmanov test korelacije), pri čemu je vrednost $p < 0.05$ označavala statističku značajnost.

REZULTATI I DISKUSIJA

Naše istraživanje je sprovedeno u toku 2012. godine. Ukupni broj intervjuisanih osoba (krajnjih korisnika) u prvoj anketi iznosio je 252. Tabela 1 pokazuje rezultate vezane za opšte podatke ispitanika (krajnjih korisnika), a rezultati ispitivanja vezani za kvalitet ambalaže i proces sledljivosti i originalnosti u lancu snabdevanja lekovima prikazani su u tabeli 2.

Od ukupnog broja ispitanika, 82,5% (208) misli da je kvalitet pakovanja leka važan za pacijente (tabela 2). Interesantan je podatak da od njih, 80,8% (168) zna za postojanje i funkcije KM ($p < 0,05$), a samo 38,9% (81) i za funkciju DM sistema ($p > 0,05$). Od broja ispitanika koji misle da je kvalitet ambalaže važan, samo 41,8% (87) smatra i da se na osnovu izgleda ambalaže može prepoznati da li je lek originalan ili je u pitanju falsifikat. Priroda raspodele između pitanja (I grupa – 1 i 6 pitanje, tabela 2), određena Hi kvadrat testom ($p > 0,05$) i Spirmanovim koeficijentom korelacije ($p > 0,05$), ukazuje da rezultati nisu statistički značajni. Iako je kvalitet ambalažnog pakovanja leka važan za pacijente, većina njih smatra da ono ne može uvek biti pokazatelj da li je u pitanju falsifikat ili ne. Danas su razvijene sofisticirane

Tabela 1. Karakteristike ispitanika – krajnjih korisnika
Table 1. Characteristics of the responders – end users

Parametar	*n* (%)
Pol	
Ženski	190 (75,4)
Muški	60 (23,8)
Nepoznato	2 (0,8)
Godine starosti	
18–25	10 (4,0)
26–35	56 (22,2)
36–50	112 (44,4)
51–65	63 (25,0)
Više od 65	11 (4,4)
Učestalost terapije lekovima u poslednjih godinu dana	
1 put	75 (31,3)
2–5 puta	88 (36,7)
6–10 puta	18 (7,5)
Neprekidno	59 (24,6)
Obrazovanje	
Osnovno	10 (4,0)
Srednje	55 (21,8)
visoko i više	186 (73,8)
Nepoznato	1 (0,4)
Priroda bolesti za koju su uzimani lekovi	
Akutna	160 (66,7)
Hronicna	80 (33,3)
Da li pripadate grupi ljudi sa posebnim potrebama? (slep, slabovid, nemoćne u aktivnostima sa rukama, stare osobe, nešto drugo)	
Ne	249 (98,8)
Da	3 (1,2)

tehnologije za falsifikovanje, tako da je teško golim okom napraviti razliku.

Veći broj ispitanika (77,8%; 196) odgovorio je pozitivno na pitanje „da li znate da svaka kutija leka mora da ima na sebi oznaku (kontrolnu markicu, KM), kojom se potvrđuje da je lek originalan i da ima odgovarajuću dozvolu za promet?", u poređenju sa odgovorima na pitanje „da li znate koju funkciju ima KM na ambalažnom pakovanju leka?" 69,8% (176), koje ne sadrži potpuno objašnjenje. Ovo se može objasniti pretpostavkom da su osobe koje su početno dale negativan odgovor, prepoznale funkciju KM u detaljnijem pitanju. Na pitanje koje ima ponuđene tri opcije u vezi postojanja KM još veći broj ispitanika je odgovorio pozitivno 86,9% (218), pa se može pretpostaviti da jedan broj ispitanika „latentno" zna ulogu KM na ambalažnom pakovanju leka. U prilog tome govore i rezultati testiranja prirode raspodele između drugog i četvrtog pitanja. Na osnovu vrednosti Hi kvadrata ($p < 0,01$) vidi se da postoji visoko statistički značajna razlika između dve varijable, a Spirmanov koeficijent korelacije ($p < 0,01$) ukazuje da je korelacija visoko statistički značajna. Rezultati testiranja prirode raspodele između pitanja (I grupa/2. pitanje) i (II grupa/odgovor pod a), pokazuju da postoji visoko značajna razlika između dve varijable (vrednost Hi kvadrata ($p < 0,01$)). Spirmanov koeficijent korelacije ($p < 0,01$) ukazuje da je korelacija visoko statistički značajna. Ovakav rezultat da veliki broj ispitanika zna tačno koja je funkcija KM i da svaka kutija leka mora da je poseduje, može se objasniti činjenicom da 73,8% (186) ispitanika ima visoko i više obrazovanje.

Urađena je i analiza značaja razlike i značaja povezanosti između odgovora gde su isptitanici znali koju funkciju ima KM i onih koji bi kupili lek bez KM. Vrednosti Hi kvadrata ($p > 0,05$) i koeficijenta korelacije ($p > 0,05$) ukazuju da rezultati nisu statistički značajni. Dobijeni rezultat ukazuje da ne postoji značajna razlika između ispitanika koji bi kupili lek i znaju i onih koji bi kupili lek i ne znaju koja je funkcija KM, što govori u prilog mišljenju da za pacijente postojanje KM na ambalažnom pakovanju leka nema velikog značaja.

Od ukupnog broja ispitanika 36,7% (92) zna koja je funkcija Data matrix (DM) obeležja (tabela 2). Od toga 92,4% (85) ispitanika zna koju funkciju ima i KM i DM sistem. Vrednosti Hi kvadrata ($p > 0,05$), ukazuju na to da nema statistički značajne razlike, dok koeficijent korelacije ($p < 0,05$) ukazuje na postojanje statistički značajne povezanosti. Pored toga, od ukupnog broja ispitanika koji znaju funkciju DM, 65,2% (60) bi kupilo lek bez KM, a 34,8% (32) ne bi kupilo lek bez KM ($p >$

Tabela 2. Rezultati I ankete – odgovori krajnih korisnika na pitanja vezana za kvalitet ambalže i proces sledljivosti i originalnosti u lancu snabdevanja lekovima
Table 2. Survey results (Questionnaire I) – answers of end users to questions regarding the drug packaging quality andprocess of traceability in the drug supply chain and originality of drugs

Pitanje		ne		da	
		n	%	*n*	%
	I grupa pitanja				
1	Da li mislite da je kvalitet ambalažnog pakovanja leka važno pitanje za pacijente?	44	17,5	208	82,5
2	Da li znate koju funkciju ima kontrolna markica na ambalažnom pakovanju leka?	76	30,2	176	69,8
3	Da li znate koju funkciju ima Data matrix sistem na ambalažnom pakovanju leka?	159	63,3	92	36,7
4	Da li znate da svaka kutija leka mora da ima na sebi kontrolnu markicu, kojom se potvrđuje da je lek originalan i ima odgovarajuću dozvolu za promet?	56	22,2	196	77,8
5	Da li biste kupili lek koji nema kontrolnu markicu, ukoliko u ponudi na tržištu ima samo lekova koji nemaju kontrolnu markicu, a vama je neophodno?	107	42,5	145	57,5
6	Da li mislite da se na osnovu izgleda ambalaže može prepoznati da li je lek originalan ili je u pitanju falsifikat?	151	59,9	101	40,1
	II grupa pitanja. Postojanje kontrolne markice na ambalažnoj kutiji leka ukazuje na to:				
a	da je u pitanju originalni lek koji ima odgovarajuću dozvolu za promet	33	13,1	218	86,9
b	da je u pitanju bezbedan i efikasan lek	209	83,3	42	16,7
c	da je u pitanju neka oznaka bita za proizvođača lekova	233	92,8	18	7,2

> 0,05), što takođe ukazuje na to da za ispitanike, iako znaju ulogu i KM i DM, postojanje KM na ambalažnom pakovanju leka nema velikog značaja.

Ministarstvo zdravlja je 2008. godine donelo Pravilnik o sadržaju i načinu obeležavanja spoljnog i unutrašnjeg pakovanja leka i o sadržaju uputstva za pacijenta, a svi proizvođači i uvoznici lekova dobili su obavezu da do januara 2012. godine na spoljno pakovanje leka stave kontrolne markice [31]. Ovaj Pravilnik je izazvao mnogo polemike u javnosti, naročito među proizvođačima i uvoznicima lekova. Kao razlog za uvođenje kontrolnih markica navedena je bolja kontrola lekova na tržištu i sprečavanje falsifikata. Međutim, kontrolne markice ne mogu da omoguće sistemsko praćenje svake kutije leka, od proizvođača do pacijenta, a zakonska obaveza stavljanja DM na ambalažno pakovanje leka ne postoji. Jedan od zanimljivih faktora u našem istraživanju je što Srbija nije tržište koje karakterišu falsifikovani lekovi (za poslednjih sedam godina pojavila su se tek dva ili tri falsifikata).

Druga anketa obuhvatila je 19 stručnjaka iz 7 farmaceutskih kompanija. Po tipu organizacije bilo je 16 (84,2%) samostalnih kompanija, a 3 (15,8%) su bile deo međunarodnog lanca. Po broju zaposlenih 14 (73,7%) je imalo više od 500, 1 (5,3%) između 101–300, a 4 (21,0%) manje od 50 zaposlenih. Više od 5 poslovnih jedinica u okviru organizacije imalo je 10 (52,6%) kompanija, dok je 4–5 poslovnih jedinica imalo 3 (15,8%) kompanije, a jednu poslovnu jedinicu imalo je 6 (31,6%) kompanija. Rezultati vezani za kvalitet ambalaže lekova i proces sledljivosti i originalnosti u lancu snabdevanja lekovima kod proizvođača (I grupa pitanja) prikazani su na slici 1.

Više od dve trećine stručnih osoba (68,4%; 13) smatra da uvođenje KM ne omogućava efikasnije poslovanje, što se može tumačiti samom funkcijom koju KM ima i činjenicom da domaći proizvođači nemaju problem falsifikovanja lekova iz svog proizvodnog asortimana. S druge strane, povećavaju se troškovi proizvodnje zbog nabavke proizvodne opreme za lepljenje KM, nabavke samih KM, regulatornih taksi za prijavu varijacije i utroška vremena za organizovanje svih aktivnosti vezanih za KM. Obzirom da od januara 2012. godine, kada su proizvođači bili dužni da uvedu KM, nije bilo nikakvih incidenata u vezi sa falsifikovanjem lekova i da je ovaj period vrlo kratak, za sad ne postoji potvrda o koristi uvođenja KM. Zaštita od falsifikata je posao od najvećeg interesa, kako za građane koji koriste lekove i za državu koja na taj način uvodi red u ovu oblast, tako i za same proizvođače lekova. Dvadesetogodišnje iskustvo iz kovnice novca sa sistemom izdavanja akciznih markica za alkohol i duvan (premda lekovi svakako ne spadaju u istu grupu), ukazuje da je sâm sistem veoma razrađen i delotvoran [32]. Manje od polovine ispitanika (47%; 9) smatra da uvođenje KM predstavlja ulaganje koje za posledicu ima značajne dugoročne pozitivne efekte za kompaniju. Iako većina (84,2%; 16) proizvođača smatra da bi uvođenje GS1 Datamatrix-a omogućilo kompletnu sledljivost leka od proizvođača do krajnjeg korisnika, samo 22,2% (4) je počelo sa aktivnostima na uvođenju ovog sistema za svoje proizvode, a samo 15,8% (3) ima na svojim proizvodima neku dodatnu zaštitu od falsifikovanja. Obzirom da je uvođenje svake novine u farmaceutskoj industriji skup i dugotrajan proces, a tržište Srbije ne karakterišu falsifikovani lekovi, jasno je zašto domaći proizvođači nemaju veliki

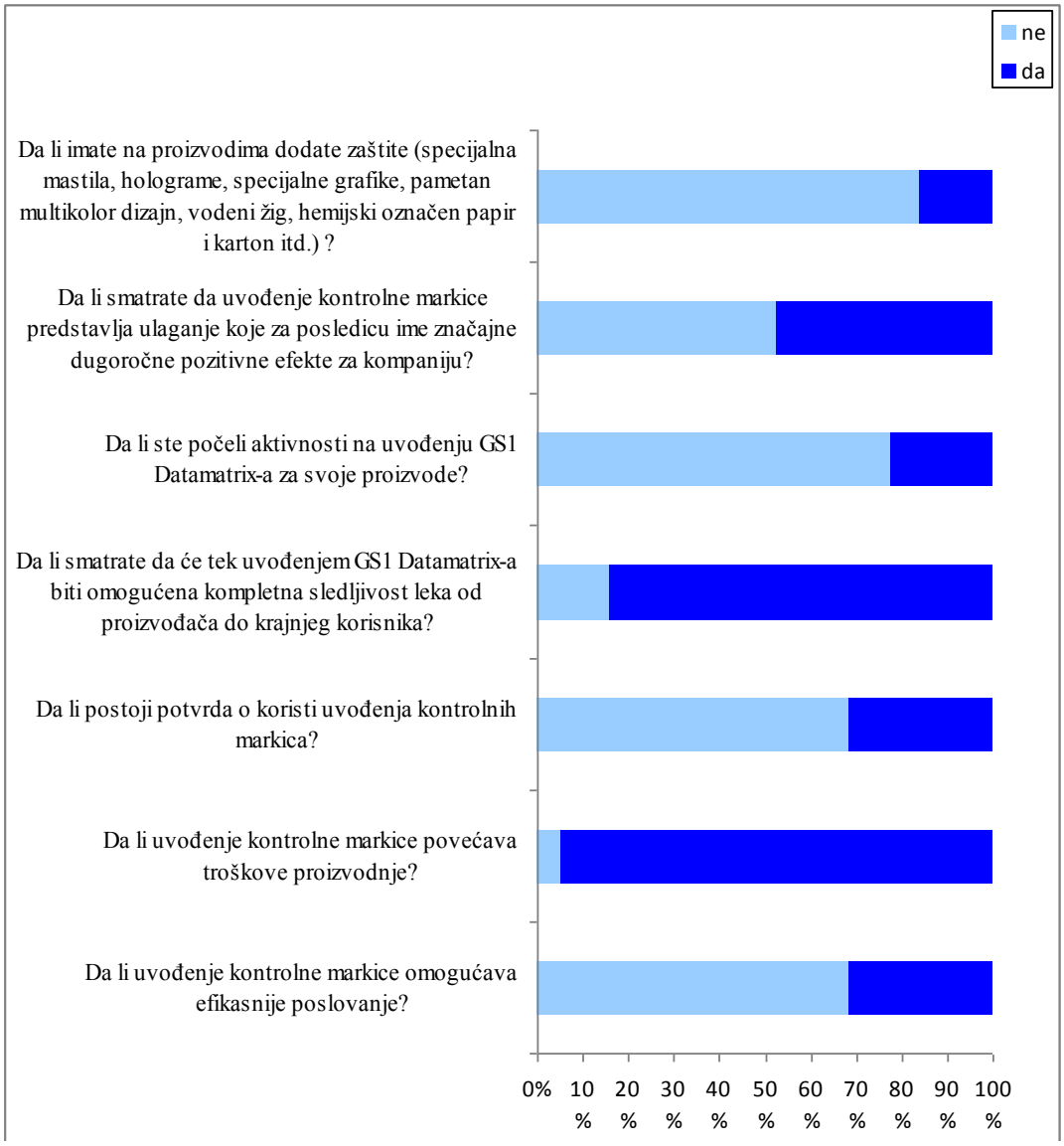

Slika 1. Rezultati II ankete – odgovori stručnih osoba na pitanja vezana za kvalitet ambalaže i proces sledljivosti i originalnosti u lancu snabdevanja lekovima.
Figure 1. Survey results (questionnaire II) – answers of experts to questions regarding the drug packaging quality quality and process of traceability in the drug supply chain and originality of drugs.

interes za uvođenjem dodate zaštite na svojim proizvodima (specijalna mastila, holograme, specijalne grafike, pametan multikolor dizajn, vodeni žig, hemijski označen papir i karton, itd.).

Na pitanje „Da li Vaša kompanija ima sisteme za sprovođenje sledljivosti i navedite koje?" svi ispitanici su dali pozitivan odgovor. Implementacija GMP i ISO standarda je način za identifikaciju i sledljivost proizvoda i procesa u svim anketiranim kompanijama, u kojima svi materijali imaju svoje šifre, kontrolne brojeve, EAN kod i farmakod, a gotovi proizvodi serijski broj. U većim kompanijama materijalima se upravlja kompjuterizovanim sistemom, što omogućava laku manipulaciju, proveru skladištenog materijala i bezbedno memorisanje podataka. U jednoj od anketiranih kompanija za sprovođenje aktivnosti sledljivosti koriste se integrisana softverska rešenja koja obuhvataju ključne poslovne funkcije organizacije, kao što je najpoznatija softverska aplikacija SAP ERP (*Enterprise Resource Planning*). Ispitanici iz jedne kompanije naveli su da je praćenje materijala i procesa omogućeno simultanim radom više kompjuterskih sistema, kao što je Mecalux Easy aplikacija za upravljanje skladištem (WMS – *Warehouse Menagement System*), čija je osnovna svrha da kontroliše ulaz, skladištenje i izlaz materijala, a povezan je sa HOST eksternim sistemima upravljanja i sistemom za automatsko razmeravanje. Ove veze sa eksternim sistemima omogućavaju elektronski prijem informacija

(punjenje i ažuriranje baze podataka, najave materijala koji ulaze u sistem, prijem zahteva za izdavanje materijala).

Svi ispitanici su naveli da praćenje sledljivosti leka od proizvođača do krajnjeg korisnika postižu brojnim kompleksnim aktivnostima koje su regulisane zakonskim propisima [33–36] i da imaju interes za poboljšanje poslovnih performansi i unapređenje kvaliteta ambalažnog pakovanja lekova u ukupnom procesu sistema menadžmenta kvalitetom. Ovakvi odgovori se mogu tumačiti time da je veći broj ispitanika 73,7% (14) bio iz velikih kompanija koje imaju više od 500 zaposlenih, sa više od 5 poslovnih jedinica u organizaciji.

Na pitanje „Da li su po vašem mišljenju ambalažni materijal i svi procesi vezani za ambalažni materijal kritična tačka za bezbednost proizvoda i zaštitu kompanije od velikih ekonomskih gubitaka, gubitka ugleda pa čak i totalnog propadanja od nelegalih aktivnosti kao što su: kopiranje, zamena, falsifikovanje, krađa, nelegalna paralelna trgovina prizvoda, itd.?”, 68,5% (13) ispitanika dalo je negativan odgovor.

Na pitanje „Da li su po vašem mišljenju isplativa velika finansijska ulaganja u sistem bezbednosti celog lanca od dobavljača materijala, bezbednosti kretanja materijala tokom celog proizvodnog ciklusa do završne faze proizvodnje i nakon toga do krajnjeg korisnika?” 15,8% (3) ispitanika odgovorilo je pozitivno jer smatraju da su to dugoročna ulaganja koja štite proizvod. Znatno veći broj ispitanika (16; 84,2%) smatra da velika finansijska ulaganja u ceo lanac nisu isplativa, već su dovoljna samo ona koja unapređuju kvalitet sistema sledljivosti unutar kompanije. Obrazloženje za ovaj stav je nemogućnost postizanja konkurentne cene na tržištu. Pored toga, stav većine domaćih proizvođača da sledljivost u lancu snabdevanja i zaštitu od zloupotrebe za svoje proizvode mogu da postignu implementacijom standarda, propisa i aplikacijom kompjuterskih sistema, može se tumačiti činjenicom da je tržište na koje plasiraju svoje proizvode relativno malo, zbog čega imaju dobar uvid u stanje, kao i to da to tržište ne karakterišu falsifikati. Ovi odgovori mogu se objasniti strukturom kompanija iz kojih su bili ispitanici: samo 3 (15,8%) kompanije su deo međunarodnog lanca, dok je 16 (84,2%) samostalnih. Veliki svetski proizvođači, koji imaju proizvodnje izmeštene u različitim delovima sveta, kao i distribuciju svojih proizvoda u celom svetu, imaju i veći interes za ulaganje u lanac sledljivosti i sisteme za praćenje i povećanu bezbednost svojih proizvoda. U prilog tome ide i visok procenat ($\bar{x}$ = 90) pozitivnog odgovora na pitanje „U kom procentu je efikasan sistem za sprovođenje sledljivosti koji imate u vašoj kompaniji?” što govori o tome da su svi ispitanici iz farmaceutskih kompanija zadovoljni funkcionisanjem sistema koji koriste. Ovo potkrepljuje i odgovor ($\bar{x}$ = 91) da je sistem sledljivosti koji imaju implementiran i da omogućava sprovođenje procesa farmakovigilance.

ZAKLJUČAK

U ovom istraživanju prikupljene su informacije o značaju kvaliteta ambalažnog pakovanja leka kao pokazatelja procesa sledljivosti u lancu snabdevanja i originalnosti za krajnje korisnike (pacijente) i za proizvođače lekova. Većina anketiranih korisnika (82,5%) smatra da je kvalitet ambalažnog pakovanja leka bitan za kvalitet proizvoda, ali da pakovanje ne može uvek biti pokazatelj originalnosti leka. Postojanje KM na ambalažnom pakovanju leka nema velikog značaja, jer bi se veći deo ispitanika odlučio da kupi lek i bez KM, iako zna njenu funkciju.

Više od dve trećine anketiranih stručnih osoba zaposlenih u farmaceutskoj industriji (68,4%) smatra da uvođenje KM ne omogućava efikasnije poslovanje i da povećava troškove proizvodnje. Rezultati ovog istraživaja će otvoriti prostor za dugoročnije sagledavanje opravdanosti postojanja KM na ambalaži, obzirom da se veći broj ispitanika izjasnio da za sad ne postoji potvrda o koristi uvođenja KM, za unapređenje procesa sledljivosti i zaštitu od falsifikovanja. Mada veći broj ispitanika (84,2%) smatra da će uvođenjem GS1 Datamatrix-a biti omogućena kompletna sledljivost leka od proizvođača do krajnjeg korisnika, samo 22,2% je počelo sa aktivnostima na uvođenju ovog sistema za svoje proizvode. Ovo istraživanje je pokazalo da domaći proizvođači nemaju veliki interes za uvođenje dodatne zaštite (specijalna mastila, holografi, specijalne grafike, pametan multikolor dizajn, vodeni žig, hemijski označen papir i karton, itd.) na svoje proizvode, s obzirom na to da samo 15,8% anketiranih ima na svojim proizvodima neku dodatnu zaštitu od falsifikovanja. Svi ispitanici bili su u visokom procentu zadovoljni funkcionisanjem sistema sledljivosti koji imaju u svojim kompanijama. Poboljšanje kvaliteta ambalažnog pakovanja lekova većina ispitanika vidi kao deo unapređenja sistema sledljivosti unutar kompanije u ukupnom procesu sistema upravljanja kvalitetom; velika finansijska ulaganja u ceo lanac sledljivosti nisu isplativa zbog nemogućnosti postizanja konkurentne cene na tržištu. Obzirom da su samo 3 anketirane kompanije bile deo međunarodnog lanca, ovo otvara prostor za nova istraživanja koja bi uključila i multinacionalne proizvođače lekova iz regiona, kako bi se u potpunosti sagledao značaj ulaganja u lanac sledljivosti leka i zaštitu od falsifikovanja, kao deo ukupnog procesa upravljanja kvalitetom u farmaceutskoj industriji.

Zahvalnica

Ovaj rad je podržan od strane Ministarstva prosvete, nauke i tehnološkog razvoja Republike Srbije, u okviru projekta 179001.

LITERATURA

[1] D.A. Dean, E.R. Evans, I.H. Hall, Pharmaceutical packaging technology, 2 rd ed., Taylor & Francis, London and New York, 2005.

[2] V.D. Marinković, T.V. Šibalija, V.D. Majstorović, Lj.Tasić, Analiza uticaja uspostavljenog sistema menadžmenta kvaliteta na performanse poslovanja u farmaceutsko-hemijskoj industriji Srbije, Hem. Ind. **67** (2013) 535–546.

[3] Marucheck, N. Greis, C. Mena, L. Cai, Product safety and security in the global supply chain: Issues, challenges and research opportunities, J. Oper. Manag. **29** (2011) 707–720.

[4] Grackin, Counterfeiting and piracy of pharmaceuticals, IEEE Eng. Med. Biol. **27**(6) (2008) 66–69.

[5] C.S. Tang, Making products safe: process and challenges, International Commerce Review, ECR J. **8** (2008) 48–55.

[6] G. Jackson, Faking it: the dangers of counterfeit medicine on the internet, Int. J. Clin. Pract. **63** (2009) 181.

[7] H. Forcinio, Pill-Level Product Protection, Pharmaceut. Tech. **33**(9) 2009.

[8] R.Y. Shah, P.N. Prajapati, YK. Agrawal, Anticounterfeit packaging technologies, J. Adv. Pharm. Tech. Res. **1**(4) (2010) 368–373.

[9] H. Forcinio, Verification through Telecommunication, Pharmaceut. Tech. **35**(9) (2011) 40–43.

[10] A. Bellman, Product Traceability in the Pharmaceutical Supply Chain: An Analyzis of the Auto-ID Approach, Master of Engineering in Logistic, Massachusetts Institute of Technology, 2003.

[11] H. Forcinio, New Systems for Counterfeit Protection and Quality Control, Pharmaceut. Tech. **6**(29) 2005.

[12] N. Niven, Monitored dose packaging: A win-win situation, Innovat. Pharmaceut. Tech. **35** (2010) 64–67.

[13] Paxton, Current challenges with supply-chain integrity and the threat to the quality of marketed drugs, Clin. Pharmacol.Ther. **89** (2011) 316–319.

[14] R. Schnettler, I. Müller, C. Wawretschek, The 15th GMP Conference: From the EU pharmaceutical package to supplier management. EU Pharmaceutical Package/Risk management systems/GMP inspections/Supplier qualification/15th Drug Law amendment, (Conference Paper), Pharmazeut. Ind. **72**(1) (2010) 132–140.

[15] H. Forcinio, Adopting Serialization, Pharmaceut. Tech. **34**(8) 2010.

[16] R. Koppel, T. Wetterneck, J. L. Telles, B.T. Karsh, Workarounds to Barcode Medication Administration Systems: Their Occurrences, Causes, and Threats to Patient Safety, J. Am. Med. Inform. Assn. **15**(4) (2008) 408–423.

[17] Pharmaceutical Anti-counterfeiting Strategies and Commercial Analysis 2010-2020, Visiongain, BSG House, London, EC1V 2QY, UK, 2010.

[18] Pharmaceutical anti-counterfeiting technologies: market analysis 2011-2021, Visiongain, BSG House, London, EC1V 2QY, UK, 2011.

[19] Radio Frequency Identification (RFID) in Pharmaceuticals: Supply Chain Security Concerns Provide Impetus for RFID Adoption, GBI Research, 2010.

[20] P.Harrop, T. Crotch-Harvey, RFID for Healthcare and Pharmaceuticals 2008–2018, Securing Industry Ltd., UK, 2008.

[21] Filling the Holes in the Drug Supply Chain (Strategic Focus), Datamonitor, [3] DMTC2266, 2009.

[22] R. Das, P. Harrop, RFID Forecasts, Players and Opportunities: 2009–2019, Securing Industry Ltd. UK, 2009.

[23] H. Forcinio, Temperature-Controlled Shippers, Pharmaceut. Tech. **36**(9) (2012) 34–36.

[24] H. Forcinio, Preventing Temperature Abuse, Pharmaceut. Tech. **35**(2) (2011) 34–37.

[25] L. Médioni, C. Hay, SmartLog: a Swiss drug traceability pilot, in GS1 Healthcare Reference Book, 2009/2010, pp. 1–4.

[26] J. Jenkins Associates and WP6 partners, Pharma Traceability Pilot, Problem analysis, BRIDGE Project, 2007.

[27] P. Taylor, Traceability of medicines in EU: feasible, but challenging, Securing Pharma, 2009.

[28] B. Mitić, Pokrenut pilot projekat u zdravstvu, E-bilten GS1 Srbija Info (4), 2011.

[29] Elektronska identifikacija lekova, Inovia bilten, Fond proizvođača inovativih lekova INOVIA, 2011.

[30] D. Miljević, GS1 DataMatrix, u Sibologija koja dolazi, E-bilten GS1 Srbija Info (1), 2009.

[31] Pravilnik o sadržaju i načinu obeležavanja spoljnjeg i unutrašnjeg pakovanja leka, dodatnom obeležavanju, kao i sadržaju uputstva za lek, Sl. glasnik RS, br. 41/2011.

[32] http://www.pharmanetwork.rs/, datum pristupa: oktobar 2012.

[33] Zakon o lekovima i medicinskim sredstvima, Sl. glasnik RS, br.30/2010.

[34] EU Guidelines to Good Manufacturing Practice, Medicinal Products for Human and Veterinary Use, the European Commission, http://ec.europa.eu/health/documents/ eudralex/vol-4/index_en.htm, datum pristupa: novembar 2012.

[35] Smernice dobre proizvodjačke prakse, Sl. glasnik RS, br. 28/2008. i 35/2008 (ispr.).

[36] ICH guideline Q10, Pharmaceutical Quality System, 2011, EMA/INS/GMP/79818/2011.

SUMMARY

ANALYSIS OF THE IMPORTANCE OF DRUG PACKAGING QUALITY FOR END USERS AND PHARMACEUTICAL INDUSTRY AS A PART OF THE QUALITY MANAGEMENT SYSTEM

Irma M. Lončar[1], Janko M. Cvijanović[2]

[1]*Galenika a.d., Belgrade, Serbia*
[2]*Economics Institute, Belgrade, Serbia*

(Scientific paper)

In this study, we collected and analyzed information on the importance of drug packaging quality to end users and pharmaceutical industry, as an indicator of the process of traceability and originality of drugs. Two surveys were conducted: one among the end users of drugs (252 patients) and the other among professionals working in seven pharmaceutical companies in Serbia. For most end users (82.5%), the quality of the packaging was important, but only 41.8% of them thought that the appearance of the packaging could be an indicator of genuinity of drugs. The existence of the control marks (KM) on drug packaging was not of great importance, since most of the users (86.9%) know its function, but the majority (60.2%) would nevertheless decide to buy the drug without KM. Regarding the experts from the pharmaceutical industry, more then two thirds (68.4%) believed that the existance of KM did not contribute to efficient operations. Although a great number of pharmaceutical industry professionals (84.2%) answered that the introduction of GS1 DataMatrix system would allow for complete traceability of the drug from the manufacturer to the end user, only 22.2% of them introduced this system to their products. This study also showed that domestic producers did not have a great interest for additional protection (special inks, holograms, special graphics, smart multicolor design, watermark, chemically labeled paper and cardboard, etc.) on their products, given that only 15.8% of them had some kind of additional protection against counterfeiting. Monitoring drug traceability from a manufacturer to end user is achieved by many complex activities regulated by law. A high percentage of responders said they were satisfied with the functionality of traceability systems used in their companies. As a way to increase the quality of drug packaging and business performance, most responders saw in the continuous improvement of the system of traceability within the company's overall quality management system. For them, a big financial investment in the complete traceability chain was not feasible because of the inability to achieve competitive prices in the market. Since only three of the surveyed companies were part of international chains, these findings open the path for new research that would include more multinational drug manufacturers from the region, in order to fully comprehend the importance of investing in the drug chain traceability and protection against counterfeiting, as a part of total quality management process in the pharmaceutical industry.

Keywords: Drug packaging quality • Traceability • Pharmaceutical industry

Prilog projektovanju vodonepropusnih slojeva deponija

Milica Karanac[1], Mića Jovanović[2], Eugène Timmermans[3], Huib Mulleneers[3], Marina Mihajlović[1], Jovan Jovanović[1]

[1]*Inovacioni centar Tehnološko–metalurškog fakulteta u Beogradu, Univerzitet u Beogradu, Beograd, Srbija*
[2]*Tehnološko–metalurški fakultet u Beogradu, Univerzitet u Beogradu, Beograd, Srbija*
[3]*Trisoplast Mineral Liners International BV, The Netherlands*

Izvod

Deponije predstavljaju složen sistem koji potencijalno može zagaditi životnu sredinu, što se sprečava obezbeđenjem vodonepropusnosti prilikom njihovog projektovanja. Prvi deo preglednog rada bavi se analizom odgovarajućih tehničkih propisa, tumačenja i preporuka iz SAD, EU i Srbije, u cilju podsticanja valjanog usaglašavanja domaće prakse i propisa sa najboljim dostupnim tehnikama na međunarodnom nivou. U drugom delu rada uporedno su analizirane alternative prilikom projektovanja vodonepropusnih slojeva za oblaganje dna i prekrivanje deponija. Opisane su slabosti i prednosti korišćenja prirodne gline, bentonita, geosintetičke glinene obloge i različitih mešavina peska, bentonita i polimera. Rad zaključno formuliše predlog unapređenja nacionalnog propisa o odlaganju otpada na deponije.

Ključne reči: *projektovanje deponija, veštačka geološka barijera.*

Dostupno na Internetu sa adrese časopisa: http://www.ache.org.rs/HI/

PREGLEDNI RAD

UDK 628.4/.8:502/5045

Hem. Ind. **67** (6) 961–973 (2013)

doi: 10.2298/HEMIND121227012K

U većini zemalja odlaganje otpada na deponije je sastavni deo integrisanog sistema upravljanja otpadom. I pored smanjenja otpada nekom vrstom tretmana (reciklaža, spaljivanje, kompostiranje, itd.), iz otpada ostaje određena količina koja se neminovno odlaže na deponije. U domaćoj naučnoj literaturi, izučavanje problematike zaštite životne sredine sa aspekta otpadnih materijala relativno malo je zastupljeno [1–9], dok je izučavanje problematike deponovanja otpada vrlo skromno [10–12]. Sa druge strane, u svetu naučna literatura bavi se mnogim aspektima izgradnje i rada deponija, posebno njenom stabilnošću, problemom vodonepropusnosti, osobinama materijala koji se koriste pri deponovanju, itd. [13–17]. Budući da deponije potencijalno mogu zagaditi životnu sredinu, neophodno je da se njihovo projektovanje vrši prema važećim propisima. U Evropskoj uniji je 1999. godine, po ugledu na propise Sjedinjenih Američkih Država, doneta je Direktiva o deponijama (u daljem tekstu Direktiva) [18]. U Republici Srbiji, po ugledu na evropsku Direktivu, 2010. godine, doneta je Uredba o odlaganju otpada na deponije (u daljem tekstu Uredba) [19].

Savremena deponija se ogleda u pravilnom odabiru lokacije za njenu izgradnju, valjanim projektovanjem i izgradnjom iste, upravljanjem i monitoringom tokom faze punjenja i valjanim zatvaranjem deponije i nadzorom nakon zatvaranja. Na savremenim deponijama odlažu se određeni tipovi otpada za koje je deponija projektovana, te postoje deponije za opasan, neopasan i inertan otpad [18]. Zahtevi koji se pri projektovanju deponija moraju ispuniti različiti su za svaku vrstu deponija i od velikog značaja su za sprečavanje ili smanjenje negativnih uticaja na zdravlje stanovništva i životnu sredinu, tako da se obezbedi kontrolisano upravljanje procednim vodama i izdvojenim gasovima [19]. Deponije predstavljaju složen sistem, koji je po pravilu, sastavljen od: donje zaštitne obloge, sistema za sakupljanje i odvođenje procednih voda (često i tretmana procednih voda, sa ili bez recirkulacije), drenažnog sloja, sistema za sakupljanje (često i tretman) otpadnih gasova, kao i sistema za monitoring gasnih emisija, procednih voda, zagađivanja podzemnih voda od strane deponije i prekrivnog sloja. Potencijalno zagađenje sprečava se postavljanjem barijera koje obezbeđuju vodonepropusnosti: a) dna deponije tokom faze eksploatacije, a zatim i b) prekrivnog sloja, nakon zatvaranja deponije, kako opasnog tako i neopasnog otpada. Poslednjih 20–30 godina korišćeni su različiti prirodni i veštački materijali za izgradnju vodonepropusnih slojeva deponija. Mnogi autori su se bavili ispitivanjem mogućih rešenja za oblaganje i prekrivanje deponija, posebno karakteristikama različitih pogodnih materijala [20–25], kao i njihovim interakcijama sa procednim vodama [26,27]. U prošlosti vladalo je mišljenje da prirodna glina može valjano obezbediti vodonepropusnost. Vremenom je pokazano da postoje znatno bolja rešenja, te se za tu svrhu danas nudi više različitih veštačkih materijala zasnovanih na oplemenjenim prirodnim sirovinama. U literaturi postoje tvrdnje da najveću otpornost prema procednim vodama ima mešavina peska, bentonita i polimera, koja takođe pokazuje

Prepiska: M. Jovanović, Tehnološko–metalurški fakultet u Beogradu, Univerzitet u Beogradu, Karnegijeva 4, 11000 Beograd, Srbija.
E-pošta: mica@tmf.bg.ac.rs
Rad primljen: 27. decembar, 2012
Rad prihvaćen: 28. januar, 2013

izuzetnu otpornost na vlažno/suve cikluse, što je slabost prirodne gline [28,29].

Zatvaranje deponija vrši se nanošenjem prekrivnog, zaštitnog sloja koji sprečava dotok i prodor atmosferskih voda u telo deponije, kao i prodor otpadnih gasova iz tela deponije u okolinu. Zbog toga je veoma važan odabir valjanog materijala koji obezbeđuje nepropusnost deponije. Zatvorena, dobro projektovana i izgrađena, nepropusna deponija može biti iskorišćena da se iznad nje izgrade parkovi, sportski tereni, aerodromi, itd.

Cilj rada je da, vezano za problematiku projektovanja deponija, da doprinos pri izboru valjanih rešenja koje bi u potpunosti ispunila zahteve za obezbeđivanjem vodonepropusnosti deponija. Osnova za definisanje zahteva pri projektovanju deponija su važeći međunarodni i domaći propisi, te njihova tumačenja i preporuke. U radu se uporedno analiziraju moguće alternative prilikom projektovanja vodonepropusnih slojeva za oblaganje dna i prekrivanje deponija. Pitanje izgradnje vodonepropusnih slojeva deponija u Srbiji izuzetno je važno, jer su u toku aktivnosti sanacije, zatvaranja i rekultivacije vrlo velikog broja divljih deponija, izgradnje novih industrijskih deponija i izgradnje regionalnih sanitarnih deponija [30].

ANALIZA PROPISA ZA OBEZBEĐIVANJE VODONEPROPUSNOSTI

Projektovanje deponija zasniva se na primeni odgovarajućih nacionalnih propisa. Prve propise, sedamdesetih godina prošlog veka, uvele su Sjedinjene Američke Države (SAD). Usledili su srodni propisi zemalja Evropske Unije (EU), sa različitom koncepcijom i rešenjima, posebno u zahtevima za obezbeđivanjem vodonepropusnosti deponija, sastava zaštitnog sloja, debljine slojeva i vrednosti keoficijenta propustljivosti. Odgovarajući propis Republika Srbija (RS) uvela je 2010. god. sa pretenzijom da isti u potpunosti bude usaglašen sa evropskim.

Sjedinjene Američke Države

Propisi iz oblasti upravljanja otpadom postoje od sedamdesetih godina prošlog veka i od tada su više puta menjani. Prema vrsti otpada doneti su propisi koji se odnose na opasan i neopasan-komunalni čvrsti otpad [31,32]. Smernice Američke agencije za zaštitu životne sredine US EPA (eng. *United States Environmental Protection Agency*), zahtevi za oblaganje deponijskog dna i preporuke za izgradnju prekrivke deponije, u pogledu vodopropusnosti – K i debljine, prikazane su na slikama 1 i 2 [33].

U prošlosti su u SAD, za obezbeđenje nepropusnosti, primenjivana sledeća rešenja: jednoslojna obloga izrađena od gline, takozvani sabijeni glineni sloj (eng. *Compacted Clay Liner, CCL*), geomembrane/fleksibilne membranske obloge (eng. *Flexible Membrane Liner, FML*) i geosintetički materijali (eng. *Geosynthetic Clay Liner, GCL* – bentonitna glina ojačana geomembranom ili geotekstilom).

Prema važećim propisima u SAD prilikom projektovanja deponije trebalo bi obezbediti sledeće:

– Dvoslojna kompozitna obloga (geomembrana, mineralni sloj) za dno deponije i sistem za sakupljanje procednih voda. U poređenju sa jednoslojnom oblogom obezbeđuje se dodatna zaštita podzemnih voda, omogućava se detekcija i sakupljanje procednih voda, takođe, povećava se kapacitet deponije. Kompozitna obloga se sastoji od dva ili više nisko propustljivih slojeva (geomemrana u kombinaciji sa geosintetičkom oblogom)

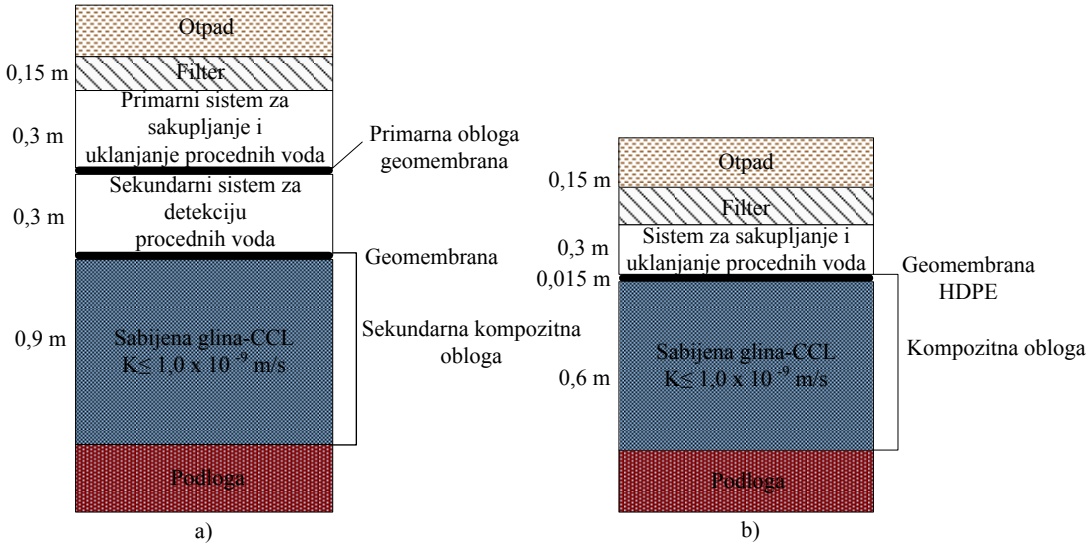

Slika 1. Zahtevi USA EPA za oblaganje dna deponije: a) opasnog i b) komunalnog čvrstog otpada.
Figure 1. U.S. EPA requirements for the bottom lining of the landfill: a) for hazardous and b) for MSW.

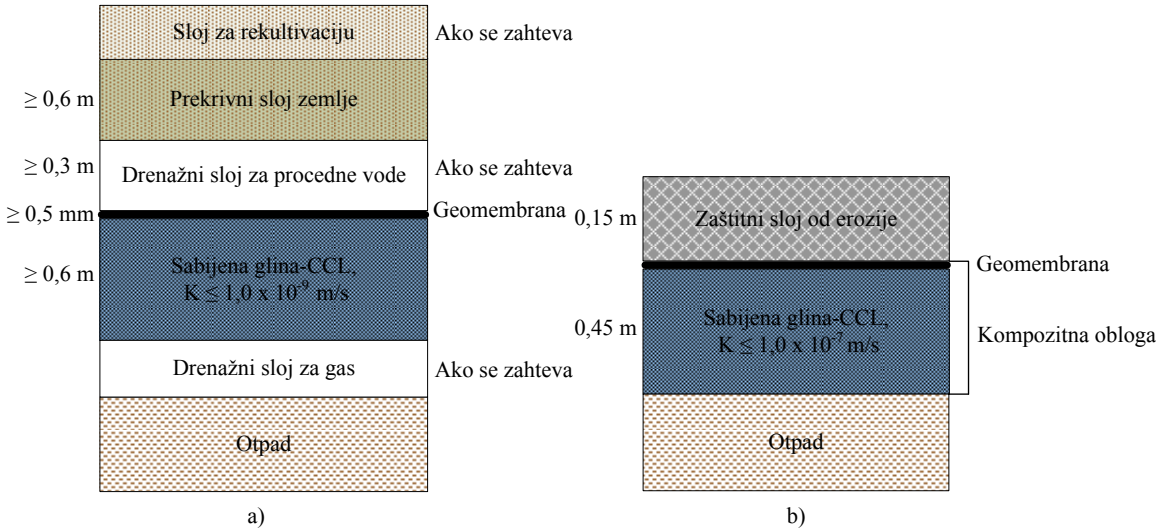

Slika 2. Preporuka USA EPA za prekrivni sloj deponije: a) opasnog i b) komunalnog čvrstog otpada.
Figure 2. U.S. EPA recommendation for the landfill cover: a) for hazardous and b) for MSW.

odvojenih drenažnim slojem. Dvoslojna obloga pruža efikasniju zaštitu javnog zdravlja i životne sredine po razumnoj ceni.

– Prekrivka deponije treba da bude sačinjena od: zaštitnog sloja sabijene gline ili geomembrane, drenažnog sloja i površinskog sloja, ekvivalentne propustljivosti ili manje kao obloga dna. Prekrivka treba da obezbedi zaštitu od erozije i infiltracije atmosferskih voda. Ukoliko se polietilen visoke gustine (eng. *High-Density Polyethylene, HDPE*) folija koristi za oblaganje dna deponije, onda za prekrivanje deponije nije neophodno korišćenje HDPE folije [34,35].

Evropska Unija

U Evropskoj uniji postoje brojni propisi koji se odnose na oblast upravljanja otpadom [36–41]. Poblematiku izgradnje deponija otpada uređuje Direktiva o deponijama koja propisuje opšte kriterijume deponovanja otpada i određene tehničke standarde za deponije [18]. Tamo gde Direktiva ne obezbeđuje relevantne tehničke zahteve, primenjuju se opšti principi IPPC Direktive [42–44]. Sve zemlje Evropske unije su u obavezi da svoje nacionalne propise u potpunosti usklade sa zahtevima za projektovanje deponija propisanih u Direktivi.

Ključni tehnički zahtev, nezavisno od tipa deponije, je sprečavanje njenog zagađenja voda i zemljišta. Zaštita voda i zemljišta se postiže postavljanjem geološke barijere (eng. *geological barrier*), zaptivnog sloja i prikupljanjem procednih voda. Geološka barijera je određena geološkim i hidrogeološkim karakteristikama lokacije i sačinjena je od kombinacije geološke barijere i donje obloge deponije tokom radne faze i kombinacije geološke barijere i prekrivke nakon zatvaranja deponije. Kriterijumi za oblaganje dna i strana deponija u smislu vodopropusnosti i debljine geološke barijere su sledeći:

– deponije opasnog otpada: $K \leq 1{,}0\times10^{-9}$ m/s; debljina ≥ 5 m;

– deponije neopasnog otpada: $K \leq 1{,}0\times10^{-9}$ m/s; debljina ≥ 1 m;

– deponije inertnog otpada: $K \leq 1{,}0\times10^{-7}$ m/s; debljina ≥ 1 m.

Prema Direktivi o deponijama, tamo gde geološka barijera prirodno ne ispunjava propisane uslove zaštitni sloj se može završiti i veštački ojačati drugim materijalima koji pružaju ekvivalentnu zaštitu. Sloj veštački uspostavljene geološke barijere (eng. *artificially established geological barrier*) bi trebalo da bude minimalno 0,5 m (slika 3). Napominje se da prirodni teren može biti deo veštački uspostavljene barijere, pri debljini od 41 cm, zajedno sa 9 cm veštačkog sloja, koja ispunjava zahtevane uslove [45].

Veštačka zaptivna obloga koja se postavlja između geološke barijere i drenažnog sloja je obavezan element deponija opasnog i neopasnog otpada. U praksi se najčešće koristi HDPE. Geomembrana postavlja se po dnu deponije i po unutrašnjim kosinama nasipa, odnosno u delovima deponija u kojima dolazi do kontakta otpada i okruženja.

U evropskoj Direktivi nisu navedeni zahtevi za prekrivni sloj, već odgovarajući tehnički elementi koji imaju karakter preporuke za izgradnju zaštitne obloge sastavljene od: vodonepropusnog, drenažnog sloja za vodu i gas i sloja za rekultivaciju (slika 4).

Nakon zatvaranja deponije narednih 30 godina neophodno je vršiti procenu rizika na životnu sredinu i ispitivanja trajnosti ugrađene barijere, primenom određenih metodologija u cilju pravilnog upravljanja deponijama [46].

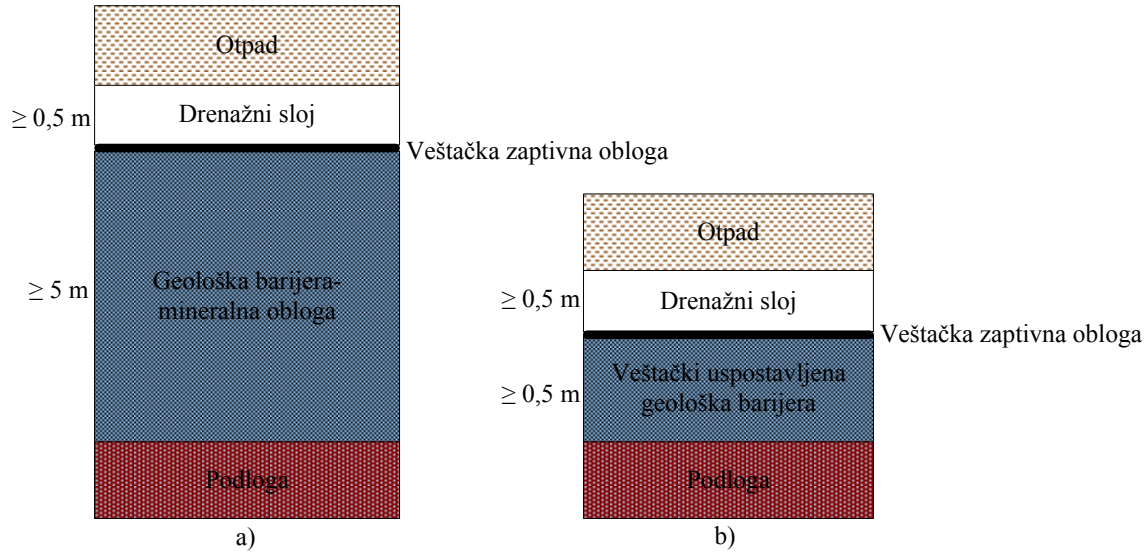

Slika 3. Zahtevi Direktive za oblaganje dna deponije opasnog otpada: a) prirodna i b) veštačka barijera.
Figure 3. Directive requirements for the bottom liner of the hazardous waste landfill: a) natural and b) an artificial barrier.

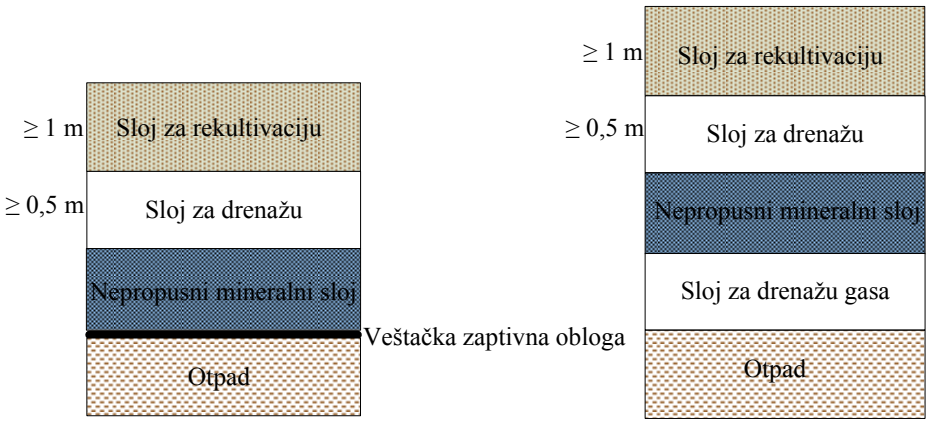

Slika 4. Preporuka Direktive za prekrivanje deponije.
Figure 4. Directive recommendation for the landfill cover.

Na osnovu napred navedenog, vodonepropusnost obezbeđuje se zaptivnom oblogom i geološkom barijerom za koju su propisane vrednosti koeficijenta vodopropusnosti i debljine. Napominje se i da Evropska komisija još uvek nije izradila referentni dokument sa najbolje dostupnim tehnikama (eng. *Best Available Techniques Reference Document, BREF*) za deponije, odnosno da predmetna Direktiva predstavlja najbolju dostupnu tehniku [44].

Republika Srbija

U Republici Srbiji se od decembra 2010. g. primenjuje Uredba o odlaganju otpada na deponije [19]. Uredba propisuje uslove i kriterijume za određivanje lokacije, tehničke i tehnološke uslove za projektovanje, izgradnju i rad deponija, odlaganje otpada na deponiju, način i procedure rada i zatvaranja deponije, način monitoringa kao i održavanje nakon zatvaranja deponije.

Cilj Uredbe je da u potpunosti obezbedi primenu evropskih standarda za predmetnu oblast u Republici Srbiji. U tom smislu Uredba mora u potpunosti, nedvosmisleno, kao minimalno, primeniti zahteve, rešenja i preporuke sadržane u Direktivi. Prema Uredbi, kao i prema Direktivi, dno i bočne strane treba da se sastoje od prirodne geološke barijere i dodatne zaštite od migracije procednih voda (veštačka zaptivna obloga – folija i drenažni sloj).

Zahtevi Uredbe u pogledu vodopropusnosti i debljine prirodne geološke barijere su isti kao u Direktivi. Kada prirodna geološka barijera ne zadovoljava propisane vrednosti, ona se obezbeđuje oblaganjem deponijskog dna sintetičkim materijalima ili prirodnim mineralnim tamponom koji mora biti tako konsolidovan da se dobije ekvivalentna vrednost dna u smislu njegovih vodopropusnih svojstava. Prirodni mineralni tampon ne sme biti manji od 0,5 m (slika 5). Važno je napomenuti da je zahtev u vezi sa nepropusnosti dna deponije u

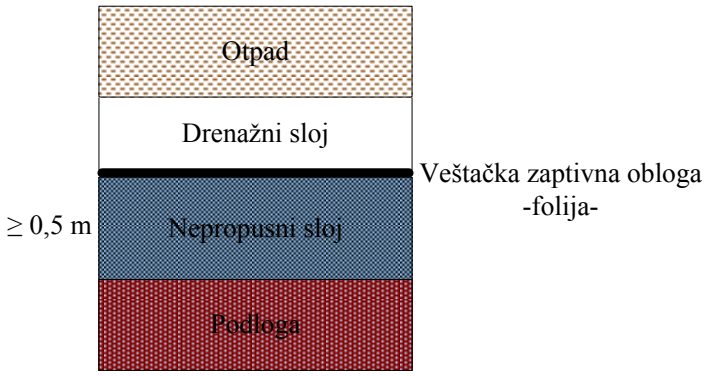

Slika 5. Zahtevi Uredbe za oblaganje dna.
Figure 5. Regulation requirements for the bottom lining.

Uredbi drugačije formulisan nego u Direktivi, te da u pojedinim elementima bitno menja njegovu sadržinu. Ovo se odnosi na mogućnost da se vodonepropusnost obezbedi oblaganjem deponijskog dna sintetičkim materijalima ili prirodnim mineralnim tamponom, u odnosu na zahtev Direktive za veštački uspostavljenom geološkom barijerom.

Nakon zatvaranja deponije, Uredba zahteva i formiranje gornjeg prekrivnog sloja, kako je prikazano na slici 6.

Komparativna analiza

Komparativna analiza zahteva, ograničenja i preporuka za izradu vodonepropusnih slojeva deponija izvedena je na dva nivoa. U prvom se porede rešenja koja se zahtevaju u SAD i EU. Na drugom nivou se za zemlje EU i RS porede pojedinačna rešenja koja dopunski razrađuju Direktivu. U tom smislu, posebno su značajna službena tumačenja predmetnih propisa iz različitih zemalja, odnosno podzakonski akti koji predstavljaju razradu osnovnih propisa.

U SAD je u prošlosti bilo propisano oblaganje dna jednoslojnom glinenom oblogom. Vremenom su uočeni nedostaci koji su smanjili njenu efikasnost, tako da je uvedeno i tehničko rešenje sa dvoslojnom kompozitnom oblogom. Kada su geološki uslovi na izabranoj lokaciji dobri može se postaviti jednoslojna obloga, a kada je neophodna dodatna zaštita uvodi se dvoslojna obloga. Pojedine države SAD bavile su se ispitivanjem efikasnosti višeslojnih, dvoslojnih sistema zaštite i u skladu sa njima koristile pravo da propišu i oštrije zahteve, umanjujući primenu jednoslojne obloge, tako da većina država danas zahteva (skuplju) dvoslojnu kompozitnu oblogu, što je stručno diskutabilno [47].

Prema nacionalnim propisima u zemalja EU neophodan element za oblaganje dna deponija je geološka barijera, koja alternativno prirodnoj može biti i veštački uspostavljena. Pojedine zemlje EU i Srbija, su odlučile da u svoje propise ubace zahteve koji su iznad nivoa onih definisanih u Direktivi. Važno je istaći da se, po pravilu, ne navode ili preciziraju materijali koji se imaju koristiti za obezbeđenje vodonepropusnosti i zaptivanje. Od ovog stava odstupa Uredba koja eksplicitno precizira da je veštačka zaptivna obloga – folija. Napominje se i da EU Direktiva ne sprečava da se deponije

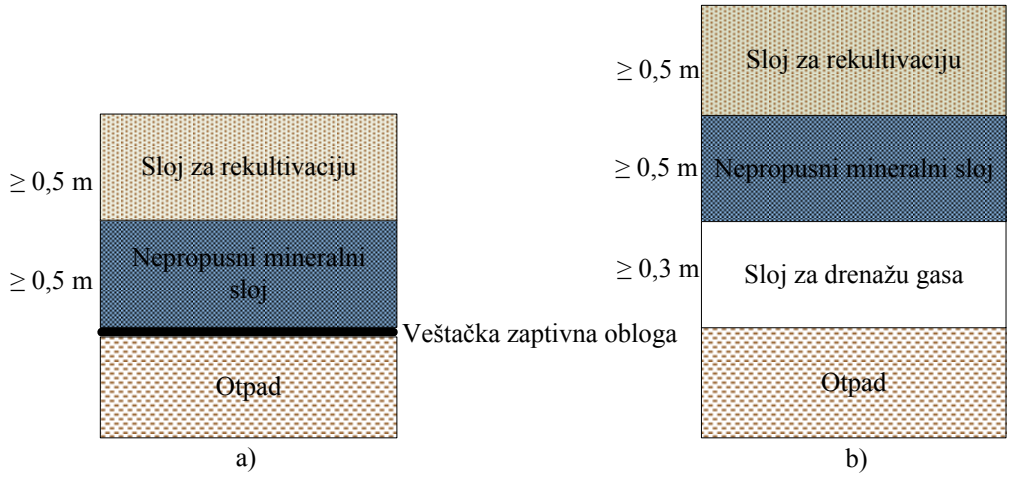

Slika 6. Zahtevi Uredbe za prekrivku deponije: a) opasnog i b) neopasnog otpada.
Figure 6. Regulation requirements for the landfill cover: a) hazardous and b) non-hazardous waste.

projektuju sa dvoslojnim dnom po ugledu na SAD, ali se ovo rešenje u praksi ne susreće, jer je skuplje.

EPA Velike Britanije (eng. *United Kingdom Environmental Protection Agency, UK EPA*) je razvila čitav niz dokumenata koja razrađuju problematiku deponovanja [44,48–56]. Posebno je značajno ukazati da neke deponije podležu IPPC Direktivi, a neke ne [44]. Prema EPA UK obavezan element deponija su geološka barijera i veštačka zaptivna obloga. Geološka barijera se postavlja po dnu i stranama deponije. Odabir geološke barijere se vrši prema proceni rizika za ispuštanje zagađujućih materija tokom životnog ciklusa deponije i procene stabilnosti [19]. Kada prirodna geološka barijera ne pruža dovoljnu zaštitu, može se veštački ojačati. Na osetljivim lokacijama moguće je u potpunosti koristiti samo veštački uspostavljenu geološku barijeru. Veštačka barijera u skladu sa Direktivom, ne sme biti manja od 0,5 m. Prema tome, geološka barijera ne može se ojačati samo pomoću geosintetičke obloge. Tumačenje UK EPA je da postoje dva elementa koja se mogu veštački obezbediti: a) sloj koji ojačava geološku barijeru, odnosno veštački uspostavljena minerala geološka barijera i b) veštačka zaptivna obloga. Nije moguće koristiti jednu veštačku zaptivnu oblogu za ispunjenje zahteva vodonepropusnosti postojeće, nedovoljno dobre, geološke barijere. Za odabir veštačke zaptivne obloge koristi se vodič za upotrebu geomembrana [48]. Mineralna veštačka zaptivna obloga može se koristiti na lokacijama gde postoji značajna prirodna geološka barijera. Posebno važno tumačenje ukazuje da je mala verovatnoća da se jedan mineralni sloj može posmatrati i kao veštački uspostavljena geološka barijera i kao veštačka zaptivna obloga. Ako je mineralna obloga prihvatljiva kao veštačka zaptivna obloga, preporuka je da se dodatno zaštiti od spoljašnjih uticaja, erozije, vremenskih uslova i sušenja [44]. Na osnovu napred iznetog HDPE folija koja se obično koristi kao veštačka zaptivna obloga, ne može biti upotrebljena kao veštački uspostavljena geološka barijera. Takođe, nije obavezno da se isključivo folija koristi kao veštačka zaptivna obloga.

U Holandiji se veliki deo teritorije nalazi ispod ili na nivou mora, odnosno ima visok nivo podzemnih voda, tako da se vodonepropusnost obezbeđuje formiranjem veštačkih barijera koje imaju ulogu geoloških barijera [57]. Kriterijumi za obezbeđivanje vodonepropusnosti su strožiji. Propisani zahtevi za opasan otpad primenjuju se i za deponije neopasnog otpada. Dopunski zahtevi su, na primer, debljina veštački uspostavljene geološke barijere koja za sve klase deponija iznosi 0,5 m, a debljina geomembrane – HDPE 2 mm. Debljina drenažnog sloja je 0,3 m. Vodonepropusnost obezbeđuje se sa gornje strane, kao i u ostalim zemljama, ali posebna pažnja obraća se obezbeđivanju stabilnosti deponije u odnosu na uticaj visokog nivoa podzemnih voda. Podzemne vode usled visokog hidrauličkog pritiska mogu da razbiju sloj – veštačku geološku barijeru, čime bi ona izgubila osobine vodonepropusnosti. To podrazumeva, postavljanje dodatne podloge ispod geološke mineralne barijere. Izgradnja vodonepropusnih obloga podvrgnuta je velikom broju ispitivanja i odgovarajućem obezbeđenju kvaliteta, posebno pri izboru materijala [57]. Napominje se da prirodna glina u Holandiji (kao i u većini zemalja u svetu) ne ispunjava zahtevane uslove vodopropusnosti, pa je primena veštački uspostavljene geološke barijere obavezna. Holandski propisi ne navode eksplicitno koji se materijali moraju koristiti, ali su predložene njihove karakteristike i način izgradnje. Bilo koji materijal koji se koristi mora biti ispitan i prihvaćen od nadležne institucije. Takođe, važno je projektom deponije utvrditi i verifikovati životni vek barijere, od koga zavisi visina takse koja se plaća pri izgradnji deponije. Bolje i dugovečnije barijere uslovljavaju manje troškove taksi, a slabije, sa manjim životnim vekom znatno više.

U Nemačkoj se predlaže da glavna komponenta za oblaganje dna deponija opasnog i neopasnog otpada bude kompozitna obloga [58]. Propisi i njihova tumačenja zahtevaju upotrebu geološke barijere i sistema obloga. Ukoliko geološka barijera na osnovu svojih prirodnih karakteristika ne ispunjava navedene, minimalne evropske zahteve za K i d, takva barijera može biti izrađena, završena ili ojačana putem tehničkih mera. U tom slučaju debljina barijere može biti minimalno 0,5 m, pružajući ekvivalentnu zaštitu. Osnovni sistem obloga sastoji se od mineralne komponente, zaštitnog sloja i mineralnog drenažnog sloja. Mineralna komponenta može biti sačinjen od više slojeva, plastičnog zaptivnog sloja (ili asfaltne membrane) čija debljina ne sme biti manja od 2,5 mm i mineralne komponente minimalne debljine 0,5 m sa $K \leq 5\times10^{-10}$ m/s, na gradijentu pritiska od i = 30. Debljina drenažnog sloja je 0,5 m. Pre izgradnje deponije, neophodno je dokazati svojstva odabranog materijala ili posedovati sertifikat koji izdaje Savezni institut za istraživanja i ispitivanja materijala. Sertifikat je priznat na nivou Savezne Republike Nemačke. Mora biti pokazano da će odabrani sistem obloga u periodu od 100 godina biti stabilan, odnosno da ne podleže spoljnim uticajima i interakcijama. U suprotnom, najmanje 30 godina bi trebalo sprovoditi merenja i ispitivanja provodnosti barijera [59].

Tekst važeće Uredbe u Srbiji u odnosu na Direktivu sadrži neodgovarajuće formulacije (ili prevode), što je otvorilo mogućnosti za različita tumačenja pri projektovanju vodonepropusnih slojeva deponija u praksi. Uredba (Prilog 2 pod 1, odeljak 2) propisuje: “Kada prirodna geološka barijera ne zadovoljava propisane vrednosti, ona se obezbeđuje oblaganjem deponijskog dna sintetičkim materijalima ili prirodnim mineralnim tamponom koji mora biti tako konsolidovan da se dobije ekvivalentna vrednost dna u smislu njegovih vodopropusnih

svojstava. Prirodni mineralni tampon ne sme biti manji od 0,5 m". Takođe, Uredba zahteva da veštačka zaptivna obloga bude folija, ali propisuje i da se za zaptivanje mogu koristiti i druge metode i tehnike. Tekst Direktive je u detaljima drugačiji i propisuje (*Annex* I, 3.2.): „Tamo gde geološka barijera prirodno ne može da zadovolji propisane uslove, može biti veštački završena i ojačana drugim sredstvima dajući ekvivalentnu zaštitu. Veštački uspostavljena geološka barijera ne sme biti manja od 0,5 m". Drugačija formulacija veštački uspostavljene geološke barijere u Uredbi, dovodi u pitanje da li se oblaganjem deponijskog dna sintetičkim materijalima ili prirodnim mineralnim tamponom može obezbediti propisana vrednost koeficijenta vodopropusnosti. Postavlja se pitanje da li veštački uspostavljena geološka barijera može biti npr. prirodni mineralni tampon pri debljini od 0,5 m kako Uredba dozvoljava. Skreće se pažnja na propise i tumačenja u pojedinim evropskim zemljama [21,44] koji to eksplicitno zabranjuju. Postavlja se tehnološko pitanje, da li pri navedenoj debljini prirodni mineralni tampon (najčešće glina) može obezbediti zahtevanu vodonepropusnost K (za ispucale gline od 5×10^{-2} do 5×10^{-7} m/s i neispucale gline, $k < 5\times10^{-7}$ m/s [28]). Pojedini autori smatraju da se geološka barijera veštački može ojačati materijalima sa drugih lokacija, dovoženjem dodatnog sloja gline, dajući jednaku zaštitu [60]. Uredba, takođe, ograničava mogućnost upotrebe drugih materijala kao veštačka zaptivne obloge, jer specificira da je to ista folija.

Ključni problem na koji se ukazuje je korišćenje termina „prirodni mineralni tampon" u Uredbi na mestu izvornog termina „veštački uspostavljena geološka barijera" iz Direktive. Napred citirani tekst Uredbe ne postoji u Direktivi, ne zna se kako je nastao, stručno je sporan, za njega nema zvaničnih tumačenja, te sveukupno izaziva nedoumice.

Za razliku od Direktive, koje daje preporuke za prekrivku deponije, Uredba je odlučila da za prekrivku propiše zahteve čiji je uporedni prikaz dat u tabeli 1. Podseća se da Uredba može biti tehnički zahtevnija od Direktive, ali mora ispuniti minimum zahteva iz nje. U skladu sa tim, skreće se pažnja i da Uredba zahteva manju debljinu sloja za rekultivaciju, definiše debljinu nepropusnog mineralnog sloja i drenažnog sloja za gas kod deponija neopasnog otpada, dok drenažni sloj za vodu nije naveden.

ANALIZA MOGUĆIH REŠENJA ZA OBEZBEĐIVANJE VODONEPROPUSNOSTI

Projektovanje modernih deponija trebalo bi da se zasniva na upotrebi dugovečne geološke barijere. Budući da u propisima nije navedeno koji materijali se imaju upotrebiti za izgradnju vodonepropusnog sloja, različiti pristupi projektovanju obloge i prekrivke deponija svode se na njihov izbor. Za izradu obloge/barijere deponija koriste se prirodni i/ili veštački materijali. U praksi se često, sa ciljem poboljšanja svojstava, kombinuju prirodni i sintetički materijali, u slojevima ili kao višeslojni „gotovi proizvod" (kompoziti, geosintetičke glinene obloge, itd.).

Materijali koji se koriste za izradu barijera moraju da zadovolje niz propisanih kriterijuma među kojima je najvažnija vodopropusnost, dugoročna kompatibilnost sa hemikalijama, visok kapacitet sorpcije i nizak koeficijent difuzije [61]. Takođe, moraju imati visoku otpornost na oštećenja i deformacije tokom izgradnje i eksploatacije, jednostavnu konstrukciju i nisku cenu.

Prirodni materijali

Prirodni materijali koji se upotrebljavaju imaju sposobnost bubrenja i sprečavanja prodiranja tečnosti. Najčešće korišćen prirodni materijal za izradu vodonepropusnih slojeva deponija je glina. Sabijena glina sastavljena je od prirodnih mineralnih materijala iskopanih na lokaciji deponije ili je dovežena sa drugih lokacija. Sloj sabijene gline je poslednjih 15–20 godina korišćen kao podloga za geomembrane, deo dvoslojne ili kompozitne obloge. U pojedinim zemljama dozvoljeno je korišćenje gline ako ispunjava propisane vrednosti vodopropusnosti. Pored gline mogu se upotrebljavati pesak, šljunak, bentonit, kamena prašina, itd. [62,63].

Tabela 1. Uporedni prikaz Uredbe i Direktive pri izgradnji prekrivke
Table 1. Comparative review of Regulation and Directive in the construction of cover layer

Komponente za sloj prekrivke	Opasan otpad		Neopasan otpad	
	Uredba	Direktiva	Uredba	Direktiva
Sloj za drenažu deponijskog gasa	Ne zahteva se	Ne zahteva se	Zahteva se, $d \geq 0{,}3$ m	Zahteva se
Veštačka vodonepropusna obloga-folija	Zahteva se	Zahteva se	Ne zahteva se	Ne zahteva se
Nepropusni mineralni sloj	Zahteva se, $d \geq 0{,}5$ m	Zahteva se	Zahteva se, $d \geq 0{,}5$ m	Zahteva se
Drenažni sloj	Nije naveden	Zahteva se, $d > 0{,}5$ m	Nije naveden	Zahteva se, $d > 0{,}5$ m
Sloj za rekultivaciju	Zahteva se, $d \geq 0{,}5$ m	Zahteva se, $d > 1$ m	Zahteva se, $d \geq 0{,}5$ m	Zahteva se, $d > 1$ m

Primena samo gline kao vodonepropusnog sloja ima izvesna ograničenja. Usled različitog sleganja sabijenog sloja otpada, kao i vremenskih uslova, dolazi do fizičkog oštećenja gline. Formiranjem pukotina (slika 7) nakon samo par godina glina gubi svojstvo vodonepropusnosti, odnosno gubi zaštitni efekat [21]. Takođe, hemijska reakcija procednih voda sa glinom vremenom povećava vodopropusnost gline [64].

Slika 7. Ispucala glina.
Figure 7. Cracked clay.

Pored navedenih ograničenja, trebalo bi uzeti u obzir da je propisana debljina prirodne barijere za deponijsko dno u rasponu od 1–5 m, što može imati uticaj sa aspekta kapaciteta i troškova budućeg deponovanja. U praksi se često koristi kombinacija različitih vrsta glina, takozvana multimineralna barijera [24]. Ranije se smatralo da 0,5 m gline može zameniti geomembranu, međutim takvo rešenje je odbačeno jer nema dugoročni efekat.

Jednostavni materijali na bazi bentonita i veštačkih materijala

Kao prirodni materijal, u praksi se veoma često se koristi bentonit koji sadrži glineni mineral, monmorilonit [24]. Primenom tzv. bentonitnih tepiha, ili u literaturi poznatijim pod nazivom „geosintetičke glinene obloge“ – GCL u praksi su prevazilažena ograničenja gline [23,65].

GCL je kompozitna obloga sačinjena od sloja natrijum- ili kalcijum-bentonita u kombinaciji sa slojem ili slojevima nekog od geosintetičkih materijala [23,66,67]. U prirodi se nalazi uglavnom nalazi Ca bentonit, ali češće se upotrebljava Na bentonit zbog svojstva bubrenja, niske vodopropusnosti i ojačanja deponija [68,69].

Kao sintetički materijali koriste se geotekstili, geomreže, georešetke ili geomembrane.

Geotekstili mogu biti tkani ili netkani, sačinjeni od polipropilena, poliestera, poliamida, itd. Geomreže su sačinjene od istih materijala kao i geotekstil, češće se koriste za obezbeđivanje sigurnosti nestabilnih padina. Geomembrane se mogu koristiti same ili u kombinaciji sa drugim materijalima kada nastaju kompozitni materijali. Postoje različite vrste geomembrana: polivinilhlorid (PVC), polipropilen (PP), polivinilhlorid (PVC), polietilen visoke gustine (HDPE), bitumenske membrane, itd.

Giroud je vršio poređenje efikasnosti CCL-a i GCL-a koje se koriste sa geomembranama za formiranje kompozitnog sloja [70]. Rowe je u svom radu opisao trajnost, najčešće korišćene HDPE geomembrane [71], jer funkcionalnost deponije veoma zavisi od trajnosti geomembrane [72]. Vodopropusnost i unutrašnja erozija u zavisnosti su od podloge na koju se postavlja GCL [66]. Kada glina nije dostupna na samoj lokaciji predviđenoj za izgradnju deponije, upotreba geomembrane je ekonomičnija i povoljnija za održavanje.

Na tržištu postoje različite vrste materijala, uglavnom sačinjenih od kombinacije natrijum-bentonita i polipropilenskog geotekstila različitih oblika, povezanih na različite načine. Vezivanje bentonita i geosintetičkih materijala obavlja se lepljenjem, zašivanjem iglama ili „lepljenjem sa prošivanjem“ [21]. Veoma je važno pažljivo i pravilno spajanje materijala, jer postoji mogućnost oštećenja prilikom postavljanja i spajanja geomembrana čime se gubi svojstvo vodonepropusnosti.

Mane geosintetičkih obloga upravo jesu kompleksan proces instalacije, oštećenja u spojevima materijala, gubitak mehaničke stabilnosti usled bubrenja bentonita i klizanja slojeva u bentonitnom tepihu i pojave unutrašnje erozije [73]. Takođe, ograničenja i nedostaci postoje i usled različitih vremenskih uslova (na primer sušenje), stabilnosti kosina, propustljivosti gasa i prodiranje korova kroz sloj [74]. S obzirom na to da je neophodno obezbediti dugoročnu stabilnost i efikasnost [21], navedeni nedostaci prethodno pomenutih obloga ograničavaju njihovu primenu.

Danas postoji mnogo mogućnosti za obezbeđenje vodonepropusnosti primenom tradicionalnih ili inovativnih barijera. Upotreba reaktivnih barijera, modifikovanih glina (dodatak zeolita u monmorilonit) kojom se smanjuje vodopropusnost [74]. Jonska razmena ili adsorpcija se može poboljšati dodatkom aditiva u barijeru, npr. dodatkom zeolita u bentonit, organski modifikovana glina ima povećanu adsorpcionu moć organskih jedinjenja [75].

Složeni materijali na bazi bentonita

Složeni, tzv. kompozitni materijali daju najbolje rezultate u dugoročnoj zaštiti životne sredine. Kroz mnoga ispitivanja uočena je njihova visoka i dugoročna efikasnost [73]. Ispitivana je i reaktivnost organskih zagađujućih materija sa kompozitnim oblogama [26], kao i migracija zagađujućih materija kroz višeslojnu mineralnu barijeru [67].

GCL obloge se mogu ojačati dodatkom polimera. Pojedini autori smatraju da upotreba polimera, radi poboljšanja kvaliteta obloge, ne bi trebalo da se istražuje, jer je u praksi teško dokazati dugoročnu provodljivost [65]. EPA daje smernice za upotrebu GCL i

smatra da ne bi trebalo podsticati primenu polimera [48]. Međutim, novija istraživanja su dokazala upotrebu polimera kao veoma efikasno rešenje [77].

Jedno od rešenja za izgradnju vodonepropusnog sloja je veštačka mineralna barijera sačinjena od mešavine bentonita i peska ojačane sa polimerom (eng. *Polymer Enhanced Bentonite–Sand Mixture, PEBSM*). Komercijalni naziv ove mešavine, koja je razvijena i patentom zaštićena od strane GID Milieutechniek, je TRISOPLAST® [78].

Ova veštačka mineralna barijera, odlikuje se mnogobrojnim prednostima u odnosu na tradicionalne materijale. U poređenju sa zahtevima iz Direktive, u pogledu vodopropusnosti i debljine geološke barijere, PEBSM ima karakteristike koje nadmašuju propisane vrednosti. Pored izrazito niske vrednosti koeficijenta vodopropusnosti (1×10^{-12} m/s < K < 5×10^{-11} m/s), karakterišu ga visoka mehanička, termička i hemijska stabilnost [74]. U poređenju sa glinom on sprečava pojavu rupa i pukotina jer ima svojstvo samoobnavljanja i veoma je otporan na cikluse suvo/vlažno [28]. Takođe, prisustvo polimera ne predstavlja nikakav rizik za upotrebu PEBSM, jer je prema istraživanjima nerazgradiv čak i pod ekstremnim mikrobiološkim uslovima.

PEBSM je ekološki povoljan materijal. Komponente od kojih je sačinjen su uglavnom prirodne sirovine: pesak (oko 87 %), bentonit (oko 13 %) i vezivni polimer (samo 2 % od iznosa bentonita). Proizvodi se na licu mesta, prema utvrđenom brzom, lakom i pouzdanom načinu. Proizvodnja Trisoplasta se sprovodi prema tačno definisanim standardima obezbeđenja kvaliteta, kompletne kontrole od strane nezavisne, akreditovane laboratorije standardom ISO 17025.

Ugradnjom PEBSM upija vodu iz okoline sa kojom dođe u kontakt. Bentonitna glina tako nabubrava i stvara nepropusnu mrežu hemijskih veza čime sa rastopljenim polimerom nastaje gusta, umrežena gel struktura, sa peskom dispergovanim u njoj. Pesak osigurava mehaničku čvrstoću, a gel betonit – polimer mu pruža neophodnu elastičnost i vodonepropusnost koja je čak 100 do 1000 puta veća nego kod drugih tradicionalnih mineralnih barijera. Visok ugao unutrašnjeg trenja sa izrazitom kohezijom omogućava primenu PEBSM na strmim kosinama bez dodatne stabilizacije. Mehaničke osobine prilikom sabijanja neznatno su promenjene [79]. Zahvaljujući stvaranju gel strukture, u mnogim evropskim zemljama je dokazano da sloj Trisoplasta debljine od 0,07–0,09 m, nanesen na podlogu, može zameniti 1–5 m obloge od gline, čime omogućava i uštedu prostora za odlaganje (slika 8) [80].

Trisoplast se može primenjivati kako za oblaganje dna, tako i za prekrivanje deponija, za izgradnju puteva, skladišta uglja, remedijaciju zemljišta i uređenje terena [81,82]. Primenom Trisoplasta, troškovi održavanja deponija nakon zatvaranja se značajno umanjuju [77]. Jedna od najvažnijih svojstava Trisoplasta je dug životni vek, preko 100 godina, bez promenjenih svojstava [83,84]. Moguće je da početni troškovi izgradnje deponije prilikom upotrebe Trisoplasta budu nešto veći u odnosu na alternativne proizvode, ali nakon zatvaranja, troškovi održavanja su manji, jer funkcionalnost Trisoplast obloge produžava životni vek deponije [84]. Trisoplast ima ekonomske prednosti na lokacijama gde je pesak pristupačan po niskim cenama.

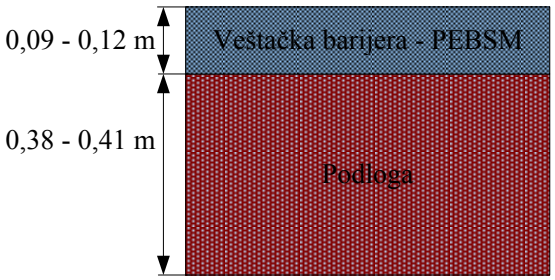

Slika 8. Poprečni presek veštački uspostavljene PEBSM barijere.
Figure 8. Cross-section of artificial established PEBSM barrier.

ZAKLJUČAK

U radu je izvršena detaljna analiza pojedinih propisa u pogledu obezbeđivanja vodonepropusnosti prilikom projektovanja deponija. Poređenjem propisa konstatovano je da važeći nacionalni propis – Uredba – nije usaglašen sa Direktivom. Ocenjuje se da je neophodno izmeniti tekst Uredbe u Prilogu 2 pod 1, odeljak 2, iza definicije koeficijenta vodopropusnosti. Predlaže se da se tekst: „Kada prirodna geološka barijera ne zadovoljava propisane vrednosti, ona se obezbeđuje oblaganjem deponijskog dna sintetičkim materijalima ili prirodnim mineralnim tamponom koji mora biti tako konsolidovan da se dobije ekvivalentna vrednost dna u smislu njegovih vodopropusnih svojstava. Prirodni mineralni tampon ne sme biti manji od 0,5 m“ zameni sa „Tamo gde geološka barijera prirodno ne može da zadovolji propisane uslove, može biti veštački završena i ojačana drugim sredstvima dajući ekvivalentnu zaštitu. Veštački uspostavljena geološka barijera ne sme biti manja od 0,5 m“. Takođe, termin „prirodni mineralni tampon“ bi trebalo zameniti izvornim terminom „veštački uspostavljena geološka barijera“.

Ukazuje se da se geološka barijera ne može ojačati isključivo pomoću sintetičke obloge, odnosno HDPE folije, koja se obično koristi kao veštačka zaptivna obloga. HDPE folija ne može biti upotrebljena kao veštački uspostavljena geološka barijera i nije obavezno da se isključivo folija koristi kao veštačka zaptivna obloga, što Uredba zahteva.

Pri projektovanju deponija u RS neophodno je da projektant proračunom dokaže karakteristike upotrebljenih materijala u smislu vodopropusnosti, a da se u

procesu tehničke kontrole valjanost ovih proračuna provere i potvrde [85]. Odgovarajuća praksa izrade tehničke dokumentacije ukazuje da: a) projektima deponija često nedostaje tehnološki projekat sa odgovarajućim proračunima i b) da pomenutih proračuna nema, odnosno da se materijali za obezbeđenje vodonepropusnosti biraju bez odgovarajućih valjanih, proverljivih podloga, što je neprihvatljivo.

Kroz poređenje životnog ciklusa materijala, može se konstatovati da nedostaci CCL-a i GCL-a, smanjuju njihov životni vek, dok najduži životni vek i najniži koeficijent vodopropusnosti ima PEBSM. CCL, nakon veoma kratkog vremena usled gubitka vlage puca, čime gubi svojstvo vodonepropusnosti. Tokom instalacije GCL-a najčešći problem je u spojevima bentonita i sintetičkog materijala, česta mehanička oštećenja dovode do smanjenja životnog ciklusa materijala. Navedene karakteristike PEBSM nemoguće je postići alternativnim mineralnim, konkurentskim proizvodima (tabela 2).

Tabela 2. Poređenje alternativnih materijala
Table 2. Comparison of alternative materials

Svojstvo	Veštačka barijera – PEBSM		Veštačka barijera – GCL	Geološka barijera – CCL		
Debljina barijere, d / m	0,007	0,009	0,01	1,00	1,00	5,00
Koeficijent vodopropusnosti, $K\times10^9$ / m s^{-1}	0,03	0,03	0,03	100	1	1

Veštački uspostavljena geološka barijera sastavljena od 0,09 m PEBSM i 0,41 m prirodnog materijala može u potpunosti obezbediti vodonepropusnost i zameniti 1–5 m obloge od gline.

PEBSM predstavlja ekološki povoljan materijal, jer je najvećim delom sastavljen od prirodnih sirovina. Mehanički, hemijski i termički je stabilan materijal i jedini je otporan na cikluse suvo/vlažno. Dug životni vek PEBSM, bez promenjenih svojstava, značajno umanjuje troškove održavnja deponija nakon zatvaranja.

Zahvalnica

Istraživanja u ovom radu izvršena su u okviru aktivnosti na projektu TR 34009 koji finansira Ministarstvo prosvete, nauke i tehnološkog razvoja Republike Srbije.

LITERATURA

[1] M. Savić, M. Jovanović, J. Tanasijević, O. Ocić, A. Spasić, P. Jovanić, I. Nikolić, Primena algoritma za redukovanje otpada u analizi uticaja na životnu sredinu: primer proizvodnje bitumena, Hem. Ind. **65**(2) (2011) 197–204.

[2] D. Stanojević, M. Rajković, D. Tošković, Upravljanje korišćenim gumama, dometi u svetu i stanje u Srbiji, Hem. Ind. **65**(6) (2011) 727–738.

[3] A. Mitovski, D. Živković, LJ. Balanović, N. Štrbac, Ž. Živković, Analiza životnog ciklusa bezolovnih lemnih legura sa aspekata zaštite životne sredine, Hem. Ind. **63**(3) (2009) 163–169.

[4] H. Stevanović-Čarapina, J. Stepanov, D. Savić, A. Mihajlov, Emisija toksičnih komponenti kao faktor izbora najbolje opcije za upravljanje otpadom primenom koncepta ocenjivanja životnog ciklusa, Hem. Ind. **65**(2) (2011) 205–209.

[5] M. Rajković, Klasifikacija fosfogipsa kao otpadnog proizvoda sa aspekta životne sredine, Hem. Ind. **58**(1) (2004) 26–32.

[6] M. Životić, D. Stojiljković, Al. Jovović, V. Čudić, Mogućnost korišćenja pepela i šljake sa deponije termoelektrane „Nikola Tesla“ kao otpada sa upotrebnom vrednošću, Hem. Ind. **66**(3) (2012) 403–412.

[7] Š. Tisovski, V. Valent, Recilovanje poliolefinskog otpada kao energenta, Hem. ind. **62**(6) (2008) 361–364.

[8] A. Kostić-Pulek, S. Marinković, S. Popov, J. Đinović, Investigation of the possibility of the reutilization of some industrial wastes, J. Serb. Chem. Soc. **70**(6) (2005) 843–851.

[9] A. Milutinović-Nikolić, J. Dostanić, P. Banković, N. Jović-Jovičić, S. Lukić, B. Rosić, D. Jovanović, A new type of bentonite-based non-woven composite, J. Serb. Chem. Soc. **76**(10) (2011) 1411–1425.

[10] M.Đ. Ristić, M.D. Marjanović, Concentrations of Cu, Zn, Cd and Pb in urban soils in parks and green areas of Belgrade, Serbia, CI&CEQ **12**(4) (2006) 236–240.

[11] M. Marjanović, M. Vukčević, D. Antonović, S. Dimitrijević, Đ. Jovanović, M. Matavulj, M. Ristić, Heavy metals concentration in soils from parks and green areas in Belgrade, J. Serb. Chem. Soc. **74**(6) (2009) 697–706.

[12] N. Ćalić, M. Ristić, Ispitivanje karakteristika procednih voda deponije “Vinča” metodom izluživanja, Hem. Ind. **60**(7–8) (2006) 171–175.

[13] N. Dixon, K. Zamara, D.R.V. Jones and G. Fowmes, Waste/Lining System Interaction: Implications for Landfill Design and Performance, Geotech. Eng. J. SEAGS AGSSEA **43**(3) (2012), ISSN 0046-5828.

[14] D.R.V. Jones, N. Dixon, Landfill lining stability and integrity: the role of waste settlement, Geotext. Geomembr. **23** (2005) 27–53.

[15] N. Dixon, D. Russell, V. Jones, Engineering properties of municipal solid waste, Geotext. Geomembr. **23** (2005) 205–233.

[16] A. Damgaard, S. Manfredi, H. Merrild, S. Stensøe, TH. Christensen, LCA and economic evaluation of landfill leachate and gas technologies, Waste Manage. **31** (2011) 1532–1541.

[17] P.V. Divya, B.V.S. Viswanadham, J.P. Gourc, Influence of geomembrane on the deformation behaviour of clay-based landfill covers, Geotext. Geomembr. **34** (2012) 158–171.

[18] Council Directive 1999/31/EC of 26 April 1999 on the landfill of waste (OJ L 182, 16.7.1999, p. 1–19).

[19] Uredba o odlaganju otpada na deponije, („Sl. glasnik RS“, broj 92/2010).

[20] T. Katsumi, C.H. Benson, G.J. Foose, M. Kamon, Performance – based design of landfill liners, Eng. Geol. **60** (2001) 139–148.

[21] G. Heerten, R. Koerner, Cover systems for landfills and brownfields, Land Contam. Reclam. **16**(4) (2008) 343––356.

[22] P.J. Fox, D.J. De Battista, D.G. Mast, Hydraulic performance of geosynthetic clay liners under gravel cover soils, Geotext. Geomembr. **18** (2000) 179–201.

[23] A. Bouazza, Geosynthetic clay liners, review article, Geotext. Geomembr. **20** (2002) 3–17.

[24] D. Koch, Bentonites as a basic material for technical base liners and site encapsulation cut-off walls, Appl. Clay Sci. **21** (2002) 1–11.

[25] A. Bouazza, W. F. Van Impe, Liner design for waste disposal sites, Environ. Geol. **35**(1) (1998) 41–45.

[26] U. Kalbe, W.W. Müller, W. Berger, Jürgen Eckardt, Transport of organic contaminants within composite liner systems, Appl. Clay Sci. **21** (2002) 67–76.

[27] J.P. Giroud, K. Badu-Tweneboah, K.L. Soderman, Comparison of Leachate Flow Through Compacted Clay Liners and Geosynthetic Clay Liners in Landfill Liner Systems, Geosynthetics International **4**(3–4) (1997) 391–431.

[28] S. Melchior, Wechselwirkungen zwischen mineralischen Komponenten von Oberflächenabdichtungssystemen, 28. Fachtagung „Die sichere Deponie 2012 - Sicherung von Deponien und Altlasten mit Kunststoffen“ SKZ - ConSem GmbH, Würzburg und AK GWS Arbeitskreis Grundwasserschutz e. V., Berlin.

[29] D. Guyonnet, D. Cazaux, H. Vigier-Gailhanou, B. Chevrier, M. Gamet, TRISOLIX: compatibility testing of TRISOPLAST®, Final Report, 2008, BRGM/RP-56850-FR.

[30] Strategija upravljanja otpadom za period 2010–2019. godine, http://www.ekoplan.gov.rs/src/upload-centar/ /dokumenti/zakoni-i-nacrti-zakona/propisi/strategija_upravljanja_otpadom_konacno.pdf (februar 2012).

[31] U.S. Environmental Protection Agency, Code of Federal Regulations, Title 40, Part 264 Subtitle C, Standards for Owners and Operators of Hazardous Waste Treatment, Storage, and Disposal Facilities, http://www.wbdg.org/ /ccb/EPA/40cfr264.pdf (jun 2012).

[32] [U.S. Environmental Protection Agency, Code of Federal Regulations, Title 40, Part 258 Subtitle D, Criteria for Municipal Solid Waste Landfills, http://www.epa.gov/ /wastes/wyl/tribal/pdftxt/40cfr258.pdf (jun 2012).

[33] U.S. Environmental Protection Agency, Survey of Technologies for Monitoring Containment Liners and Covers, Solid Waste and EPA542-R-04-013 Emergency Response June 2004 (5102G), Washington, DC 20460, http:// //www.epa.gov/tio/download/char/epa542r04013.pdf (jun 2012)

[34] Discussion Document Proposed Modifications to the Solid Waste Management Facility Regulations 310 cmr 19.000, may 24, 2004, http://www.mass.gov/dep/ /recycle/laws/swregbgd.pdf (avgust 2012).

[35] U.S. Environmental Protection Agency Center for Environmental Research Information Office of Research and Development, Requirements for Hazardous Waste Landfill Design, Construction, and Closure, Technology Transfer E PA162514-89lO22, August 1989, http://infohouse.p2ric.org/ref/17/16909.pdf (jul 2012).

[36] Directive 2008/98/EC of the European Parliament and of the Council of 19 November 2008 on waste and repealing certain Directives (Text with EEA relevance) (OJ L 312, 22.11.2008, pp. 3–30).

[37] Directive 2000/76/EC of the European Parliament and of the Council of 4 December 2000 on the incineration of waste (OJ L 332, 28.12.2000, pp. 91–111).

[38] Regulation (EC) No. 1013/2006 of the European Parliament and of the Council of 14 June 2006 on shipments of waste (OJ L 190, 12.7.2006, pp. 1-98).

[39] European Parliament and Council Directive 94/62/EC of 20 December, 1994, on packaging and packaging waste (OJ L 365, 31.12.1994, pp. 10–23).

[40] Directive 2006/66/EC of the European Parliament and of the Council of 6 September, 2006, on batteries and accumulators and waste batteries and accumulators and repealing Directive 91/157/EEC (Text with EEA relevance) (OJ L 266, 26.9.2006, pp. 1–14).

[41] Directive 2002/96/EC of the European Parliament and of the Council of 27 January, 2003, on waste electrical and electronic equipment (WEEE) – Joint declaration of the European Parliament, the Council and the Commission relating to Article 9 (OJ L 37, 13.2.2003, pp. 24–39).

[42] Directive 2008/1/EC of the European Parliament and of the Council of 15 January, 2008, concerning integrated pollution prevention and control (Codified version) (Text with EEA relevance) (OJ L 24, 29.1.2008, pp. 8–29).

[43] Zakon o integrisanom sprečavanju i kontroli zagađivanja životne sredine, „Sl. glasnik RS“, broj 135/2004.

[44] Environment Agency, LFE5 Guidance for the Landfill Sector, Technical Requirements of the Landfill Directive and Integrated Pollution Prevention and Control (IPPC S5.02), April 2007, http://cdn.environment-agency.gov.uk/geho0407bmho-e-e.pdf (jul 2012).

[45] Alterra, Dutch governmentally installed expertise network for soil protection, Wageningen, The Netherlands, 2002.

[46] A. Pivato, Landfill Liner Failure: An Open Question for Landfill Risk Analysis, J. Environ. Prot. **2**(3) (2011) 287––297.

[47] J. Munie, Illinois Environmental Protection Agency, A Study of the merits and effectiveness of anternate liner systems at Illinois landfills, A research paper Submitted in Fulfillment of House Resolution 715 State of Illinois 92nd General Assembly January 2003, http:// //www.epa.state.il.us/land/regulatory-programs/ /permits-and-management/alternate-landfill-liner-study/alternate-landfill-liner-study.pdf (jul 2012).

[48] Environment Agency, LFE5 – Using geomembranes in landfill engineering, http://cdn.environment-agency.gov.uk/geho0409bpnh-e-e.pdf (avgust 2012).

[49] Environment Agency, LFE8 – Geophysical testing of geomembranes used in landfills, http://cdn.environ-

ment-agency.gov.uk/geho0409bpnm-e-e.pdf (avgust 2012).

[50] Environment Agency, LFE10 - Using bentonite enriched soils in landfill engineering, http://cdn.environment--agency.gov.uk/geho0409bpnw-e-e.pdf (avgust 2012).

[51] Environment Agency, Environmental Permitting Regulations (England and Wales) 2010, Regulatory Guidance Series, No LFD 1, Understanding the Landfill Directive, http://www.environment-agency.gov.uk/static/documents/Business/RGN_LFD1_Landfills_(v2.0)_30_March_2010.pdf (avgust 2012).

[52] Environment Agency, LFE6 – Guidance on using landfill cover materials, http://cdn.environment-agency.gov.uk/ /geho0409bpni-e-e.pdf (avgust 2012).

[53] Environment Agency, Guidance on Financial Provision for Landfill http://www.environment-agency.gov.uk/ /static/documents/Business/Guidance_-_financial_provision_for_landfill.pdf (avgust 2012).

[54] Environment Agency, LFE 2 – Cylinder testing geomembranes and their protective materials, A methodology for testing protector geotextiles for their performance in specific site conditions, http://cdn.environment--agency.gov.uk/geho0611btuw-e-e.pdf (avgust 2012).

[55] Environment Agency, LFE4 – Earthworks in landfill engineering, Design, construction and quality assurance of earthworks in landfill, http://cdn.environment-agency.gov.uk/geho0211btlr-e-e.pdf (avgust 2012).

[56] Environment Agency, How to comply with your environmental permit Additional guidance for: Landfill (EPR 5.02), March 2009, http://cdn.environment-agency.gov.uk/geho0409bput-e-e.pdf (avgust 2012).

[57] D. Boels, Quality assurance of liner construction in The Netherlands, Landfill Construction Quality Assurance Seminar, Helsinki, Finland, Oct. 19, 2006 http:// //www.ygoforum.fi/boelstex.pdf (maj 2012).

[58] Technical Committee on Geotechnics of landfill Engineering, German Geotechnical Society, Technical Committee Landfill Technology, Chapter 2.2, Principles of Bottom Barrier Systems, Erwin Gartung, Nürnberg Germany, Hans-Günter Ramke, Höxter, July 2009.

[59] Ordinance Simplifying Landfill Law Of 27 April 2009, Federal Law Gazette I No. 22 of 29 April 2009, p. 900 http://www.bmu.de/files/pdfs/allgemein/application/pdf/ordinance_simplifiying_landfill_law.pdf (jun 2012).

[60] Lj. Obradović, M. Bugarin, Z. Stevanović, M. Ljubojev, Z. Milijić, Odlaganje opasnog otpada na deponije u skladu sa Direktivom Evropske Unije o deponijama br. 1999/31/EU, Rudarski radovi, Broj 2, 2010, str. 123–133.

[61] C.H. Benson, A. Bouazza, E. Fratalocchi, M. Manassero, Traditional and Innovative Barriers Technologies and Materials, TC5 Report, September 2005, http:// //www.ce.utexas.edu/prof/zornberg/pdfs/TR/Shackelford_etal_2005.pdf (jul 2012).

[62] G. Gjetvaj, P. Kvasnička, Ž. Veinović, Diffusion through Pulverized Stone Compared to Other Mineral Barrier Materials, Geologia Croatica **57/16**(3) (2004) 95–101.

[63] Ž. Veinović, Mogućnosti uporabe otpadne kamene prašine za izradu brtvenih slojeva odlagališta, bib.irb.hr/ /datoteka/48629.ZGO_Zlim.doc (maj 2012).

[64] A. Allen, Containment landfills: the myth of sustainability, Eng. Geol. **60** (2001) 3–19.

[65] K. P. Von Maubeuge, C. M. Quirk, Geosynthetic Clay Liners and long-term slope stability, http://www.bentofix.com/naue/p/waste2000_shear.pdf (april 2012).

[66] R. Kerry Rowe, C. Orsini, Effect of GCL and subgrade type on internal erosion in GCLs under high gradients, Geotext. Geomembr. **21** (2003) 1–24.

[67] P. Phillips and M. Eberle, The use of Geosynthetic Clay Liners (GCL's) in containment applications – an Australian perspective, http://www.bentofix.com/naue/ /p/geo_env2001.pdf (april 2012).

[68] D. Guyonnet, P. Perrochet, B. Côme, J.-J. Seguin, A. Parriaux, On the hydro-dispersive equivalence between multi-layered mineral barriers, J. Contam. Hydrol. **51** (2001) 215–231.

[69] J.G. Zornberg, Geosynthetic Reinforcement in Landfill Design: US Perspectives, GSP 141 International Perspectives on Soil Reinforcement Applications, http:// //www.ce.utexas.edu/prof/zornberg/pdfs/CP/Zornberg_2005a.pdf (jun 2012).

[70] J.P. Giroud, N.S. Rad, J.A. McKelvey, Evaluation of the Surface Area of a GCL Hydrated by Leachate Migrating Through Geomembrane Defects, Geosynth. Inter. **4**(3–4) (1997) 433–462.

[71] R. Kerry Rowe, Henri P. Sangam, Durability of HDPE geomembranes, Geotext. Geomembr. **20** (2002) 77-95.

[72] Y. Hsuan, Waste Containment Technology – Lifetime Prediction of The Landfill Liner, www.gatewaycoalition.org/files/NewEH/htmls/Hsuan.doc (maj 2012).

[73] Scottish Environment Protection Agency, Framework for Risk Assessment for Landfill Sites The Geological Barrier, Mineral Layer and the Leachate Sealing and Drainage System August 2002, http://www.sepa.org.uk/ (maj 2012).

[74] Y. Yukselen-Aksoy, Characterization of two natural zeolites for geotechnical and geoenvironmental applications, Appl. Clay Sci. **50** (2010) 130–136.

[75] A. Kaya, S. Durukan, Utilization of bentonite-embedded zeolite as clay liner, Appl. Clay Sci. **25** (2004) 83– 91.

[76] F.-G. Simon, W.W. Müller, Standard and alternative landfill capping design in Germany, Environ. Sci. Policy **7** (2004) 277–290.

[77] J. Wammes, M. Naismith, H. Mulleneers, New developments for environmental protection demonstrated on the polymer enhanced mineral barrier Trisoplast®, Answai conf 2009, http://conference.nswai.com/ /1%29%20J.wammes-TRISOPLAST.pdf (februar 2012).

[78] US2010/0087580 Method of produciong a modified smectite or smectite – containing substance capable of taking up and releasing water in a reversible manner 04-08-2010 (februar 2012).

[79] S.S. Agus, Y. F.Arifin, T. Schanz, Hydro-mechanical characteristic of a polymer-enhanced bentonite-sand mixture for landfill applications, International Workshop "Hydro-Physico-Mechanics of Landfills" LIRIGM, Grenoble 1 University, France, 2005, http://www.gbf.ruhr--uni-bochum.de/forschung/pdf/32_AGUS.PDF (februar 2012).

[80] M. Naismith, J. Wammes, H. Mulleneers, Soil & Groundwater protection by the mineral barrier Trisoplast (Applications and new developments), Remediation Technologies Symposium (RemTech^{TM}, 2001) in Baff, Canada) http://www.esaa-events.com/remtech/2009//pdf/09-Naismith-paper.pdf.pdf (Jun 2012).

[81] D. Đurović, D. Urošević, J. Tanasijević, M. Savić, J. Jovanović, M. Jovanović, A. Spasić, Power plant coal storage design: prevention of water pollution, 43rd International October Conference on Mining and Metallurgy, October, Kladovo, Serbia, 2011, pp. 12–15.

[82] J. Tanasijević, M. Savić, J. Jovanović, M. Jovanović, Improved Technical Solution of Power Plant Coal Storage, International Conference Innovation as a Function of Engineering Development, November, Niš, Serbia, 2011, pp. 25–26.

[83] D. Boels, Comparing performance of Trisoplast with different mineral liner materials, T.C. Christensen, R. Cossu, R. Stegmann (eds.), Barriers, waste mechanics and groundwater pollution; Sardinia 2001, eighth international waste management and landfill symposium; Proceedings, Vol. 3, S.l., Italy, CISA, 2001, pp. 45–54.

[84] D. Boels, S. Melchior, B. Steinert, Are Trisoplast barriers sustainable? An evaluation of old barriers in landfill caps, AlterraReport 541, 2003.

[85] Pravilnik o sadržini i načinu vršenja tehničke kontrole glavnih projekata, „Sl. glasnik RS“, broj 93/2011.

SUMMARY

IMPERMEABLE LAYERS IN LANDFILL DESIGN

Milica Karanac[1], Mića Jovanović[2], Eugène Timmermans[3], Huib Mulleneers[3], Marina Mihajlović[1], Jovan Jovanović[1]

[1]*Innovation Center, Faculty of Technology and Metallurgy, University of Belgrade, Belgrade, Serbia*
[2]*Faculty of Technology and Metallurgy, University of Belgrade, Belgrade, Serbia*
[3]*Trisoplast Mineral Liners International BV, The Netherlands*

(Review paper)

Landfills are complex systems that could potentially contaminate the environment. This needs to be prevented by providing impermeability during the landfill design. In this aim, the related regulations should be followed and adequate materials that provide impermeability should be used. The first part of the paper presents a review of the current regulations, interpretations, and recommendations from the U.S., EU and Republic of Serbia. Knowing that the Serbian regulation should fully follow the related European Directive, some inadequate formulations and terms were observed in the analyses related to the Directive Annex I, 3.2. Request of the Regulation that deals with the bottom of the landfill leakage is formulated differently than in the Directive as well. The mentioned problems enable some design solutions that are not among the best available techniques. In the second part, the paper presents a comparative analysis of possible alternatives in impermeable layer design, both for the bottom and landfill cover. Some materials like clay, CCL, GCL might not be able to satisfy the prescribed requirements. The longest lifetime and the lowest coefficient of permeability, as well as excellent mechanical, chemical and thermal stability, show the mixture of sand, bentonite and polymers (PEBSM).

Keywords: Landfill design • Landfill impermeability • Artificial geological barrier

Desorpcija ^{137}Cs iz mahovine *Homalothecium sericeum* (Hedw.) Schim. slabo kiselim rastvorima

Ana A. Čučulović[1], Dragan S. Veselinović[2]

[1]*INEP – Institut za primenu nuklearne energije, Univerzitet u Beogradu, Zemun, Srbija*
[2]*Fakultet za fizičku hemiju, Univerzitet u Beogradu, Beograd, Srbija*

Izvod

Desorpcija ^{137}Cs iz mahovine *Homalothecium sericeum* (Hedw.) Schim. vršena je korišćenjem pet uzastopnih desorpcija sa pet identičnih zapremina rastvora. Za desorpciju su korišćeni rastvori: H_2SO_4, HNO_3 i njihova smeša, H_2SO_4–HNO_3, pH vrednosti 4,61; 5,15 i 5,75; kao i destilovana voda pH 6,50. Posle pet sukcesivnih desorpcija iz mahovina je od sorbovane kiseline desorbovano od 22,8% (rastvor H_2SO_4–HNO_3 pH 5,75) do 33,2% (rastvor H_2SO_4–HNO_3 pH 4,60) ^{137}Cs, a destilovanom vodom 31,3% ^{137}Cs. Prvom desorpcijom iz mahovine desorbuje se najviše ^{137}Cs, od 9,0 do 17,9%. Srednje vrednosti procenta ukupno desorbovanog ^{137}Cs iz mahovine su slične: za rastvor H_2SO_4 28,8%; HNO_3 25,7% i H_2SO_4–HNO_3 28,6%, što ukazuje da NO_3^- i SO_4^{2-} nemaju uticaj na desorpciju Cs^+. Korišćene pH vrednosti rastvora ne utiču značajno na desorpciju ^{137}Cs iz mahovine. Posle pet sukcesivnih desorpcija iz mahovine ^{137}Cs se ne desorbuje u značajnoj meri. U intervalu pH od 4,61 do 6,50 desorpcione supstance su H_2O i H^+, a manji uticaj imaju SO_4^{2-} i NO_3^-. Postoje dva mesta sorpcije, odnosno dve vrste sorpcije, pri čemu je jedna dominantna.

Ključne reči: *desorpcija ^{137}Cs, Homalothecium sericeum (Hedw.) Schim. mahovina, kisele kiše.*

Dostupno na Internetu sa adrese časopisa: http://www.ache.org.rs/HI/

NAUČNI RAD

UDK 66.081.5:582.32

Hem. Ind. **67** (6) 975–980 (2013)

doi: 10.2298/HEMIND121211014C

U periodu od 1959–1963. godine izvršene su mnoge nuklearne probe čime su bile oslobođene i velike količine raznih radionuklida, među kojima su za živi svet najznačajniji ^{137}Cs, ^{134}Cs i ^{90}Sr, zbog njihovog dugog fizičkog vremena poluraspada ($t_{1/2}$ = 30,2; 2,1 i 28 godina, redom) i biološke aktivnosti u organizmu. Zbog zadovoljavanja energetskih potreba izgrađene su nuklearne elektrane, ali zbog faktora čovek u periodu od 1945. do 1987. godine desilo se 28 akcidenata, od kojih su za zagađenje životne sredine radionuklidima najznačajniji: Kištim (1957.), Vindskejl (1957.), Ostrvo Tri milje (1979.) i Černobilj (1986.). Akcidentom u Černobilju, na području bivše Jugoslavije je deponovano 2,4% od ukupno ispuštenih radionuklida (bez inertnih gasova), odnosno oko 5% ^{131}I i oko 10% ^{137}Cs. ^{137}Cs je hemijski i biohemijski homolog kalijuma i u organizmu prati njegov metabolizam. Od dužine zadržavanja ^{137}Cs u organizmu zavisi i telesno oštećenje organizma koje je zagađeno ovim radionuklidom [1–6].

Mahovine su veoma stara i primitivna grupa organizama, koja se odlikuje posebnom građom i specifičnom ekologijom u odnosu na više biljke. Nemaju razvijene biljne organe u pravom smislu reči: cela biljka (talus) se sastoji od rizoida koga čine pojedinačne ćelije, stabalce i listići, nemaju kutikulu, ni stome kojima bi regulisale transpiraciju i lako upijaju zagađujuće supstance iz svoje okoline (radionuklide, teške metale, pesticide...). Usvajanje, odnosno, sadržaj zagađujućih supstanci u talusu mahovina je posledica unutrašnjih i spoljašnjih činilaca. Glavni sadržaj fisionih radionuklida je u gornjim, zelenim, delovima biljke i procenjuje se da je akumulacija radionuklida proporcionalna unosu [7].

Mahovine su pioniri vegetacije i značajni organizmi jer naseljavaju nepristupačne predele, stvaraju humus, sedru i treset, smanjuju eroziju duž reka i potoka, regulišu vlažnost u ekosistemima i omogućavaju naseljavane ostalih biljaka. Buseni mahovina su miniekosistemi i staništa sitnim beskičmenjacima i nekim bakterijama. Mahovine imaju veliku upotrebnu vrednost: koriste se u medicini, farmaciji i veterini, neke vrste služe za prehranu i ishranu divljači u zimskim mesecima, a upotrebljavaju se kao đubrivo za određene tipove hortikulture.

Mahovine su dobri bioindikatori (imaju sposobnost da ukažu na prisustvo zagađujućih supstanci iz sredine u kojoj se nalaze) i biomonitori (daju kvantitativnu informaciju o nivoima zagađenja i ukazuju na promene sa vremenom) zagađenja životne sredine. Pomoću mahovina se mogu prikupiti verodostojne informacije o prostornoj i vremenskoj podeli i trendovima zagađenja vazduha i okoline zagađujućim supstancama, na pr. radionuklidima, posebno u uslovima nuklearne nesreće i nekontrolisane emisije fisionih produkata [8–20].

Atmosferske padavine dolaze do mahovina suvim ili vlažnim padavinama. Kisele kiše se obrazuju kako od SO_2, tako i od NO_2, koji H_2SO_4 i HNO_3 grade nakon oksidacije u toku atmosferskog prenosa [1]. Ako mahovina

Prepiska: A.A. Čučulović, INEP – Institut za primenu nuklearne energije, Univerzitet u Beogradu, Banatska 31b, 11080 Zemun, Srbija.
E-pošta: anas@inep.co.rs
Rad primljen: 11. decembar, 2012
Rad prihvaćen: 4. februar, 2013

sorbuje određenu supstancu (na pr. ^{137}Cs), ona postaje njome zagađena, a kada se mahovina unese u vodu ili se povremeno obliva kišom ili drugim rastvorima, koja ne sadrže supstancu koja je sorbovana u mahovini, ta supstanca podleže desorpciji iz mahovine. Navedenim procesom dolazi do prenosa supstance iz čvrste faze u tečnu, odnosno, ako se radi o zagađujućoj supstanci, dolazi do njenog prenosa u tečnu fazu. Ovo je osnovni proces koji se dešava kada se mahovina, unese u vodu ili ako biva oblivana kišom. U prvom slučaju radi se o sistemu sa jednokratnom desorpcijom, a u drugom, kada se imitira povremeno padanje kiše, radi se o sistemu koji radi na principu sukcesivnih desorpcija. S obzirom na to da od sastava kiše, tj. kiselosti kiše kao desorpcionog rastvora, zavisi količina desorbovane supstance, to će i prenos zagađujuće supstance desorbovane sa kišom dovesti do prenosa i širenja zagađenja u većoj ili manjoj meri u okolinu [21].

Mahovine kao objekat bioindikacije su znatno manje korišćene od lišajeva, možda zbog toga što ima znatno više vrsta epifitskih lišajeva koji su pogodni za biomonitoring zagađenosti životne sredine.

U našim prethodnim radovima praćena je desorpcija ^{137}Cs iz lišaja *Cetraria islandica* kiselim rastvorima različitih pH vrednosti od 2,00 do 5,75 [21–26]. Znajući da su kisele kiše padavine pH vrednosti manje od 5,60 i da ne postoje podaci o desorpciji ^{137}Cs iz mahovine *Homalothecium sericeum* rastvorima koji imaju sastav sličan sastavu kiselih kiša, u ovom radu je ispitivana desorpcija ^{137}Cs iz mahovine *H. sericeum* rastvorima pH vrednosti 4,61; 5,15 i 5,75. S obzirom na to da Cs pripada grupi alkalnih metala, to je od interesa razmatranje uticaja H^+, na njegovu desorpciju, bez jednovremenog delovanja i drugih katjona, što je cilj ovog rada.

EKSPERIMENTALNI DEO

U radu su korišćene hemikalije: H_2SO_4 p.a., Merck (Nemačka), HNO_3 p.a., Alkaloid (Skoplje, Makedonija). Destilovana voda (D), pH vrednosti 6,50.

Za merenje pH vrednosti rastvora korišteni su pH metar Iskra MA 5730 i puferski rastvori, pH 4,00 i 7,00, Carlo Erba (Italija).

Rastvori A i B su napravljeni tako što je u 200 mL destilovane vode dodavana koncentrovana H_2SO_4, odnosno HNO_3 dok nije postignuta pH vrednost 4,61; 5,15 i 5,75 (rastvori H_2SO_4: A_1, A_2 i A_3, i HNO_3: B_1, B_2 i B_3). Rastvor C je dobijen mešanjem 100 mL rastvora A i 100 mL rastvora B (rastvori C_1, C_2 i C_3).

Masa je merena na analitičkoj vagi Mettler (osetljivosti 0,1 mg).

Korišćen je standardni filter papir, Merck (Nemačka) za filtraciju rastvora koji su dobijeni desorpcijom mahovine rastvorom A, B, C ili destilovanom vodom (D).

Uzorci mahovine *Homalothecium sericeum* (Hedw.) Schimp., sakupljeni su u Crnoj Gori (Andrijevica) 2002. godine i čuvani u papirnim vrećama. Osušeni, očišćeni od nečistoća koje su vizuelno mogle da se uoče i mehanički usitnjeni uzorci mahovina su odmeravani na analitičkoj vagi, u količini od 10 g i stavljeni u plastične posude prečnika 7,5 cm i zapremine 150 cm^3. U tako pripremljenim uzorcima meren je nivo aktivnosti ^{137}Cs. Prilikom rada nije bilo razaranja biljnog materijala.

U eksperimentu je 10 g suve mase mahovine, nakon merenja aktivnosti, preliveno sa 200 mL destilovane vode (D) ili rastvorima koji imitiraju sastav kisele kiše: A – H_2SO_4; B – HNO_3 i C – H_2SO_4–HNO_3 (smeša, 1:1), a zatim je ostavljeno da stoji radi uravnotežavanja 24 časa.

Desorpcije su vršene na sobnoj temperaturi (22 °C) u trajanju od 24 časa uz povremeno mešanje. Posle svake desorpcije, od ukupno 5, nakon filtracije, uzorci mahovina su sušeni na sobnoj temperaturi u otvorenoj posudi do konstantne mase. Izmerene su aktivnosti uzoraka, a i aktivnosti dobijenih rastvora posle desorpcije. Zatim su sa po 200 mL rastvora vršene naredne sukcesivne desorpcije, ponavljajući postupak filtracije i sušenja. Urađeno je po pet sukcesivnih desorpcija. Sve serije ponovljene su 2 puta.

Za određivanje aktivnosti u uzorcima mahovina korišćena je gamaspektrometrijska metoda. Uzorci su mereni na gamaspektrometru sa HPGe detektorom, proizvođača Ortec-Ametek sa 8192 kanala, rezolucije 1,65 keV i efikasnosti 34% na 1,33 MeV ^{60}Co sa greškom merenja ispod 5,0%. Za obradu spektara korišćen je softver Gamma Vision-32 [27]. Pre merenja izvršene su energetska kalibracija i kalibracija efikasnosti spektrometra pomoću kalibracionog izvora koji sadrži smešu radionuklida poznatih aktivnosti. Nivo aktivnosti ^{137}Cs meren je u uzorcima pre i posle svake desorpcije, pod istim geometrijskim uslovima, u trajanju od 1 časa. Izračunate su specifične aktivnosti (Bq/kg) uzoraka. Sadržaj ^{137}Cs u svakom uzorku izražen je kao procenat preostalog cezijuma u uzorku nakon svake desorpcije u odnosu na njegov sadržaj u polaznom uzorku. On je dobijen izražavajući aktivnost uzorka nakon svake desorpcije kao procenat aktivnosti polaznog uzorka.

Smanjenje mase uzoraka posle svih desorpcija je zanemarljivo, jer je manje od greške merenja. Greška merenja je standardna devijacija svih pojedinačnih merenja istog tipa (pH vrednosti) nezavisno od vrste rastvora.

REZULTATI I DISKUSIJA

U tabeli 1 prikazani su nivoi aktivnosti ^{137}Cs (Bq/kg) u mahovini *H. sericeum*, pre desorpcije, procenat desorbovanog ^{137}Cs iz mahovine posle svake od pet uzastopnih desorpcija rastvorima A–C i destilovanom vodom (D), kao i procenat ukupno desorbovanog ^{137}Cs iz mahovine.

Tabela 1. Srednje vrednosti aktivnosti ^{137}Cs (Bq/kg) u mahovini H. sericeum pre desorpcije, procenat nedesorbovanog ^{137}Cs posle svake uzastopne desorpcije rastvorima A–C i destilovanom vodom (D). Sobna temperatura ≈22 °C. Srednja greška merenja: 3,5%
Table 1. Mean ^{137}Cs activity (Bq/kg) in H. sericeum moss before desorption, percentage of non-desorbed ^{137}Cs after each consecutive desorption using solutions A–C and distilled water (D). Room temperature ≈22 °C . Mean measurement error: 3.5%

pH	4,60			5,15			5,75			6,50
Rastvor	A	B	C	A	B	C	A	B	C	D
Desorpcija	Nivo aktivnosti ^{137}Cs u mahovini pre desorpcije A_0 (Bq kg^{-1})									
	552	513	498	538	476	493	550	505	490	523
	Procenat nedesorbovanog ^{137}Cs u lišaju posle svake uzastopne desorpcije									
I	83,2	85,1	82,3	82,1	84,1	83,2	91,0	87,5	89,1	87,9
II	78,5	81,1	77,2	76,9	80,3	80,0	85,6	81,1	86,4	82,0
III	74,8	78,6	73,5	72,9	77,2	77,1	83,1	78,5	81,8	76,9
IV	71,8	76,7	68,7	70,2	75,1	73,5	77,5	77,1	78,8	71,1
V	68,2	75,2	66,8	69,3	71,1	70,3	76,1	76,6	77,2	68,7
	Ukupno desorbovano ^{137}Cs iz lišaja, %									
	31,8	24,8	33,2	30,7	28,9	29,7	23,9	23,4	22,8	31,3

Nivoi aktivnosti ^{137}Cs u uzorcima mahovine *H. sericeum* je bio od 476 do 552 Bq/kg. Posle pet desorpcija iz mahovina je desorbovano od 22,8% (rastvor C, pH 5,75) do 33,2% (rastvor C, pH 4,61) ^{137}Cs od početne vrednosti. Destilovanom vodom (D) iz mahovine je desorbovano 31,3% ^{137}Cs od početne vrednosti. Prvom desorpcijom iz mahovine desorbuje se ^{137}Cs u najvećem procentu (od 9,0 do 17,9%). Srednja vrednosti desorpcija ^{137}Cs iz mahovina rastvorom A je 28,8%, B 25,7%, C 28,6%. Na osnovu rezultata zaključuje se da pH vrednost rastvora ne utiče značajno na desorpciju ^{137}Cs iz mahovine i da se posle pet sukcesivnih desorpcija ^{137}Cs ne desorbuje značajno iz mahovine. Ovi rezultati ukazuju da je u intervalu pH od 4,61 do 6,50 dominantna desorpciona supstanca H_2O, a manji uticaj imaju SO_4^{2-}, NO_3^- i H^+.

Ako se uporede rezultati naših prethodnih istraživanja desorpcije ^{137}Cs iz lišaja *Cetraria islandica* rastvorima iste pH vrednosti i istog sastava sa rezultatima prikazanim u ovom radu zaključuje se da se iz lišaja približno dva puta više desorbuje ^{137}Cs nego iz mahovina. Pretpostavlja se da je to posledica različite građe navedenih biljnih vrsta, selektivnosti njihovih polupropustljivih membrana, sorpcije ^{137}Cs u talusu, starosti biljke, mesta nalaženja. Rezultati ukazuju na složenost apsorpcionog i desorpcionog sistema tj. biljnih vrsta [26].

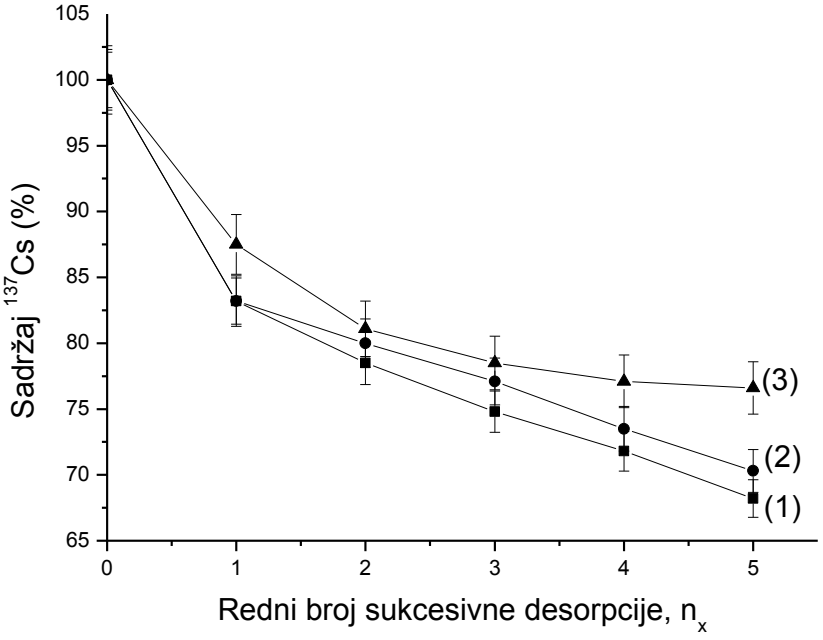

Slika 1. Sadržaj ^{137}Cs u mahovini H. sericeum u odnosu na početni sadržaj (100%), u zavisnosti od rednog broja sukcesivnih desorpcija, n_x, rastvorima A, pH 4,61 (1), B, 5,75 (3) i C, pH 5,15 (2).
Figure 1. ^{137}Cs content in H. sericeum moss in realtion to the starting content (100%), depending on the consecutive desorption number, n_x, using solutions A, pH 4.61 (1), B, 5.75 (3) and C, pH 5.15 (2).

Promena desorbovane količine ^{137}Cs od broja uzastopnih desorpcija, daje eksponencijalne krive, koje ne zavise od pH vrednosti i vrste rastvora (Slika 1).

Naša prethodna istraživanja su pokazala da se uzastopnim desorpcijama sa jednakim zapreminama desorbensa menja i količina preostale sorbovane supstancije (C_x) sa brojem desorpcija (n_x), što se može prikazati jednačinom (1):

$$\ln C_x = \ln C_0 - \underline{a} n_x \quad (1)$$

gde su C_0 – sadržaj sorbovane supstance u lišaju pre desorpcije, $\underline{a}$ – konstanta, n_x – broj sukcesivnih desorpcija jednakim zapreminama desorpcionog rastvora (kojih je bilo 5), C_x – količina sorbovane supstance pri određenoj vrednosti n_x.

Kada postoji samo jedan tip sorpcije, ili ako jedan od više tipova preovlađuje (pa se ostali mogu da zanemare), kada se koristi jednačina (1) za realni sistem se dobija da je zavisnost logaritma količine sorbovane supstancije u čvrstoj fazi linearna funkcija broja sukcesivnih zapremina rastvora korišćenog pri desorpciji, n_x. Ako sorbent ima mogućnost da sorbovanu supstanciju veže različitim tipovima sorpcije, odnosno na različita mesta sorbenta kada se koristi jednačina (1) dobija se da je zavisnost logaritma količine sorbovane supstancije u čvrstoj fazi nelinearna funkcija broja sukcesivnih zapremina rastvora korišćenog pri desorpciji, n_x. tj. dolazi do odstupanja od prave linije.

U ovim istraživanjima, dobijen je samo jedan tip krivih, slika 2, koji čine prave linije, čiji je presek sa ordinatnom osom, tj. vrednost C_0 manja od 100%.

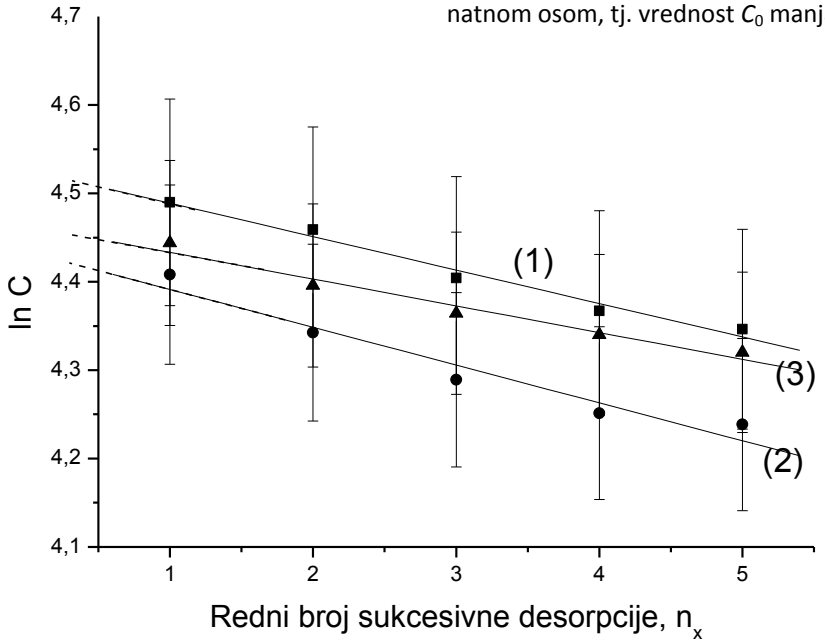

Slika 2. Logaritam sadržaja (%) ^{137}Cs u mahovini H. sericeum, ln C, u zavisnosti od broja sukcesivnih desorpcija (n_x) rastvorima: C, pH 5,75 (1), A, pH 5,15 (2) i B, pH 4,61 (3). Početni sadržaj: C_0 = 100%.
Figure 2. Logarithm of the ^{137}Cs content (%) in H. Sericeum moss, ln C, depending on the consecutive desorption number (n_x) using solutions: C, pH 5.75 (1), A, pH 5.15 (2) and B, pH 4.61 (3). Starting content C_0 = 100%.

Tabela 2. Vrednosti početnih aktivnosti ^{137}Cs (C_{0e}), određenih ekstrapolacijom pravih (Slika 2), i razlika (ΔC_0) u odnosu na izmerene početne aktivnosti C_0 (100%)
Table 2. Values of starting activity of ^{137}Cs (C_{0e}), determined by extrapolation of straight lines (Figure 2), and differences (ΔC_0) in relation to measured starting activitiesof C_0 (100%)

Desorpcioni rastvor	pH	C_{0e} / %	$\Delta C_0 = 100 - C_{0e}$ (%)
A	4,61	84,8	15,2
	5,15	84,6	15,4
	5,75	84,6	15,6
B	4,61	82,7	17,3
	5,15	85,6	14,4
	5,75	85,2	14,8
C	4,61	92,8	7,2
	5,15	86,5	13,5
	5,75	90,9	9,1
Destilovana voda	6,50	90,0	10,0

Ekstrapolacijom dobijenih pravih linija dobijene su vrednosti ln C_{0e} za n = 0 koje su prikazane u tabeli 2. Iz tabele 2 sledi da su vrednosti ΔC_0 (gde je ΔC_0 = 100 – – C_{0e}) od 7,2 do 17,3%. Dobijene vrednosti ukazuju da su prisutne najmanje dve vrste sorpcije ^{137}Cs koje se znatno razlikuju po jačini veza. Slabije je vezan deo ^{137}Cs koji se desorbuje korišćenim zapreminama desorpcionog rastvora. Ostali deo sorbovanog ^{137}Cs je daleko jače vezan, pa su i koncentracije desorbovanog ^{137}Cs daleko niže, i ne utiču na značajniju izmenu ravnotežnih koncentracija dobijenih u korišćenim zapreminama ekstragensa. Ovo dovodi do toga da grafik jednačine (1) ne odstupa od prave linije.

ZAKLJUČAK

Posle pet desorpcija iz mahovina je desorbovano od 22,8 do 33,2% ^{137}Cs od početne vrednosti. Destilovanom vodom (D) iz mahovine je desorbovano 31,3% ^{137}Cs od početne vrednosti. Srednje vrednosti desorpcija ^{137}Cs iz mahovina rastvorima A, B su 29,9% tj. 29,8%, dok je za rastvor C nešto niža (23,3%). Prvom desorpcijom iz mahovine desorbuje se ^{137}Cs u najvećem procentu (od 9,0 do 17,9%).

Promena desorbovane količine ^{137}Cs od broja uzastopnih desorpcija, daje eksponencijalne krive, koje ne zavise od pH vrednosti i vrste rastvora.

U ovim istraživanjima, dobijen je samo jedan tip krivih, koji čine prave linije, čiji je presek sa ordinatnom osom, tj. vrednost C_0 manja od 100%.

Zahvalnica

Ovaj rad finansiralo je Ministarstvo prosvete, nauke i tehnološkog razvoja Republike Srbije (Projekat broj: III 43009).

LITERATURA

[1] D. Veselinović, I.A. Gržetić, Š.A. Đarmati, D. Marković, Stanja i procesi u životnoj sredini, Fizičkohemijski osnovi zaštite životne sredine, knjiga I, Udžbenici Fizičke hemije, Fakultet za fizičku hemiju, Univerziteta u Beogradu, Beograd, 1995.

[2] M. Jovanović, Jonizujuća zračenja i životna sredina, Vojnoizdavački zavod, Beograd, 1983, str. 107–190.

[3] N. Xavkes, G. Lean, D. Leigh, R. McKie, P. Pringle, A. Wilson, Najgora nesreća na svijetu, Černobil: kraj nuklearnog sna, Globus, Zagreb, 1987.

[4] Savezni komitet za rad, zdravstvo i socijalnu zaštitu, Nivo radioaktivne kontaminacije čovekove sredine i ozračenost stanovništva Jugoslavije 1986. godine usled havarije nuklearne elektrane u Černobilju, Beograd, 1987.

[5] F.W. Whicker, Impacts of large radionuclide releases on plant and animal populations, in: Ciba Foundation, Health Impacts of Large Releases of Radionuclides, John Wiley, London, 1997, pp. 74–93.

[6] A.L. Nichols, E. Hunt, Nuclear data table, in: G. Longworth, Ed., The radiochemical manual, Howell, 1998.

[7] D.H.S. Richardson, The Biology of Mosses, Blackwell Scientific Publications, Oxford, 1981

[8] A. Basile, S. Sorbo, G. Aprile, B. Conte, R. Castaldo Cobianchi, Comparison of the heavy metal bioaccumulation capacity of an epiphytic moss and epiphytic lichen, Environ. Pollut. **151** (2008) 401–407.

[9] S. Chakrabortty, G.T. Paratkar, Biomonitoring of Trace Element Air Pollution Using Mosses, Aerosol, Air Quality Res. **6** (2006) 247–258.

[10] A. Čučulović, D. Popović, R. Čučulović, J. Ajtić, Natural radionuclides and ^{137}Cs in moss and lichen in Eastern Serbia, Nucl. Technol. Radiat. **27**(1) (2012) 44–51.

[11] A. Čučulović, D. Veselinović, Mosses as biomonitors for radioactivity following the Chernobyl accident, Arch. Biol. Sci. Belgrade **63**(4) (2011) 1117–1125.

[12] A. Čučulović, R. Čučulović, M. Sabovljević, D. Veselinović, Activity concentrations of ^{137}Cs and ^{40}K in mosses from spas in Eastern Serbia, Arch. Biol. Sci., Belgrade **64**(3) (2012) 917–925.

[13] A. Čučulović, R. Čučulović, S. Nestorović, D. Veselinović, Levels of activity of ^{40}K and ^{137}Cs in samples of bioindicators from the National park Đerdap, in Proceedings of XIX International Scientific and Professional meeting ecological Trouth Eco-ist 11, University of Belgrade, Technical Faculty in Bor, Bor, 2012, pp. 18–23.

[14] C. Delfanti, C. Papucci, C. Benco, Mosses as indicators of radioactivity deposition around a coal-fired power station, Sci. Total Environ. **227** (1999) 49–56.

[15] E.F. Elstner, R. Fink, W. Höll, E. Lengfelder, H. Ziegler, Natural and Chernobyl-caused radioactivity in mushrooms, mosses and soil-samples of defined biotops in SW Bavaria, Oecologia **73** (1987) 553–558.

[16] C. Giovani, G. Bolognini, P.L. Nimis, Bryophytes as indicators of radioactive deposition in northeastern Italy, Sci. Total. Environ. **157** (1994) 35–43.

[17] R.E. Longton, The role of bryophytes and lichens in terrestrial ecosystems, Bryophytes and Lichens in a Changing Environment, J.W. Bates, A.M. Farmer, Eds., Clarendon press, Oxford, 1992.

[18] C. Papastefanou, M. Manolopoulou, T. Sawidis, Lichens and mosses: Biological monitors of radioactive fallout from the Chernobyl reactor accident, J. Environ. Radioact. **9** (1989) 199–207.

[19] C. Papastefanou, M. Manolopoulou, T. Sawidis, Residence time and uptake rates of ^{137}Cs in lichens and mosses at temperate latitude (40° N), Environ. Int. **18** (1992) 397–401.

[20] T. Sawidis, L. Tsikritzis, K. Tsigaridas, Cesium-137 monitoring using mosses from W. Macedonia, N. Greece, J. Environ. Manag. **90** (2009) 2620–2627.

[21] A. Čučulović, Desorpcija ^{137}Cs i drugih metala iz lišaja *Cetraria islandica* kiselim rastvorima, doktorska disertacija, Fakultet za fizičku hemiju, Univerzitet u Beogradu, Beograd, 2007.

[22] A. Čučulović, D. Veselinović, Š. S. Miljanić, Extraction of ^{137}Cs from *Cetraria islandica* lichen with water, J. Serb. Chem. Soc. **71**(5) (2006) 565–571.

[23] A. Čučulović, D. Veselinović, Š. S. Miljanić, Extraction of ^{137}Cs from *Cetraria islandica* lichen using acid solutions, J. Serb. Chem. Soc. **72**(7) (2007) 673–678.

[24] A. Čučulović, D. Veselinović, Š. S. Miljanić, ^{137}Cs Desorption from lichen Using Acid Solutions, Russ. J. Phys. Chem., A **83**(9) (2009) 1547–1549.

[25] A. Čučulović, D. Veselinović, Š. S. Miljanić, Desorption of ^{137}Cs from *Cetraria islandica* (L.) Ach. using solutions of acids and their salts mixtures, J. Serb. Chem. Soc. **74**(6) (2009) 663–668.

[26] A. Čučulović, D. Veselinović, Š.S. Miljanić, Desorpcija radiocezijuma-137 iz lišaja *Cetraria islandica* (L.) Ach. rastvorima koji simuliraju kisele kiše, Hem. Ind. **66**(5) (2012) 701–708.

[27] Gamma Vision-32: Gamma-Ray Spectrum Analysis and MCA Emulator, Software User´s Manuel, ORTEC.

SUMMARY

DESORPTION OF ^{137}Cs FROM *Homalothecium sericeum* (Hedw.) Schim. MOSS USING WEAKLY ACID SOLUTIONS

Ana A. Čučulović[1], Dragan S. Veselinović[2]

[1]*INEP – Institute for the Application of Nuclear Energy, University of Belgrade, Zemun, Serbia*
[2]*Faculty of Physical Chemistry, University of Belgrade, Belgrade, Serbia*

(Scientific paper)

Desorption of ^{137}Cs from *Homalothecium sericeum (*Hedw.) Schim. moss was performed using five consecutive desorptions with five identical solution volumes. The following solutions were used for desorption: H_2SO_4, HNO_3 and their mixture H_2SO_4–HNO_3, with pH values of 4.61; 5.15 and 5.75; and also distilled water pH 6,50. After five consecutive desorptions from 22.8% (solution H_2SO_4–HNO_3, pH 5.75) to 33.2% (solution H_2SO_4–HNO_3, pH 4.60) of ^{137}Cs was desorbed by the sorbed acid, while by distilled water 31.3% of ^{137}Cs was desorbed. The highest amount of ^{137}Cs was desorbed by the first desorption, from 9.0 to 17.9%. Mean values of the total percentage of desorbed ^{137}Cs from moss were similar: for solution H_2SO_4 28.8%; HNO_3 25.7% and H_2SO_4–HNO_3 28.6%, which indicates that NO_3^- and SO_4^{2-} do not have an influence on Cs^+ desorption. The used pH values of solutions do not significantly influence ^{137}Cs desorption from moss. After five consecutive desorptions ^{137}Cs was not significantly desorbed from moss. In the pH interval of 4.61 to 6.50 the desorbed substances were H_2O and H^+, while SO_4^{2-} and NO_3^- had a smaller influence.There are two sorption points, *i.e.*, two sorption types where one is dominant.

Keywords: ^{137}Cs desorption • *Homalothecium sericeum* (Hedw.) Schim. • Acid rain

Deformation behaviour of two continuously cooled vanadium microalloyed steels at liquid nitrogen temperature

Dragomir M. Glišić, Abdunnaser H. Fadel, Nenad A. Radović, Djordje V. Drobnjak, Milorad M. Zrilić

University of Belgrade, Faculty of Technology and Metallurgy, Belgrade

Abstract

The aim of this work was to establish the deformation behavior of two vanadium microalloyed medium carbon steels with different contents of carbon and titanium by tensile testing at 77 K. Samples were reheated at 1250 °C for 30 min and continuously cooled in still air. Beside acicular ferrite as the dominant morphology in both microstructures, the steel with lower content of carbon and negligible amount of titanium contains considerable fraction of grain boundary ferrite and pearlite. It was found that Ti-free steel exhibits a higher strain hardening rate and significantly lower elongation at 77 K than the fully acicular ferrite steel. The difference in tensile behavior at 77 K of the two steels has been associated with the influence of the pearlite, together with higher dislocation density of acicular ferrite.

Keywords: Co(II) determination, Sn(II) determination, kinetic spectrophotometric method.

Available online at the Journal website: http://www.ache.org.rs/HI/

SCIENTIFIC PAPER

UDC 669.14.01/.09

Hem. Ind. **67** (6) 981–988 (2013)

doi: 10.2298/HEMIND121214015G

Traditional medium carbon forging steels achieve their strength and toughness in additional separate processes of quenching and tempering after forging [1––4]. In order to reduce production costs and avoid usual problems associated with quenching, especially long products, vanadium microalloyed forging steels had been developed [5]. These steels achieve required level of strength during air cooling directly from hot forging temperature, due to V(C,N) precipitation in ferrite. However, the toughness of the air cooled steels is lower, because coarsening of austenite grains at temperatures used in conventional forgings produces coarse ferrite-pearlite structure. Microalloying with titanium provided austenite grain refinement by Zener pinning effect of highly insoluble TiN particles [6,7]. Fine ferrite-pearlite structures with improved toughness had been achieved. On the other hand, coarse TiN particles, usually larger than 1 μm [1], act as fracture nucleation sites and are detrimental to the toughness of the steel.

Further toughness improvement had been achieved in medium carbon Ti–V microalloyed steels with acicular ferrite structure [1–4]. Acicular ferrite, often considered as intragranulary nucleated bainite [8], consists of fine interlocking plates with random crystalographic orientation. It is assumed that acicular ferrite plate boundaries effectively resist propagation of microcracks nucleated at brittle particles [3,9]. However it remains unclear whether it is grain size or particle size that controls cleavage fracture.

Correspondence: D. Glišić, Department of Metallurgical Engineering, Faculty of Technology and Metallurgy, University of Belgrade, Karnegijeva 4, 11120 Belgrade, Serbia.

E-mail: gile@tmf.bg.ac.rs

Paper received: 14 December, 2012

Paper accepted: 29 January, 2013

In order to examine the cleavage process itself in microalloyed medium carbon steels with acicular ferrite structure, and predict fracture behaviour, it is necessary to have knowledge of deformation behaviour in conditions close to nil ductility. Therefore, in the present work, deformation behavior at liquid nitrogen temperature of two medium carbon vanadium microalloyed steels with different amount of carbon and titanium was analyzed by means of tensile testing at liquid nitrogen temperature.

EXPERIMENTAL PROCEDURE

Two commercial medium carbon V-microalloyed steels with different content of carbon and titanium received as hot-rolled rods were investigated. The chemical composition of the steels is given in Table 1, where numbers in labels “A19” and “B22” indicate the rod diameter in milimeters. In order to eliminate as-received microstructure 200 mm long samples were homogenized at 1250 °C for 4 h and quenched in oil. In order to provide homogeneous solid solution, samples were afterward reaustenized at 1250 °C for 30 min and cooled in still air. In all heat treatments, argon was used as a protective atmosphere.

In order to measure previous austenite grain size, the following procedure was applied. After quenching in water, samples were tempered at 450 °C for 24 h, in order to allow phosphorous segregation on previous austenite grain boundaries, and then slowly cooled in still air to room temperature. Polished samples were etched by a solution of 10 g of picric acid ($C_6H_3N_3O_7$), 50 ml of sodium alkylsulfonate and 1 ml of HCl in 100 ml of distilled water. The solution was heated to 90 °C and

Table 1. Chemical composition of the steels (wt.%)

Steel	C	Si	Mn	P	S	Cr	Ni	Mo	V	Ti	Al	Nb	N
A19	0.256	0.416	1.451	0.0113	0.0112	0.201	0.149	0.023	0.099	0.002	0.038	0.002	0.0229
B22	0.309	0.485	1.531	0.0077	0.0101	0.265	0.200	0.041	0.123	0.011	0.017	0.003	0.0228

the samples were immersed for 25 s. Grain size determination was done *via* standard linear intercept method.

The transverse metallographic specimens were polished and etched in a 2% nital solution. Microstructure was examined using optical microscopy.

Cylindrical specimens of 5 mm diameter and 30 mm gauge length were machined and tensile tested at liquid nitrogen temperature at a cross-head velocity of 0.1 mm/min, giving an initial strain rate of $5.5 \cdot 10^{-5}$ s^{-1}.

RESULTS

Microstructure of steel A19 (0.256 wt.% C, 20 ppm Ti) is characterized by dominant presence of acicular ferrite, with some ferrite and pearlite along previous austenite grain boundaries (Figure 1). Within the generally continuous layer of grain boundary ferrite, both polygonal idiomorphs and thin elongated allotriomorphs are present. A few examples of Widmanstätten saw-teeth ferrite emanating from grain boundary ferrite allotriomorphs can also be seen. Fine interlocking structure of acicular ferrite inside prior austenite grain interiors is in many cases separated from the grain boundary ferrites by pearlite. Some inragranullary nucleated coarse plates could be recognized as Widmanstätten ferrite [4], although it is not always easy to distinguish it from the acicular ferrite at optical microscopy level.

Predominant morphology in the microstructure of the steel B22 (0.309 wt.% C, 110 ppm Ti) is acicular ferrite (Figure 2). As opposed to the steel A19, the structure of the steel B22 is almost free of pearlite and the grain boundary ferrite layer is thinner and discon-

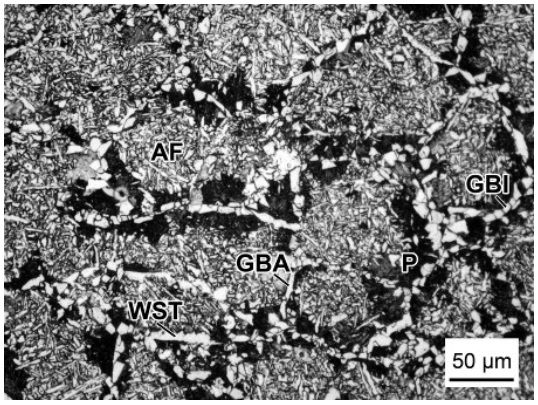

(a)

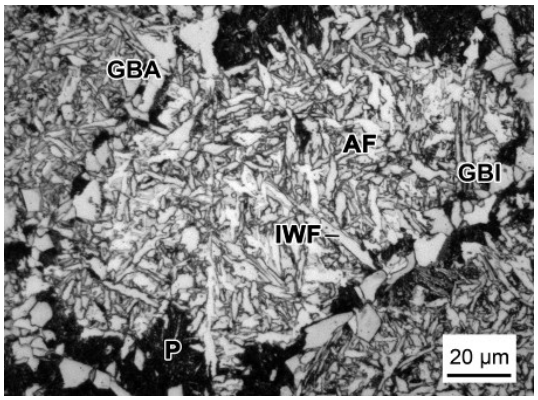

(b)

Figure 1. Microstructure of steel A19 (air-cooled from the austenitization at 1250 °C for 30 min). GBI – grain boundary idiomorph, GBA – grain boundary allotriomorph, P – pearlite, AF – acicular ferrite, WSF – Widmanstätten saw-teeth ferrite, IWF – intragranular Widmanstätten ferrite.

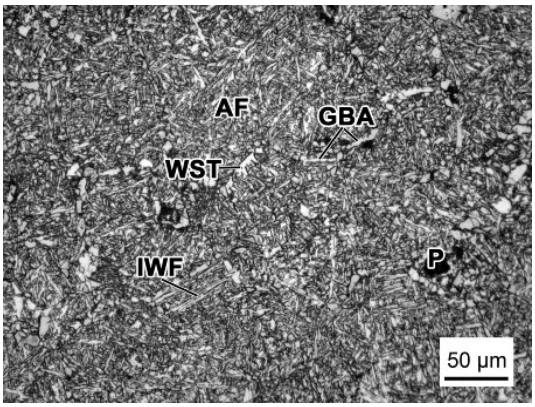

(a)

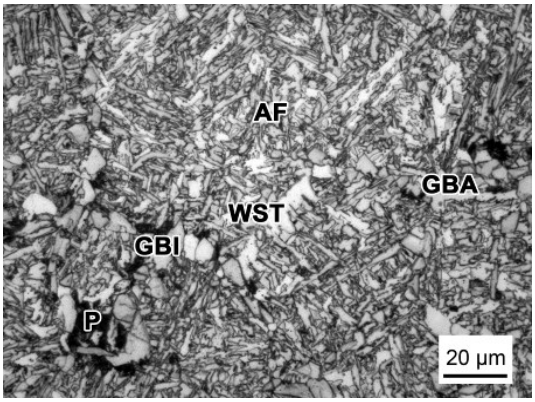

(b)

Figure 2. Microstructure of steel B22 (air-cooled from the austenitization at 1250 °C for 30 min). GBI – grain boundary idiomorph, GBA – grain boundary allotriomorph, P – pearlite, AF – acicular ferrite, WSF – Widmanstätten saw-teeth ferrite, IWF – intragranular Widmanstätten ferrite.

tinuous. Widmanstätten ferrite sideplates nucleated at the grain boundary directly at grain boundary allotriomorphs could be noticed too.

Previous austenite grain size (PAGS) is given in Table 2.

Table 2. Prior austenite grain size in tested steels

Steel	Austenitization, temperature/time	PAGS, μm
A19	1250 °C/30 min	100 ± 10
B22	1250 °C/30 min	80 ± 10

True stress-strain curves for the steels A19 and B22 tested at 77 K are shown in Figure 3. The steel B22 exhibits considerably higher elongation than the steel A19, while the latter show higher level of strain hardening. Instantaneous strain hardening rate as a function of true stress is given in Figure 4 and it demonstrates again higher level of strain hardening for the A19 steel. Stress-strain curves show gradual increase of flow stress, *i.e.*, there is no sharp yield point. Therefore, offset yield strength was established.

Table 3 summarizes tensile properties at 77 K, alongside with the values of yield stress to ultimate tensile stress ratio. Steel B22 exhibit yield stress higher by 123 MPa and ultimate tensile stress by 64 MPa than for steel A19. Total elongation for steel B22 is also higher (10.0 comparing to 5.0%), while steel A19 has a somewhat higher strain hardening index.

DISCUSSION

Microstructure

As shown in Figures 1 and 2, the dominant microstructure in both steels is acicular ferrite, while difference in pearlite content being the dominant difference. Hardenability of steel B22 is higher than for steel

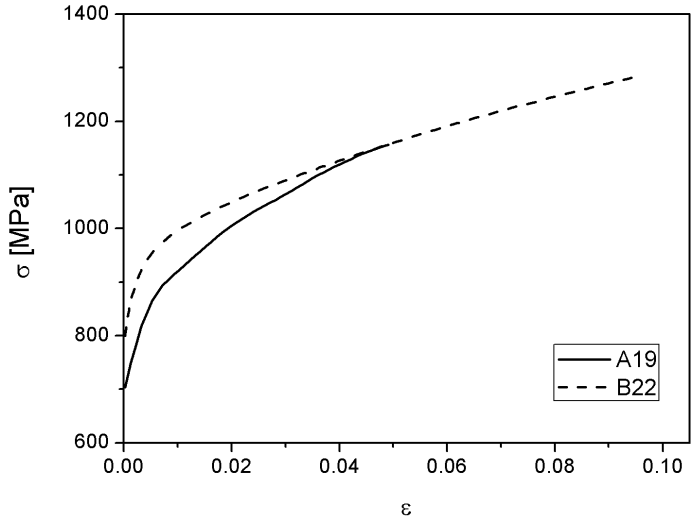

Figure 3. Tensile true stress – true strain curves at 77 K.

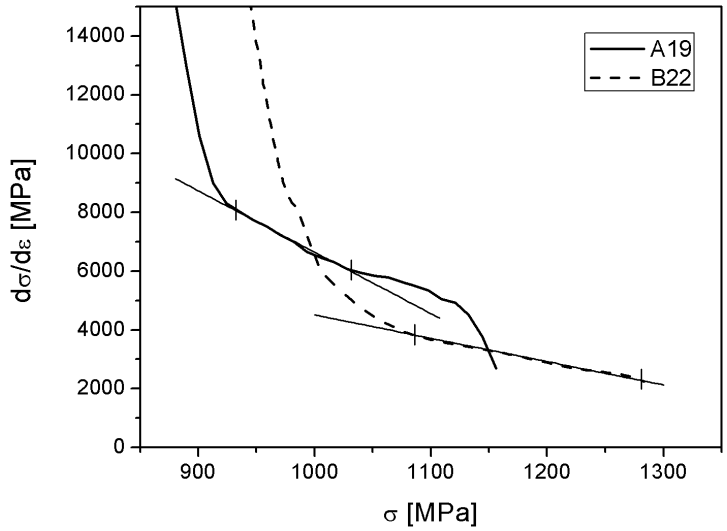

Figure 4. Strain hardening rates as a function of a true stress at 77 K.

Table 3. Tensile properties of the steels tested at 77 K; Room temperature values for the steels with equivalent chemical composition and the same termomechanical treatment is given for comparison

Steel	$\sigma_{0.2}$ / MPa	σ_m / MPa	e_t / %	$\sigma_{0.2}/\sigma_m$	n	Test temperature, K	Ref.
A19	775	1105	5.0	0.70	0.17	77	This work
B22	898	1169	10.0	0.77	0.16	77	This work
Ti-free	531	853	17.0	0.62	-	298	[10]
Ti-V	555	864	18.5	0.64	-	298	[10]

A19, since structure of the latter contains considerable fraction of pearlite. In steel B22 pearlite reaction is for the most part inhibited, even though samples were cooled at still air (about 60 °C/min). Manganese is well known to have the strongest retarding effect on diffusional decomposition of austenite, for elements present in both steels [11-13]. Since its content is practically equal in both steels, the higher hardenability in steel B22 is attributed to higher carbon content. Differences in other alloying element contents are not significant either, except for the titanium. Titanium is added for the purpose of austenite grain refinement and grain size control [6,7]. Its influence on hardenability is indirect, because grain boundaries are preferential nucleation sites for ferrite and pearlite. Bainite also nucleates intergranularly and larger grain sizes will slow down the kinetics in favor of intragranular nucleation. Furthermore, by increasing the grain size the probability of trapping inclusions/precipitates within austenite grain is also enlarged [14,15]. At austenitization temperature of 1250 °C, the measured austenite grain size is 100 μm for steel A19 and 80 μm for steel B22. Such large grain should enhance acicular ferrite formation in detriment of bainite by increasing the ratio between intragranular and grain boundary nucleation sites. However, in the case of the steels studied here, the effect of titanium on hardenability seems to be negligible, considering modest prior austenite grain size difference and that in both steels acicular ferrite intragranular nucleation predominated.

Temperatures for complete dissolution of VN and VC and distribution of main alloying elements are summarized in Table 4. It is assumed that total amount of Ti is contained within TiN particles, which are insoluble at reheating temperature of 1250 °C. Distribution of alloying elements was calculated assuming that on cooling from austenitization temperature precipitation of VN particles precedes VC precipitation and also taking into account stochiometric ratios of Ti:N = 3.4 and V:N = 3.6. Excess vanadium is available for VC precipitation or solid solution strengthening. It is assumed that VC does not precipitate separately from VN, but in fact as V(C,N) [16]. Temperatures for complete dissolution of VN and VC were calculated using equations for solubility products [17]:

$$\log[V][N] = -7840/T_{VN} + 3.02 \quad (1)$$

$$\log[V][C] = -9500/T_{VC} + 6.72 \quad (2)$$

Vanadium-nitride particles are favorable sites for nucleation of acicular ferrite [3,18,19]. Nitrogen available after TiN precipitation during solidification of the steels is available for VN precipitation. The reheating temperature of 1250 °C is above the temperature for complete dissolution of VN and taking into account similar values of vanadium content in both steels, quantity of VN particles should not be significantly different. According to the balance of Ti, V and N content (Table 4), all nitrogen is spent by precipitation of the alloying elements and thus vanadium is in excess. It was reported that vanadium solutes segregation render prior austenite grain boundaries inactive for nucleation of grain boundary ferrite [20], similarly to the well-known effect of boron [21]. Baring in mind precipitation of VC at lower temperatures than for VN, significant amount of free vanadium solute in steel A19 is not expected ($[V]_{excess}$ = 0.018 wt.%), as opposed to the steel B22 where excess amount of vanadium is higher ($[V]_{excess}$ = 0.052 wt.%) and some vanadium in solid solution could be expected. Nevertheless, it seems that vanadium solutes in steel B22 did not affect the nucleation of grain boundary ferrites and therefore its influence on hardenability is not conclusive.

Mechanical properties

Higher yield strength of the steel B22 is an understandable consequence of higher carbon content than in steel A19. The observed gradual yielding, typical for bainitic structures, is mainly due to higher density of mobile dislocations [8]. Multiple phases in structure with marked difference in strength can also contribute gradual yielding, because only the softer phase would

Table 4. Temperatures for complete dissolution of VN and VC and distribution of V, Ti and N

Steel	T_{VN} / °C	T_{VC} / °C	[V] / wt.%	[Ti] / ppm	[N] / ppm	$[N]_{TiN}$ / ppm	$[V]_{VN}$ / wt.%	$[V]_{excess}$ / wt.%	$[N]_{VN}$ / ppm
A19	1108.1	869.2	0.099	20	229	6	0.081	0.018	223
B22	1117.3	893.9	0.123	110	228	32	0.071	0.052	196

deform until it attained the strength of the harder phase [8]. The previously observed effect of yield strength decrease with temperature in bainitic medium carbon steels [22] is actually the effect of continuous-yielding, characteristic for low temperature deformation of these steels (see sketch in Figure 5). It is ascribed to the presence of retained austenite in the structure [22]. Elsewhere authors believe that it is a consequence of the higher mobile dislocation density in bainite, or in this case acicular ferrite [8].

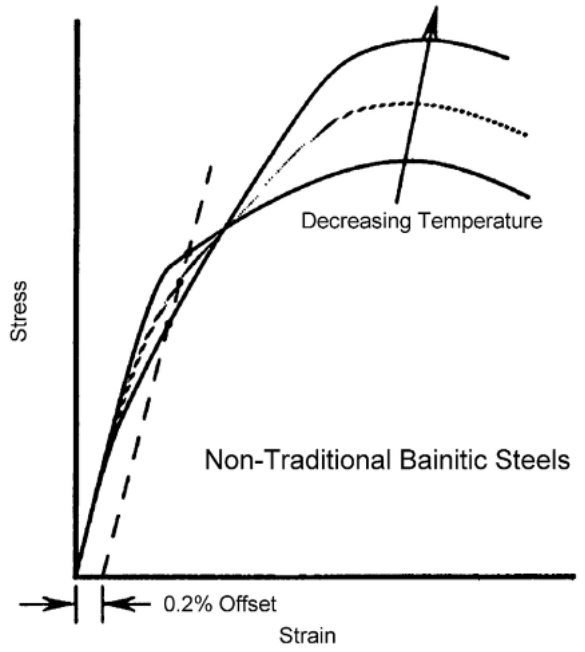

Figure 5. Schematic representatiom of the effect of test temperature on yield point of medium carbon bainitic steels [22].

According to the Kocks-Mecking model the linear part of the $d\sigma/d\varepsilon$-σ curve (stage III hardening) represents the rate of strain hardening decrease [23, 24]. The slope of the linear part of the curve for steel A19 indicates a faster strain hardening decrease than for steel B22. Strain hardening rate at low temperatures is basically resulting effect of two opposite processes: suppression of cross-slip and yield strength increase [25]. In this work, it seems that the latter is attributed to the presence of mobile dislocations in bainite. It is established before that strain hardening rate of the steel increases with increasing pearlite fraction in steel [26]. With considerable pearlite fraction in the structure of steel A19, as opposed to the steel B22, the high strain rate hardening at 77 K is understandable.

According to the classical view on the precipitation hardening, V(C,N) particles precipitated in ferrite coherent or partially coherent with the matrix, possess the highest effect [27], particularly on yield strength [25]. Therefore, it is expected that VN precipitates affect predominantly the strength of steel A19, since it incurporates considerable fraction of ferrite, including both grain boundary ferrite and pearlitic ferrite. On the other hand, in steel B22 where volume fraction of proeutectoid ferrite is lower and the amount of pearlite is almost negligible, hardening contribution of the VN particles should be neglected. The high strain hardening rate of steel A19 and low yield strength compared to B22 seem to disprove this point of view, especially taking into account the notable increase in difference of yield strengths between the two steels at room and at liquid nitrogen temperature (from less than 50 MPa to 120 MPa, Table 3).

There is also an opinion based on thermodynamic calculations that V(C,N) precipitation in austenite region at high temperatures, as in bainite or acicular ferrite at low temperatures is sluggish and that only interphase precipitation during transformation of austenite to ferrite produce particle dispersion capable for significant strengthening effect [16]. More recent findings imply that V(C,N) particles are incoherent even in ferrite [28,29] and that their strengthening contribution is primarily through Orowan-Ashby mechanism of dislocations bypassing the particles [30]. A possibility for this mechanism of strain hardening rate increase observed in steel A19 should be taken into consideration. The observed incoherency leads also to the conclusion that V(C,N) particles precipitated in austenite also could contribute to the strengthening of the steel [31, 32]. Given the similar conditions for precipitation in both steels (same reheating temperature, similar cooling rate, approximate T_{VN}) it doesn't seem that VN particles, presumably precipitated in austenite and thus randomly distributed in overall structure, have an observable influence on strengthening.

Despite the higher level of strain hardening rate, and therefore higher value of strain hardening exponent, *n*, total elongation for steel A19 is low compared to steel B22. Failure of the tensile specimen at the 77K is far beyond tensile instability condition, which is a consequence of the incapacity of the material for further hardening. It is well known that pearlite has a detrimental effect on ductility of the steel, as it brings increased strain hardening rate in combination with numerous potential sites for crack nucleation at ferrite/cementite interfaces [11]. Steep increase of stress in these conditions can give rise to processes of microcracks nucleation whether on cementite lamelaes or at second phase particles. When stress reaches a critical value for fracture, cleavage ensues.

Noticeable differences in yield strength increase when deformation temperature changes from room to liquid nitrogen temperature (47% increase for A19 and 62% for B22, Table 3), cannot be associated only with increased Peierls-Nabarro stress, stress needed for dislocation movement or solid solution strengthening con-

tribution. It is believed that grain refinement and dislocation density are the most effective in strengthening of acicular ferrite or bainitic steels [8,30]. Based on this view and with earlier considerations in mind, it can be assumed that the fine-grained structure of AF alongside with increased dislocation density has more pronounced effect at liquid nitrogen temperature.

The beneficial effect of acicular ferrite on ductility is well documented. Beside benefit of grain refinement at low temperatures, ferrite laths of random spatial orientation force cleavage crack to deflect, spending a considerable part of the energy input [1,2,33]. In classical quenched and tempered medium carbon steels with ferrite-pearlite structure, preferential cleavage nucleation sites are cementinte lamelaes or coarse TiN particles [9]. Giving that steel A19 has a negligible amount of titanium, coarse TiN particles are not expected. Volume fraction of the MnS particles should not be any different in the two steels investigated, as it is already concluded in the case of V(C,N) particles. This leads to conclusion that the main reason for the observed difference in total elongation is probably the presence of pearlite in the structure of steel A19, as opposed to the structure of B22 with acicular ferrite as the predominant constituent.

CONCLUSION

The dominant morphology of the two steels examined after continuous cooling in still air from the austenitization temperature of 1250 °C is acicular ferrite. A considerable fraction of pealite in the microstructure of the V-microalloyed steel A19, as opposed to the almost pearlite free microstructure of the steel Ti-V-microalloyed steel B22, is attributed to the different content of carbon.

The notable differences in deformation behavior of the steels investigated cannot be related just to the different content of carbon and titanium. The high strain hardening rate of steel A19 is attributed to the presence of pearlite in the structure and is concerned to be the main reason for lower tensile ductility. The marked increase of yield strength of steel B22 alongside with higher total elongation than of steel A19 at liquid nitrogen temperature indicates the influence of smaller grain size and high dislocation density of acicular ferrite.

Acknowledgement

The authors are indebted to Ministry of Education, Science and Technological Development of the Republic of Serbia for financial support (Project OI174004) and Serbian Oil Company for supplying experimental material. Abdunnaser Fadel acknowledges the Ministry of Education of Libya for providing PhD scholarship.

REFERENCES

[1] M.A. Linaza, J.L. Romero, J.M. Rodriguez-Ibabe, J.J. Urcola, Improvement of Fracture Toughness of Forging Steels Microalloyed with Titanium by Accelerated Cooling After Hot Working, Scripta Metall. Mater. **29** (1993) 1217–1222.

[2] M.A. Linaza, J.L. Romero, J.M. Rodriguez-Ibabe, J.J. Urcola, Cleavage Fracture of Microalloyed Forging Steels Scripta Metall. Mater. **32** (1995) 395–400.

[3] F. Ishikawa, T. Takahashi, The Formation of Intragranular Ferrite Plates in Medium-carbon Steels for Hot-forging and Its Effect on the Toughness, ISIJ Int. **35** (1995) 1128–1133.

[4] DJ. Drobnjak, A. Koprivica in: C.J. Van Tyne, G. Krauss, D.K. Matlock (Eds.), Microalloyed Bar and Forging Steels, TMS, Golden, 1996, pp. 93–107.

[5] M.J. Balart, C.L. Davis, M. Strangwood, Cleavage initiation in Ti–V–N and V–N microalloyed ferritic – pearlitic forging steels, Mater. Sci. Eng., A **284** (2000) 1–13.

[6] W. Roberts, in: J.M. Gray (Ed.), HSLA Steels Technology and Applications, ASM International, Beijing, 1986, pp. 33.

[7] T. Gladman, in: G. Tither and Z. Shouhua (Eds.), HSLA Steels, Processing, Properties and Applications, TMS, Warrendale, 1992, pp. 3.

[8] H.K.D.H. Bhadeshia, Bainite in Steels: Transformations, Microstructure and Properties, 2nd ed., IOM Communications Ltd., London, 2001.

[9] M.J. Balart, C.L. Davis, M. Strangwood, J.F. Knott, Cleavage Initiation in Ti–V–N and V–N Microalloyed Forging Steels, Mater. Sci. Forum **500**–**501** (2005) 729––736.

[10] A. Koprivica, Structure and properties of medium carbon V-microalloyed steels, PhD Thesis, TMF, Belgrade, 1998 (in Serbian).

[11] H.K.D.H. Bhadeshia, R.W.K. Honeycombe, Steels: Microstructure and Properties, 3rd ed., Elsevier, 2006.

[12] D. Glišić, N. Radović, A. Koprivica, A. Fadel, DJ. Drobnjak, Influence of Reheating Temperature and Vanadium Content on Transformation Behavior and Mechanical Properties of Medium Carbon Forging Steels, ISIJ Int. **50** (2010) 601–606.

[13] A. Fadel, D. Glišić, N. Radović, DJ. Drobnjak, Influence of Cr, Mn and Mo Addition on Structure and Properties of V Microalloyed Medium Carbon Steels, J. Mater. Sci. Technol. **28** (2012) 1053–1058.

[14] C. Capdevila, F. G. Caballero, C. Garcia de Andres, Relevant Aspects of Allotriomorphic and Idiomorphic Ferrite Transformation Kinetics, Mater. Sci. Tech. **19** (2003) 195–201.

[15] C. Capdevila, F.G. Caballero, C. Garcia-Mateo, C. Garciaa de Andres, The Role of Inclusions and Austenite Grain Size on Intragranular Nucleation of Ferrite in Medium Carbon Microalloyed Steels, Mater. Trans. **45** (2004) 2678–2685.

[16] S. Zajac, T. Siwecki, W.B. Hutchinson, R. Lagneborg, Strengthening Mechanisms in Vanadium Microalloyed

Steels Intended for Long Products, ISIJ Int. **38** (1998) 1130–1139.

[17] H. Adrian, in: Microalloying '95, ISS, Warrendale, 1995, pp. 285.

[18] C. Garcia-Mateo, C. Capdevila, F.G. Caballero, C.G.D. Andrés, Influence of V Precipitates on Acicular Ferrite Transformation Part 1: The Role of Nitrogen, ISIJ Int. **48** (2008) 1270–1275.

[19] C. Garcia-Mateo, J. Cornide, C. Capdevila, F.G. Caballero, C.G.D. Andrés, Influence of V Precipitates on Acicular Ferrite Transformation Part 2: Transformation Kinetics, ISIJ Int. **48** (2008) 1276–1279.

[20] H. Adrian, A mechanism for effect of vanadium on hardenability of medium carbon manganese steel, Mater. Sci. Tech. **15** (1999) 366–378.

[21] G. Thewlis, Transformation kinetics of ferrous weld metals, Mater. Sci. Tech. **10** (1994) 110–125.

[22] D.K. Matlock, G. Krauss, J.G. Speer, Microstructures and properties of direct-cooled microalloy forging steels, J. Mater. Process. Tech. **117** (2001) 324–328.

[23] U.F. Kocks, Laws for Work-Hardening and Low-Temperature Creep, J. Eng. Mater. T. ASME **98** (1976) 76–85.

[24] H. Mecking, U.F. Kocks, Kinetics of flow and strain-hardening, Acta Metall. Mater. **29** (1981) 1865–1875.

[25] DJ. Drobnjak, Fizička metalurgija fizika čvrstoće i plastičnosti 1, treće izdanje, TMF, Beograd, 1990 (in Serbian).

[26] K.W. Burns, F.B. Pickering, Deformation and Fracture of Ferrite-Pearlite Structures, J. Iron Steel I. **202** (1964) 899–906.

[27] L. Meyer, C. Strassburger, C. Schneider, in: HSLA Steels: Metallurgy and Applications, J. M. Gray, T. Ko, Z. Shouhua, W. Baorong and X. Xishan (Eds.), American Society for Metals, Metals Park, OH, 1986, pp. 29–44.

[28] E.V. Morales, J. Gallego, H.-J. Kestenbach, On coherent carbonitride precipitation in commercial microalloyed steels, Phil. Mag. Lett. **83** (2003) 79–87.

[29] H.-J. Kestenbach, S.S. Campos, E.V. Morales, Role of interphase precipitation in microalloyed hot strip steels, Mater. Sci. Tech. **22** (2006) 615–626.

[30] A.J. DeArdo, M.J. Hua, K.G. Cho, C.I. Garcia, On strength of microalloyed steels: an interpretive review, Mater. Sci. Tech. **25** (2009) 1074–1082.

[31] H.-J. Kestenbach, J. Gallego, On dispersion hardening of microalloyed hot strip steels by carbonitride precipitation in austenite, Scripta. Mater. **44** (2001) 791–796.

[32] M.D.C. Sobral, P.R. Mei, H.-J. Kestenbach, Mater. Sci. Eng., A **367** (2004), 317–321.

[33] Madariaga I., Gutierez, I., Acicular Ferrite Microstructures and Mechanical Properties in a Medium Carbon Forging Steel, Mater. Sci. Forum **284–286** (1998) 419––426.

ИЗВОД

ДЕФОРМАЦИОНО ПОНАШАЊЕ ДВА КОНТИНУИРАНО ХЛАЂЕНА ВАНАДИЈУМ МИКРОЛЕГИРАНА ЧЕЛИКА НА ТЕМПЕРАТУРИ ТЕЧНОГ АЗОТА

Драгомир М. Глишић, Abdunnaser H. Fadel, Ненад А. Радовић, Ђорђе В. Дробњак, Милорад М. Зрилић

Универзитет у Београду, Технолошко–металуршки факултет, Београд

(Научни рад)

Челици микролегирани ванадијумом и титаном развијани су са циљем да замене каљене и отпуштене средњеугљеничне челике. Иако ове челике карактерише добра комбинација чврстоће и жилавости, с друге стране захтевају накнадну термичку обраду, која значајно повећава трошкове производње. Технологија добијања континуирано хлађених челика треба да обезбеди микроструктуру захтеваних особина после хлађења на ваздуху. Из тог разлога је овим челицима промењен састав, а добре особине се обезбеђују присуством ацикуларног ферита. Ацикуларни ферит карактерише нуклеација унутар претходног аустенитног зрна и велика разлика у кристалографској оријентацији појединих зрна, односно феритних плочица. Ова испреплетана структура обезбеђује повећан отпор кретању прскотине и жилавост која је на нивоу жилавости код традиционалних каљених и отпуштаних челика. У раду су испитивана два континуирано хлађена микролегирана челика са додатком ванадијума. Структура челика без титана и са мањим садржајем угљеника (“A19”) састоји се од континуиране мреже проеутектоидног ферита уз који се издвојио перлит, за којим следи ацикуларни ферит издвојен унутар некадашњег аустенитног зрна. Структура челика са титаном и већим садржајем угљеника (“B22“) састоји се готово у потпуности од ацикуларног ферита. Деформационо понашање на 77 K испитивано је једноосним затезањем. Укупно издужење узорака челика B22 знатно је веће него код челика A19 (10 у односу на 5%). Челик B22 такође поседује већу границу течења и затезну чврстоћу, што је разумљиво с обзиром на већи садржај угљеника. Значајна разлика у дуктилности на температури течног азота у вези је са присуством перлита код челика A19, у односу на структуру ацикуларног ферита код челика B22. Брзина деформационог ојачавања се повећава са повећањем удела перлита у структури, чиме деформација постаје отежана, док истовремено конкурентни процес настајања микропрскотина на кртим цементитним ламелама или честицама секундарних фаза, брзо доводи до кртог лома на 77 K. С друге стране, ацикуларни ферит карактерише повећана густина дислокација, што се манифестује смањењем брзине деформационог ојачавања, а тиме и повећаним капацитетом деформационог ојачавања и већим издужењем код челика B22.

Кључне речи: Средње угљенични челици • Ванадијум микролегирани челици • Ацикуларни ферит • Температура течног азота • Брзина деформационог ојачавања

Analytical application of the reaction system phenyl fluorone–hydrogen peroxide for the kinetic determination of cobalt and tin traces by spectrophotometry in ammonia buffer media

Sofija M. Rančić[1], Snežana D. Nikolić-Mandić[2], Aleksandar Lj. Bojić[1]

[1]*Department of Chemistry, Faculty of Sciences and Mathematics, University of Niš, Serbia*
[2]*Faculty of Chemistry, University of Belgrade, Belgrade, Serbia*

Abstract

The present paper describes two new, simple, rapid, selective and sensitive kinetic spectrophotometric methods for Co(II) and Sn(II) determination in solution at room temperature, based on their effect on phenyl fluorone (PF) oxidation by hydrogen peroxide in ammonia buffer. The new method was elaborated for nano amounts of Co(II) determination, based on its catalytic effect on the oxidation of PF by H_2O_2 in the presence of citric acid (CA) as an activator. Also, the new method for micro amounts of Sn(II) determination was developed based on its inhibitory effect upon the same reaction. Comparison of the results showed that the activated catalytic reaction has better sensitivity than the inhibitory one. Methods were validated by the analysis of chemical substances and results were confirmed by examining the same samples by the AAS method.

Keywords: Co(II) determination, Sn(II) determination, kinetic spectrophotometric method.

Available online at the Journal website: http://www.ache.org.rs/HI/

SCIENTIFIC PAPER

UDC 546.73:543.42:544

Hem. Ind. **67** (6) 989–997 (2013)

doi: 10.2298/HEMIND121114016R

The significant reactivity of Co(II) ion in the comparison with Sn(II), and also its ability to form complexes with numerous compounds, caused a development of far more methods for cobalt determination. Although there are published AAS, ASV, ET-LEAFS, FI--PDA, CPE, polarografic, etc. methods, there is no doubt that kinetic and spectrophotometric methods have a significant part in cobalt determinations.

Kinetic methods, published in the last decade, determined Co(II) as the catalyst of various reactions of oxidation with hydrogen peroxide or KIO_4 as the oxidant and different substances like TADAB, FPKH, SPADNS, SPTSQ, SPAQ, cianex, etc. as the reductant. Recently, two methods were published: in 2006, the method for Co(II) determination in a reaction of oxidation of red artificial color Ponceau 4R with hydrogen peroxide [1], and the method for Co(II) determination as a catalyst of the reaction of oxidation of Sunset Yellow, by the same oxidant, in 2009 [2]. Also, some kinetic as well as spectrophotometric methods were published for simultaneous determination of cobalt, nickel, copper, zinc and iron in natural waters and laboratory mixtures, without prior separation [3–11]. Karayannis and Pettas suggested a simultaneous kinetic determination of cobalt, nickel and iron in mixtures by coupling stopped-flow techniques and charge coupled device detection [12]. Fernandez *et al.* [13] described the kinetic determination of Co, Cu, Zn and Ni at trace levels by first and second order multivariate calibration. There are interesting kinetic methods for Co(II) determination in the air, natural waters, pharmaceutical products, tea and hair [14–20]. Kinetic methods are also developed for cobalt determination in alloys, oils and ashes [21–24], coal, tobacco, etc. Kamble *et al*. developed a reliable analytical method for synergistic extractive spectrophotometric detection of Co(II) from alloys and nano composite samples [25]. The spectrophotometric method was published for simultaneous detection of trace amounts of Co, Ni and Cu, after the preconcentration of their 2-aminocyclopentene-1--dithiocarboxylate complexes on microcrystalline naphthalene [26].

Today, tin and organic tin compounds have been increasingly used in a variety of agricultural and industrial applications, as well as ship coats, and have become a serious environmental threat. Aquatic organisms in sea and river waters can effectively accumulate TBT and TPT: fishes, shells, plants and algae and also in marine and river sediments and sludges. Tin is a component of many alloys and it is the material for can production; thus, it can affect the environment by industrial wastewaters. Some biological investigations showed that Sn(II) and Sn(IV) chlorides inhibit growth and chlorophyll content of *Cyanobacterium* cultures under alkaline conditions [27]. Tin content in canned foods, according the WHO, is not supposed to exceed the concentration of 250 μg/g. In fact, sometimes even the tin concentration of 200 μg/g could cause serious

Correspondence: A.Lj. Bojić, Department of Chemistry, Faculty of Sciences and Mathematics, University of Niš, Višegradska 33, 18000 Niš, Serbia.
E-mail: bojica@gmail.com
Paper received: 14 November, 2012
Paper accepted: 13 February, 2013

gastrointestinal effects in human organism. Sn(II) forms complexes with compounds like ferroin, rhodamine 6G, catechol, tropolone, chloranilic acid, and propyl gallate, 8-hydroxiquinoline, and bromopyrogallol red, etc. and also spectrophotometric methods were published for tin determination in different samples. A spectrophotometric method for tin determination in canned food was elaborated in 1997 [28], and fluorimetric methods in 1985 [29] and 2006 [30]. Tin was determined in powdered coffee and milk [31], fruit juices [32], biological materials (kidney, liver hearth and muscles) [33], human hair [34], sea water [35], marine sediments [36], river sediments, soils and sludges [37], fly ashes, industrial effluents and alloys [38], etc.

Sn(II) can perform both as the inhibitor of the reactions of oxidation and the catalyst of the reactions of reduction in aqueous medium, but there are only a few kinetic methods published recently for tin determination. The kinetic spectrophotometric method was published for simultaneous determination of Sn(II) and Sn(IV) in water and fruit juices samples without prior separation steps [39]. The method is based on the difference in the rate of reactions of Sn(II) and Sn(IV) with pyrocatechol violet at pH 4.0. Tin was also determined as the catalyst of the reaction of reduction of chromium blue K in phosphoric acid medium and method was applied for tin determination in geological samples [40].

EXPERIMENTAL

Apparatus

Spectrophotometric measurements were performed on a UV–Vis spectrophotometer Shimadzu UV--1650 PC (Shimadzu, Japan). AAS measurements were performed on an Analyst A300 Perkin Elmer (USA). The cylindrical cells were thermostated at 20.00±0.02 °C using a thermocirculating bath (Julabo MP-5A). The pH measurements were performed using a Hach H260G pH-meter with a non-glass pH probe PH77SS (Hach, USA). Also, stopwatch Agat (Russia) was used.

Reagents and chemicals

Analytical grade reagents, provided by Merck, Germany, unless indicated otherwise and deionised water (Micro Med high purity water system, TKA Wasseraufbereitungs system GmbH) or ammonia buffer were utilized for solutions preparation. Ammonia buffers were prepared by mixing NH_3(aq) and NH_4Cl solutions (0.2 mol dm^{-3}) and their pH values were checked using pH-meter. A stock Co(II) solution (1×10^{-3} g cm^{-3}) was prepared by dissolving the exactly measured $CoCl_2\cdot4H_2O$ in deionised water. The concentration of the stock solution was checked electrogravimetically. Basic Sn(II) solution (1×10^{-3} g cm^{-3}) was prepared by dissolving 1.00 g of metallic tin (99.999%) in 100 cm^3 of concentrated HCl. The solution was diluted to 1.00 dm^3 by deionised water and its concentration was checked by iodometric titration. The concentrations of H_2O_2 solutions were verified by $KMnO_4$ titration. The phenyl fluorone basic solution was prepared by dissolving the exactly measured dry substance in ammonia buffer. All the polyethylene containers and the glassware were washed by diluted hydrochloric acid (1:1), solution of potassium hydroxide in ethanol and then repeatedly well rinsed by tap, distilled and deionized water. All concentrations described here are the initial concentrations in the reaction mixture at time zero after mixing. Each kinetic result is the average of five determinations.

Procedure

In order to obtain good mechanical and thermal stability, the instruments were run for 10 min before the first measurement. Selected volumes of reactants and deionized water were poured separately in the reaction mixture vessel with four compartments (Budarin vessel) up to a predeterminated total volume of 10 cm^3. The solution of Co(II), during cobalt determination, and Sn(II), during tin determination, was measured in one compartment of Budarin vessel for catalytic, *e.g.*, inhibitory reaction, and the same volume of deionized water was measured for non-catalytic and non-inhibitory reaction. After thermostating for ten minutes, the reagents were mixed and simultaneously the stopwatch was turned on. The solution was immediately added to a properly rinsed spectrophotometer cell with a path length of 10 cm and absorbance was measured every 15 s, starting from the 45^{th} s of reaction, up to 10 min of the reaction.

The reaction was tested by examination the influence of each component of the reaction mixture upon the reaction rate of catalytic and non-catalytic reaction for cobalt method development and inhibitory and non-inhibitory reaction for tin method development. The concentration of each component was changing consecutively, while the concentration of other components, as well as the working temperature, were kept constant.

RESULTS AND DISCUSSION

As the reaction progresses, the initial red color of the solution fades and the colorless reaction product forms. The exact mechanism of reaction and the nature of reaction products were not the main interest of our investigation. All spectrophotometric measurements were performed at the wavelength of absorption maximum of phenyl fluorone in ammonia buffer (493.6 nm, Figure 1).

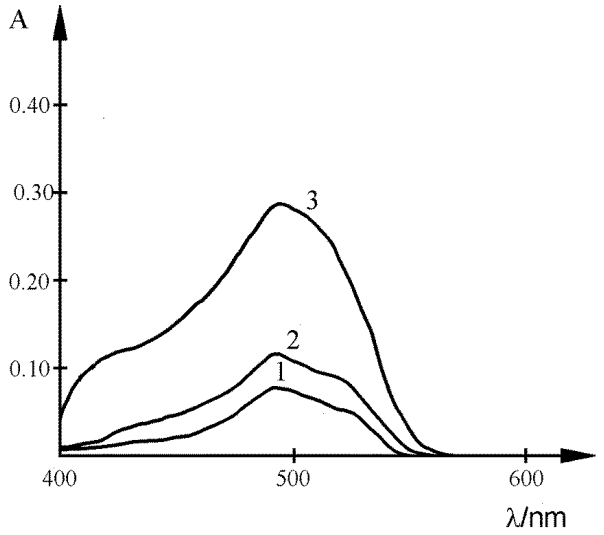

Figure 1. Absorption spectra of PF in ammonia buffer. Initial conditions: 1.5×10^{-5} mol dm^{-3} PF; 20.00±0.02 °C; pH: 1) 10.2; 2) 10.6; 3) 11.9.

The logarithm of absorbance-time curves are linear during the first five to ten minutes of reaction for different Co(II) and Sn(II) concentrations, so all kinetic results were treated by the integral variant of tangent method [41]. The rate of reaction was obtained using the slope of the kinetic curves of the absorbance-time plot.

According to the our preliminary investigations, the kinetic catalytic reaction of Co(II) is faster in the the presence of citric acid, so citric acid was added in the reaction mixture as an activator, during cobalt method investigations.

The influence of the pH value of selected ammonia buffers on the rate of both the catalytic and non-catalytic reaction for cobalt method development was examined in the pH interval from 10 to nearly 12. Within this range, both reactions showed complex dependence on the pH value of ammonia buffer (Figure 2). The value of 11.7 was selected as the most appropriate one, because it provides the adequate difference of the reaction rates of the catalytic and non-catalytic reaction. So, the ammonia buffer pH 11.7 was used in all subsequent investigations.

The influence of pH value of ammonia buffer upon the rate of both inhibitory and non-inhibitory reaction for tin method development was examined in pH interval from nearly 9.0 to nearly 11.5. In this range, both reactions show complex dependence of pH value of ammonia buffer (Figure 3). The ammonia buffer 10.4 was used in all following investigations.

The rates of both catalytic and non-catalytic reactions, for cobalt method investigation, are of the first order dependence on the reductant concentration (Figure 4) within the range of 1.8×10^{-5} to 7.3×10^{-5} mol dm^{-3}. Consequently, a concentration of 7.3×10^{-5} mol dm^{-3} was selected as optimal for the subsequent measurements.

In the range of PF concentration from 1.0×10^{-5} to 6.0×10^{-5} mol dm^{-3}, the rates of both inhibitory and non-inhibitory reaction, for tin method investigation, are in the first order dependence upon the reductant concentration (Figure 5). The concentration of 4.0×10^{-5} mol dm^{-3} was selected as optimal for the following measurements.

The dependence of the rate of the catalytic and non-catalytic reaction on the oxidant concentration was monitored within the concentration range of about 1.0 to about 3.2 mol dm^{-3} H_2O_2. Within this interval, the rate of catalytic reaction (in the presence of Co(II))

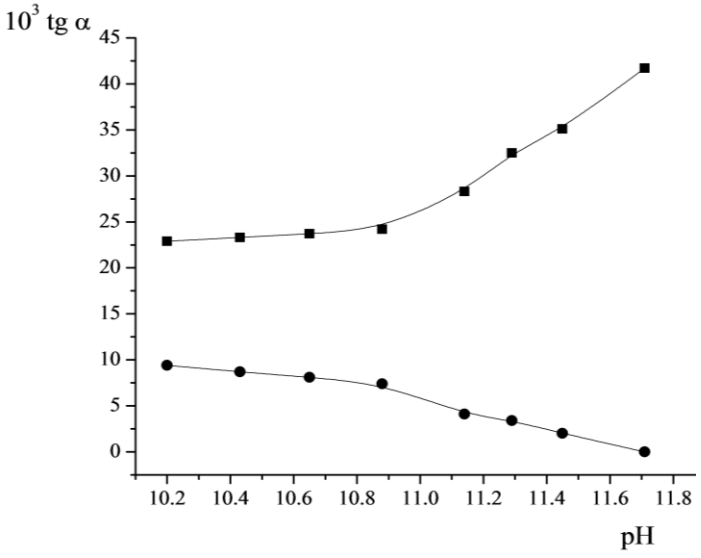

Figure 2. Dependence of the reaction rate on pH for cobalt method development. Initial conditions: 9.1×10^{-3} mol dm^{-3} CA; 7.3×10^{-5} mol dm^{-3} PF; 1.8 mol dm^{-3} H_2O_2; 1.8×10^{-7} g cm^{-3} Co(II); 20±0.02 °C; 1 – catalytic reaction; 2 – non-catalytic reaction.

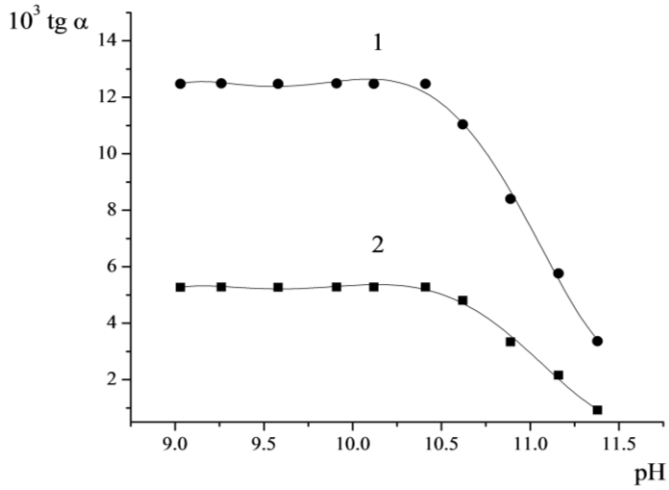

Figure 3. Dependence of the reaction rate on pH for tin method development. Initial conditions: 5.0×10^{-5} mol dm^{-3} PF; 3.92 mol dm^{-3} H_2O_2; 2.5 μg cm^{-3} Sn(II); 20.00±0.02 ℃; 1 – inhibitory reaction; 2 – non-inhibitory reaction.

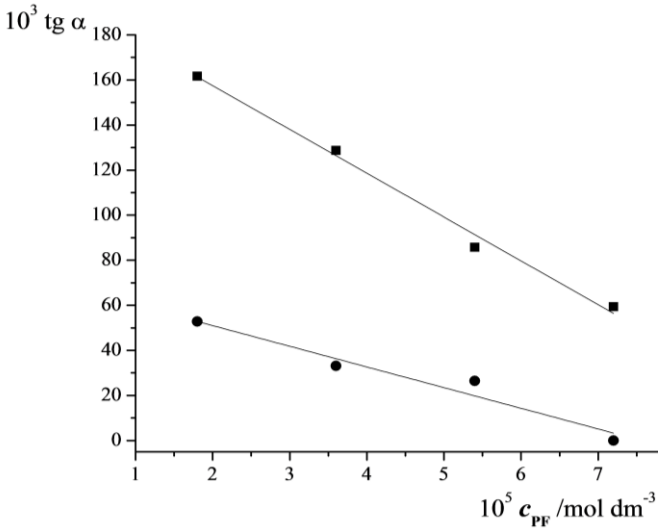

Figure 4. Dependence of the reaction rate on PF concentration for cobalt method development. Initial conditions: 9.1×10^{-3} mol dm^{-3} CA; 1.8 mol dm^{-3} H_2O_2; 1.8×10^{-7} g cm^{-3} Co(II); pH 11.7; 20±0.02 ℃; 1 – catalytic reaction; 2 – non-catalytic reaction.

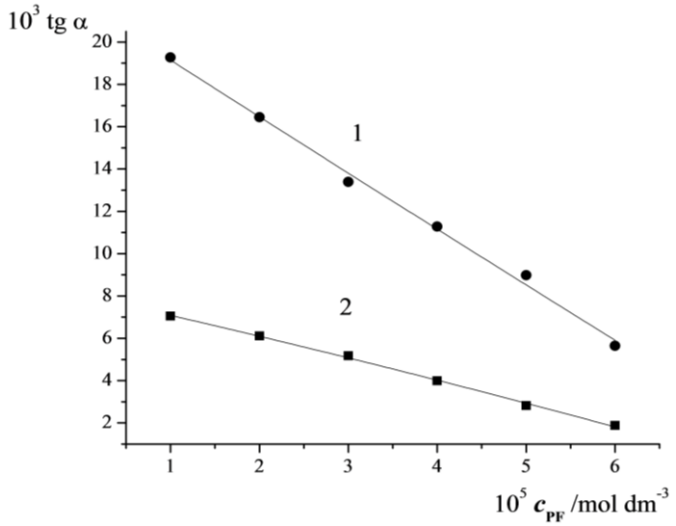

Figure 5. Dependence of the reaction rate on PF concentration for tin method development. Initial conditions: 3.92 mol dm^{-3} H_2O_2; 2.5 μg cm^{-3} Sn(II); pH 10.4, 20.00±0.02 ℃; 1 – inhibitory reaction; 2 – non-inhibitory reaction.

shows a complex dependence, whereas the non-catalytic one is of the zero order dependence within the concentration range of about 1.0 to about 2.0 mol dm^{-3} H_2O_2 (Figure 6). As optimal, a concentration of 1.3 mol dm^{-3} H_2O_2 was selected.

The dependence of inhibitory and non-inhibitory reaction rate on the oxidant concentration for tin method was followed for the concentration range of about 2.4 to about 4.4 mol dm^{-3} H_2O_2. In this interval, both reactions show the first order dependence of H_2O_2 concentration (Figure 7). The concentration of 2.94 mol dm^{-3} H_2O_2 was selected for further investigations.

The influence of the concentration of activator was examined only for catalytic and non-catalytic reaction for cobalt method development (Figure 8). Inside the investigated concentration range of citric acid of nearly 4.5×10^{-3} to nearly 27.0×10^{-3} mol dm^{-3}, the catalytic reaction exhibited a complex dependence, while the non-catalytic reaction showed zero order dependence. Citric acid concentration of 4.5×10^{-3} mol dm^{-3} was selected for further work.

Hence, the optimal conditions for performing the reaction for cobalt determination were found to be: pH 11.7, $c_{PF} = 7.3\times10^{-5}$ mol dm^{-3}, $c_{H2O2} = 1.3$ mol dm^{-3}, $c_A = 4.5\times10^{-3}$ mol dm^{-3}. In addition, the optimal conditions for performing the reaction for tin determination were found to be pH 10.4, $c_{PF} = 4.0\times10^{-5}$ mol dm^{-3}, $c_{H2O2} = 2.94$ mol dm^{-3}.

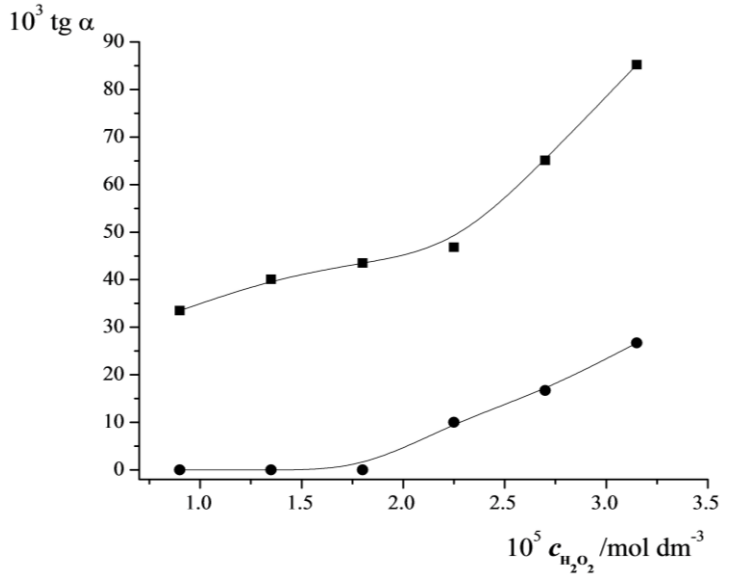

Figure 6. Dependence of the reaction rate on H_2O_2 concentration for cobalt method development. Initial conditions: 9.1×10^{-3} mol dm^{-3} CA; 7.3×10^{-5} mol dm^{-3} PF; 1.8×10^{-7} g cm^{-3} Co(II); pH 11.7; 20±0.02 °C; 1 – catalytic reaction; 2 – non-catalytic reaction.

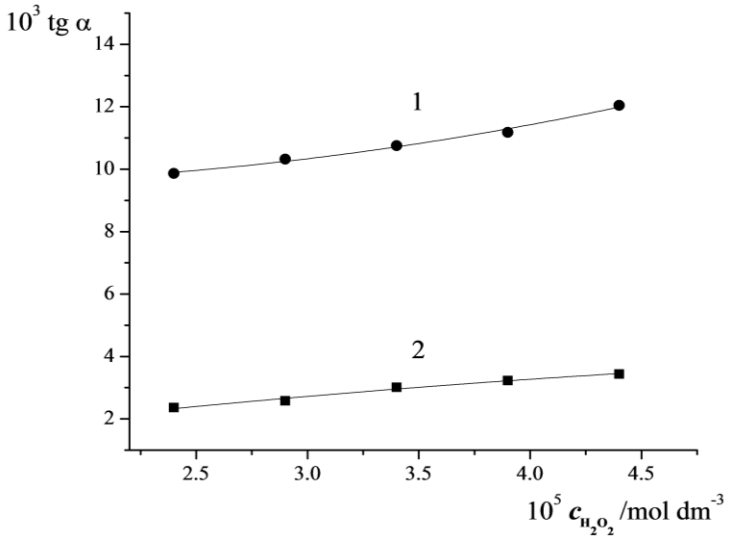

Figure 7. Dependence of the reaction rate on H_2O_2 concentration for tin method development. Initial conditions: 4.0×10^{-5} mol dm^{-3} PF; 2.5 μg cm^{-3} Sn(II); pH 10.4; 20.00±0.02 °C; 1 – inhibitory reaction; 2 – non-inhibitory reaction.

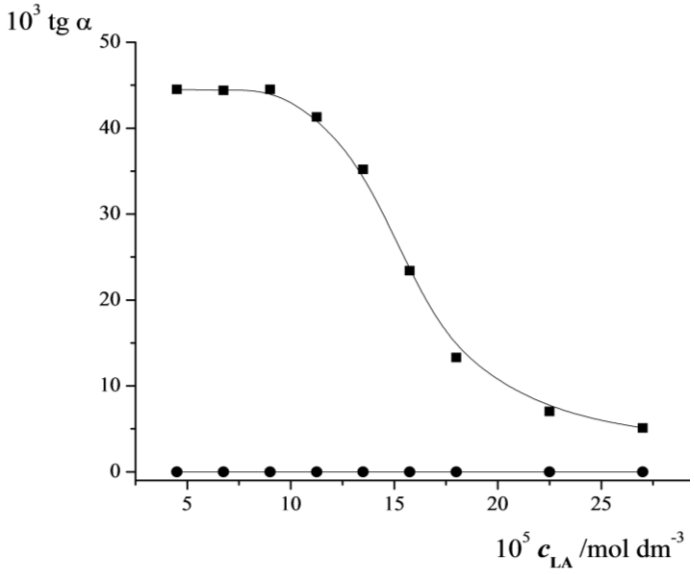

Figure 8. Dependence of the reaction rate on CA concentration for cobalt method development. Initial conditions: 7.3×10^{-5} mol dm^{-3} PF; 1.3 mol dm^{-3} H_2O_2; 1.8×10^{-7} g cm^{-3} Co(II); pH 11.7; 20±0.02 °C; 1 – catalytic reaction; 2 – non-catalytic reaction.

Under the selected conditions, the dependence of catalytic reaction rate on the Co(II) concentration was observed at 20±0.02 °C. The linear dependence of calibration curve falls within the range of 5×10^{-9} to 18×10^{-8} g cm^{-3} Co(II).

The adequate equation of calibration curve for 20±0.02 °C is:

$$\text{Slope} = (0.00253\pm0.00001)c + (0.00178\pm0.00008) \quad (1)$$

where c is Co(II)×10^{-8} concentration in g cm^{-3}.

Under selected conditions, dependence of inhibitory reaction rate on the Sn(II) concentration at 20.00±0.02 °C was tested. The linear range of calibration curve was found to be 0.4 to 4.0 μg cm^{-3} Sn(II).

The adequate equation of calibration curve for 20.00±0.02 °C is:

$$\text{Slope} = (-0.00276\pm0.00002)c + (0.01192\pm0.00017) \quad (2)$$

where c is Sn(II)×10^{-6} concentration in g cm^{-3}.

The accuracy and precision of the methods were checked for three different Co(II) and Sn(II) concentrations within the range of adequate calibration curves. Five repeated measurements were performed for each concentration. Satisfactory results were obtained for both methods. For Co(II) concentrations of 64, 91 and 108 ng cm^{-3}, RSD values were found to be 5.9, 3.6 and 1.5%, respectively. For Sn(II), concentrations of 1.0, 2.5 and 3.5 μg cm^{-3}, *RSD* was found to be 6.2% , 4.2 and 1.3%, respectively.

The selectivity of both methods was established by interference studies: selected ions were separately added in the reaction mixture. The tolerance limit was estimated as the concentration of the added ion that gives up to a 3% relative error in the determination of cobalt and tin. Cations were added as chlorides or nitrates and anions were added as sodium or potassium salts. Each ion was added in six known concentration ratios (0.01:1, 0.1:1, 1:1, 10:1, 100:1 and 1000:1) against the constant Co(II) concentration of 91.0 ng cm^{-3}, for cobalt method investigation and constant Sn(II) concentration of 2.0 μg cm^{-3}, for tin method investigation. The measurements were performed at 20±0.02 °C, and about 30 most frequently used cations and anions were tested (Na^+, K^+, Ag^+, Ca^{2+}, Sr^{2+}, Ba^{2+}, Mg^{2+}, Zn^{2+}, Cd^{2+} Cu^{2+}, Pb^{2+}, Ni^{2+}, Hg^{2+}, Bi^{3+}, Fe^{3+}, Al^{3+}, As^{3+}, Sb^{3+}, Bi^{3+}, acetates, tartarates, oxalates, molybdates, wolframates, Br^-, I^-, Cl^-, NO_3^-, SO_4^{2-}, CO_3^{2-} and PO_4^{3-}) and Sn^{2+} in cobalt method investigation and Co^{2+} in tin method investigation. The results presented in Table 1 reveal that proposed methods for cobalt and tin determination have a very good selectivity.

As it could be noticed, only the presence of Ni^{2+}, in the ratio 1000:1 and Bi^{3+} and Cd^{2+}, in the ratio 10:1, catalyzes the determination of cobalt, while Sn^{2+}, in the ratio 10:1, inhibits the determination of cobalt by this method. The method for tin determination also has very good selectivity because only the presence of Mg^{2+}, in the ratio 100:1 and wolframates, in the ratio 1:1, interferes the tin determination. Co^{2+} and Bi^{3+}, both in the ratio 0.1:1 to the tin concentration, have the catalytic effect to the tin determination by this method. The ions that interfere in the determination of cobalt and tin can be easily removed by standard analytical methods, like masking, precipitation, etc., depending on the sample nature.

The newly developed methods were successfully applied to cobalt and tin determination in chemical

Table 1. Selected results of interference studies for cobalt and tin determination

Added ion	Ion ratio: Co(II)	Cobalt determination	Ion ratio: Sn(II)	Tin determination
Ni(II)	1000	Catalyzes	100	–
Cd(II)	10	Catalyzes	1	–
Mg(II)	100	–	100	Interferes
Bi(III)	10	Catalyzes	0.1	Catalyses
Co(II)	–	–	0.1	Catalyses
Sn(II)	10	Inhibits	–	–
WO_4^{2-}	1000	–	1	Interferes

substances: Co(II) determination in KNO_3 and tin determination in zinc powder.

Solutions containing a known quantity of cobalt were prepared by dissolving the substance in deionised water. The solutions were analyzed by application of both the presented kinetic method and AAS method. The results are shown in Table 2. A good agreement between the results of both methods can be seen.

The solution for tin determination was prepared by dissolving the zinc powder with addition of HNO_3 (1:1) and the small volume of H_2SO_4 (1:3). The solution was vaporized to dry and the residue was dissolved in adequate volume of deionized water. The analysis was performed by applying both the kinetic and AAS methods. The final results are shown in Table 3.

CONCLUSIONS

The limit of quantification (LQ) of 1.1 ng cm^{-3} was reached, and the limit of detection (LD) of 0.3 ng cm^{-3} was obtained for Co(II) determination. The optimized conditions yielded the LD value of 31.2 ng cm^{-3} for Sn(II) determination, while LQ was found to be 107.1 ng cm^{-3}. LQ was defined as the ratio signal:noise = 10:1 and LD was defined as signal 3:1 against the blank. The *RSD* value was found to be in the range 1.5–5.9% for the investigated concentration range of Co(II) and 1.3––6.2% for the investigated concentration range of Sn(II) determination. The methods allow the determination of Co(II) over the concentration range of 5.0–180.0 ng cm^{-3} and 0.4–4.0 μg cm^{-3} for Sn(II). The influence of about 30 selected ions upon the reaction rate was tested in order to assess the selectivity of both methods. The results were validated statistically and through recovery studies. The both methods were confirmed by determination in chemical substances: Co(II) was determined in KNO_3 and Sn(II) was determined in zinc powder. The obtained results were in a good agreement with results obtained by the AAS method.

The activated catalytic reaction (PF, H_2O_2, Co(II), CA) in ammonia buffer media shows better sensitivity for cobalt determination than inhibitory reaction for tin determination (PF, H_2O_2 and Sn(II)) at room temperature.

The new kinetic method for Co(II) nano amounts determination is very sensitive and provides rapid and easy performance at room temperature, with precise, reproducible results and good selectivity. Based on the obtained results, the method is recommendable for the determination of Co(II) in chemical substances of high purity grade. It could also be a good basis for further investigations in the area of kinetic methods for cobalt determination in different samples.

The new kinetic method for Sn(II) micro amounts determination is one of very few known kinetic methods for tin determination in solution. It is inexpensive, rapid, selective and simple to perform. Based on the obtained results, the method is recommendable for determination of Sn(II) in chemical substances as well as in wastewater samples and the other environ-

Table 2. Co(II) determination in KNO_3

Measured, ng cm^{-3}	Kinetic determination[a], ng cm^{-3}	Recovery, %	AAS determination[a], ng cm^{-3}	Recovery, %
10.0	12.6±1.8	126.0	10.5±0.2	105.0
30.0	31.2±1.6	104.0	29.8±0.2	99.3
50.0	50.6±1.0	101.2	50.2±0.2	100.4

[a]The mean value of five measurements±2*SD*

Table 3. Sn(II) determination in zinc powder

Kinetic determination[a], g cm^{-3}	Recovery, %	AAS determination[a], g cm^{-3}	Recovery, %	Kinetic determination[a], g cm^{-3}
$(4.06\pm0.10)\times10^{-7}$	101.5	$(4.01\pm0.02)\times10^{-7}$	100.2	$(4.06\pm0.10)\times10^{-7}$

[a]The mean value of five measurements±2*SD*

mental solutions. It could be used as a good basis for further investigations in the area of kinetic methods for tin determination.

Acknowledgments

The research was supported by the Serbian Ministry of Education, Science and Technological Development (Grant no. 172051).

REFERENCES

[1] Z.M. Grahovac, S.S. Mitić, E.T. Pecev, S.B. Tošić, Kinetic spectrophotometric determination of Co(II) ion by the oxidation of Ponceau 4R by hydrogen peroxide, J. Serb. Chem. Soc. **71** (2006) 189–197.

[2] S.S. Mitić, R.J. Micić, M.V. Budimir, Highly sensitive determination of traces of Co (II) in pharmaceuticals and urine samples using kinetic spectrophotometric method, Anal. Lett. **42** (2009) 935–947.

[3] A. Safavi, H. Abdollahi, H. Nezhad, R. Hormozi, Indirect kinetic spectrophotometric determination of Co (II) based on the reaction with iron (III) in the presence of 1,10-phenantroline, Spectrosc. Lett. **35** (2002) 681–688.

[4] J. Gashemi, A. Niazi, A. Safavi, Simultaneous catalitic determination of cobalt, nickel and cooper using resazurine sulfide reaction and partial square s calibration method, Anal. Lett. **34** (2001) 1389–1399.

[5] A. Afkami, M. Bahram, Mean centering of ratio kinetic profiles as a novel spectrophotometric method for the simultaneous kinetic analysis of binary mixtures, Anal. Chim. Acta **526** (2004) 211–218.

[6] K. Zarei, M. Atabati, Principal component-wavelet neural network as a multivariate calibration method for simultaneous determination of iron, nickel and cobalt, Anal. Lett. **39** (2006) 2085–2094.

[7] M. Gharehbaghi, F. Shemirani, M.D. Faharani, Cold-induced aggregation microextraction based on ionic liquids and fiber optic-linear array spectrophotometry detection of cobalt in water samples, J. Haz. Mat. **165** (2009) 1049–1055.

[8] M. Bahram, K. Farhadi, A. Afkami, D. Shotkatynia, F. Arjmand, Simultaneous kinetic spectrophotometric detection of Cu(II), Co(II)and Ni(II) using partial least squares (PLS) regression, Cent. Eur. J. Chem. **7** (2009) 375–381.

[9] A. Naseri, M. Bahram, M. Mabhooti, A second order standard addittionmethod based on the data treatment by calculation of variation matrix of kinetic systems analysed by MCR-ALS, J. Braz. Chem. Soc. **22** (2011) 2206–2216.

[10] M. Bahram, S. Khezri, Multivariate optimization of cloud point extraction for the simultaneous spectrophotometric determination of cobalt and nickel in water samples, Anal. Meth. **2** (2012) 384–393.

[11] H.R. Pouretedal, P. Sononi, M.H. Keshavarz, A. Semnani, Simultaneous determination of cobalt and iron using first derivative spectrophotometric and H-point standard addition methods in micellar media, Khimiya **18** (2009) 22–36.

[12] M.I. Karayannis, I.A. Pettas, Simultaneous kinetic determination of cobalt, nickel and iron by coupling stopped flow techniques and charge coupled device detection, Anal. Chim. Acta **423** (2000) 277–286.

[13] F.M. Fernandez, M.B. Tudino, O.E. Troccoli, Multicomponent kinetic determination of Cu, Zn, Co, Ni and Fe at trace levels by first and second order multivariate calibration, Anal. Chim. Acta **433** (2001) 119–133.

[14] A.K. Yatsimirskii, M.I. Nelen, A.P. Savitsky, G.V. Ponamarev, Kinetic fluorimetric determination of Cu, Zn, Fe, CO, Ni and Mn divalent ions by their incorporation reactions into a water soluble porfyrin, Talanta **41** (1994) 1699–1706.

[15] M. Otto, J. Rentsch, G. Werner, Optimized spectrophotometric detection of trace cobalt and manganese by their catalysis of the tyron-hydrogen peroxide reaction, Anal. Chim. Acta **147** (1983) 267–275.

[16] L. Romanovskaya, L. Fedorina, V. Solomonov, I. Alekseeva, Cobalt determination in environmental samples, Zavod. Lab. **56** (1990) 14–15.

[17] M.G. Angelova, A.A. Aleksiev, Kinetic spectrophotometric method for the determination of urinary cobalt based on its catalytic effect on the oxidation of L-adrenaline hydrochloride by hydrogen peroxide, Anal. Chim. Acta **290** (1994) 363–369.

[18] J. Medina-Escriche, M. Hernandez-Lorens, M. Llobat-Estelles, A. Sevillano-Cabeza, Determination of vitamin B12 as cobalt by use of a catalytic spectrophotometric method, Analyst **112** (1987) 309–311.

[19] Y. Li, Catalytic kinetic spectrophotometric determination of trace cobalt(II), Huaxue Fence **34** (1998) 408–409.

[20] X. Wang, Catalytic spectrophotometric determination of trace cobalt based on oxidation of alizarin green by H_2O_2, Yejin Fenxi **23** (2003) 17–18.

[21] K.N. Kaul, A.K. Malik, B.S. Lark, A.L.J. Rao, Spectrophotometric determination of cobalt, nickel, copper, palladium and molybdenum using sodium diethyldithiocarbamate in the presence of surfactants, Rev. Roum. Chim. **45** (2001) 221–226.

[22] A.K. Malik, K.N. Kaul, B.S. Lark, W. Faubel, A.L.J. Rao, Spectrophotometric determination of cobalt, nickel, palladium, copper, ruthenium and molybdenum using sodium isoamylxanthate in presence of surfactants, Turc. J. Chem. **25** (2001) 99–105.

[23] A.K. Malik, Spectrophotometric determination of cobalt, nickel, palladium, copper, ruthenium and molybdenum after adsorption of their isoamylxanthate complex onto microcrystalline naphthalene, Ann. Chim-Rome **90** (2000) 581–591.

[24] A.K. Malik, Spectrophotometric determination of iron, cobalt, nickel, copper and palladium using cyclohexylcarbodithioate in the presence of surfactants, Chim. Acta Turc. **26** (1999) 5–10.

[25] G. Kamble, A. Ghare, S. Kolekar, S. Han, M. Anuse, Development of an reliable analytical method for synergistic extractive spectrophotometric determination of Co(II) from alloys and nano composite samples by using chromogenic chelating ligand, Spectrochim. Acta, A **84** (2011) 117–124.

[26] M.B. Gholivand, Y. Mozaffari, S. Sobhani, J. Ghasemi, Simultaneous spectrophotometric determination of trace amounts of cobalt, nickel and copper using the partial least squares method after the preconcentration of their 2-aminocyclopentene-1-dithiocarboxylate complexes on microcrystalline naphthalene, J. Anal. Chem. **63** (2008) 232–238.

[27] B. Pawlik-Skowronska, R. Kaczorowska, T. Skowronski, The impact of inorganic tin on the planktonic cyanobacterium *Synechocystis aquatilis*, the effect of pH and humic acid, Env. Poll. **97** (1997) 65–69.

[28] X. Huang, W. Zhang, S. Han, X. Wang, Determination of tin in canned foods by UV–Vis spectrophotometry technique using mixed surfactants, Talanta **44** (1997) 817–822.

[29] S. Rubio, A. Gomez-Hens, M. Valcarcel, Fluorimetric determination of tin at the nanograms per mililitre level in canned beverages, Analyst **110** (1985) 43–45.

[30] J.L. Manzoori, M. Amjadi, D. Abolhasani, Spectrophotometric determination of tin in canned foods, J. Haz. Mat. **137** (2006) 1631–1635.

[31] A. Ribeiro, A. Moretto, M. Arruda, S. Cadore, Analysis of Powdered Coffee and Milk by ICP OES after Sample Treatment with Tetramethylammonium Hydroxide, Microchim. Acta **141** (2003) 149–155.

[32] L.F. Capitan-Vallvey, M.C. Valensia, G. Miron, Flow-injection method for the determination of tin in fruit juices using solid-phase spectrophotometry, Anal. Chim. Acta **289** (1994) 365–370.

[33] M. Burguera, J. Burguera, C. Rivas, P. Carrero, R. Brunetto, M. Gallignani, Time based device used for the determination of tin by hydride generation flow-injection atomic absorption techiques, Anal. Chim. Acta **308** (1995) 339–348.

[34] Y.H. Li, H. Long, F.Q. Zhou, Determination of trace tin by catalytic adsorptive cathodic stripping voltammetry, Anal. Chim. Acta **554** (2005) 86–91.

[35] E. Hutton, S. Hočevar, L. Mauko, B. Ogorevc, Bismuth film electrode for anodic stripping voltammetric determination of tin, Anal. Chim. Acta **580** (2006) 244–250.

[36] J. Moreda-Pineiro, P. Lopez-Mahia, S. Muniatequi-Lorenzo, E. Fernandez-Fernandez, D. Prada-Rodriguez, Tin determination in marine sediment, soil, coal fly ash and coal slurried samples by hydride generation electrothermal atomic absorption spectrometry, Anal. Chim. Acta **461** (2002) 261–271.

[37] I. Lopez-Garsia, I. Arnau-Jerez, N. Campillo, M. Hernandez-Cordoba, Determination of tin and titanium in soils, sediments and sludges using electrothermal atomic absorption spectrometry with slurry sample introduction, Talanta **62** (2004) 413–419.

[38] M.A. Taher, B.K. Puri, Differential pulse polarographic determination of tin in alloys and environmental samples after preconcentration with the ion pair of 2-nitroso--1-naphtol-4-sulfonic acid and tetradecyldimethylbenzylammonium chloride onto microcrystalline naphthaene or by column method, Talanta **48** (1999) 355–362.

[39] T. Madrakian, A. Afkhami, R. Moein, M. Bahram, Simultaneous spectrophotometric determination of Sn(II) and Sn(IV) by mean centering or ratio kinetic profiles and partial squares methods, Talanta **72** (2007) 1847––1852.

[40] Z. Zhou, D. Peng, Determination of trace tin by catalytic reduction decoloration spectrophotometry, Guangpu Shiyanshi **15** (1998) 40–43.

[41] D. Perez-Bendito, M. Silva, Kinetic methods in analytical chemistry, John Wiley & Sons, Chichester, 1988.

IZVOD

ANALITIČKA PRIMENA REAKCIONOG SISTEMA FENIL-FLUORON–VODONIK-PEROKSID ZA KINETIČKO ODREĐIVANJE TRAGOVA KOBALTA I KALAJA SPEKTROFOTOMETRIJSKI U AMONIJAČNOM PUFERU

Sofija M. Rančić[1], Snežana D. Nikolić-Mandić[2], Aleksandar Lj. Bojić[1]

[1]*Departman za hemiju, Prirodno–matematički fakultet, Univerzitet u Nišu, Srbija*
[2]*Hemijski fakultet, Univerzitet u Beogradu, Srbija*

(Naučni rad)

Pri određivanju Co(II), ostvarena je granica određivanja (LQ) od 1,1 ng cm^{-3} i granica detekcije (LD) od 0,3 ng cm^{-3}. Pod optimalnim uslovima, nađeno je da LD, pri određivanju Sn(II), iznosi 31,2 ng cm^{-3}, a LQ je 107,1 ng cm^{-3}, pri čemu je LQ definisan kao odnos signal:šum = 10:1, a LD kao signal 3:1 u odnosu na slepu probu. RSD se pri određivanju kobalta kreće u rasponu od 1,5–5,9% za ispitivani interval koncentracija Co(II), odnosno u rasponu od 1,3–6,2%, za ispitivani interval koncentracija Sn(II). Novom metodom je moguće određivanje Co(II) u opsegu od 5,0–180,0 ng cm^{-3}, kao i određivanje Sn(II) u opsegu od 0,4–4,0 μg cm^{-3}. Radi utvrđivanja selektivnosti novih metoda, ispitan je uticaj dodatka tridesetak različitih jona na brzinu, kako katalizovane, tako i inhibirane reakcije i utvrđena je njihova dobra selektivnost. Rezultati su statistički obrađeni i komentarisani. Metode su proverene određivanjem kobalta i kalaja u hemijskim supstancama: Co(II) je određivan u KNO_3, a Sn(II) u cinku u prahu. Dobijeni rezultati pokazuju dobro slaganje s rezultatima dobijenim ispitivanjem istih uzoraka AAS metodom.

Ključne reči: Određivanje Co(II) • Određivanje Sn(II) • Kinetičko spektrofotometrijska metoda

Meat quality characteristics of Duroc×Yorkshire, Duroc×Yorkshire×Wild Boar and Wild Boar

Snežana D. Ivanović[1], Zoran M. Stojanović[2], Jovanka V. Popov-Raljic[3], Milan Ž. Baltić[4], Boris P. Pisinov[1], Ksenija D. Nešić[1]

[1]*Scientific Veterinary Institute of Serbia, Belgrade, Serbia*
[2]*Serbian Environmental Protection Agency SEPA, Belgrade, Serbia*
[3]*Faculty of Agriculture, Zemun, Serbia*
[4]*Faculty of Veterinary Medicine, University of Belgrade, Belgrade, Serbia*

Abstract

Chemical composition, pH value, fatty acids profile, cholesterol content, color and sensory analysis of pork meat from Duroc×Yorkshire (D×Y), Duroc×Yorkshire×wild boar (D×Y×WB) crossbreeds and wild boars (WB) was investigated. Samples for all tests were taken from *m. longissimus dorsi*. The chemical composition and pH value were tested by ISO methods. Fatty acid and cholesterol determination was performed by gas chromatography with external standard. The color was determined instrumentally using the thristimulus colourimeter. The overall sensory quality (appearance, texture and smell) of samples of raw meat was evaluated. A scoring system was used in the evaluation of the results. Statistically significant differences ($p < 0.05$) were found in the chemical composition (moisture, fat, protein and ash) and pH values between each of the examined groups, as well as fatty acids and cholesterol content among all the examined groups. Measurments of the colour of meat from all three groups showed that the L^*, a^*, b^*, Chroma and Hue angle were also statistically significantly different ($p < 0.01$)

Keywords: meat quality, Duroc, Yorkshire, wild boar.

Available online at the Journal website: http://www.ache.org.rs/HI/

PROFESSIONAL PAPER

UDC 637.5'64.05

Hem. Ind. **67** (6) 999–1006 (2013)

doi: 10.2298/HEMIND121211017I

The quality of pork meat includes different aspects: technological (water holding capacity, pH, intensity and homogeneity of colour, firmness and processing yield), chemical (protein, fat, fatty acids profile and content of cholesterol, conjugated linoleic acid, vitamins and minerals) and sensory (colour, marbling, tenderness, juiciness and flavour). These aspects are influenced by many factors before and after the slaughtering.

The pH value in the muscle after slaughtering is the main factor that affects the meat colour, water holding capacity of binding water, water loss during cooking, processing yield, etc. Rapid acidification of muscle proteins leads to their denaturation and some irregular metabolic processes [1]. The proximate composition and intramuscular fat content are important factors that affect the meat quality and nutritional value. The proximate composition of meat depends on many factors, such as the anatomic region, type of muscle fibres and condition of animal, breed and diet. There are many differences in the fatty acid composition of meat and adipose tissue between various kinds of animals. In pigs, the adipose tissue has a higher content of fat than meat, but the fatty acid composition is similar as in meat [2]. The content of linoleic acid is higher in tissues of pigs than in tissues of cattle and small ruminants. Linoleic acid originates primarily from the feed. It passes unchanged through the intestines of pigs, then through blood vessels, and is finally incurporated into the tissue. Different fatty acid composition in meat can be achieved by adding some fatty acids in feed mixtures or using feedstuffs that have higher content of ω-3 fatty acids, such as linen seed. The recommended relation between all polyunsaturated and saturated fatty acids in nutrition is 0.4 or higher, and it is higher in pigs than in ruminants [2]. Selection of pigs in recent decades has mostly been focused on production of large amount of lean meat. New genetic lines deposit less fat in the body and they have less live weight than traditional breeds. To this aim, in modern pig breeding Duroc pigs are chosen because of suitable intramuscular fat content [3,4].

One of the most important meat attributes is colour, which is caused by concentration of myoglobin, its chemical status on the surface of meat, structure and physical status of muscle proteins and the proportion of muscular fat [5]. The colour of meat depends also on the age, condition, diet and pH values [6]. Some authors suggest that the content of myoglobin in skeletal muscle depends on race, while other authors found no differences.

Correspondence: S. Ivanović, Scientific Veterinary Institute of Serbia, Autoput 3, 11070 Belgrade, Serbia.
E-mail: snezaivanovic@gmail.com
Paper received: 11 December, 2012
Paper accepted: 22 February, 2013

The sensory perception of meat depends on many factors, such as the characteristics of the breed, weight, sex, diet and the biochemical changes that occur during further processing, slaughtering, maturation, heat treatment and cooking [7]. The eating pork quality, evaluated as sensory perceptions during consumption, consists of several attributes. Among the most important are tenderness, juiciness, flavour and absence of off-flavours [8]. In the case of raw meat bought by consumers for house consumption, the significant traits are the amount of visible fat and colour [9].

The aim of this paper was to investigate if there were any statistically significant differences between chemical composition and pH value, fatty acid composition, cholesterol content, colour and sensory characteristics of pork meat originating from Duroc×Yorkshire (D×Y), Duroc×Yorkshire×wild boar (D×Y×WB) and wild boars (WB).

MATERIALS AND METHODS

A total of 60 pigs were used for the trial: 20 castrated males Duroc×Yorkshire (D×Y), 20 castrated males Duroc×Yorkshire×wild boar (first generation crossed pig Duroc×Yorkshire with wild boar) (D×Y×WB) and samples collected from 20 shot wild boars (WB). Pigs were bred under the same conditions and fed with the same standard diet adequate for their category. Breeding of pigs was under all hygienic and zootechnical conditions. The animals were slaughtered at final live weight that was in the range 96–112 kg.

Wild boars weighed between 140 to 150 kg and aged about one year. The hunting ground is located in the southwest and southeast region Šumadija, Serbia. These are primarily habitats of steppe and steppe forest vegetation, which predominates in deciduous trees – oak, elm, linden, chestnut and hazel. The dominating herbaceous species are *Graminaceae*, *Asteraceae* and *Poaceae*, and the representative cereals are corn, wheat and barley [10].

The material used for the determination of chemical composition, fatty acids and cholesterol content was *m. longissimus dorsi* from the left side of the halves. For colour measurement, the same muscle from the right side of halves was used. Protein content was calculated from nitrogen content multiplied by 6.25 using relevant ISO standards [11]. The fat content was determined according to relevant ISO standards [12], as well as moisture content [13], ash content [14] and pH value [15]. Chemical parameters and pH were measured in the meat 24 h after slaughter. The Folch–Lees method [16] was applied for the lipid extraction from the tissue. After the lipid hydrolysis, the fatty acids were esterified to methyl esters, evaporated to dryness in a stream of nitrogen and stored at –18 °C. Analysis of FAMEs and cholesterol was performed by an external standard method using a gas chromatograph (GC6890N, Agilent Tech., USA) by comparing with standard mix of FAMEs 37 (Supelco, USA).

The colour was measured on the fresh meat cuts of the *m. longissimus dorsi pars lumborum*, from the right side of each carcass (n = 20, two times, for each sample). CIE $L^*a^*b^*$ and CIEYxy colour coordinates [17] were determined using a Minolta chromameter CR-400 (Minolta Co Ltd., Osaka, Japan) in D-65 lighting, with a standard angle of 2° of shelter and 8 mm aperture of the measuring head. In CIE $L^*a^*b^*$ results were given as the mean values: L^* – psychometer light, a^* – psychometer tone, b^* – psychometer chroma, hue angle and chroma.

The overall sensory quality (appearance, texture and smell) of all samples of raw meat from D×Y, D×Y×WB and WB was evaluated. A scoring range of 1.00 to 5.00 was used, with the possibility of assigning half- and quarter-points. For each selected quality characteristic the coefficient of importance (*CI*) was determined, which was used for the correction (multiplication) of given ratings. The coefficients were chosen according to the importance of effect of individual characteristics on the overall quality, and balanced so that their sum was 20. Addition of individual scores gave us a complex indicator that represented the overall sensory quality and was expressed as "percentage of the maximum possible quality". Dividing that value by the sum of the coefficients obtained by weighted importance mean score, which also represented the overall sensory quality of raw meat samples D×Y, D×Y×WB and WB. Rating: 1.00 – very pronounced errors, 2.00 – pronounced errors, 3.00 – noticeable deviations, 4.00–5.00 and slight differences – fully meets the requirements for quality. In evaluation of sensory characteristics of raw meat quality D×Y, D×Y×WB and WB [18], 20 experienced tasters were involved [19,20].

Data obtained in investigations were analysed by descriptive and analytical statistics, using Microsoft Excel 2003, ANOVA and the differences between two averages were compared by the t-test at the level of significance of 99% and 95%.

RESULTS

The results obtained during the investigation relating live animal weight, chemical composition and pH value of pork meat are shown in Table 1.

The wild boars had bigger live weight ($P < 0.05$) than D×Y×WB and D×Y, but D×Y did not differ ($P > 0.05$) from D×Y×WB. The average water means, expressed as percentage, showed that there were differences between all mutually compared groups ($P < 0.05$). There were also differences between all mutually compared groups ($P < 0.05$) regarding total fats, as well as

Table 1. Live animal weight, chemical composition and pH value of the m. longissimus dorsi in Duroc×Yorkshire, Duroc×Yorkshire×wild boar and wild boar (n = 20); a,b,c – row means with different superscripts differ significantly at P < 0.05

Parameter	Breeds of pigs		
	Duroc×Yorkshire	Duroc×Yorkshire×wild boar	Wild boar
Live weight, kg	100.48^{a}±4.99	100.85^{b}±4.88	144.77^{c} ±3.29
Moisture, %	74.42^{c}±0.07	74.07^{b}±0.03	72.97^{a}±0.09
Fat, %	2.78^{c}±0.05	2.26^{b}±0.04	1.87^{a}±0.11
Protein, %	21.80^{a}±0.14	22.12^{b}±0.06	23.67^{c}±0.22
Ash, %	0.84^{a}±0.08	1.33^{c}±0.03	1.26^{b}±0.11
pH, after 24 h	5.79^{b}±0.09	5.80^{c}±0.07	5.48^{a}±0.02

for average proteins values and the average ash mean. The pH value of D×Y meat did not differ ($P > 0.05$) from D×Y×WB meat, while the pH value of WB meat was significantly lower than D×Y meat and D×Y×WB meat ($P < 0.05$).

Results of examination of fatty acid composition and cholesterol content in pork from three groups D×Y, D×Y×WB and WB are presented in Table 2. This table shows that there were differences between all mutually compared groups ($P < 0.05$).

Instrumentally measured values regarding the colour characteristics of meat samples, expressed in CIE *L*a*b** system for three groups are presented in Table 3.

For the values obtained for lightness of meat (*L**) between all mutually compared groups there were differences ($P < 0.01$). Regarding redness of meat (a*) the WB meat differed ($P < 0.01$) from D×Y meat and D×Y×WB meat, while D×Y meat did not differ ($P > 0.01$) from D×Y×WB. Regarding obtained values for yellowness of meat (*b**) the WB meat differed ($P < 0.01$) from D×Y meat and D×Y×WB meat, while D×Y meat did not differ ($P > 0.01$) from D×Y×WB meat. For the hue angle, the WB meat differed ($P < 0.01$) from D×Y meat and D×Y×WB meat, but D×Y meat did not differ ($P > 0.01$) from D×Y×WB meat. The obtained chroma values in WB meat differed ($P < 0.01$) from D×Y meat and D×Y×WB meat, while in D×Y meat did not differ ($P > 0.01$) from D×Y×WB meat.

Based on sensory estimation of appearance, *i.e*., colour and surface of raw meat pieces from different breeds of pigs (visual technique), it is evident that the greatest number of points was obtained from D×Y×WB sample (20±0.25), and it had a peculiar colour. Then follows a D×Y sample (18.80±0.28), which was slightly darker than the previous sample. The sample with the lowest number of points for colour as appearance and size, was a sample of WB meat (18.00±0.28) (Table 4). Generally speaking, those were minor differences in shades, *i.e*., surface brightness, among different kinds of raw pork pieces, but still visually characterized by highly experienced and trained tasters as "conditional" different, but characteristic shades of colour. This observation is in accordance to results of instrumental colour determination, the same samples of pig raw meat, measured by the Minolta CR-400 chromameter (Table 3).

For the sample D×Y by visual technique characteristic, uniform distribution of muscle fibers at the intersection of pig meat was reported (14.00±0.25), and the corresponding characteristic hardness (15.00±0.23), evaluated by palpatory technique. Practically, for the textural properties samples of D×Y×WB raw meat

Table 2. Fatty acid composition and cholesterol of the m. longissimus dorsi of Duroc×Yorkshire, Duroc×Yorkshire×wild boar and wild boar (n = 20); a,b,c – row means with different superscripts differ significantly at P < 0.05

FAME (% of total fatty acids)	Breeds of pigs		
	Duroc×Yorkshire	Duroc×Yorkshire×wild boar	Wild boar
Myristic acid (C14:0)	1.53^{a}±0.02	2.40^{b}±0.03	3.01^{c}±0.51
Palmitic acid (C16:0)	25.55^{a}±0.09	30.34^{b}±0.41	33.20^{c}±0.30
Palmitoleic acid (C16:1)	2.69^{c}±0.07	1.76^{b}±0,03	0.65^{a}±0.01
Stearic acid (C18:0)	14.29^{a}±0.20	19.08^{b}±0.16	21.97^{c}±0.13
Oleic acid (C18:1)	43.18^{c}±0.29	40.01^{b}±0.20	36.15^{a}±0.12
Linoleic acid (C18:2)	9.28^{c} ±1.64	5.17^{b}±0.03	3.29^{a}±0.02
SFA	41.37	51.82	58.18
USFA	55.15	46.94	40.09
USFA/SFA	1.33	0.91	0.69
Cholesterol, mg/100 g	59.80^{c}±0.62	51.00^{b}±0.55	44.94^{a}±0.55

*Table 3. Colour parameters of the m. longissimus dorsi of Duroc×Yorkshire, Duroc××wild boar and wild boar expressed in CIE L*a*b* system (n = 20); a,b,c – row means with different superscripts differ significantly at P < 0.05*

Colour parameter	Breeds of pigs		
	Duroc×Yorkshire	Duroc×Yorkshire×wild boar	Wild boar
Lightness – *L**	50.50^{c}±1.00	48.40^{b}±1.10	42.16^{a}±1.47
Redness – *a**	7.58^{a}±0.50	7.75^{a}±0.40	11.97^{b}±0.44
Yellowness – *b**	14.20^{b}±0.60	14.70^{b}±0.50	8.94^{a}±0.33
Hue angle	30.50^{b}±2.10	30.30^{b}±1.70	26.13^{a}±2.21
Chroma	16.10^{b}±0.60	16.60^{b}±0.50	11.75^{a}±1.19

(12.50±0.18) and samples of raw WB meat (12.50±0.16) were evaluated with the same score (Table 4). Our results of sensory evaluation of smell of raw meat from different breeds of pigs clearly show that meat of WB had very peculiar, stable odour intensity (48.50±0.20), then the characteristic smell of D×Y×WB meat (47.50±0.13), and slightly lower, but still characteristic odour intensity of D×Y meat (46.00±0.32) (Table 4).

So we could surely say that from the sensory point (assessing odour), the highest quality was found for the meat of wild boar. The percentage of the maximum score for all evaluated characteristics, as well as the weighted mean value of ratings is shown in Table 4. Based on the total number of points that is high sensory quality, the order would be as follows: D×Y (93.80/ /4.69), D×Y×WB (92.00/4.60) and WB (92.0/4.50).

DISCUSSION

For D×Y and D×Y×WB meat, the chemical composition depends on the diet, race, manner of holding and other factors. According to Pierson [21], fats are the basic ingredient for the perception of taste in the meat, as it is characteristic for the taste of meat of different animal species. Kim *et al.* [22] in their research showed that the chemical composition is not the same in all muscles of pig carcass. They investigated 21 muscles. The muscle *longissimus dorsi* is very interesting for comparison with our results. According to these authors, the percentage of water was 75.51%, protein 21.79%, fat 2.02% and ash 0.99%. Our results were not in agreement with the results of these authors. Jukna and Jukna [23] have also investigated the chemical composition of *m. longissimus dorsi* from different pig breeds. We can compare the findings with the chemical composition of *m. longissimus dorsi* Yorkshire. Our results for water, protein and ash in the first two test groups were similar with the findings of these authors (water 74.91%, protein 22.39% and ash 1.09%), while the fat was different (1.61%). Oliver *et al.* [3] studied the chemical composition of *m. longissimus dorsi* of five different crossbreeds, which included Duroc (DU), Landrace (LR), Large White (LW) and Belgian Landrace (BL). In our research, obtained values for water, fat, protein and ash in the first two test groups were the closest to the authors who got the breed DU×(LR×LW). Their findings were 74.12% of water, fat 1.88% and 22.51% of protein. Jacyno *et al.* [24] studied chemical composition in *m. longissimus dorsi* of fleshy pigs: water 72.70%, 23.50% protein, 2.79% intramuscular

Table 4. Sensory evaluation of pigs meat

Breeds of pigs		Attribute				Percentage of maximal possible quality 100	Weighted average 100/20
		Appearance	Texture		Flavour		
		Colour surface	Visual evaluated structure	Palpatory evaluated firmness	Olfactory evaluated odour		
		Coefficient of importance					
		4	3	3	10		
Duroc×Yorkshire	M	18.80	14.00	15.00	46.00	93.80	4.69
	Sd	0.28	0.25	0.23	0.32		
	Cv	1.47	1.76	1.51	0.71		
Duroc×Yorkshire ×wild boar	M	20.00	12.50	12.00	47.50	92.00	4.60
	Sd	0.25	0.18	0.18	0.13		
	Cv	1.27	1.42	1.42	0.28		
Wild boar	M	18.00	12.50	11.00	48.50	90.00	4.50
	Sd	0.28	0.16	0.39	0.20		
	Cv	1.58	1.28	3.58	0.41		

fat. The results of these authors concerning the content of water and protein are not in agreement with our results, while the content of intramuscular masses is in line. Our results regarding fat approximate the findings of Václavková and Bečková [25], who examined the effects of various additives on the chemical composition of the *m. longissimus dorsi* of crossbreed (Czech Large White×Czech Landrace)×(Hampshire×Pietrain). Our findings of fat content in *m. longissimus dorsi* of Duroc×Yorkshire (D×Y) and Duroc×Yorkshire×wild boar (D×Y×WB) were similar to the findings of fat in *m. longissimus dorsi* of the control group (2.10±0.40 %) which was regularly fed. However, our results of intramuscular fat were different from the findings (1.6±0.4) of Simek *et al.* [26]. The same authors have determined the pH values in all lines after 24 h. The values ranged from 5.6±0.1 to 5.7±0.2, and were in accordance with the values that we noted 24 h after, by measuring samples D×Y (5.79±0.09) and the D×Y×WB (5.80±0.07). Kasprzyk *et al*. [27] measured the pH value of the crossed (Hampshire×Wild boar) after 24 h from the time of slaughter 5.75±0.22, which is consistent with our results for pH values of D×Y×WB (5.80±0.07). The same authors measured the Pulawska line (5.41±0.25), which was lower value than we had got in D×Y (5.79±0.09).

Václavková and Bečková [25] in the same experiment examined the prevalence of specific fatty acids. Their findings for myristic C14: 0 (1.29±0.17), palmitic C16: 0 (24.44±1.08), stearic C18: 0 (12.78±0.52), oleic C18: 1 (40.40±1.53) and linoleic acid C18: 2 (1.77±7.53) in a control group of pigs that were given standard feed, as our pigs in the first two groups, did not agree with our findings (Table 3). This probably happened as a result of different races. Wood *et al*. [4] studied the effect of keeping and feeding on fat deposition in muscle and presence of some fatty acids in different muscles. They investigated the composition of *m. longissimus dorsi* of Berkshire and Tamworth, Large White and Duroc line. We can compare our results from first two groups with their findings relating to the control group Duroc line that received standard feed. Their findings for myristic C14: 0 (1.59), palmitic C16: 0 (23.85), stearic C18: 0 (15.56), oleic C18: 1 (36.17), and linoleic acid C18: 2 (12.02) were significantly different from our findings, which again indicates the influence of race on the fatty acid composition of individual muscles. Furman *et al.* [28] examined the commercial fat, meat-type pigs (hybrid Large White×Slovenian Landrace mated by Pietrain, Duroc or Piertain×Slovenian Landrace) and normal fatty acid composition of *m. longissimus dorsi*. Their findings of myristic C14: 0 (1.22), palmitic C16: 0 (22.55), palmitoleic acid C16: 1 (3.23), stearic C18: 0 (11.49), oleic acid C18: 1 (40.21) and linoleic acid C18: 2 (12.75) were also significantly different from our results concerning the first two groups of pigs (Duroc×Yorkshire and Duroc×Yorkshire×wild boar). Jacyno *et al.* (2006) studied fatty acid composition in *m. longissimus dorsi* of fleshy pigs. Their findings for myristic C14: 0 (1.29), palmitic C16: 0 (22.95), palmitoleic acid C16: 1 (4.63), stearic C18: 0 (11.50), oleic acid C18: 1 (44.27) and linoleic acid C18: 2 (10.26) were not in accordance with our results. The finding by the same authors for total cholesterol was 63.2 mg/100 g which was not in agreement with our findings (59.80±0.62 mg/100 g and 51.00±0.55 mg/100 g).

Marchiori *et al.* [29] instrumentally measured the colour of *m. longissimus dorsi* in pigs that were grown under controlled conditions. *L** values (59.00±2.72), *a** (7.65±1.43), *b** (16:38±0.79) were measured after 48 h from the time of slaughter. *L** values were higher than ours (Table 4), indicating that their meat was lighter on the surface in relation to our first two groups. Oliver *et al.* [3] studied the colour of *m. longissimus dorsi* from five different crossbreeds, which included Duroc (DU), Landrace (LR), Large White (LW) and Belgian Landrace (BL). The measured values for meat of Duroc were: *L** (54.06±0.60), *a** (7.55±0.32), *b** (6.48±0.27). *L** values were higher than ours (Table 4), indicating that their meat was lighter than ours in the first two groups. On the other hand, colour of meat, measured after seven days, from *m. longissimus lumbrorum* taken from the slaughtered pig breeds Large White Landrace [30] was darker (*L** 45.9, *a** 9.3, *b** 8.1) than meat from our first two groups (Table 3).

For wild boar, Postolache *et al*. [31] investigated the chemical composition of *m. longissimus dorsi* in shot wild pigs in Romania, aged 3–4 years. Their findings were 75.36% for water, 21.81% for protein, fat 2.58%, and the pH value measured after 24 h (post mortem) was 5.56. Results regarding water, proteins and fats were not in agreement with our results, while the pH value was in accordance with our findings. That difference can be explained by a different diet and different age. With respect to pH value in the wild boars meat, our results (5.48±0.02) were consistent with the results (5.46±0.14) from Marchiori *et al*. [27], but the pH value of our measurements was the lower from pH values (5.80±0.18) that were measured by Kasprzyk *et al*. [26].

Quaresma *et al.* [32] examined intramuscular lipids, cholesterol and fatty acid composition in major muscle of shot wild boars in Portugal. They found that the fat content was 4.75%, cholesterol 58.7 mg/100 g, fatty acid – myristic C14:0 (1.00), palmitic C16:0 (20.70), palmitoleic acid C16:1 (2.20) stearic C18:0 (10.50), oleic acid C18:1 (39.70) and linoleic C18:2 (15.90). Our results were consistent with the results of these authors.

Marchiori *et al.* [27] had also measured the colour of the wild boars *m. longisimus dorsi*. *L** value

(49.00±3.48), *a** (9.50±1.46), *b** (12.99±1.33) were measured after 48 h of the moment of slaughter. *L** value was higher than ours (Table 4), suggesting that their wild boars meat was lighter than ours.

It is difficult to compare the results of sensory analysis between different authors. It is also difficult to compare different techniques. But, our results can be compared with the results of Kasprzyk *et al.* [26]. These authors evaluated Pulawska meat, wild boar and Pulawska×(Hampshire×Wild boar). In meat of those wild boars authors received the lowest rating, while the meat of the cross-breed got a perfect score. Morrison *et al.* [33] investigated the effect of different cultivation methods on sensory qualities. Evaluation was carried out by panel test. The scores varied slightly, but did not differ ($P > 0.05$) in tenderness, juiciness, pork flavour or overall desirability of pork produced from the two housing treatments. The results of Morrison *et al.* [33] were similar to ours. Although our results have got slight differences in the sensory evaluation of appearance, they did not affect the acceptability of meat.

CONCLUSIONS

1. Based on the obtained results, it can be concluded that there was a statistically significant difference ($P < 0.05$) between all three groups in the average water content, total fat, average protein value and ash content. Regarding live weight and pH values there was no statistically significant difference ($P > 0.05$) between D×Y and D×Y×WB, while it was noted between D×Y and WB, as well as between D×Y×WB and WB ($P < 0.05$).

2. According to the obtained results regarding fatty acids profile and cholesterol content there was a statistically significant difference ($P < 0.05$) between all three groups.

3. By instrumental measurements of the colour characteristics of meat samples it can be concluded that for *L** there was a statistically significant difference ($P < 0.05$) between all three groups. But, regarding *a**, *b**, hue angle and chroma there was no statistically significant difference ($P > 0.05$) between D×Y and D×Y×WB, while however it was noted between D×Y and WB, as well as between D×Y×WB and WB ($P < < 0.05$).

Based on the total number of points, *i.e.*, mean sensory quality score, the order would be as follows: D×Y (93.80/4.69), D×Y×WB (92.00/4.60) and WB (92.0/4.50).

REFERENCES

[1] P. Sellier, G. Monin, Genetics of pig meat quality, A review J. Muscle Foods **5** (1994) 187.

[2] J.D. Wood, M. Enser, A.V. Fisher, G.R. Nute, P.R. Sheard, R.I. Richardson, S.I. Hughes, F.M. Whittington, Fat deposition, fatty acid composition and meat quality, A review, Meat Sci. **78** (2008) 343–358.

[3] M.A. Oliver, P. Gou, M. Gispert, A. Diestre, J. Arnau, J.L. Noguera, A. Blasco, Comparison of five types of pig crosses. Ll. Fresh meat quality and sensory characteristics of dry cured ham, Livest. Prod. Sci. **40** (1994) 179––185.

[4] J.D. Wood, G.R. Nute, R.I. Richardson, F.M. Whittington, O. Southwood, G. Plastow, R. Mansbridge, N. da Costa, K.C. Chang, Effects of breed diet and muscle on fat deposition and eating quality in pigs, Meat Sci. **67** (2004) 651–667.

[5] I.K. Vukovic, The basics of meat technology (2nd ed.). Veterinary Chamber of Serbia, Belgrade, Serbia, 1998.

[6] USDA, The Color of Meat and Poultry, Food Safety and Inspection Service, Washington D.C., USA, 2008. Available at: http://www.fsis.usda.gov

[7] M. Flores, E. Armero, M.C. Aristoy, F. Toldrá, Sensory characteristics of cooked pork loin as affected by nucleotide content and post mortem meat quality, Meat Sci. **51** (1999) 53–59.

[8] E.A. Bryhni, D.V. Byrne, M. Rodbotten, Consumer and sensory investigations in relation to physical/chemical aspects of cooked pork in Scandinavia, Meat Sci. **65** (2003) 737–748.

[9] Resurreccion AVA, Sensory aspects of consumer choices for meat and meat products, Meat Sci. **66** (2004) 11–20.

[10] S. Jovanović, Sinekological and floristic study of ruderal vegetation on Belgrade region. DPh. thesis, University of Belgrade, Belgrade, Serbia, 1992.

[11] ISO 937 (1992), Meat and meat products - Determination of nitrogen content. International Organization for Standardization, Geneva, Switzerland.

[12] ISO 1443 (1992), Meat and meat products – Determination of total fat content. International Organization for Standardization, Geneva, Switzerland.

[13] ISO 1442 (1998), Meat and meat products – Determination of moisture content. International Organization for Standardization, Geneva, Switzerland.

[14] ISO 936 (1999), Meat and meat products – Determination of total ash. International Organization for Standardization, Geneva, Switzerland.

[15] ISO 2917 (2004), Meat and meat products – Measurement of pH, Reference method. International Organization for Standardization, Geneva, Switzerland.

[16] J. Folch, M. Lees, G.H.S. Stanley, Eine einfache Methode zur Isolierung und Reinigung der Lipide aus tierisch Gewebe, J. Biol. Chem. **226** (1957) 497–509.

[17] CIE Colorimetry Committee, Technical notes: working program on colour differences, J. Opt. Soc. Am. **64** (1986) 896–897.

[18] ISO 5492 (2000), Sensory analysis – Vocabulary. International Organization for Standardization, Geneva, Switzerland.

[19] ISO 8586-1 (1993), Sensory analysis-General guidance for the selection, training and monitoring of assessors.

International Organization for Standardization, Geneva, Switzerland.

[20] ISO 8586-2 (1994,) Sensory analysis-General guidance for the selection,training and monitoring of assessors – Part 2. International Organization for Standardization, Geneva, Switzerland.

[21] A.M. Pearson, T.A. Gillett, Processed meat (3rd ed.), Aspen Publisher Inc., Gaithersburg, ML, 1999.

[22] H.J. Kim, N.P. Seong, H.S. Cho, Y.B. Park, H.K. Hah, H.L. Yu, G.D. Lim, H.I. Hwangl, H.D. Kim, M.J. Lee, N.C. Ahn, Characterization of Nutritional Value for Twenty-one Pork Muscles, Asian-Aust J. Anim. Sci **21** (2008) 138–143.

[23] V. Jukna, C. Jukna, The comparable estimatimation of meat quality of pigs breeds and their combinations in Lithuania, Biotechnol. Anim .Husband **21** (2005)175–179.

[24] E. Jacyno, A. Pietruszka, A. Kołodziej, Influence of pig meatiness on pork meat quality, Pol. J. Food Nutr. Sci. **56** (2006) 137–140.

[25] E. Václavková, R. Bečková, Effect of linseed in pig diet on meat quality and fatty acid content. Arch. Tierz. Dummerstorf Special Issue **50** (2007) 144–151.

[26] J. Simek, M. Grolichová, Steinhauserová I, Steinhauser L, Carcass and meat quality of selected final hybrids of pigs in the Czech Republic, Meat Sci. **66** (2004) 383–386.

[27] A. Kasprzyk, A. Stasiak, M. Babicz, Meat quality and ultrastructure of muscle tissue from fatteners of Wild Boar, Pulawska and its crossbreed Pulawska × (Hamshire × Wild Boar). Arch. Tierz. 53 (2010) 184-193.

[28] M. Furman, Š. Malovrh, A. Levart, Kovač M, Fatty acid composition of meat and adipose tissue from Krškopolje pigs and commercial fatteners in Slovenia. Arch. Tierz. **53** (2010) 73–84.

[29] A.F. Marchiori, E.P. de Felício, Quality of wild boar meat and commercial pork. Sci. Agric. **60** (2003) 1–5.

[30] B. Lebret, A.N. Guillard, Outdoor rearing of cull sows: Effects on carcass, tissue composition and meat quality, Meat Sci. **70** (2005) 247–257.

[31] N.A. Postolache, R. Lazăr, C.P. Boişteanu, Researches on the characterization of physical and chemical parameters of refrigerated meat from wild boar sampled From the N-E part of Romania, Lucrări Ştiinţifice, **54** (2011) 193–197.

[32] G.M.A. Quaresma, P.S. Alves, I. Trigo-Rodrigues, R. Pereira-Silva, N. Santos, C.P.J. Lemos, S.A. Barreto, B.J.R. Bessa, Nutritional evaluation of the lipid fraction of feral wild boar (Sus scrofa scrofa) meat, Meat Sci. **89** (2011) 457–461.

[33] S.R. Morrison, J.L. Johnston, M.A. Hilbrands, The behaviour, welfare, growth performance and meat quality of pigs housed in a deep-litter, large group housing system compared to a conventional confinement system, Appl. Anim. Behav. Sci. **103** (2007) 12–24.

IZVOD

KVALITET MESA SVINJA RASE DUROK×JORKŠIR, DUROK×JORKŠIR×DIVLJI VEPAR I DIVLJI VEPAR

Snežana D. Ivanović[1], Zoran M. Stojanović[2], Jovanka V. Popov-Raljic[3], Milan Ž. Baltić[4], Boris P. Pisinov[1], Ksenija D. Nešić[1]

[1]*Naučni institut za veterinarstvo Srbije, Beograd, Srbija*
[2]*Agencija za ispitivanje životne sredine, Beograde, Srbija*
[3]*Poljoprivredni fakultet, Zemun, Srbija*
[4]*Fakultet veterinarske medicine, Univerziteta u Beogradu, Beograd, Srbija*

(Stručni rad)

Meso svinja zbog svog sastava, pre svega količine visoko vrednih proteina, i esencijlnih aminokiselina, masti i esencijalnih masnih kiselina, vitamina (svinjsko meso, na primer, sadrži visok nivo tiamina i on je 5–10 puta veći nego u mesu ostalih vrsta stoke za klanje) i minerala, predstavlja visokokvalitetnu i koncentrovanu hranu i zato ima važnu ulogu u ishrani ljudi. U zavisnosti od, rase, pola, starosti i stepena uhranjenosti, kao i položaja u telu, meso može da sadrži različite količine mišićnog, masnog i vezivnog tkiva, što neposredno uslovljava hemijski sastav ove namirnice. Cilj ovog rada je bio da se ispita hemijski sastav i pH vrednost, sastav masnih kiselina, sadržaj holesterola, boja (instrumentalno) i senzorna analiza svežeg mesa svinja za: Durok×Jorkšir, Durok×Jorkšir×divlji vepar i divlji vepar. Iz uzoraka *m. longissimus dorsi,* uzetih nakon klanja navedenih životinja, ispitivan je hemijski sastav primenom ISO metoda. Sastav masnih kiselina i sadržaj holesterola određivani su standardnom metodom primenom gasne hromatografije (GC6890N, Agilent Tech., USA) poređeni sa standardom masnih kiselina (standard mix of FAMEs 37, Supelco, USA). Boja svežeg mesa je takođe određivana u *m. longissimus dorsi* upotrebom Minolta chromameter CR-400. Senzornu analizu su radili obučeni ocenjivači u skladu sa ISO metodom. Dobijeni rezultati su statistički obrađeni primenom programa MS-Excel 2003, ANOVA i utvrđene razlike srednjih vrednosti poređene t-testom na nivou značajnosti 99 i 95%. Iz prikazanih rezultata vidi se da je postojala statistički značajna razlika u kvalitetu mesa između ispitivanih uzoraka.

Ključne reči: Kvalitet mesa • Durok • Jorkšir • Divlji vepar

Uticaj pH vrednosti na biosorpciju jona bakra otpadnom lignoceluloznom masom koštice breskve

Zorica R. Lopičić[1], Jelena V. Milojković[1], Tatjana D. Šoštarić[1], Marija S. Petrović[1], Marija L. Mihajlović[1], Časlav M. Lačnjevac[2], Mirjana D. Stojanović[1]

[1]*Institut za tehnologiju nuklearnih i drugih mineralnih sirovina, Beograd, Srbija*
[2]*Poljoprivredni fakultet, Univerzitet u Beogradu, Srbija*

Izvod

Jedan od glavnih faktora u procesu biosorpcije predstavlja pH vrednost rastvora sorbata, jer istovremeno utiče na hemijsko ponašanje prisutnih kontaminanata kao i na aktivnost funkcionalnih grupa biosorbenta. U ovom radu ispitan je uticaj pH vrednosti u procesu biosorpcije dvovalentnog bakra, nemodifikovanom otpadnom lignoceluloznom masom koštica breskve (KB). Procenat uklanjanja bakra ovim biosorbentom znatno varira u ispitivanom opsegu pH vrednosti, počev od 2,62% za pH vrednost 2, do 90,43% za pH vrednost 6, pri inicijalnoj koncentraciji bakra od 50 mg/l. Rezultati ispitivanja pokazali su da je za KB pri izabranim operativnim uslovima, proces neophodno voditi na pH 5, što je vrednost nešto viša od vrednosti nultog naelektrisanja (pH_{pzc}) koja iznosi 4,75±0,1. Potvrđena je neophodnost održavanja pH vrednosti konstantnom za vreme procesa, pri čemu je biosorpcioni kapacitet KB dvostruko veći od biosorpcionog kapaciteta bez održavanja pH vrednosti.

Ključne reči: *biosorpcija, joni bakra, koštica breskve, tačka nultog naelektrisanja, pH vrednost.*

Dostupno na Internetu sa adrese časopisa: http://www.ache.org.rs/HI/

NAUČNI RAD

UDK 66.081:54:543.554.2:634.25

Hem. Ind. **67** (6) 1007–1015 (2013)

doi: 10.2298/HEMIND121225018L

Sveprisutnije zagađenje životne sredine antropogenog porekla, predstavlja realni problem savremenog čoveka. Od svih polutanata, najčešće su prisutni joni teških metala, koji, osim što su veoma toksični, biološki i termički nerazgradivi, imaju i svojstvo akumulacije u tkivima organizama [1]. Među ovim jonima najčešće su prisutni joni olova, kadmijuma, bakra, cinka, nikla itd. U ovom radu ispitivana je biosorpcija jona bakra, obzirom da je poslednjih godina potražnja i proizvodnja ovog metala naglo porasla, pa je samim tim i njegovo prisustvo u površinskim vodama sve značajnije [2]. Za uklanjanje metalnih jona iz otpadnih voda najčešće se koriste različite konvencionalne metode, kao što su hemijska precipitacija i redukcija, filtracija, flokulacija, jonska izmena, elektrohemijski tretman, itd. [3]. Glavni nedostaci ovih metoda su nedovoljna selektivnost, generisanje otpadnog mulja koji je potrebno dalje tretirati, visoki operativni troškovi i različita tehnička ograničenja, naročito ukoliko se radi o niskim koncentracijama prisutnih polutanata, pa je zbog toga neophodno pronaći ekonomski isplativo, tehnički lako izvodljivo rešenje, kojim bi se oni efikasno uklonili [2,4].

Tokom poslednje dve decenije u svetu je došlo do povećanja ekološke svesti što je doprinelo razvoju novih, efikasnih, ekološko i ekonomsko prihvatljivih tehnologija za prečišćavanje kontaminiranih voda. Upravo se to vreme smatra početkom razvoja biosorpcije, odnosno primene bioloških materijala za uklanjanje polutanata iz vodenih rastvora. Aktuelnost ove tehnike vidi se kroz konstantan rast publikovanih naučnih radova iz ove oblasti, što samo potvrđuje kompleksnost i multidisciplinarnost biosorpcionog sistema [4–6].

Biosorpcija se definiše kao sposobnost izvesnih biomolekula da svojim aktivnim grupama vezuju ili iz vodenih rastvora koncentrišu određene jone, pri čemu su uklanjani polutanti najčešće joni metala ili organska jedinjenja [5–8]. Mehanizmi odgovorni za biosorpciju mogu biti pojedinačni ili kombinacija sledećih procesa: jonska izmena, građenje kompleksa, fizička adsorpcija ili hemisorpcija, elektrostatička interakcija, mikrotaloženje, građenje helata, itd, što umnogome zavisi od prirode samog biosorbenta, ali i osobina polutanta koji se uklanja [5].

U odnosu na konvencionalne metode, biosorpcija ima određene prednosti: selektivna je, jeftina i efikasna čak i pri vrlo niskim koncentracijama polutanata, ekološki održiva jer se kao biosorbent najčešće koristi obnovljivi izvor – biomasa, koja neupotrebljena predstavljala otpad u životnoj sredini [9]. Upotrebljenu biomasu moguće je regenerisati, pri čemu se dobija koncentrat metala i biomaterijal spreman za novi ciklus uklanjanja. Efikasnost biomase se može povećati modifikacijom fizičkim, hemijskim, termičkim ili kombinovanim tretmanima [10–12].

Generalno, biosorbenti se mogu podeliti u četiri velike kategorije [13]: bakterije, alge, gljive i kvasci, i poljoprivredni otpad, čija je primena predmet istraživanja u ovom radu. Optimizacija biosorpcionog procesa obuhvata ispitivanje uticaja karakteristika biološkog

Prepiska: Z.R. Lopičić, Institut za tehnologiju nuklearnih i drugih mineralnih sirovina, Franše d'Eperea 86, 11000 Beograd.
E-pošta: z.lopicic@itnms.ac.rs
Rad primljen: 25. decembar, 2012
Rad prihvaćen: 28. februar, 2013

materijala, koncentracije polutanta, pH vrednosti rastvora, jonske jačine rastvora sorbenta, veličine čestica, temperature, uticaja prisustva koegzistirajućih hemijskih vrsta i sl. [12]. Jedan od parametara čija se značajna uloga ističe u gotovo svakom radu na temu biosorpcije predstavlja pH vrednost rastvora sorbata, ali je u radovima retko naglašen značaj održavanja izabrane pH vrednosti konstantnom tokom celog procesa biosorpcije, što i jeste prednost ovog rada.

Adsorpcioni kapacitet, q_e, predstavlja maksimalnu količinu sorbata (mmol ili mg) koju je moguće ukloniti jediničnom masom biosorbenta (g), značajno je uslovljen svim prethodno pomenutim parametrima. Adsorpcioni kapacitet i adsorpciono vreme predstavljaju dva najvažnija parametra koji definišu primenu nekog adsorbenta [14]. Biosorpcioni kapacitet pojedine otpadne biomase, korišćenih u svrhu biosorpcije različitih metala, prikazani su u tabeli 1 [15–22]. Iz ove tabele može se videti da maksimalni adsorpcioni kapaciteti ispitivanih biosorbenata znatno variraju, ali se svi autori slažu u konstataciji da je posmatrane biosorbentne poželjno koristiti za uklanjanje ispitivanih metala.

Biosorpcija različitih polutanata umnogome zavisi od morfologije i dostupnosti površine biosorbenta, gustine i raspodele površinskog naelektrisanja koji zavise od prisustva i uticaja različitih aktivnih grupa, i od osobina same zagađujuće materije [2]. Poznato je da pH vrednost sredine ima snažan uticaj na sorpciju katjona, u prvom redu zbog uticaja na ponašanje metalnih jona u rastvoru (hidroliza, građenje kompleksa, taloženje i sl.), ali i na jonizaciju hemijski aktivnih mesta na biosorbentu [23]. Kako je pokazano u literaturi [24,25], ukupno naelektrisanje površine sorbenta može imati veoma važnu ulogu u sorpcionim procesima, pa je zbog toga korisno ispitati ponašanje biosorbenta u vodenim rastvorima, jer se na osnovu toga može delom objasniti mehanizam biosorpcije specifičnog polutanta na upotrebljenom biosorbentu. Zbog toga je u radu određena tačka nultog naelektrisanja koštica breskve i ispitan uticaj pH vrednosti vodenog rastvora sorbata na efikasnost biosorpcije. Potencijal nultog naelektrisanja (pH_{PZC}) predstavlja onu pH vrednost na kojoj je površina biosorbenta elektroneutralna. Ukoliko su radne vrednosti pH suspenzije sorbata iznad vrednosti pH_{PZC} smatra se da je površina biosorbenta negativno naelektrisana i odgovara sorpciji katjona, dok je za pH vrednosti niže od pH_{PZC} ova površina pozitivna i odgovara adsorpciji anjona. Podaci o nultom naelektrisanju diktiraju efikasnost adsorpcije katjona na mnogim pH-zavisnim materijalima (kao što je slučaj sa aktivnim ugljem), tako da se sa porastom pH vrednosti rastvora sorbata, obično povećava i adsorpcioni kapacitet za ispitivanu katjonsku vrstu [26].

EKSPERIMENTALNI DEO

Biomasa korišćena u prikazanim eksperimentima predstavlja otpadni lignocelulozni materijal (koštice breskve) poreklom iz Fabrike za preradu sokova „Vino Župa" iz Aleksandrovca, gde je klasifikovan kao otpadna biomasa. Poslednjih godina se ispituju nove mogućnosti upotrebe ovog otpada, ili putem sagorevanja biomase (što je sa jedne strane energetski zahtevno s obzirom na to da se procenat vlage u otpadu kreće od 49 do 60%), ili pronalaženjem nove upotrebne vrednosti kroz biosorpciju, pri čemu se rasterećuju već formirane deponije i sprečava formiranje novih [27].

Koštice breskve odvajane su od eventualnog zaostatka pulpe, oprane u vodi i sušene na sobnoj temperaturi. Potom su višestepenim usitnjavanjem i klasiranjem uzoraka koštica breskve (KB) dobijene različite frakcije koje su korišćene u daljim eksperimentima. Pre eksperimenata sve frakcije KB oprane su nekoliko puta u 0,01 M HCl kako bi se uklonile zaostale površinske nečistoće, a potom u destilovanoj vodi sve do negativne reakcije na Cl^-. Nakon toga uzorci KB sušeni su na temperaturi od 60 °C do konstantne mase, i uskladišteni u hermetički zatvorenim sudovima do početka eksperimenata.

Tabela 1. Primeri upotrebe različite otpadne biomase u uklanjanju teških metala biosorpcijom
Table 1. Examples of different waste materials used in biosorption of heavy metals

Biosorbent	Uklanjani metal	Maksimalni biosorpcioni kapacitet, mg/g	Ref.
Kukuruzna šaša	Cr(VI)	7,59	[15]
Stabljika grožđa	Pb(II)	49,93	[16]
	Cd(II)	27,88	
Sirova opna od pirinča	Cd(II)	8,58	[17]
Ljuska kikirikija	Cu(II)	21,25	[18]
Ljuska badema	Pb(II)	8,08	[19]
Ljuska lešnika	Pb(II)	28,18	
Pulpa šećerne repe	Cu(II)	28,50	[20]
Ječmena slama	Cu(II)	4,64	[21]
	Pb(II)	23,20	
Lišće paprati	Cu(II)	11,70	[22]

Utvrđivanje hemijskog sastava koštica breskve obuhvatio je sadržaj suve materija, vlage i pepela, sirovog proteina, masti, celuloze, lignina, neutralnih deterdžentskih vlakana (NDF), kiselih deterdžentskih vlakana (ADF) kao i bezazotnih ekstraktivnih materija (BEM). Metoda 6 objavljena u Pravilniku o metodama uzimanja uzoraka i metodama fizičkih, hemijskih i mikrobioloških analiza stočne hrane, Sl. list SFRJ 15/87, korišćena je za određivanje sadržaja suve materije i vlage, dok je po metodi 18 istog Pravilnika urađen sadržaj pepela. Sadržaj sirovih vlakana, NDF (neutralna deteredžentska vlakna) i ADF (kisela deterdžentska vlakna) određen je na uređaju ANKOM 2000 *fiber analyzer*, standardnim metodama objavljenim u Pravilniku, Sl. list SFRJ 15/87, i VDI metodama: VDI-111, VDI-118 i VDI-119 [28]. Analize su rađene u sirovom biomaterijalu sa prirodnim sadržajem vlage (PSV) i na suvoj materiji (SM).

Morfologija površine uzoraka koštica breskvi, sušenih 24 h na 60 °C, površinski naparenih tankim slojem zlata, utvrđena je skenirajućim elektronskim mikroskopom JSM-6610LV (Jeol, Japan), pri naponu od 20 kV.

Tačka nultog naelektrisanja, pHpzc, nemodifikovanih koštica breskvi određena je metodom Milonjića i autora [24]. Eksperimenti su rađeni sa tri različite jonske jačine rastvora elektrolita, 0,1, 0,01 i 0,001 M KNO_3. U seriju erlenmajera od 100 cm^3 odmereno je po 50 cm^3 rastvora KNO_3 određene koncentracije, kome su podešene početne pH vrednosti rastvora, pHi, u intervalu od 2 do 10, dodavanjem 0,1 mol/dm^3 rastvora KOH ili 0,1 mol/dm^3 HNO_3. Rastvorima sa podešenim pH vrednostima dodato je po 0,1 g uzorka KB, nakon čega su erlenmajeri sa suspenzijom postavljeni na šejker i uravnotežavani 24 h na sobnoj temperaturi. Suspenzije su profiltrirane i izmerena je pH vrednost svakog filtrata (pH_f). Tačka nultog naelektrisanja uzoraka je određena kao pH vrednost platoa grafika zavisnosti $pH_f = f(pH_i)$.

Rastvori bakarnih jona, pravljeni su rastvaranjem određene količine $Cu(NO_3)_2 \cdot 3H_2O$ (Sigma–Aldrich) u destilovanoj vodi. Koncentracija jona bakra, Cu(II), određena je upotrebom atomske adsorpcione spektrometrije (Perkyn Elmer AAS Analyst 300).

Svi eksperimenti biosorpcije izvođeni su na uzorcima KB veličine čestica od 0,1 do 0,5 mm. Koncentracija biosorbenta je bila 10 g/dm^3 sorbata, a inicijalna koncentracija jona bakra iznosila 50,0 mg/dm^3. Ogledi su izvođeni u šaržnom sistemu sa mešanjem (150 rpm) i na ambijentalnoj temperaturi od 25 °C. U tu svrhu korišćeni su stakleni erlenmajeri od 100 ml postavljeni na orbitalni šejker sa termostatom, proizvođača Heidolph, model Unimax 1010. Vrednost pH praćena je na uređaju SensION MM340, proizvođača Hach, sa integrisanom magnetnom mešalicom. Održavanje pH vrednosti konstantnom, vršeno je podešavanjem pH na željenu vrednost pre početka izvođenja eksperimenta, a potom, tokom eksperimenta, dodatkom malih zapremina (μl) 0,1 M NaOH ili 0,1 M HCl mikropipetom.

U ovom radu su prikazana tri eksperimenta izvedena sa neaktiviranim KB pri prethodno opisanim operativnim uslovima. Prvi se odnosio na praćenje promene pH vrednosti rastvora sorbata kao i rezidualne koncentracije bakra u rastvoru tokom procesa biosorpcije, tokom vremena kontakta od 500 min bez održavanja pH vrednsoti konstantnom (vreme kontakta izabrano je da bi se utvrdilo koje je vreme neophodno za uspostavljanje ravnoteže u sistemu). Drugi eksperiment odnosio se na utvrđivanje neophodnosti održavanja pH vrednosti konstantnom tokom biosorpcije, u trajanju od 240 min i odnosio se na poređenje rezultata procesa biosorpcije bez i sa održavanjem inicijalne pH vrednosti konstantnom (pH_i 4,95). Treći eksperiment izveden je na različitim pH vrednostima u opsegu 2–6 (pH održavana konstantnom sve vreme kontakta (180 min)) kako bi se utvrdila optimalna pH vrednost za izvođenje procesa biosorpcije dvovalentnog bakra neaktiviranim KB. U cilju određivanja maksimalne pH vrednosti do koje je moguće voditi proces, a da se uklanjanje Cu(II) jona može pripisati samo biosorpciji, a ne i taloženju, korišćen je grafički Medusa/Hydra program. Primenom ovog programa dobijena je specifikacija formi bakra pri izabranim radnim uslovima (slika 1).

Nakon završenog procesa biosorpcije analitički je određivana koncentracija zaostalog sorbenta, C_f, a biosorpcioni kapacitet, q (mg/g), izračunat je po jednačini:

$$q = [(C_i - C_f)V]/S \quad (1)$$

Procenat uklanjanja jona bakra, kao veličina koja opisuje efikasnost biosorpcije, izračunat je prema jednačini:

$$\text{Procenat uklanjanja} = 100[(C_i - C_f)/C_i] \quad (2)$$

V predstavlja zapreminu rastvora sorbata (dm^3), S masu biosorbenta (g), a C_i i C_f koncentracije sorbata na početku odnosno na kraju procesa biosorpcije (mg/dm^3).

Svi eksperimenti rađeni su u duplikatu, a prikazane vrednosti predstavljaju srednju vrednost dobijenih rezultata.

REZULTATI I DISKUSIJA

Rezultati hemijske analize koštica breskve pokazali su da je u suvim uzorcima KB dominantan sadržaj celuloze (62,94%) i lignina (17,93%), dok je sadržaj hemiceluloze niži i iznosi 5,42% (tabela 2). Ova tri jedinjenja obiluju hidroksilnim grupama koje su odgovorne za vezivanje metala [29].

Celulozni materijali biološkog porekla pokazuju težnju višeslojne strukture međusobno povezane sistemima kanala i pora, što im omogućava relativno veliku površinu po jedinici mase [30]. Morfologija i izgled površine mlevenih koštica breskve prikazan je na SEM

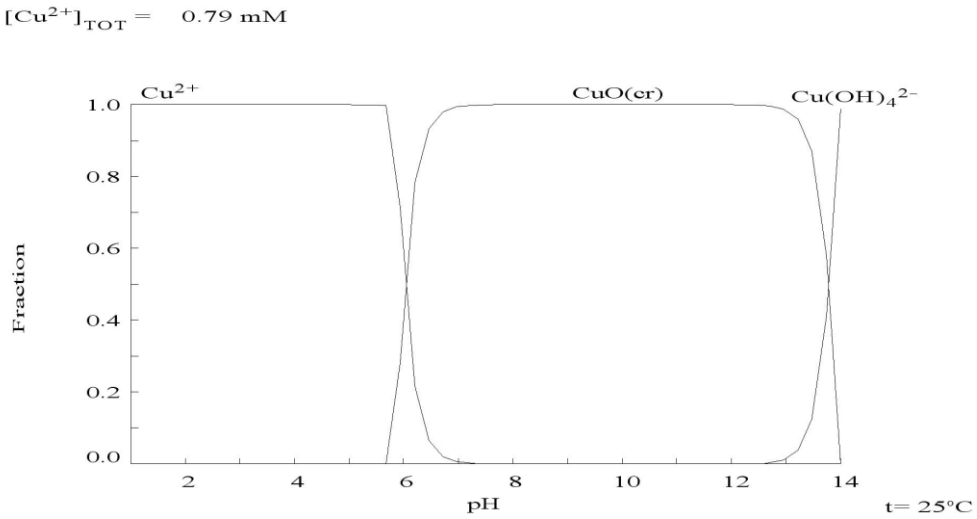

Slika 1. Frakcioni dijagram hemijskih formi bakra u funkciji od pH vrednosti.
Figure 1. Fractional diagram of chemical forms of copper in function of pH value.

Tabela 2. Hemijski sastav neaktiviranih koštica breskve (KB) [28]
Table 2. Chemical composition of untreated peach shell (PS) [28]

Karakteristika	Prirodni sadržaj vlage, %	Suva materija, %
Suva materija	92,23	100,00
Vlaga	7,77	-
Sirovi protein	1,26	1,37
Sirova mast	0,05	0,05
Sirova celuloza	58,05	62,94
Pepeo	0,42	0,46
BEM	32,45	35,18
Analiza prema van Soest-u		
Neutralna deterdžentska vlakna (NDF)	71,12	77,11
Kisela deterdžentska vlakna (ADF)	66,12	71,69
Lignin	16,54	17,93

fotografiji (slika 2) pri uvećanju od 5000 puta. Sa slike 2 može se uočiti da je u ovom biosorbentu prisutna višeslojna porozna površina, nepravilne laminarne strukture i sa različitom veličinom pora. Unutrašnja difuzija jona metala iz vodenih ratvora olakšana je prisustvom makro pora koje su dostupnije za prolaz vodene faze, pri čemu je u ovim porama olakšano mešanje i prenos mase konvekcijom. Takođe je moguće uočiti veliki broj pora prečnika oko 1 μm, koje su pogodne za difuziju metalnih jona i njihovu adsorpciju na aktivnim grupama na površini biosorbenta [31].

Tačka nultog naelektrisanja, rađena za tri različite jonske jačine, prikazana je na slici 3.

Na slici se može uočiti da tačka nultog naelektrisanja iznosi 4,75±0,1 i poklapa se za sve tri jonske jačine elektrolita, što ukazuje da je ovaj elektrolit inertan za ispitivani biosorbent jer se joni ovog elektrolita (K^+ i NO_3^-) ne sorbuju specifično na površini nemodifikovane KB (nema hemijske već samo fizičke biosorpcije) [32]. Vrednost nultog naelektrisanja predstavlja onu pH vrednost iznad koje će uklanjanje katjona, u ovom slučaju jona dvovalentnog bakra, biti favorizovano, što su potvrdili i rezultati prikazani u daljem toku ispitivanja. Vrednosti nultog naelektrisanja različitih biosorbenta opisane u literaturi znatno variraju u zavisnosti od sastava aktivnih grupa na ovršini biosorbenta, od 3,32 za piljevinu [33], preko 4,80 za poliporoznu biomasu [34], do 6,91 za strugotinu Mansoni drveta [35].

Kako je površina biosorbenta sastavljena od mnoštva molekula koji u sebi sadrže različite aktivne grupe, pH vrednost rastvora sorbata se značajno menja tokom procesa biosorpcije što je ilustrovano na slici 4. Grafik promene pH vrednosti dobijen je merenjem ove veličine tokom posmatranog vremena kontakta, a uporedo sa ovim merenjima, praćena je i koncentracija rastvora sorbata, što je takođe prikazano na slici 4.

Na slici 4 se može uočiti, tokom posmatranog vremena kontakta od 500 min, da se pH vrednost rastvora

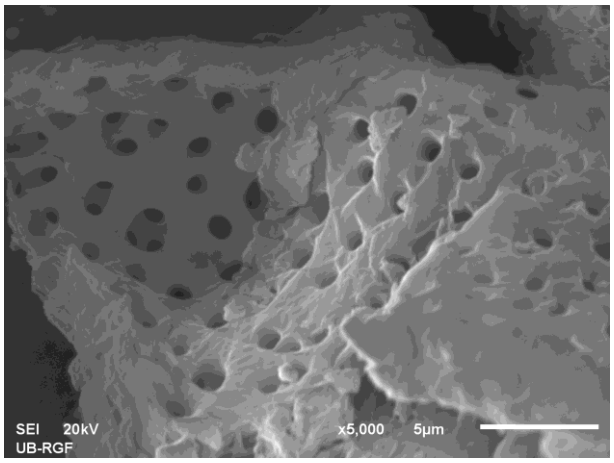

Slika 2. SEM mikrografija površine KB pri uvećanju od 5000×.
Figure 2. SEM surface microgrphs of unmodified PS with amplification of 5000×.

bakra promeni od inicijalne vrednosti rastvora sorbata (koja je iznosila 4,95) do krajnje vrednosti 3,68, zahvaljujući disocijaciji karboksilnih grupa koje su značajno prisutne u lignoceluloznom materijalu koštica breskve. Sa slike 4 jasno se može uočiti brzo inicijalno uklanjanje jona bakra tokom prvih 30 min, sa početnih 52,6 na 30,5 mg/dm^3, nakon čega sledi desorpcija jona bakra praćena snižavanjem pH vednosti i porast koncentracije bakra do finalne vrednosti od 41,0 mg/dm^3. Porast koncentracije jona bakra u rastvoru predstavlja posledicu porasta koncentracije H^+ usled disocijacije karboksilnih grupa (što je praćeno snižavanjem pH vrednosti), koji se pritom ponašaju kao joni konkurentni jonima metala, i doprinose njihovoj desorpciji sa površine biosorbenta.

Trendovi zavisnosti promene pH vrednosti i koncentracije bakarnih jona, istovremeno su i potvrdili uticaj značaja održavanja pH vrednosti konstantom tokom procesa, što pokazuju i rezultati prikazani na slici 5.

Sa slike 5 se jasno vidi da je pod istim operativnim uslovima procenat uklanjanja bakra pri održavanju pH vrednosti konstantnom, i to na onoj vrednosti koja je jednaka inicijalnoj pH vrednosti rastvora (pH 4,95), iznosi 68,16%, dok je pri istim operativnim uslovima ali bez održavanja pH, ovaj procenat daleko manji, i iznosi 22,43% nakon izabranog vremena kontakta. U isto vreme biosorpcioni kapacitet koštica breskve više je nego dvostruko veći u uslovima kada je pH vrednost tokom biosorpcije održavana konstantnom i iznosio je 3,29 mg/g KB, u odnosu na 1,18 mg/g KB kada pH vrednost nije održavana konstantnom tokom procesa biosorpcije.

Zbog svega iznetog, postavlja se pitanje koja je optimalna pH vrednost koju je potrebno držati konstantnom tokom procesa biosorpcije. U tu svrhu sprovedeno je ispitivanje uticaja različitih pH vrednosti na uklanjanje jona bakra biosorpcijom u opsegu 2–6. Ispitivanje nije bilo moguće sprovesti na višim vrednostima od 6, jer se već na vrednostima iznad 5, javlja transformacija bakra iz Cu^{2+} u $Cu(OH)^+$ ili taloženje u vidu hidroksida $Cu(OH)_2$, pa se smanjenje koncentracije dvovalentnih jona u rastvoru ne može pripisati samo procesu biosorpcije [36]. Rezultati ispitivanja uticaja različitih pH vrednosti na biosorpciju bakra prikazani su na slici 6.

Na osnovu grafikona prikazanog na slici 6 može se uočiti da je proces biosorpcije najbolje izvoditi na pH vrednosti oko 5. Ovo se objašnjava činjenicom da su na

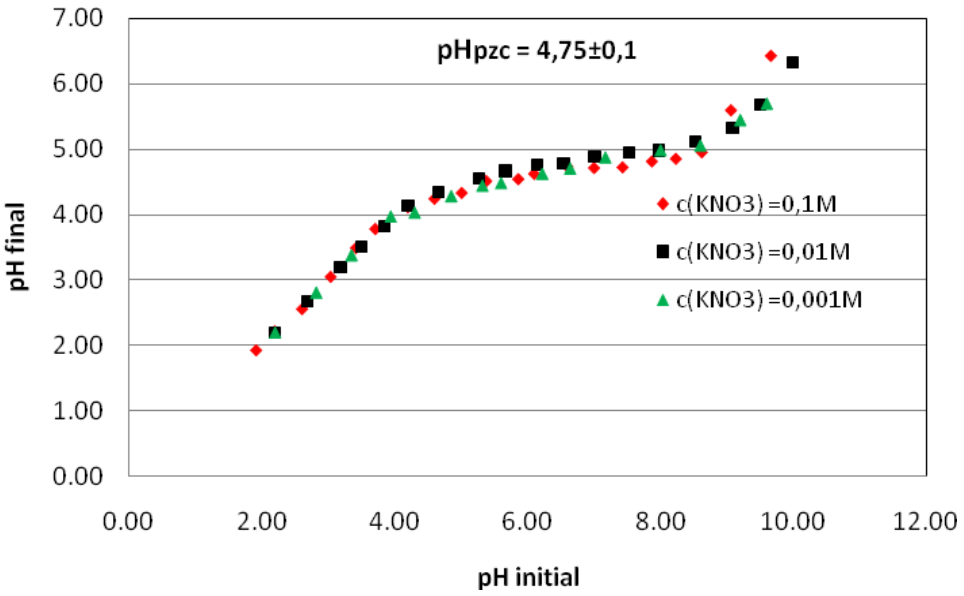

Slika 3. Zavisnost krajnje (pH_f) od inicijalne pH vrednosti (pH_i) za nemodifikovane KB.
Figure 3. Dependance of the final pH values (pH_f) from the initial pH values (pH_i) for unmodified PS.

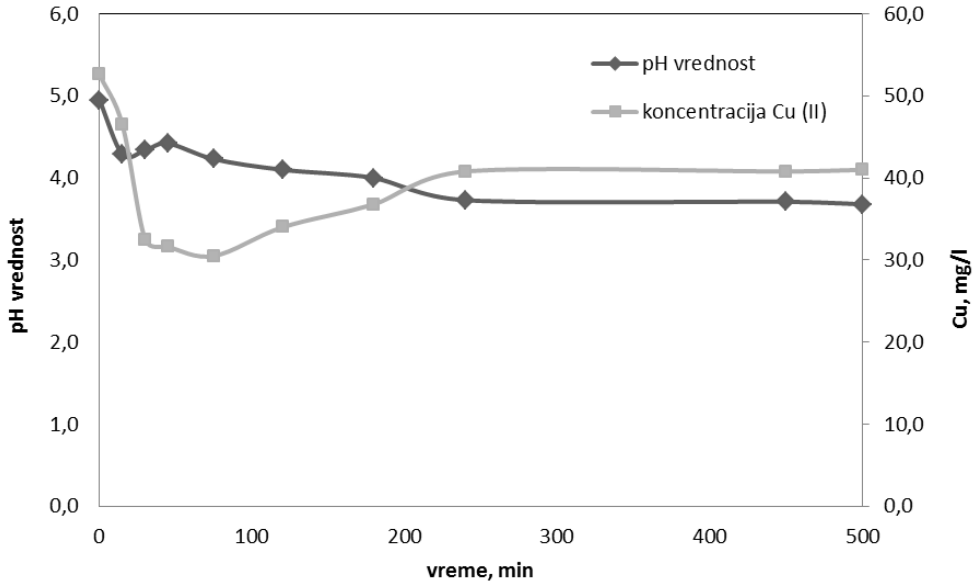

Slika 4. Promena pH vrednosti i polazne koncentracije bakarnih jona tokom kontakta.
Figure 4. Change in pH value and initial copper concentration during the contact time.

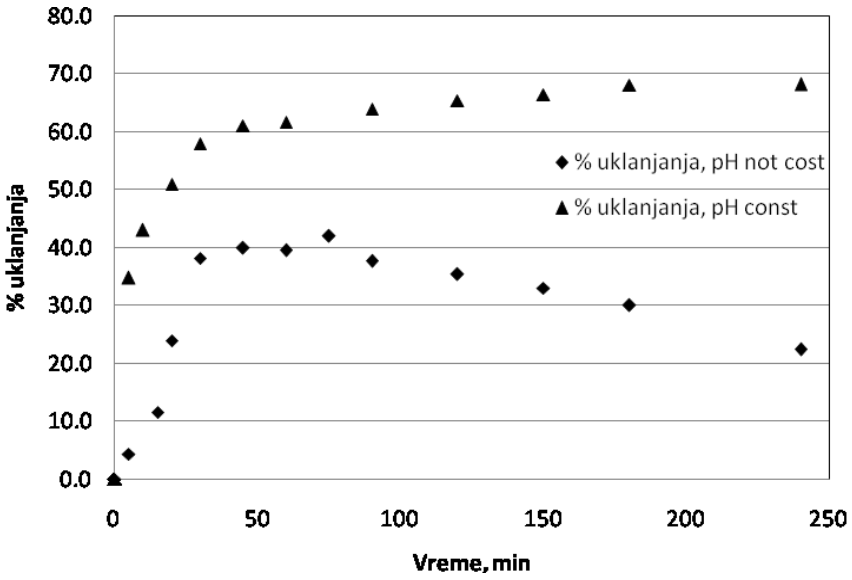

Slika 5. Uticaj pH vrednosti na procenat uklanjanja Cu(II) jona (d = 0,5+0,1 mm, C_i = 50mg/dm^3, M/V = 10g/dm^3, pH 5 (▲) const. i pH non const. (◆)).
Figure 5. The effect of pH value on the percentage removal of Cu(II) ions (d = 0.5+0.1 mm, C_i = 50mg/dm^3, M/V = 10g/dm^3, pH 5 (▲) const. and pH not const. (◆)).

niskim pH vrednostima ligandi biosorbenta okruženi hidronijum jonima tako da aktivna površina postaje pozitivna što izaziva elektrostatičko odbijanje katjona metala sa površine biosorbenta [37]. Sa porastom pH vrednosti dolazi do deprotonacije površine biosorbenta pri čemu gustina negativnog naelektrisanja raste, povećavajući pri tome uklanjanje metala iz rastvora. Ova pH vrednost je u skladu sa teorijskim objašnjenjem da je biosorpcija katjona optimalna na pH vrednostima većim od tačke nultog naelektrisanja, koja za ovaj tip biosorbenta iznosi 4,75±0,1.

ZAKLJUČAK

Rezultati prikazani u ovom radu ističu značajan uticaj pH vrednosti na proces biosorpcije, naglašavajući da je neophodno proces voditi na konstantnoj, prethodno definisanoj pH vrednosti, jer, iako se najveći procenat metala ukloni relativno brzo, neodržavanje pH vrednosti dovodi do smanjenja procenta uklanjanja sa 68,16 na 22,43%, a biosorpcionog kapaciteta za 64,13%. Održavana pH vrednost je pritom, najčešće iznad pH_{PZC}, koja za ovaj tip biosorbenta iznosi 4,75±0,1. Međutim,

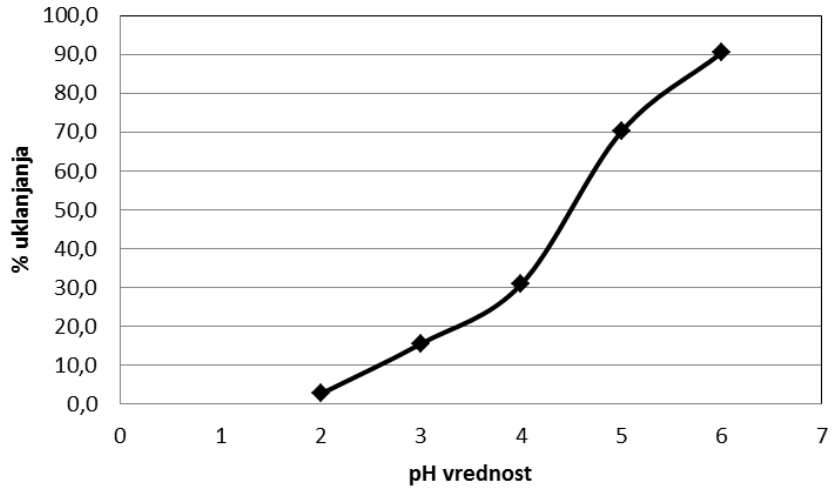

Slika 6. Uticaj pH vrednosti na biosorpcioni kapacitet KB (d = 0,5+0,1 mm, C_i = 50 mg/dm^3, M/V = 10 g/dm^3).
Figure 6. Effect of pH values on PS biosorption capacity (d = 0.5+0.1 mm, C_i = 50 mg/dm^3, M/V = 10 g/dm^3).

pri izabranim operativnim uslovima, hemijsko ponašanje samog metala dovodi do taloženja hidroksida na pH vrednostima višim od 5,5 pa je biosorpciju dvovalentnog bakra košticama breskve najbolje izvoditi na pH vrednosti oko 5, pri čemu je biosorpcioni kapacitet KB iznosio 3,31 mg/g. Ovo poklapanje optimalne pH vrednosti sa pH_{PZC} navodi na zaključak da je jedan od mehanizama vezivanja jona dvovalentnog bakra za neaktivirane čestice KB elektrostatičke prirode.

Dosadašnja ispitivanja biosorpcije bakra upotrebom nemodifikovane otpadne biomase, koštice breskve, pokazala su opravdanim predviđena istraživanja, s obzirom na to da se dobijene vrednosti biosorpcionog kapaciteta reda veličine drugih biosorbenata objavljenih u literaturi (tabela 1). U literaturi je moguće naći objavljena istraživanja sa košticom breskve, ali ne u njenoj prirodnoj formi već u formi pepela ili aktivnog uglja, što doprinosi originalnosti ovim istraživanjima. Primena aktivnog uglja na bazi otpadne biomase zahteva dodatnu energiju, poskupljujući tako sam proces uklanjanja, što je u ovom radu izbegnuto polazeći od suštine biosorpcijie – ekonomska isplativost [38]. Biosorpcija kao nova i kompleksna tehnologija pruža šansu zemljama koje poseduju veće količine neiskorišćene otpadne biomase da razviju efikasne, ekološki održive i ekonomski isplative materijale za uklanjanje polutanata iz otpadnih voda.

Zahvalnica

Autori rada se ovom prilikom zahvaljuju Ministarstvu prosvete, nauke i tehnološkog razvoja Republike Srbije, koje je svojim finansiranjem kroz projekat br. TR 31003 pomoglo opisana istraživanja. Takođe se zahvaljuju Kompaniji „Vino Župa“ iz Aleksandrovca, koja je participacijom kroz pomenuti projekat podržala opisana istraživanja.

LITERATURA

[1] J. Wang, C. Chen, Biosorbents for heavy metals removal and their future, Biotechnol. Adv. **27** (2009) 195–226.

[2] Y. Li, B. Helmreich, H. Horn, Biosorption of Cu(II) Ions from Aqueous Solution by Red Alga (Palmaria Palmata) and Beer Draff, Mater. Sci. Appl. **2** (2011) 70–80.

[3] A.V. Ochie, K. Trilestari, J. Sunarso, N. Indraswati, S. Ismadji, Recent progress on biosorption of heavy metals using low cost biosorbents: characterization, biosorption parameters and mechanism studies, Clean, 36 (2008) 937–962.

[4] B. Volesky, Biosorption and me, Water Res. **41** (2007) 4017–4029.

[5] G.M. Gadd, Biosorption: Critical review of scientific rationale, environmental importance and significance for pollution treatment, J. Chem. Technol. Biotechnol. **84** (2009) 13–28.

[6] R.H. Vieira, B. Volesky, Biosorption: a solution to pollution, Int. Microbiol. **3** (2000) 17–24.

[7] D. Sud, G. Mahajan, M.P. Kaur, Agricultural waste material as potential adsorbent for sequestering heavy metal ions from aqueous solutions – A review, Bioresour. Technol. **99** (2008) 6017–6027.

[8] M. Rao, A.V. Parwate, Utilization of low-cost adsorbents for the removal of heavy metals from wastewater – A review, J. Environ. Pollut. Contr. **5** (2002) 12–23.

[9] J. Wang, C. Chen, Biosorption of heavy metals by *Saccharomyces cerevisiae* – A review, Biotechnol. Adv. **24** (2006) 427–451.

[10] W.S. Wan Ngah, M.A.K.M. Hanafiah, Removal of heavy metal ions from wastewater by chemically modified plant wastes as adsorbents – A review, Bioresour. Technol. **99** (2008) 3935–3948.

[11] M. Emin, S. Dursun, M. Karatas, Removal of Cd(II), Pb(II), Cu(II) and Ni(II) from water using modified pine bark, Desalination **249** (2009) 519–527.

[12] B. Belhalfaoui, A. Aziz, E.H. Elandaloussi, M.S. Ouali, L.C. De Ménorva, Succinate-bonded cellulose: A regenerable

and powerful sorbent for cadmium-removal from spiked high-hardness groundwater, J. Hazard. Mater. **169** (2009) 831–837.

[13] N. Das, R. Vimala, P. Karthika, Biosorption of heavy metals-an overview, Indian J. Biotechnol. **7** (2008) 159––169.

[14] W.E. Marshall, L.H. Wartelle, D.E. Boler, M.M. Johns, C.A. Toles, Enhanced metal adsorption by soybean hulls modified with citric acid, Bioresour. Technol. **69** (1999) 263–268.

[15] V. Vinodhini, V. Anabarasu, D. Nilanjana, Screening of natural waste products for the removal of Cr (VI) ions from industrial effluents, Indian J. of Nat. Prod. Resour. **1** (2010) 174–180.

[16] M. Martınez, N. Miralles, S. Hidalgo, N. Fiol, I. Villaescusa, J. Poch, Removal of lead(II) and cadmium(II) from aqueous solutions using grape stalk waste, J. Hazard. Mater. **133** (2006) 203–211.

[17] U. Kumar, M. Bandyopadhyay, Sorption of cadmium from aqueous solution using pre-treated rice husk, Bioresour. Technol. **97** (2006) 104–109.

[18] C.S. Zhu, L.P. Wang, W.B. Chen, Removal of Cu (II) from aqueous solution by agricultural by-product: peanut hull, J. Hazard. Mater. **168** (2009) 739–746.

[19] E. Pehlivan, T. Altun, S. Cetin, M.I. Bhanger, Lead sorption by waste biomass of hazelnut and almond shell, J. Hazard. Mater. **167** (2009) 1203–1208.

[20] Z. Aksu, I.A. Isoglu, Removal of copper (II) ions from aqueous solution by biosorption onto agricultural waste sugar beet pulp, Process Biochem. **40** (2005) 3031–3044.

[21] E. Pehlivan, T. Altun, S. Parlayici, Utilization of barley straws as biosorbents for Cu^{2+} and Pb^{2+}, J. Hazard. Mater. **164** (2009) 982–986.

[22] Y.S Ho, Removal of copper ions from aqueous solution by tree fern, Water Res. **37** (2003) 2323–2330.

[23] A. Kumar, S. Kumar, D.V. Gupta, Adsorption of phenol and 4-nitro phenol on granular activated carbon in basal salt medium: Equilibrium and kinetics, J. Hazard. Mater. **147** (2007) 155–166.

[24] S.K. Milonjić, A.L. Ruvarac, M.V. Sušić, The heat of immersion of natural magnetite in aqueous solutions, Termochim. Acta **11** (1975) 261–266.

[25] N. Fiol, I. Villaescusa, Determination of sorbent point zero charge: usefulness in sorption studies, Environ. Chem. Lett. **7** (2009) 79–84.

[26] M.Z. Momčilović, M.M. Purenović, M.N. Miljković, A.Lj. Bojić, A.R. Zarubica, M.S. Ranđelović, Praškasti aktivni ugljevi dobijeni iz biljnog komunalnog otpada, Hem. Ind. **65** (2011) 241–247.

[27] Z. Lopičić, M. Stojanović, Č. Lačnjevac, J. Milojković, M. Mihajlović, T. Šoštarić, The copper biosorption using unmodified agricultural waste materials, Zaštita materijala **52** (2011) 189–193.

[28] M. Stojanović, Z. Lopičić, J. Milojković, Č. Lačnjevac, M. Mihajlović, M. Petrović, A.Kostić, Biomass waste material as potential adsorbent for sequestering pollutants, Zaštita materijala **53** (2012) 231–238.

[29] R.F. Nascimento, F.W. de Sousa, V.O.S. Neto, P. B. A. Fechine, R. N. P. Teixeira, P. de Tarso, C. Freire, M.A.Araujo-Silva, in D. Sebayang (Eds.), Electroplating: Biomass Adsorbent for Removal of Toxic Metal Ions From Electroplating Industry Wastewater, InTech, http://www.intechopen.com/books/electroplating/biomass-adsorbent-for-removal-of-toxic-metal-ions-from-electroplating-industry-wastewater, 2012, pp. 101–136.

[30] M.A. Hubbe, S.H. Hasan, J.J. Ducoste, Metal ion sorption – Review, Bioresour. **6** (2011) 2167–2287.

[31] G. Tan, H. Yuan, Y. Liu, D. Xiao, Removal of lead from aqueous solution with native and chemically modified corncobs, J. Hazard. Mater. **174** (2010) 740–745.

[32] M.M. Kragović,A. S. Daković, S.Z. Milićević, Ž.T.Sekulić, S.K. Milonjić, Uticaj sorpcije organskog katjona na tačku nultog naelektrisanja prirodnog zeolita, Hem. Ind. **63** (2009) 325–330.

[33] W. Zou, H. Bai, S. Gao, K. Li, Characterization of modified sawdust, kinetic and equilibrium study about methylene blue adsorption in batch mode, Korean J. Chem. Eng. **30** (2013) 111–122.

[34] M. Suguna, N. Siva Kumar, Equilibrium, kinetic and thermodynamics studies on biosorption of lead (II) and cadmium (II) from aqueous solutions by polypore biomass, Indian J. Chem. Technol. **20** (2013) 57–69.

[35] A.E. Ofomaja, Y.S. Ho, Effect of temperatures and pH on methyl violet biosorption by Mansonia wood sawdust, Bioresour. Technol. **99** (2008) 5411–5417.

[36] H.A. Elliott, C.P. Huan, Adsorption characteristics of some Cu(II) complexes on aluminosilicates, Water Res. **15** (1981) 849–855.

[37] A. Sari, D. Mendil, M. Tuzen, M. Soylak, Biosorption of palladium(II) from aqueous solution by moss (*Racomitrium lanuginosum*) biomass: Equilibrium, kinetic and thermodynamic studies, J. Hazard. Mater. **162** (2009) 874–879.

[38] E.O. Oyelude, U.R. Owusu, Adsorption of Methylene Blue from Aqueous Solution Using Acid Modified *Calotropis procera* Leaf Powder, J. Appl. Sci. Environ. Sanit. **6** (2011) 477–484.

SUMMARY

INFLUENCE OF pH VALUE ON Cu(II) BIOSORPTION BY LIGNOCELLULOSE PEACH SHELL WASTE MATERIAL

Zorica R. Lopičić[1], Jelena V. Milojković[1], Tatjana D. Šoštarić[1], Marija S. Petrović[1], Marija L. Mihajlović[1], Časlav Lačnjevac[2], Mirjana D. Stojanović[1]

[1]*Institute for Technology of Nuclear and Other Mineral Raw Materials, Belgrade, Serbia*
[2]*Agricultural Faculty, University of Belgrade, Serbia*

(Scientific paper)

In the last decade, pollution from anthropogenic sources has reached high levels. Special attention is being paid to heavy metals because of their high toxicity, persistence and bioaccumulation tendency. Since the conventional methods for their removal are either too expensive or create large quantities of toxic sludge, attention has been turning to new technologies such as biosorption, technology that use cheap, abundant, organic waste for sequestering pollutants from contaminated mediums. Among the other factors that affect biosorption process, pH value is one of the most important because it directs both the metal solution chemistry as well as the activity of the biomass functional groups. In this paper, the influence of pH value on biosorption of Cu (II) by unmodified low-cost lignocellulose biosorbent – peach shell (PS) particles, has been studied. The chemical composition of PS, point of zero charge (pHPZC), as well as its surface morphology is also presented. The results showed that this biosorbent contains mainly cellulose and lignin, the components that carry the functional groups responsible for metal binding. Its multilayer surface contains many pores and channels that help diffusion in deeper layers and force biosorption process. Point of zero charge determination was performed with three different KNO3 ionic strengths: 0.1, 0.01 and 0.001 M. The obtained value for pHPZC was 4.75±0.1 and showed that this biosorbent is non-sensitive to the ionic strength of the electrolyte applied. Biosorption experiments were done with peach shell particles of diameters 0.5+0.1 mm at 25 °C. The initial copper (II) concentration was 50 mg/dm^3 while the biosorbent concentration was 10 g/dm^3. Experiments were performed with and without keeping the pH constant. The influence of pH on biosorption process was examined in a pH range of 2–6. The percentage of Cu (II) removed by PS reached its maximum at pH 6, with 90.43% removal, but this percentage can also be attributed to the precipitation of metal at this pH value. However, under the same operational conditions, but at pH 2, the retention of copper was equal to 2.62%. The results also indicate that it is necessary to lead the biosorption process with keeping the pH constant at all times, since the copper removal was about 46% less when the pH value was not kept constant during the biosorption process. The pH value obtained as optimal was slightly higher than the pH_{PZC} value, which indicates that electrostatic attraction is one of the possible binding mechanisms in biosorption process. The results have showed that the removal of Cu (II) with peach shell particles is very sensitive to solution pH and that this parameter should be thoroughly investigated and strongly controlled during the whole removal process.

Keywords: Biosorption • Copper ions • Peach stone • Point of zero charge • pH Value

SADRŽAJ VOLUMENA 67.

Sveska 1

Sveska 2

Sveska 3

Sveska 4

Sveska 5

Sveska 6

Polimeri

INDEKS AUTORA 2013